

NAM

Dynamic behaviour of Groningen peat

Analysis and parameter assessment

Deltares

M. Konstantinou, dr.ir. C. Zwanenburg and dr.ir. P. Meijers

Date October 2017

Editors Jan van Elk & Dirk Doornhof

General Introduction

The accelerations experienced at surface as a result of the earthquakes induced by the production of gas from the Groningen field is locally dependent on the shallow geological and soil conditions (Ref. 1). This is called the site response effect.

NAM has asked Deltares to build a detailed model of the shallow subsurface below Groningen (Ref. 2 to 5). In preparing this model of the shallow subsurface below Groningen, Deltares has made use of the beta-version of the GEOTOP database of TNO Geologische Dienst Nederland (TNO-NITG) supplemented by more recent data. Additional data collected over the years in support of foundation design and other activities was sourced from Fugro and Wiertsema. These are mainly CPT measurements (cone penetrations tests). Additionally, data measured in the shallow geophone wells was used.

For these calculations of the site response, soil parameters related to stiffness and damping (amongst others) are also necessary. For sand and clay these parameters are derived from well accepted correlations in the literature. However, the properties of locally present peat layers need to be measured in the laboratory. This report and the accompanying report (Ref. 6) present the measurements performed by Deltares on peat samples from Groningen, the analysis of the experimental data and the assessment of peat properties.

References

1. De ondergrond van Groningen: een Geologische Geschiedenis, Erik Meijles, April 2015.
2. Geological schematisation of the shallow subsurface of Groningen (For site response to earthquakes for the Groningen gas field) – Part I, Deltares, Pauline Kruiver, Ger de Lange, Ane Wiersma, Piet Meijers, Mandy Korff, Jan Peeters, Jan Stafleu, Ronald Harting, Roula Dambrink, Freek Busschers, Jan Gunnink
3. Geological schematisation of the shallow subsurface of Groningen (For site response to earthquakes for the Groningen gas field) – Part II, Deltares, Pauline Kruiver, Ger de Lange, Ane Wiersma, Piet Meijers, Mandy Korff, Jan Peeters, Jan Stafleu, Ronald Harting, Roula Dambrink, Freek Busschers, Jan Gunnink
4. Geological schematisation of the shallow subsurface of Groningen (For site response to earthquakes for the Groningen gas field) – Part III, Deltares, Pauline Kruiver, Ger de Lange, Ane Wiersma, Piet Meijers, Mandy Korff, Jan Peeters, Jan Stafleu, Ronald Harting, Roula Dambrink, Freek Busschers, Jan Gunnink
5. Modifications of the Geological model for Site response at the Groningen field, Deltares, Pauline Kruiver, Ger de Lange, Ane Wiersma, Piet Meijers, Mandy Korff, Jan Peeters, Jan Stafleu, Ronald Harting, Roula Dambrink, Freek Busschers, Jan Gunnink
6. Assessment of dynamic properties for peat, Factual Report, Deltares, C. Zwanenburg and M. Konstantinou.

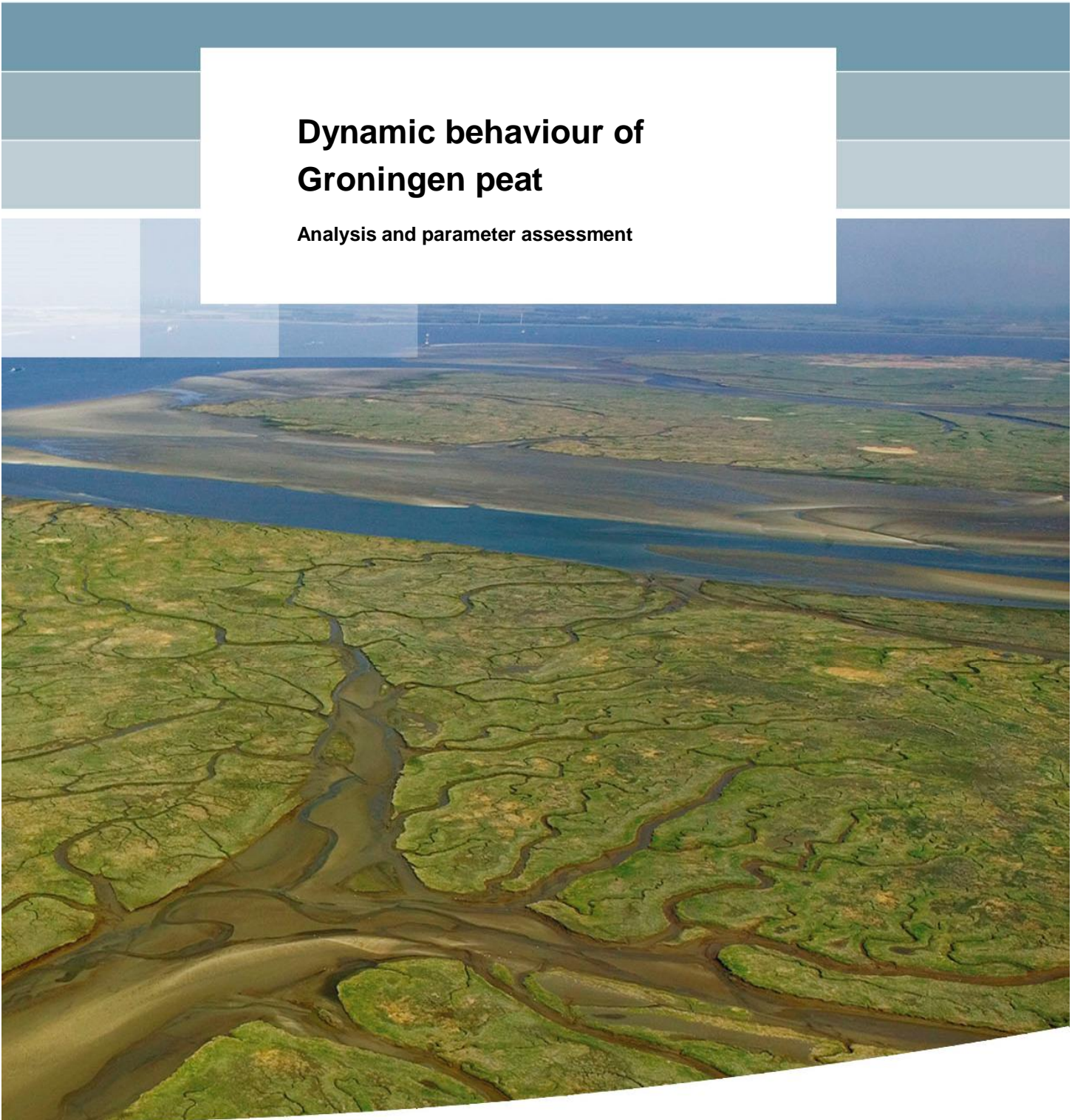


NAM

Title	Dynamic behaviour of Groningen peat Analysis and parameter assessment		Date	October 2017
			Initiator	NAM
Autor(s)	M. Konstantinou, dr.ir. C. Zwanenburg and dr.ir. P. Meijers	Editors	Jan van Elk and Dirk Doornhof	
Organisation	Deltares	Organisation	NAM	
Place in the Study and Data Acquisition Plan	<p><u>Study Theme:</u> Ground Motion prediction (local conditions)</p> <p><u>Comment:</u> The accelerations experienced at surface as a result of the earthquakes induced by the production of gas from the Groningen field is locally dependent on the shallow geological and soil conditions. This is called the site response effect. NAM has asked Deltares to build a detailed model of the shallow subsurface below Groningen. In preparing this model of the shallow subsurface below Groningen, Deltares has made use of the beta-version of the GEOTOP database of TNO Geologische Dienst Nederland (TNO-NITG) supplemented by more recent data. Additional data collected over the years in support of foundation design and other activities was sourced from Fugro and Wiertsema. These are mainly CPT measurements (cone penetrations tests). Additionally, data measured in the shallow geophone wells was used. For these calculations of the site response, soil parameters related to stiffness and damping (amongst others) are also necessary. For sand and clay these parameters are derived from well accepted correlations in the literature. However, the properties of locally present peat layers need to be measured in the laboratory. This report and the accompanying report present the measurements performed by Deltares on peat samples from Groningen, the analysis of the experimental data and the assessment of peat properties.</p>			
Directly linked research	(1) Ground Motion Prediction (2) Quaternary geology of the Groningen area			
Used data	Laboratory Experiments on local Peat Samples			
Associated organisation	Deltares			
Assurance	Internal Deltares			

Dynamic behaviour of Groningen peat

Analysis and parameter assessment



Dynamic behaviour of Groningen peat

Analysis and parameter assessment

M. Konstantinou
dr.ir. C. Zwanenburg
dr.ir. P. Meijers

1209862-011

Title
Dynamic behaviour of Groningen peat

Client	Project	Reference	Pages
NAM	1209862-011	1209862-011-GEO-0005- gbh	90

Keywords
Peat, dynamic parameters, interpretation, laboratory testing

Summary
In order to conduct a risk and hazard assessment for earthquakes in Groningen dynamic sub soil properties are needed. For clays and sands well established properties are available. However, for peats literature provides only limited information on the dynamic behaviour. Therefore a series of laboratory tests on peat samples from Groningen have been conducted.

In total 26 Resonant Column tests, 10 cyclic Direct Simple Shear tests, 20 static Direct Simple Shear tests and 20 k_0 -CRS tests, have been conducted at Ruhr Universität Bochum, Norwegian Geotechnical Institute and Deltares. Bender element measurements have been conducted on the specimens used for resonant column tests. For each tested sample the density, dry density, particle density, water content and loss on ignition is determined.

The results are reported in two reports. A companion report, referred to as *Factual report*, provides all the measurement data, working procedures and applied test conditions. This report discusses the analysis of the data and the actual parameter assessment.

References
Contract UI46802

Version	Date	Author	Initials	Review	Initials	Approval	Initials
1	March 2017	Dr. C. Zwanenburg		Dr. M. Korff		J. van Ruijven MSc	
		M. Konstantinou MSc					
		Dr. P. Meijers					
2	Nov. 2017	Dr. C. Zwanenburg		Dr. M. Korff		J. van Ruijven MSc	
		M. Konstantinou MSc					
		Dr. P. Meijers					

State
final

Contents

1	Introduction	1
1.1	Background	1
1.2	Research objectives	1
1.3	Research plan	1
1.4	Report set-up	1
2	General introduction to peat behaviour	3
3	Literature review dynamic behaviour of peat	8
3.1	Required parameters for site response calculations	8
3.2	Available published MRD curves	10
3.3	Shear modulus reduction curves	12
3.4	Damping curves	16
3.5	Effect of frequency	19
3.6	Effect organic content	21
3.7	Summary and conclusions on literature data for peats	22
4	Characterisation of the tested material	23
4.1	General material description	23
4.2	Subsoil stresses and yield stress	24
4.3	Classification parameters	27
4.3.1	General	27
4.3.2	Water content, densities and loss on ignition	27
4.3.3	Stress – strain curves	32
4.3.4	Undrained shear strength characteristics	35
4.3.5	Statistical analysis; background theory	37
4.3.6	Statistical analysis, differences in tested material for the different sample locations	39
4.3.7	Statistical analysis, differences between humified and non – moderate humified peat	40
4.3.8	Statistical analysis, differences in material tested by different laboratories	42
4.4	Small strain stiffness G_0	43
4.5	Summary and Conclusions	50
5	Construction of MRD-curves	52
5.1	Introduction	52
5.2	Shear modulus degradation curve	52
5.3	Trends in shear modulus reduction curve	55
5.3.1	Normalised graphs	55
5.3.2	Comparison with literature data	62
5.4	Damping curve	64
5.5	Trends in damping curve	68
6	Parameter Assessment	71

6.1	Introduction	71
6.2	Comparison of test data with existing MRD curves	71
6.3	Fitting measured data	75
6.3.1	Fitting shear modulus reduction curve	75
6.3.2	Fitting material damping	79
6.4	Derivation general curves for Groningen peat	81
6.4.1	Selected approach	81
6.4.2	Derivation general modulus reduction curve	82
6.4.3	Comparison with literature data	83
6.4.4	Damping curves	87
6.4.5	Summary recommended MRD curves for Groningen peat	89
7	Summary and conclusions	90
Appendices		
	References	1
	A Characterisation parameters for the tested material	A-1
	B Expressions for the MRD curves	B-1
B.1	Expressions Kishida	B-1
B.2	Expressions Darendeli for sand and clay	B-2
B.3	Adjusted Darendeli expression for peat	B-3
	C External review on draft report	C-1
	D External review on final report	D-1

1 Introduction

1.1 Background

In accordance to contract UI46802, 10 July 2014, Deltares is contributing to the risk and hazard assessment for earthquakes in the Groningen area. The risk assessment includes site response calculations to establish the amplification of the earthquakes in the shallow subsoil. For these calculations, soil parameters related to stiffness and damping (amongst others) are necessary. For sand and clay the parameters are derived from well accepted correlations in the literature. In Groningen, also peat layers are present. The dynamic properties of peat, needed for the calculations, have so far been derived by general, worldwide applicable correlations, but show a large uncertainty (Meijers, Rodriguez, 2017). To improve the site response analysis for peat layers, a field and laboratory study is conducted, of which the results are presented in two reports. A companion report (Zwanenburg & Konstantinou, 2016) provides an overview of all the test results and testing details. This report, the analysis report, provides an analysis of the data and the actual parameter assessment.

1.2 Research objectives

The objective of this study is to derive dynamic parameters for peat layer(s) present in the Groningen area. The required parameters consist of shear wave velocity, shear modulus reduction curve and damping curve.

1.3 Research plan

The research was conducted following these steps:

- At the start a literature survey was conducted to gather the (limited) available information on the dynamic parameters of peat. The literature review is given in chapter 2.
- Based on the results of the literature survey and the geology of the area locations were selected for soil sampling where peat samples were taken.
- The required parameters consist of shear wave velocity, shear modulus reduction curve and damping curve. Parameter assessment requires dynamic testing, bender element and resonant column testing. The dynamic testing is conducted by GEO-RUHR Bochum, Germany.
- A number of dynamic tests are conducted in duplo at the Norwegian Geotechnical Institute, NGI.
- Dynamic testing involves small strain testing. However information on larger strain is also needed. Therefore, static tests were conducted at Deltares. The results of the static tests are also used for classification and comparison to literature data.
- In discussion with NGI and RUB it was decided to add a series of dynamic Direct Simple Shear tests.
- Following the testing, the results were interpreted and the parameters of interest and uncertainties were assessed.

1.4 Report set-up

This report starts with an introduction to the project in chapter 1. Chapter 2 provides a general introduction to peat behaviour. Chapter 3 gives an overview of the available literature on dynamic behaviour of peats, followed by a discussion on the characteristics of the peat samples obtained in the Groningen area in chapter 4. Chapter 5 combines results of the different laboratory tests to the modulus reduction and damping curves, MRD-curves and

makes a first comparison to literature data. Chapter 6 provides a detailed analysis of the MRD-curves and makes a suggestion for the MRD curve to be used in the risk and hazard assessment for earthquakes in the Groningen area. Chapter 7 finalises with a summary and conclusions. This report has been reviewed externally. The review was conducted in two phases. First, the draft report was reviewed. Based on the reviewer's comments the draft report was finalised. Second, the final report was reviewed. Appendix C provides the review on the draft report. Appendix D provides the review on the final report.

2 General introduction to peat behaviour

Peat layers are generally developed by a successive deposition of organic material for which the rate of deposition exceeds the rate humification. An extended description of the development of peat deposits and the influence of the conditions during deposition on the mechanical behaviour of peat is given by Hobbs (1986). Due to the organic nature of peats, their mechanical behaviour is complex. The mechanical behaviour is characterised by low stresses, due to the low density, strong deformations when loaded, due to the low stiffness of the material, the strong susceptibility for creep and a fibre matrix, which influences the strength and stiffness of the material.

In geology, the botanical background is often used to classify different types of peat. It should be noted that for many types of peat the roots contribute mostly to the peat deposit. The presence of a fibre matrix is important in classifying organic material. Organic material, Gytja or Detritus might have a high organic content, however due to the lack of a fibre matrix it is usually classified as (highly) organic clay rather than peat.

Several researchers have worked on mechanical models that incorporate the influence of the fibre matrix (a.o. Landva, 2007, Cola & Cortellazzo, 2005 Hendry et al, 2012). Although these models provide valuable insight how the presence of fibres influences mechanical behaviour, the models are not generally used in engineering practice. These models assume a dominating fibre direction, usually horizontal and use the strength and stiffness of the fibres as input parameter, which are usually not known.

More recent publications on peat behaviour include images of the studied material (a.o. Mesri & Ajlouni 2007, Hendry et al. 2012). Figure 2.1 shows the results of a MRI scan on a peat sample that has been compressed in an oedometer test. It should be noted that longest side, 63 mm, was originally, before sampling, orientated in the horizontal direction. The shortest side was originally orientated in the vertical direction. The sample contains mainly *Phragmites* (Reed) with *Carex* (Sedge) inclusions. This is a type of peat that is generally available in The Netherlands, also in the Groningen area. The sample shown in Figure 2.1 was retrieved at Uitdam, approximately 15 km north of Amsterdam.

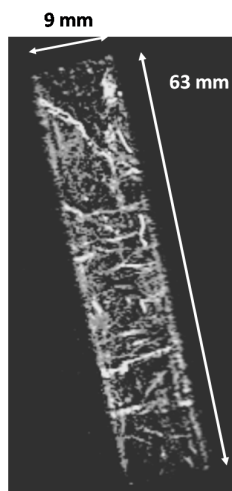


Figure 2.1 MRI scan of a peat sample after compression in oedometer test, Longest side was originally horizontal. The sample comprises *Phragmites* (Reed) with *Carex* (Sedge) inclusions

The white parts shown by Figure 2.1 represent the organic material, the dark parts represent the pore volume. The fibres are clearly visible and do not seem to have a uniform fibre direction. Some of the large fibres seem to have a vertical orientation, along the shortest direction of the sample. While small fibres seem to have a more horizontal orientation. The complex fibre pattern makes it complicated to use models based on a general fibre orientation.

Figure 2.1 also shows that some of the large fibres have a length in the same order of magnitude as the sample dimensions. Therefore it is to be expected that size effects play a role in laboratory tests on peat. Zwanenburg & Van (2015) show size effects in triaxial tests on peat. Conventional sized samples, diameter of 66 mm height of 130 mm, show strong deformation in triaxial testing, with a continuing increase in mobilised shear strength. No clear peak strength is found. Large sized samples, diameter of 400 mm and height of 800 mm, however, do show a clear peak strength and develop a failure plane. This is explained by the sliding or rupture of the fibres which is dominated by the actual displacements of fibres rather than applied strain. So, although the applied strains are the same for conventional sized and large sized samples the displacements are different leading to failure of the matrix in the large sized samples. It should be noted that the deformation characteristics up to failure are comparable. Therefore, conventional sized samples are considered relevant for determination of stiffness parameters.

It is to be expected that different botanical background might lead to different fibres and therefore to differences in peat behaviour. So far, to the author's knowledge, no successful correlation between engineering properties and botanical background of peat is established.

Strongly humified material no longer contains a clear matrix. den Haan & Kruse (2007) show differences in behaviour of strongly humified and non humified material. The non humified material shows anisotropy in shrinkage upon drying which the humified material does not show. This is explained by the presence of fibres in the non humified material. The problem in relating engineering properties to a degree in humification is the lack of a clear method for assessment of the humification degree. The degree humification is usually established visually by the van Post classification (von Post, 1922) or related, simplified, methods. The outcome of the von Post classification strongly depends on the experience of the person who makes the classification. This hampers the establishment of clear correlation between degree of humification and engineering properties. In this study it is chosen to classify the peat in two classes. First strongly humified for which the organic background of the material can no longer be recognised. Second the non to moderate humified material in which the individual organic components can be recognised. In the relation to the von Post classification, the category non to moderate humified material represents the classes H1 – H7. The humified material represents the classes H8 to H10.

As explained above the botanical background does not provide a useful frame work for correlation with engineering properties. In literature, especially in the earlier papers the botanical background is often not given. Instead, engineering properties of peats are related to mechanical properties like water content, organic content, dry, bulk or particle density. Also in this study the mechanical properties are used for correlation purposes and not too much effort is put in a detailed botanical description of the tested material.

The water content is defined by:

$$w = \frac{M_w}{M_s} \times 100\% \quad (2.1)$$

in which:

M_w = mass of pore water

M_s = mass of solid material

For peats the water mass easily exceeds the solid mass. For peats in The Netherlands, w can reach values up to beyond 1000%, Zwanenburg & Jardine (2015). The higher values, above 800%, are found for non-compressed, fresh, peats. The lower values, 200 – 400 %, are found for strongly compressed and / or strongly humified peats.

The organic content, OC , can be found from the loss on ignition, LOI . The loss on ignition is defined as the percentage of material mass lost when heating for 4 hours at 550 °C:

$$LOI = \frac{m_s - m_1}{m_s} (\times 100\%) \quad (2.2)$$

In which:

m_s = the solid mass, the remaining mass after heating the sample at 105°C for 24 h

m_1 = the remaining mass after heating the sample at 550 °C for 4 hours

When heating the sample to 550 °C not only organic, but also some inorganic, material will be lost. Skempton & Petley (1970) estimate this loss to give a 4% error providing the following relation between LOI and OC :

$$OC = 100 - 1.04(100 - LOI) \quad (2.3)$$

In which both, OC and LOI , are given as a percentage. This report provides the LOI for the individual tested samples since the LOI is directly measured. Only for comparing to literature data the OC is determined using equation(2.3).

To illustrate the applicability of the use of mechanical properties in correlating engineering properties three examples are given by Figure 2.2 to Figure 2.4. The figures originate from den Haan & Kruse (2007), which give an overview of Dutch experience in soft soils. Besides illustrating the applicability of correlations, the Figures also show three typical characteristics of peats.

Figure 2.2 shows the correlation of virgin compression index, b (den Haan, 1999), as a function of density for range of materials. Large density, $\rho = 1.7 \text{ t/m}^3$ represents stiff clays and silts. Low density, $\rho = 1.0 \text{ t/m}^3$, represents peats. Although it might be expected that presence of a fibre matrix influences the stiffness behaviour, the influence of a matrix is not found in the data. The Figure shows a gradual transition from the stiff, high density, materials which do not have a fibre matrix, to the soft, low density, materials that do have a fibre matrix. This might explain the successful application of settlement theories that have been developed for clay behaviour, to calculate the compressibility of organic soils (Molendijk & Dykstra, 2003).

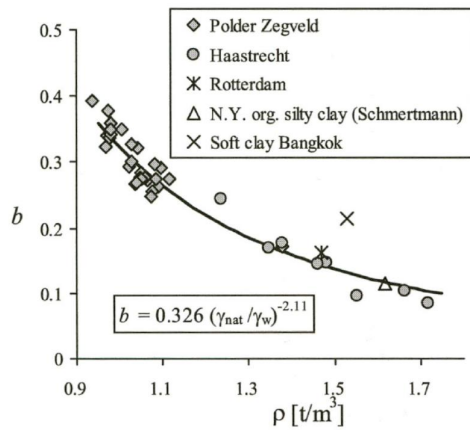


Figure 2.2 Correlation between density and virgin compression index b , from den Haan & Kruse (2007)

Figure 2.3 shows the correlation between density and earth pressure coefficient at rest, K_0 , for a range of materials. For low densities, $\rho = 1.0 \text{ t/m}^3$, which represents peat, low values for K_0 are found. A low K_0 value might indicate a large friction angle. Assuming that Jacky's formula, equation (2.4) is also applicable for peats, as indicated by Mesri & Hayat(1993), $K_0 = 0.2$ would yield $\varphi' = 53^\circ$.

$$K_0 = 1 - \sin(\varphi') \tag{2.4}$$

Evidence of these high φ' values is found in triaxial testing (a.o. Yamaguchi et al, 1985, Zwanenburg et al 2012, landva, 2007, Mesri & Ajlouni, 2007).

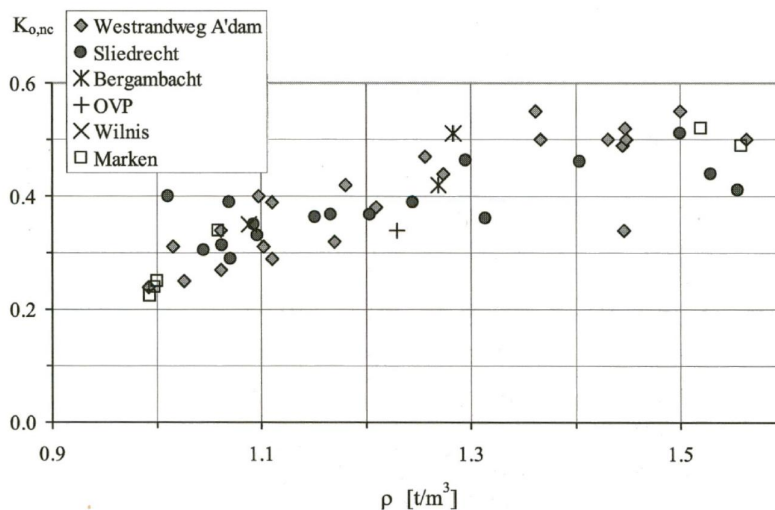


Figure 2.3 Correlation between density and earth pressure coefficient K_0 , from: den Haan & Kruse (2007)

Figure 2.4 shows the correlation between the density and the shear stress ratio of s_u / σ'_{vy} , in which s_u represents the undrained shear strength and σ'_{vy} the vertical yield stress. For low densities, $\rho = 1.0 \text{ t/m}^3$, which represents peat, a relatively high value is found. This corresponds to the increase in s_u – ratio for increasing organic content given by a.o. Wood (1990), Mesri & Ajlouni (2007).

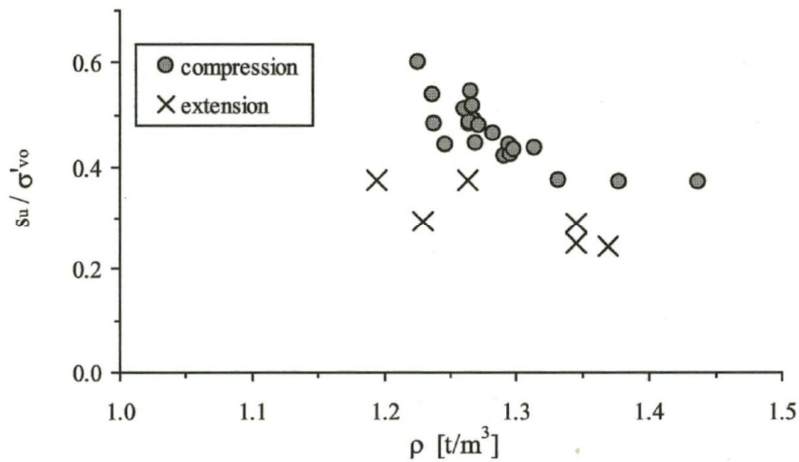


Figure 2.4 Correlation between density and shear stress ratio, from den Haan & Kruse (2007)

The high values for φ' and s_u -ratio do not comply to the general experience of peat as a soft, not strong, material. Regarding the strength of peats it should be noted that:

- 1 A relatively large deformation is needed to mobilise the maximum shear strength
- 2 Due to the low density of peat, the stresses, especially for superficial deposits remain small. Therefore, despite the relatively high φ' and s_u -ratio values, the maximum mobilised shear strength remains small.

3 Literature review dynamic behaviour of peat

3.1 Required parameters for site response calculations

For site response calculations the following parameters are necessary: shear wave velocity, shear modulus reduction curve and damping curve. The last are also known as MRD (Modulus Reduction and Damping) curves. These curves give the value of the shear modulus and the damping as function of the shear strain amplitude. With increasing shear strain amplitude the shear modulus decreases and the damping increases, as sketched in Figure 3.1.

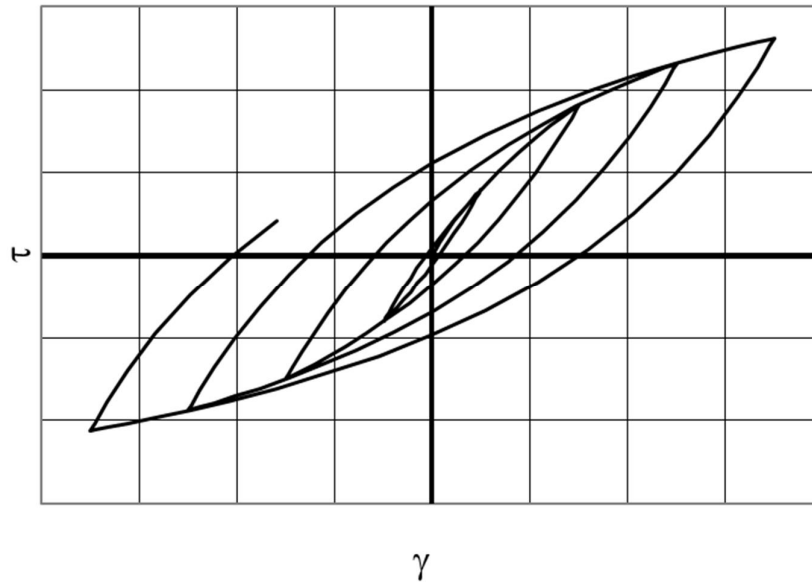


Figure 3.1 Illustration non-linear stress-strain behaviour at cyclic loading, showing decreasing shear modulus $G = \tau/\gamma$ at increasing shear strain amplitude. τ represents the shear stress, γ represents the shear strain

Hardin and Drnevich (1972) developed a model for the modulus reduction curve of a soil by assuming a hyperbolic stress-strain relation. Researchers at the University of Texas modified the basic hyperbolic model to develop modulus reduction curves for sands, gravels and clays (Darendeli 2001, Menq 2003). The model for peat used in this report is based on the modified hyperbolic model. The shear modulus reduction curve is given by:

$$\frac{G}{G_{max}} = \frac{1}{1 + \left(\frac{\gamma}{\gamma_{ref}} \right)^a} \quad (3.1)$$

with:

G = shear modulus at shear strain amplitude γ

G_{max} = small strain shear modulus

γ = shear strain amplitude

γ_{ref} = reference shear strain amplitude

With the given equation the reference shear strain amplitude is the shear strain amplitude at which $G/G_{max} = 0.5$.

The damping is a measure of the dissipated energy per cycle. The parameter D is defined as

$$D = \frac{W_{dis}}{4\pi W_{el}} \quad (3.2)$$

with:

D = damping

W_{dis} = dissipated energy per cycle

W_{el} = elastic energy $E_{el} = 0.5 \cdot \tau_{max} \cdot \gamma_{max}$

τ_{max} = amplitude shear stress

γ_{max} = amplitude shear strain

The dissipated energy per unit volume is given by the area within the hysteresis loop:

$$W_{dis} = \int \sigma d\varepsilon^p \quad (3.3)$$

with:

W_{dis} = dissipated energy

σ = applied stress

$d\varepsilon^p$ = plastic strain increment

For a DSS test, with τ representing shear stress and γ shear strain, the energy dissipation per cycle is given by, see Figure 3.2:

$$W_{dis} = \int \tau d\gamma = \int \tau(t) \dot{\gamma}(t) dt \quad (3.4)$$

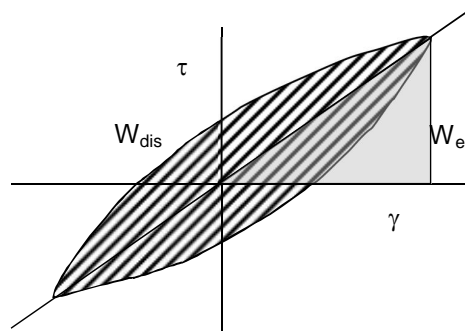


Figure 3.2 Illustration stress-strain behaviour during cyclic loading, the grey area is the elastic energy, the area with inclined lines is the dissipated energy per cycle

In resonant column testing the damping can be found by comparing the amplitude for the first cycle, after actively vibrating the sample is stopped to the amplitude of n^{th} cycle, in which $n < 10$, see ASTM D4015-15. In deriving the damping from resonant column testing, correction of the damping by the system is important. The formulae's to be applied are given in ASTM D4015-15

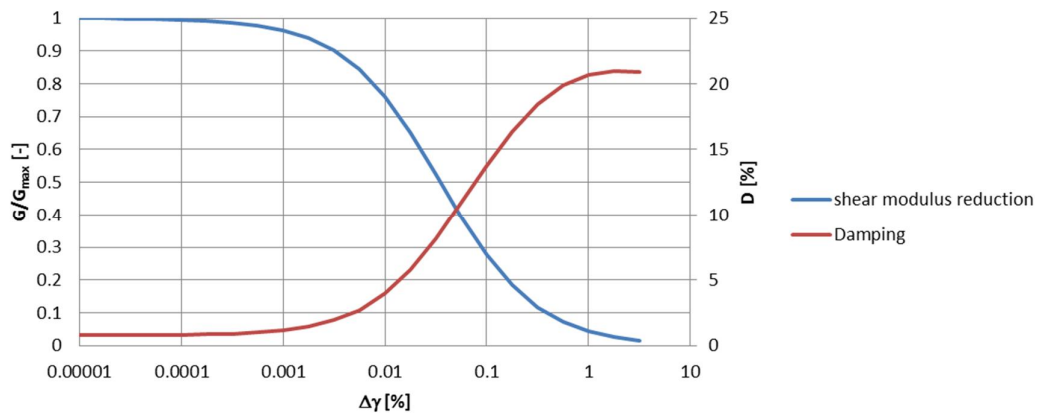


Figure 3.3 Illustration of typical MRD curve

Figure 3.3 sketches how general MRD curves look like. Initially, at small strain increments, a relatively large shear modulus and low damping is found. When strain increments increase, shear modulus decreases at increasing damping.

It should be noted that there is a strong correlation between the shear modulus reduction and the damping curve. A small shear modulus reduction (G/G_{max} close to 1) implies a nearly linear-elastic behaviour and hence hardly energy dissipation. At the other extreme a large shear modulus reduction (small value of G/G_{max}) implies a large non-linear effect and hence a large energy dissipation per cycle.

Several authors have published published measured MRD curves. An overview of published tests results for peat is given in section 3.2. Also correlations for determining the curves have been published. The most widely used are those by Darendeli (2001) for sand and clay and by Menq (2003) for sand. For peat Kishida et al (2009) has published a set of equations for assessing the MRD curves.

3.2 Available published MRD curves

With a literature review as much as possible data on the measured shear modulus reduction and damping curves for peats are collected. The results are summarised in Table 3.1. For each of the peat types, the consolidation stress (related to depth), the organic and ash content and the density are reported if given. These factors are necessary to compare the peats from literature with the Groningen peats.

Source	Location	σ_c [kPa]	Organic content ¹⁾	Ash content ¹⁾	Density ²⁾	Used test device ³⁾	Remark
Seed 1970	Union Bay [USA]	Unknown	unknown	unknown	1.003 – 1.058 ton/m ³	'repeated loading test', no further description given	a
Kramer 1996/2000	Mercer Slough [USA]	1,5		19.7 – 27.4%	1.0 – 1.04 ton/m ³	RC and CTX	
		12,5		19.7 –			

Source	Location	σ_c [kPa]	Organic content ¹⁾	Ash content ¹⁾	Density ²⁾	Used test device ³⁾	Remark
		19		27.4% 19.7 – 27.4%			
Stokoe & Santamarina 2000	Queensboro bridge [USA]	114		37-65%		RC and torsional shear	b
Boulanger et al. 1997	Sherman Island [USA]	132/200		36-65%	11.1 – 11.8 ton/m ³	CTX, special device for a wide range of strains	
Wehling et al. 2001	Sherman Island [USA]	78		48-68%	1.06 – 1.23 ton/m ³	CTX, designed for shear strain amplitude between 5E-4 and 10%	
		45					
		12					
Kishida et al. 2009	Montezuma Slough [USA]	17	42%		1.06 – 1.33 ton/m ³	CTX	
		35	44%				
		51	23%				
		67	15%				
Kishida et al. 2009	Clifton Court [USA]	55 - 69	14-35%		1.19-1.46 ton/m ³	RC and CTX	
Zwanenburg 2005	Breukelen [NL]	10 30/55		44.7%	1.04 ton/m ³	DSS	c
Tokimatsu-Sekiguchi 2006	Ojiya P-1 [Japan]					Cyclic torsional shear	
	Ojiya P-2						
Kallioglou et al 2009	Greece	370/400	48-62%		13/14 kN/m ³	RC, to a shear strain amplitude of 0.3%	d

Table 3.1 Summary available data on peat, σ_c = consolidation stress

- 1) Either the organic content or the ash content is reported in this table, depending on the parameter used in the original publication
- 2) Either the mass or the density is reported in this table, depending on the parameter used in the original publication
- 3) RC: Reasonant column; CTX: Cyclic Triaxial test; DSS: Direct Simple shear

Remarks:

- a) Damping curve not measured, data on PI, water content etc. are taken from (Kramer 1996)
- b) data taken form (Kramer 2000) and (Boulanger et al 1997)
- c) damping curve not measured
- d) Peat from two locations in Greece, sampling depth 35 m 85 m

The available test data are from a limited number of locations, mainly from the west coast of the USA. Only a few publication for locations in Europe and Asia are available. Figure 3.4 shows the geographic distribution of the locations. Stress levels vary from very low (1.5 kPa) to quite high (400 kPa).

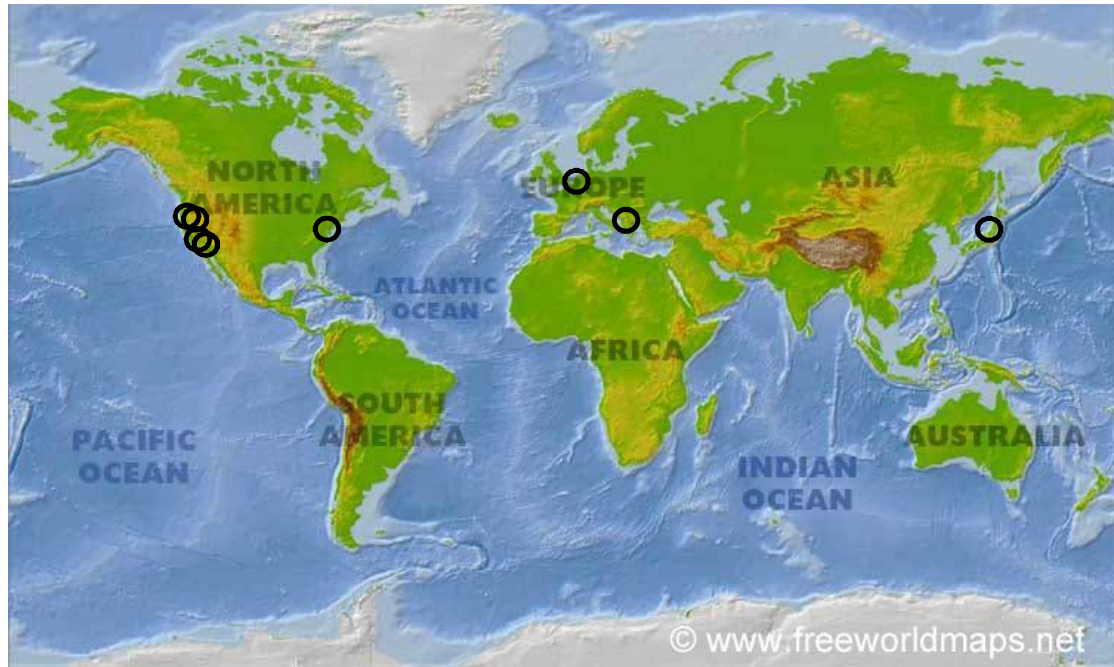


Figure 3.4 Approximate location available peat data, map from: <http://www.freeworldmaps.net/physical.html>

3.3 Shear modulus reduction curves

This section investigates the influence of the organic content, *OC* and the consolidation stress on the MRD curves. One might expect that the type of peat indicated by the botanical background and / or degree of humification might also play a role. However, in the published data the type of peat is rarely described and is therefore not considered in analysing the literature data.

Figure 3.5 shows a summary plot of all collected shear modulus reduction curves from literature (Table 3.1). In Figure 3.6 to Figure 3.8 a subdivision is made between three different ranges of the consolidation stress. The used ranges are: $\sigma' < 17$ kPa (Figure 3.6), 17 kPa $< \sigma' < 51$ kPa (Figure 3.7) and $\sigma' > 51$ kPa (Figure 3.8). These boundaries are selected based on the available set of curves. They do not imply or suggest an expected change in peat behaviour for the three considered ranges of consolidation stresses.

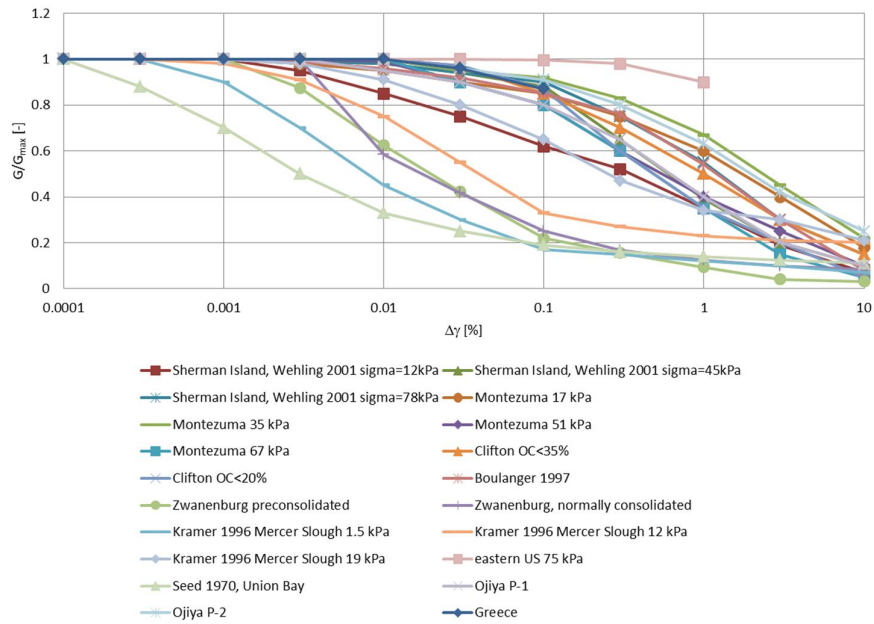


Figure 3.5 Summary all available shear modulus reduction curves

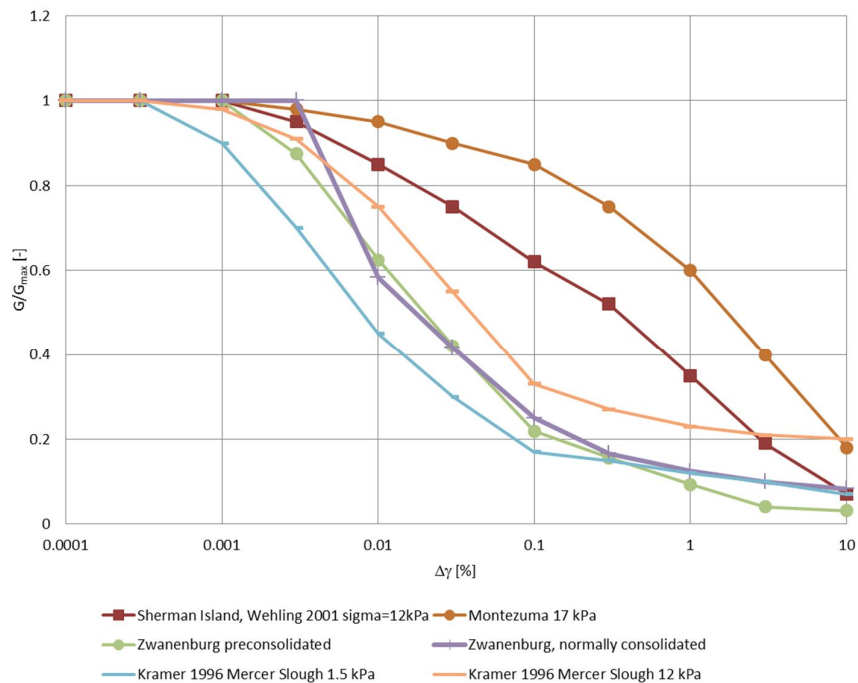


Figure 3.6 Summary available shear modulus reduction curves, low consolidation stress (< 17 kPa)

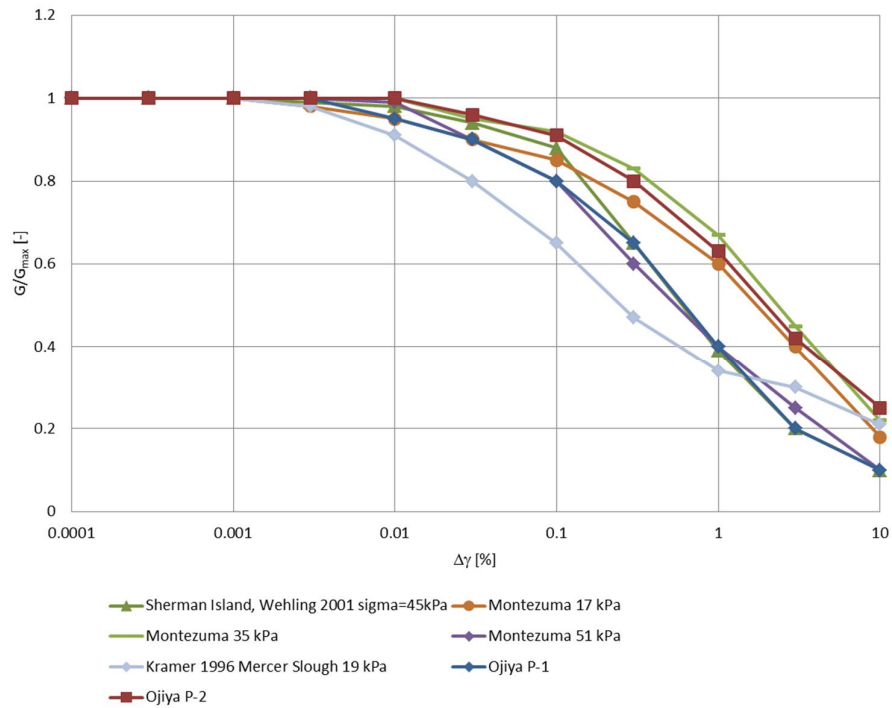


Figure 3.7 Summary available shear modulus reduction curves, medium consolidation stress (between 17 kPa and 51 kPa)'

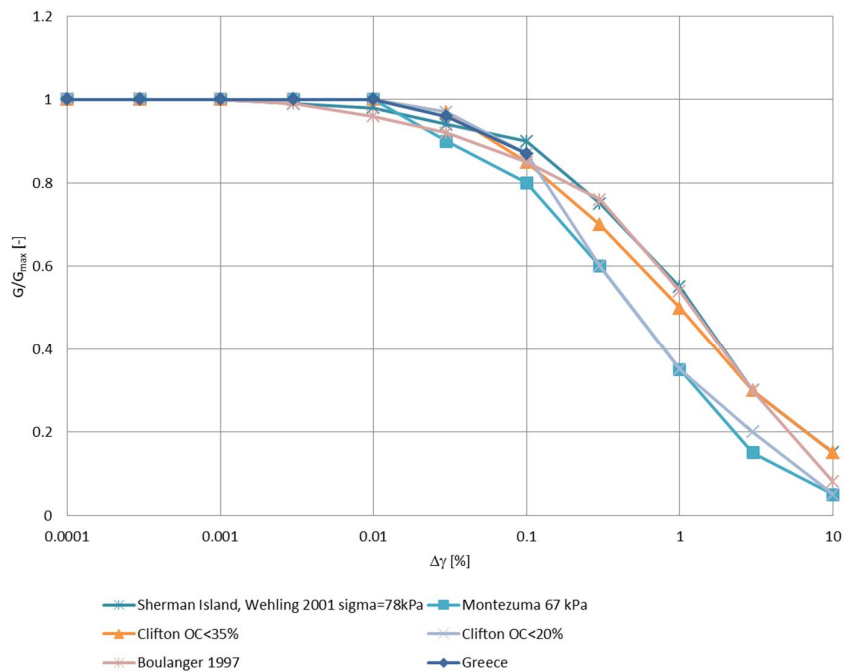


Figure 3.8 Summary available shear modulus reduction curves, high consolidation stress (> 51 kPa)

In general, there is a relation between the position of the curve in the $G/G_{max} - \Delta\gamma$ space and the consolidation stress. With increasing stress level the peat behaves linear-elastic (no shear modulus reduction) over a larger strain amplitude range. Some exceptions are:

- Montezuma 17 kPa: The curve shows much higher values for G/G_{max} relative to the other curves from literature for the low consolidation stress range. The form of the Montezuma 17 kPa curve resembles the other curves at a consolidation stress of 40 kPa.
- Queensboro bridge: This curve lies above all other curves encountered for a consolidation stress of 100 kPa and above.

Additionally, some curves in the $\sigma' > 50$ kPa range (Figure 3.8) fall within the range of the curves for $15 < \sigma' < 50$ kPa (Figure 3.7).

A measure for the position of the shear modulus reduction curve is the shear strain amplitude at which $G/G_{max} = 0.5$. This shear strain amplitude is often referred to as the reference strain γ_r . Figure 3.9 shows this reference shear strain as function of the stress level. The points for Mercer Slough are marked in green as they have a high organic content, close to the values obtained for the tested Groningen peat. The horizontal axis gives the vertical effective stress, however all tests are conducted on isotropically consolidated samples. Although a wide scatter is present the general trend is an increase of this reference shear strain with stress level.

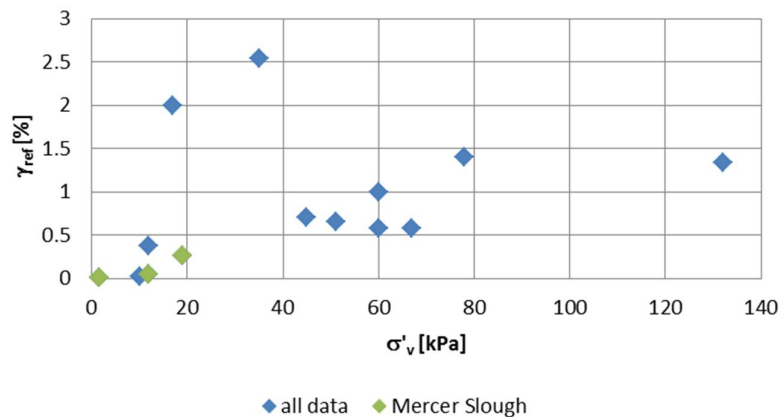


Figure 3.9 Reference shear strain γ_r as function of the stress level

The organic content is also expected to influence the reference shear strain. This is shown in Figure 3.10 for four stress ranges.

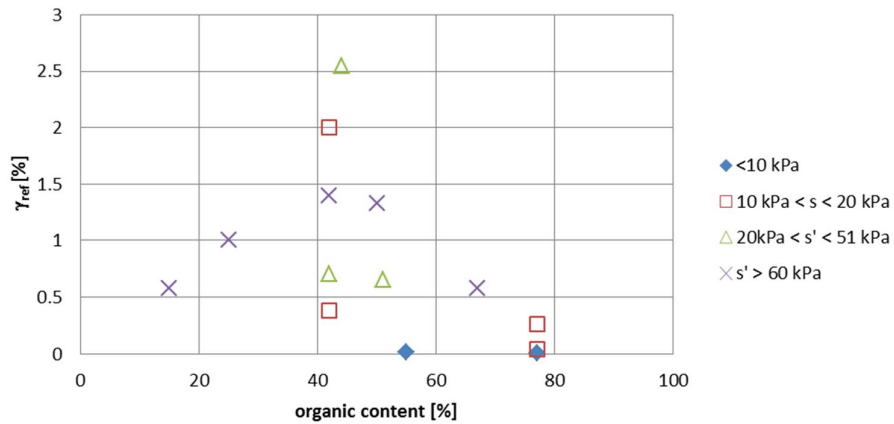


Figure 3.10 Reference shear strain γ_r as function of the organic content

No clear relation between the reference shear strain and the organic content is visible, even including the effect of the stress level does not improve the relation.

3.4 Damping curves

Figure 3.11 shows all damping curves available for peat from literature (Table 3.1). Again, the curves are plotted for three consolidation stress ranges to get a better view. Figure 3.12 gives the data for $\sigma' < 17$ kPa, Figure 3.13 for $17 \text{ kPa} < \sigma' < 51$ kPa and Figure 3.14 for $\sigma' > 51$ kPa.

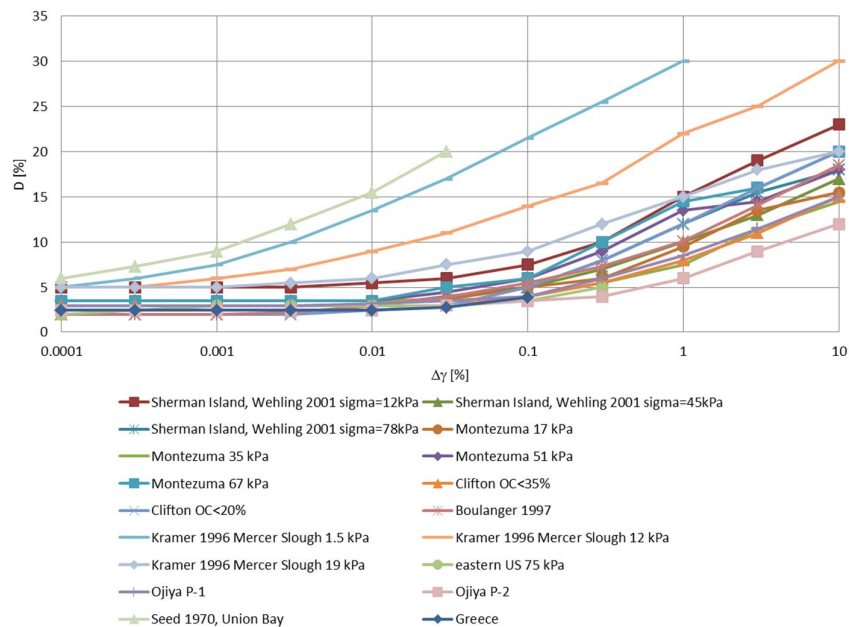


Figure 3.11 Summary all available damping curves

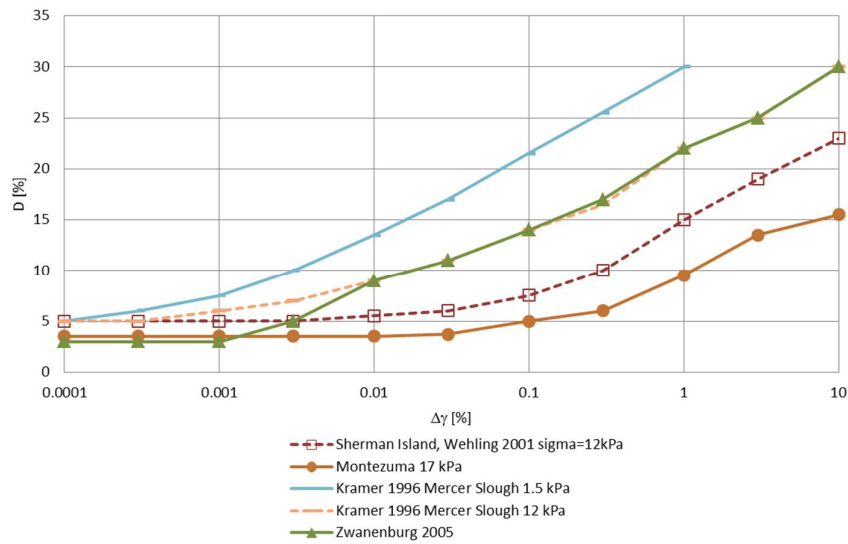


Figure 3.12 Summary available damping curves, low consolidation stress ($\sigma' < 17$ kPa)

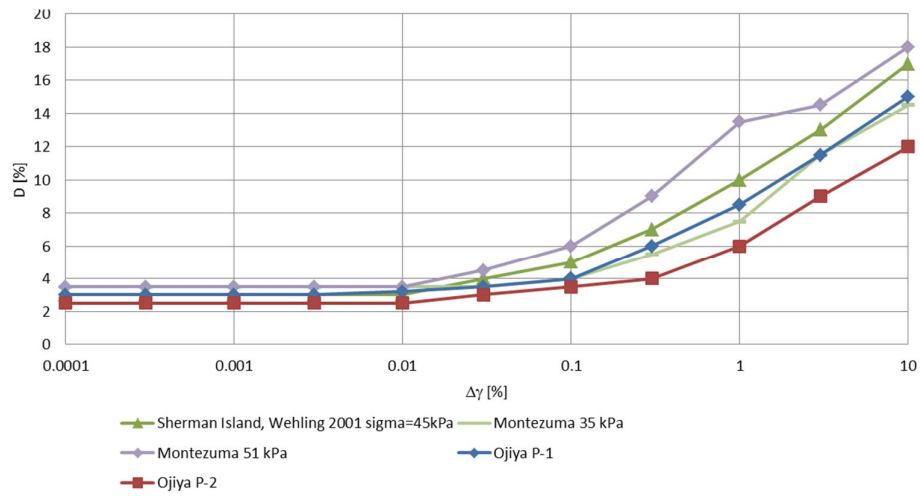


Figure 3.13 Summary available damping curves, medium consolidation stress (between 17 kPa and 51 kPa)

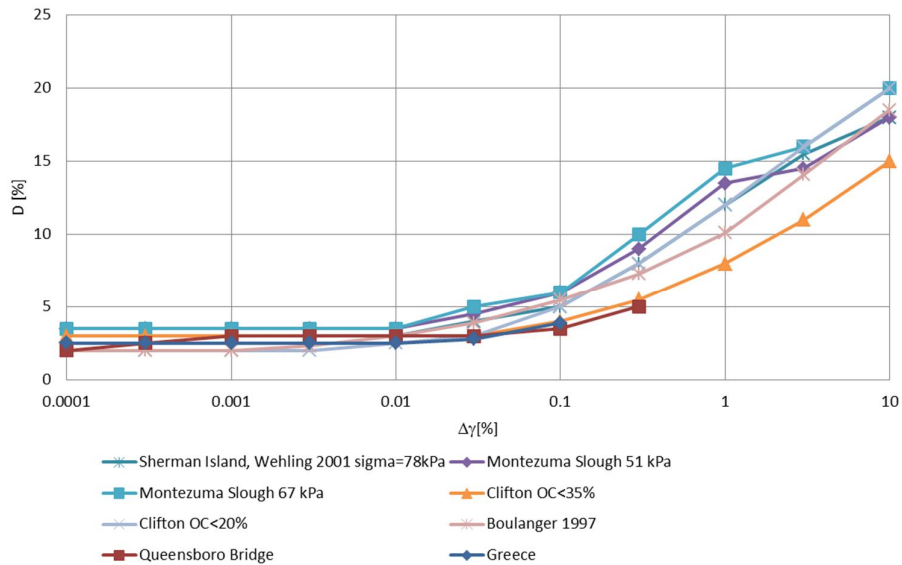


Figure 3.14 Summary available damping curves, high consolidation stress (> 51 kPa)

The curves show large variation for the lower stress levels, and much less variation for higher stress levels.

One of the parameters determining the damping is the damping at small shear strain amplitudes D_{min} . Figure 3.15 shows the value of D_{min} , as obtained from the published test data. This parameter is found to increase with decreasing consolidation stress.

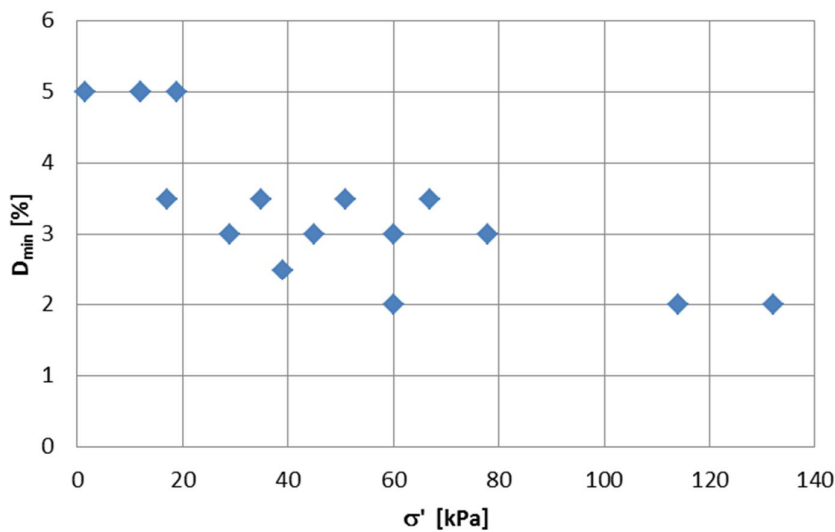


Figure 3.15 Value of D_{min} from published test data

3.5 Effect of frequency

Boulangier et al (1997, 1998) performed tests at 0.01 Hz and 1 Hz, see Figure 3.16. This figure shows that increasing the loading frequency from 0.01 Hz to 1 Hz results in an increase in the secant shear modulus with about 25%, irrespective of the shear strain amplitude. This corresponds to an increase in the stiffness with about 10-15% per each 10-fold increase in loading frequency. As this is the case for the three shear strain amplitudes shown it may be expected that the influence on the shear modulus reduction curve G/G_{max} will be negligible.

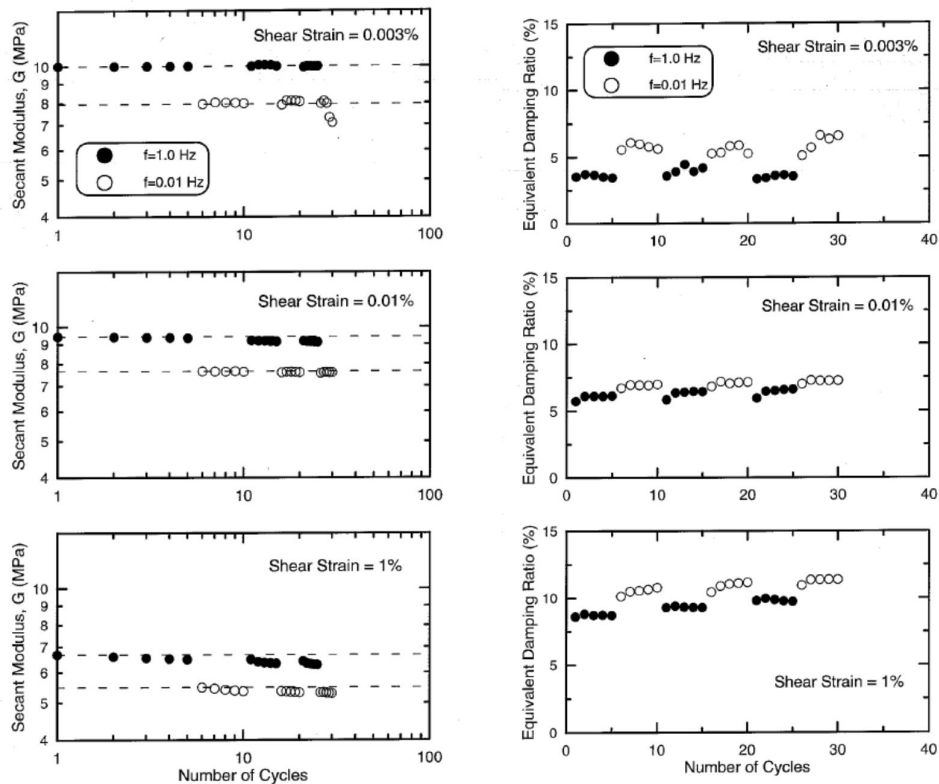


Figure 3.16 Test data from Boulangier et al (1997, 1998)

In Figure 3.16 the damping decreases with increasing frequency. This is in line with the general observation in that stiffness and damping are somehow correlated. As a consequence the damping derived from tests at 0.1 Hz may slightly overestimate the actual damping during an earthquake.

Kramer (2000) used a larger variation of frequencies, varying it between 0.0006 Hz and 10 Hz. Main results are shown in Figure 3.17.

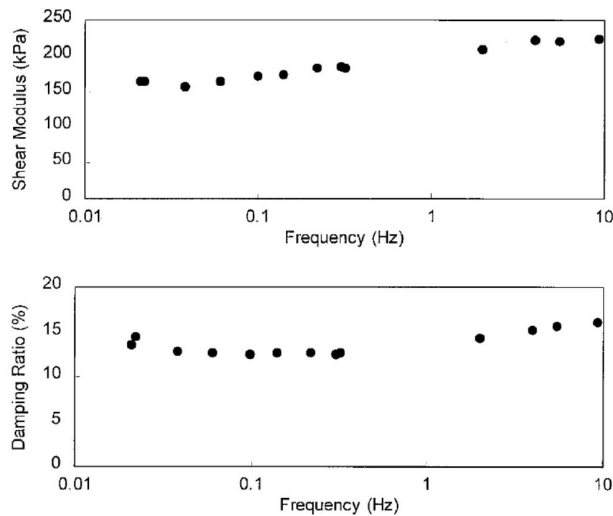


Figure 3.17 Effect of loading frequency on shear modulus and damping

Kramer (2000) does not mention the used shear strain modulus for drafting Figure 3.17. The original text by Kramer suggests that it is for higher shear strain amplitude. In Figure 3.18 the results are normalised by the shear modulus found at 0.1 Hz. This figure shows that the shear modulus at 1 Hz loading frequency is about 20% in excess of the value at 0.1 Hz. Unfortunately the published test data by Kramer do not allow to check the influence of the frequency on the G/G_{max} curve.

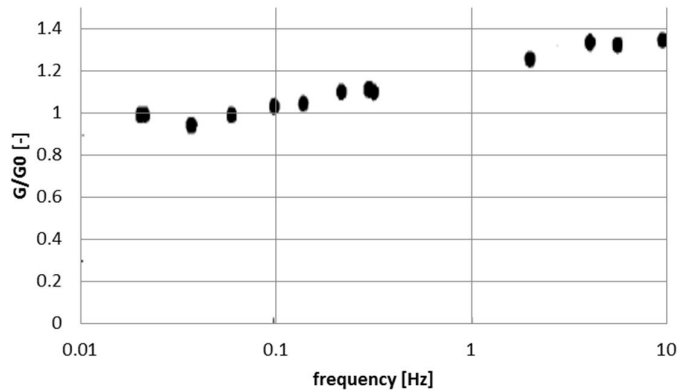


Figure 3.18 Normalised data from (Kramer 2000)

Figure 3.19 shows the damping as function of the frequency. This graph shows that for $0.05 \text{ Hz} < f < 1 \text{ Hz}$ the damping is independent of the frequency, for higher frequencies the damping tends to increase with frequency.

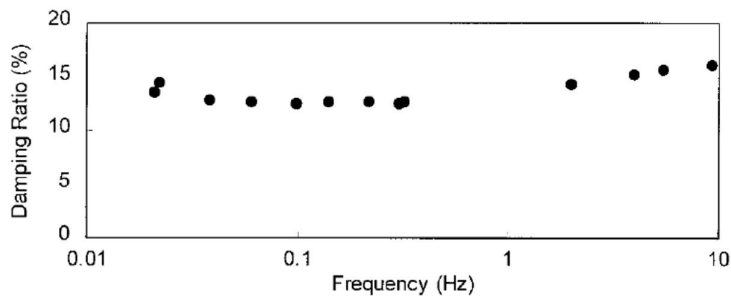


Figure 3.19 Damping as function of the frequency, from (Kramer 2000)

3.6 Effect organic content

Kishida et al (2009) looked into the effect of the organic content when deriving his equations. Figure 3.20 and Figure 3.21 shows the effect of the organic content on the MRD curves. It should be realised that these plots are prepared using the derived MRD equations and are not showing actually measured curves.

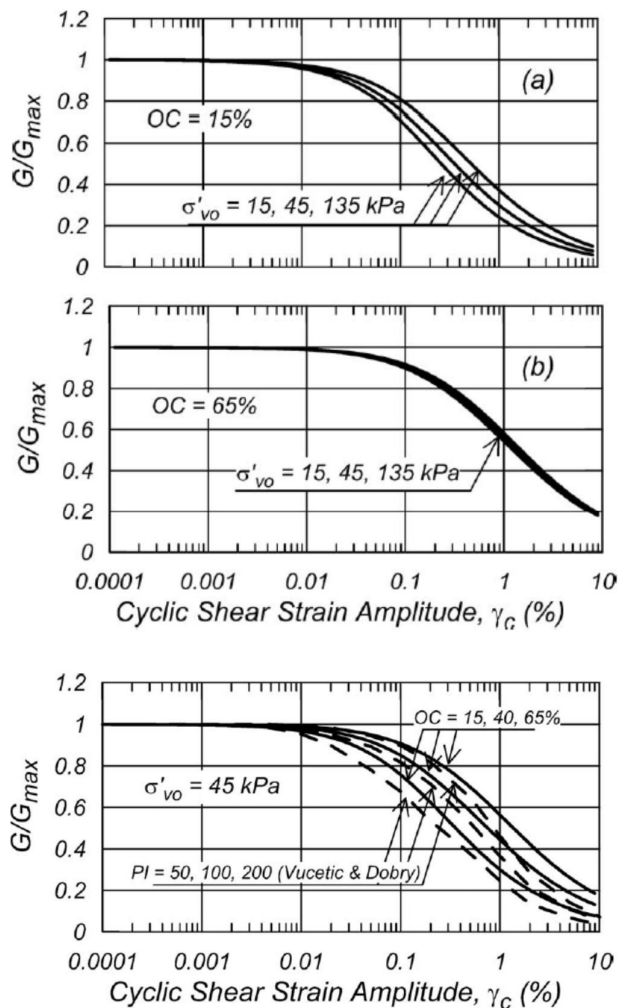


Figure 3.20 Effect of organic content on the shear modulus reduction curve, from (Kishida et al 2009)

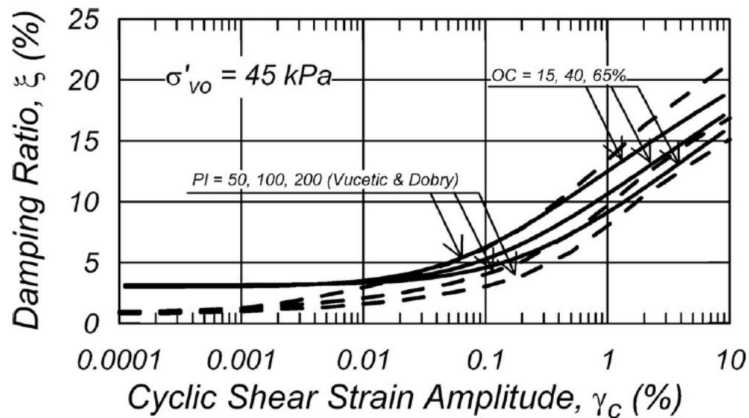


Figure 3.21 Effect of organic content on the damping curve, from (Kishida et al 2009)

According to the interpretation of Kishida et al (2009) there is an influence of the organic content on the MRD curve. Increasing the organic content increases the value of G/G_{max} and decreases the damping. The tested range of organic content however is from 15% to 65 %, which is lower than the organic content of the tested Groningen peat.

3.7 Summary and conclusions on literature data for peats

The number of published test data on peat is limited. Most published test data are from sites at the west coast of the USA. The organic content of the tested samples is in general around 50%. This is below the organic content of the tested Groningen peat with an organic content in the range of 80 – 90%. Only the peat from Mercer Slough, an organic content of 77%, has an organic content comparable to this value.

A general trend is that the shear modulus reduction curve shifts to the right with increasing stress level. Figure 3.20 shows that this effect is stronger for materials with a low organic content. For large organic content the effect of consolidation stress seems small.

Figure 3.20 shows that organic content influences the shear modulus degradation curve. For increasing organic content, the G/G_{max} curve tends to shift to the right. This effect however is not clearly shown in Figure 3.10.

The frequency of loading has some influence on the measured shear modulus. The limited available data suggest that the shear modulus increases with 10 % to 20% at a 10-fold increase in frequency. The effect on the shear modulus reduction curves seems to be limited. The effect on the damping is not clear but seems to be limited as well.

From the literature review it is concluded that organic content and (pre) consolidation stress are the dominating factors in determining the shear modulus reduction curve and damping curve. The tested samples should include a relevant range of organic content and (pre) consolidation stress found in the Groningen peat deposit. The laboratory tests conducted in the research presented in this report contain resonant column tests and cyclic Direct Simple Shear tests. In these different types of testing different frequencies are applied. In this report the cyclic simple shear data are corrected, using Figure 3.18. This is further discussed in section 6.3.1.

4 Characterisation of the tested material

4.1 General material description

As explained in section 1.1 the study focusses on the peat deposits in the Groningen area. Two deposits can be found in the area. This study focusses on the superficial peat deposits geologically classified as the Nieuwkoop formation. The basal peat layer has a limited thickness in this area. It is expected that the thicker Nieuwkoop peat has a larger impact on the site response calculations than the basal peat, which can also, because of its thickness, not be properly sampled and tested. Due to the heterogeneity of peats, the Nieuwkoop formation contains a variety of peat types with different characteristics. To emphasize that only peat samples from the area of interest has been tested, this report refers to the tested material as Groningen peat.

In the factual report (Zwanenburg & Konstantinou, 2016) the selection and selection criteria for the sample location are discussed. Samples were taken from three locations, see Figure 4.1:

- Nieuwolda.
- Siddeburen.
- Schildmeer.



Figure 4.1 Sample locations

In summary, locations were selected which show a difference in stress conditions and degree of humification. As explained in chapter 2 the degree in humification is difficult to establish. Therefore samples were classified as either non to moderate humified or strongly humified. It should be noted that the strongly humified peat layers are thin compared to the specimen dimensions needed for testing. Therefore, fewer samples of strongly humified peat compared to non to moderate humified peat are available.

The non to moderate humified peat found at the three locations mainly comprises *Phragmites* (Reet) and *Carex* (Sedge). At the Nieuwolda site inclusions of *Sphagnum* (Sphagnum) and *Eriophorum* (Cotton grass) were found. At the Schildmeer site a few *Eriophorum* (Cotton grass) inclusions were observed. It should be noted that a botanical description of the strongly humified material cannot be given.

For the different sites the following remarks are given:

Nieuwolda:

At the Nieuwolda site, the subsoil consists of a 2 – 3 m thick clay deposit followed by a 3-4 m thick layer of organic material. This organic layer consists of peat with some Gyttja layers. Just like peat, Gyttja consists mainly of organic material; however, it lacks the fibrous structure usually found in peats. Therefore, Gyttja is often described as strongly organic clay. In many engineering applications Gyttja has the same or equivalent behaviour as peat. In the conducted laboratory tests only peat samples, no Gyttja, have been tested.

The peat layer includes some strongly humified layers. These layers were relatively thin and therefore hard to sample.

Schildmeer:

At this location a top clay layer of approximately 1 m is present on top of the peat deposit. Locally the peat deposit has a thickness of 2 – 2.5 m. The relatively thin top clay layer induces a low effective stress level in the peat layer. Therefore it was expected beforehand that the yield stress in the peat at this site is also relatively low.

Siddeburen:

At Siddeburen the peat deposit is found practically at surface level. A 0.1 – 0.2 m thick top clay layer is present at the site. The field stress level at this site is low, due to the combination of the low peat density and the ground water table, which, at this site, is found in the top of the peat layer. Due to natural fluctuations in the ground water table a moderate level of pre-consolidation stress was to be expected at the ground water table level. At deeper levels the yield stress might be lower. The exact values are presented and discussed in the next section.

4.2 Subsoil stresses and yield stress

Figure 4.2 plots the stresses at the three sample locations. To derive the total stress, the density was derived from top layer samples. The pore pressure was derived from information on the groundwater level and hydraulic heads measured in the sand layer below the peat and clay deposits. All relevant information on densities, ground water tables and hydraulic heads are presented in the factual report (Zwanenburg & Konstantinou, 2016). The pore pressures shown in Figure 4.2 are found by interpolation between the groundwater table and the hydraulic heads measured in the sand layer. Especially at the Siddeburen location a considerable fluctuation in groundwater table is found, see (Zwanenburg & Konstantinou, 2016). Figure 4.2 shows the pore pressure and effective stresses given by the highest ground water level in black and for the lowest ground water level in grey. Fluctuations of hydraulic head in the deeper sand layer are considered to be small and are not taken into account.

Figure 4.2 clearly shows the difference in stress level, both in total and effective stresses, found at the Nieuwolda site and at the other two sites. Figure 4.2 also plots the yield stress found in 20 K0-CRS tests. The yield stresses found at the Siddeburen location seem large in comparison to the values found at the Schildmeer location, although both locations show low-stress conditions. The difference can be explained by the position of the tested specimens. At the Siddeburen location, both tested specimens are located in the zone within which the water table fluctuates. This zone might be subjected to suction forces when the phreatic line is low. The occurrence of the suction forces might explain the high yield stresses. At the Schildmeer location the tested specimens come from a larger depth, well below the zone in which the water table fluctuates. Except for one test, the Schildmeer samples show a lower pre consolidation stress.

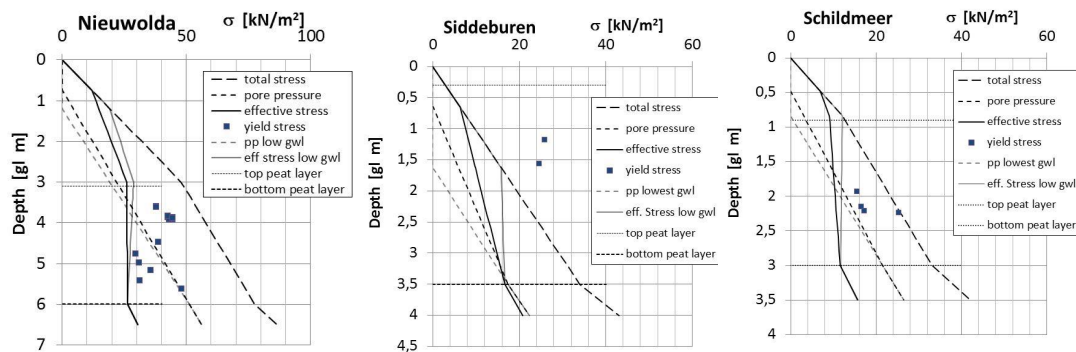


Figure 4.2 Sub soil stresses for the three sample locations, gl = ground level, gw = ground water level, pp = pore pressure

At the three locations, the lower bound level of the ground water table is in agreement with the hydraulic head found in the underlying sand layer. For the upper bound level, the ground water table exceeds the hydraulic head causing a non-hydrostatic pore pressure development in the peat layer. The density of the peat at the three locations is close to the density of water. Therefore, within the peat layer the effective stress level is nearly constant. Only at the Siddeburen location for high water tables an increase in effective stress over the peat layer is found.

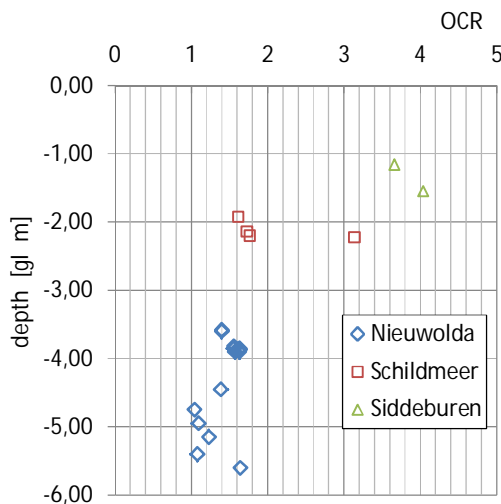


Figure 4.3 Overconsolidation ratio, OCR versus depth for the three sample locations, gl = ground level

Figure 4.3 presents the overconsolidation ratio, defined as $OCR = \sigma'_{vy} / \sigma'_{vi}$. In which σ'_{vy} represents the yield stress found in the K0-CRS tests and σ'_{vi} the vertical effective stress in the field. It should be noted that the results for the three different locations are shown in the same graph. At the Nieuwolda site a decrease in σ'_{vy} with depth is found, with a rapid increase at lower depth near the transition to the underlying sand layer. At the locations Siddeburen and Schildmeer the number of tests are too small to show a clear depth profile. For these locations a relatively high OCR is found near the groundwater table. The depth

profiles are equivalent to OCR depth-profiles found at other locations in The Netherlands, Uitdam, Zwanenburg & Jardine (2015) and Booneschans, Zwanenburg et al (2012).

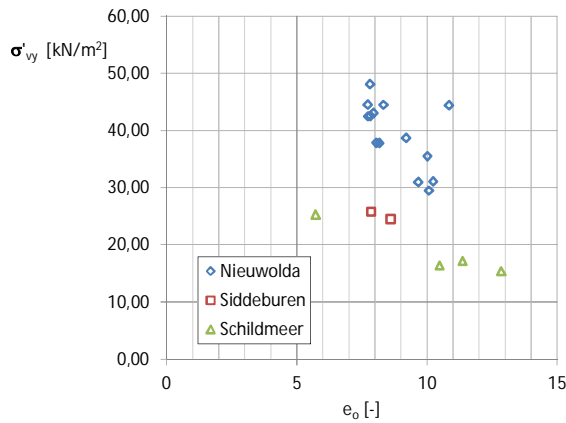


Figure 4.4 Yield stress, σ'_{vy} versus initial void ratio e_0

Figure 4.4 shows the relation between the yield stress and the initial void ratio. For the different locations σ'_{vy} seems to correlate to e_0 . Figure 4.5 shows fits for the σ'_{vy} - e_0 relation. Several fits have been tested. The figure shows the best fit, highest weighted least squares sum, R^2 , for all data points and for the Nieuwolda case. The left graph shows the best fit using an exponential function:

$$\sigma'_{vy} = 91.366 e_0^{-0.116} \quad (4.1)$$

The weighted least squares sum, $R^2 = 0.29$, indicates a poor correlation. A possible explanation for the poor correlation might be the origin of the yield stress. Yield stress follows from stress history and aging. The Siddeburen and Schildmeer samples were taken at a depth where stresses are influenced by ground water fluctuations. Here, σ'_{vy} might be mainly induced by stress history whereas the Nieuwolda samples come from a greater depth. For the Nieuwolda case aging might have a stronger influence.

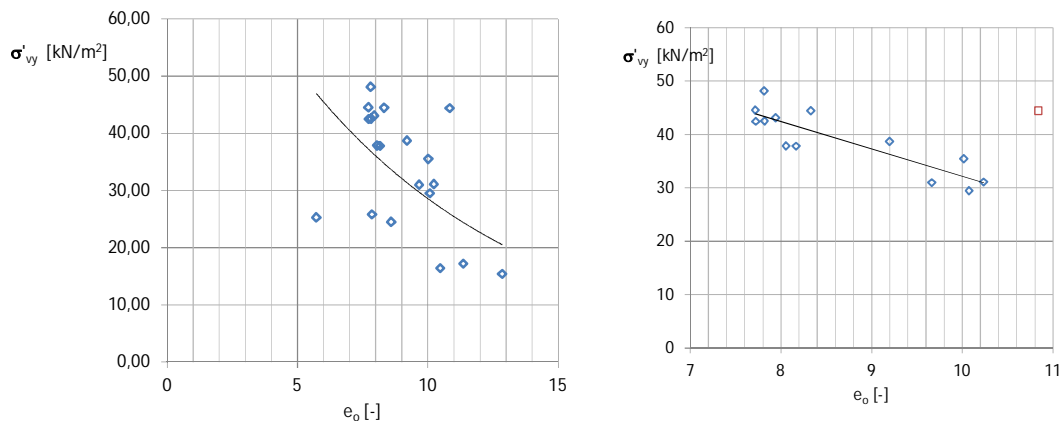


Figure 4.5 Fits for yield stress σ'_{vy} and initial void ratio e_0 relation, left best fit for all data, right best fit for Nieuwolda data, red mark is data point omitted in the fit as outlier

The right graph in Figure 4.5 shows the best fit found for the Nieuwolda data, using the least squares method. In finding the best fit one outlying data point is omitted (test NW1A2-A5-1C, $e_0 = 10.84, \sigma'_{vy} = 44.42 \text{ kN/m}^2$). Differences in fitting linear, exponential or power laws are small. For simplicity a linear relation is fitted:

$$\sigma'_{vy} = -5.1079e_0 + 82.284 \quad (4.2)$$

The weighted least squares sum, $R^2 = 0.75$. It should be noted that equation (4.2) is only valid for the peat deposit at the Nieuwolda site. No fits are made for the Siddeburen and Schildmeer locations since the number of tests at those locations is considered to be too small. More fit results will be discussed in the next section after discussion the classification parameters.

4.3 Classification parameters

4.3.1 General

To get a basic understanding of the tested material classification parameters like, density, dry density, particle density, void ratio, water content and loss on ignition are determined. Also stress strain curves from the constant rate of strain tests and the small strain shear modulus G_0 from bender element measurements provide a basic understanding of the tested material. The classification parameters, mentioned above are determined on each tested specimen. The bender element measurements are applied on each specimen tested in the Resonant Column test. The factual report explains the procedures used in determining the parameters.

The following text first discusses the classification parameters in section 4.3.2, the stress strain curves in section 4.3.3 and undrained shear strength characteristics in section 4.3.4. Section 4.3.5 to 4.3.8 characterizes the peat samples from the different locations, checks the uniformity of the samples retrieved from the different sample locations and checks the classification of the samples in humified and non to moderate humified peat, based upon the classification parameters. The results of the Bender element testing are discussed in section 4.4.

4.3.2 Water content, densities and loss on ignition

Figure 4.6 shows the depth profiles of the water content, w , for the three different locations. At the Nieuwolda site a concave profile is found with the highest water contents found just below the centre of the peat deposit. For the Nieuwolda site, the depth profile of the water content mirrors the OCR profile, Figure 4.3. The lowest OCR is found at the same depth as the highest water content. Equivalent findings are found for other peat deposits in The Netherlands, Zwanenburg & Jardine (2015) and are explained by the fact that to some extent the water content and yield stress are related to stress history. For the Siddeburen and Schildmeer locations this phenomenon is not found.

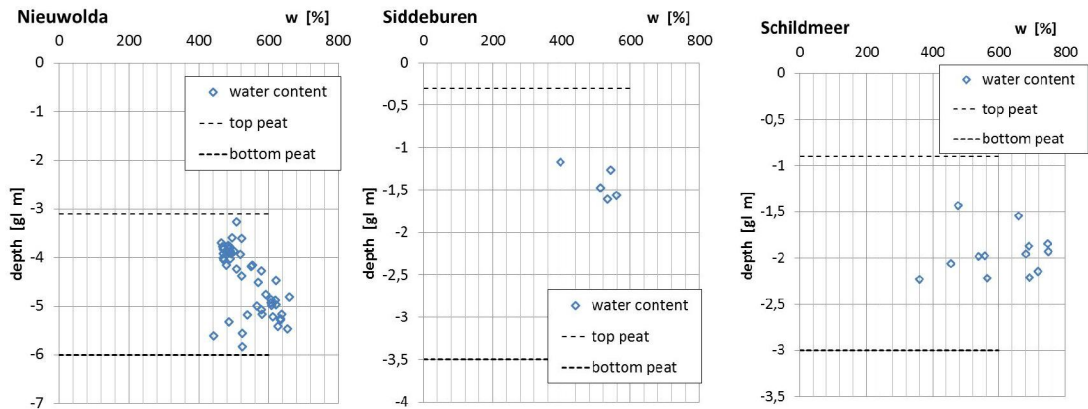


Figure 4.6 Depth profiles of water content, w , for the peat deposits at the three sample locations

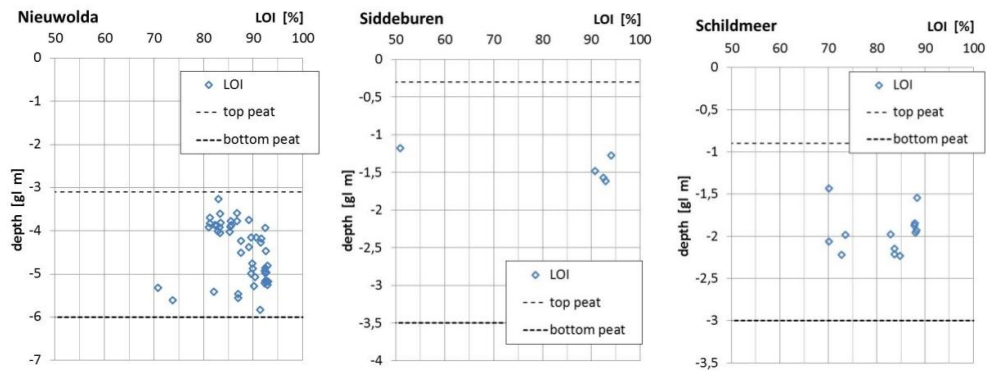


Figure 4.7 Depth profiles of loss on ignition, LOI for the peat deposits at the three sample locations

Figure 4.7 gives the depth profiles of the loss on ignition, LOI, for the peat layer at the three sample locations. The LOI is a measure for the organic content. The procedure to determine the LOI uses heating the sample by which some organic material will be lost. Skempton & Petley (1970) indicates that the difference between the organic content and LOI is in the range of 4%. This correction is not applied to the data given by Figure 4.7.

Figure 4.7 shows a small decrease in LOI in the top of the peat deposit at the Nieuwolda location and some scatter at the bottom. At the other locations no clear pattern is found. In general, LOI ranges between 70 and 95% for the tested material, with one exception at the Siddeburen site. It should be noted that the LOI is significantly higher than generally found for the data presented in the literature overview as discussed in chapter 2.

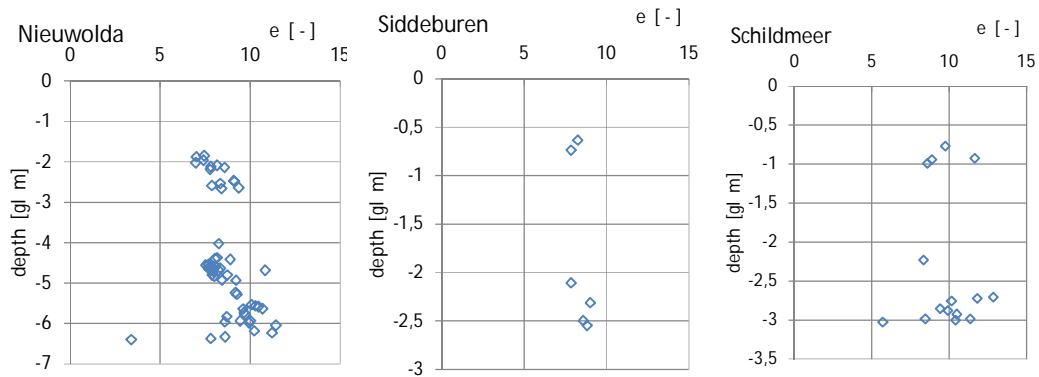


Figure 4.8 In depth profiles of void ratio, e

Figure 4.8 shows the depth profiles of the void ratio e . For the Nieuwolda site, there seems a small increase in depth.

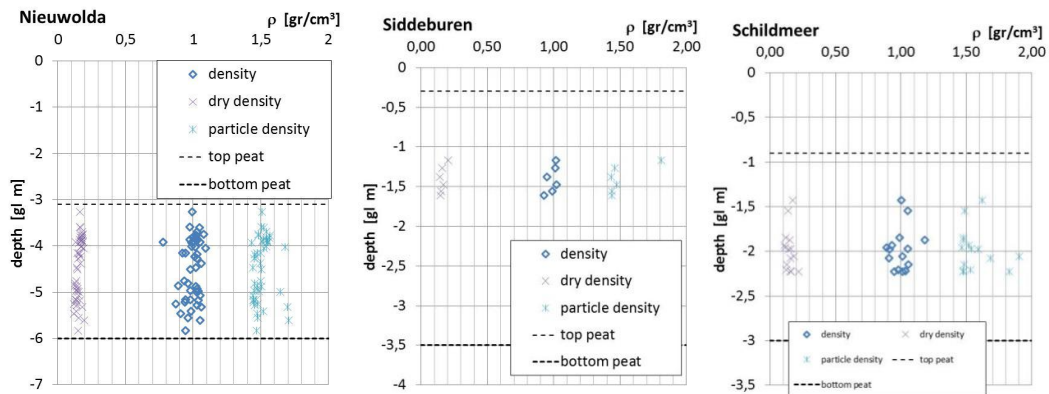


Figure 4.9 Depth profiles of density, ρ , dry density, ρ_{dry} and particle density, ρ_s for the peat deposits at the three sample locations

Figure 4.9 shows the depth profiles of the density, ρ , dry density, ρ_{dry} and particle density, ρ_s for the peat deposits at the three sample locations. A remarkable small scatter is found for the dry density. A small scatter for the ρ_{dry} is also reported by den Haan & Kruse (2007), where data for five different locations in The Netherlands is compared. den Haan & Kruse (2007) relate the water content to ρ and ρ_{dry} . Figure 4.10 reproduces this graph and plots the Groningen data on top. The data for ρ_{dry} , the left line of data points in Figure 4.10, fits well to the graph. For ρ , the right line of data points in Figure 4.10, the Groningen data show more scatter. In general the Groningen data fits well to the data presented by den Haan & Kruse (2007).

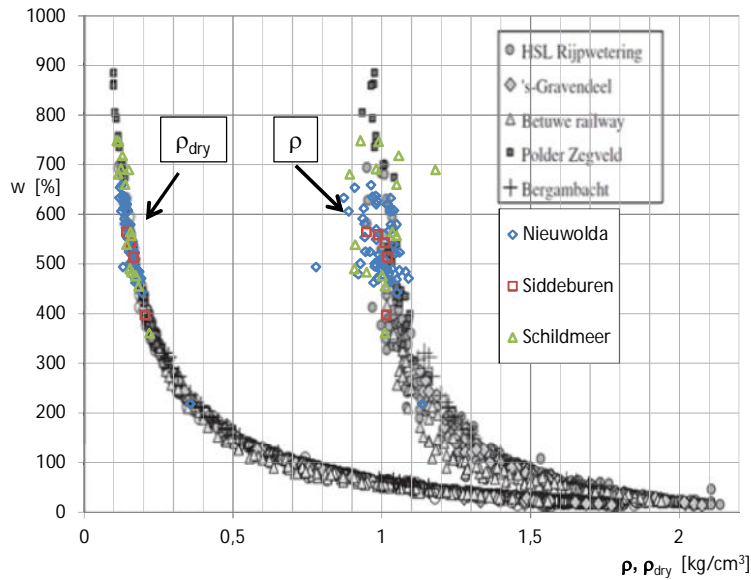


Figure 4.10 Water content versus density, the Groningen data are plotted in colour, background data given by den Haan & Kruse 2007

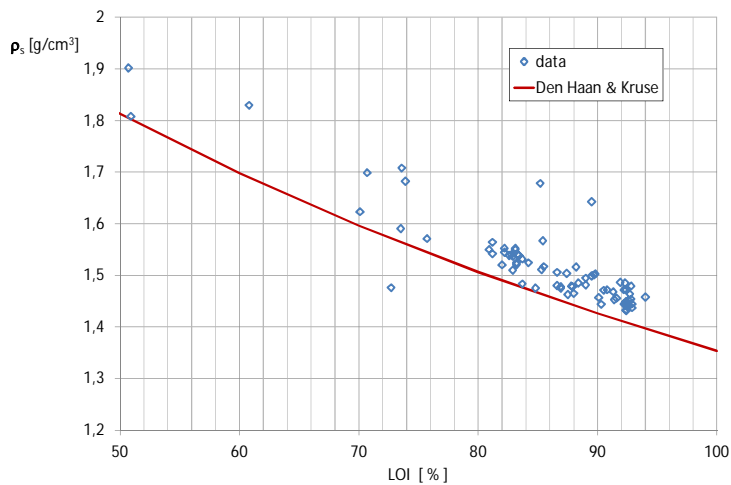


Figure 4.11 Particle density, ρ_s versus Loss on Ignition, LOI comparison between the Groningen data and the relation provided Den Haan & Kruse (2007)

den Haan & Kruse (2007) also present a relation between particle density, ρ_s and loss on ignition, LOI, see equation (4.3):

$$\frac{1}{\rho_s} = \frac{LOI/100}{1.354} + \frac{1-LOI/100}{2.746} \quad (4.3)$$

Figure 4.11 compares the Groningen data to the relation given by equation (4.3). The Groningen data lay above equation (4.3). However, the general trend is the same.

For peats, the void ratio is not only be determined by the stress level or stress history alone. The organic nature of the peat also has an influence. Equation (4.4) fits a relation between the void ratio e_0 , the yield stress σ'_{vy} and the loss on ignition, LOI .

$$e_0 = 9.508 - 0.107\sigma'_{vy} + 0.033LOI \quad (4.4)$$

The weighted sum of residual squares, $R^2 = 0.61$. Equation (4.4) shows that e_0 decreases for increasing σ'_{vy} and increases for increasing LOI . Figure 4.12 shows equation (4.4) graphically.

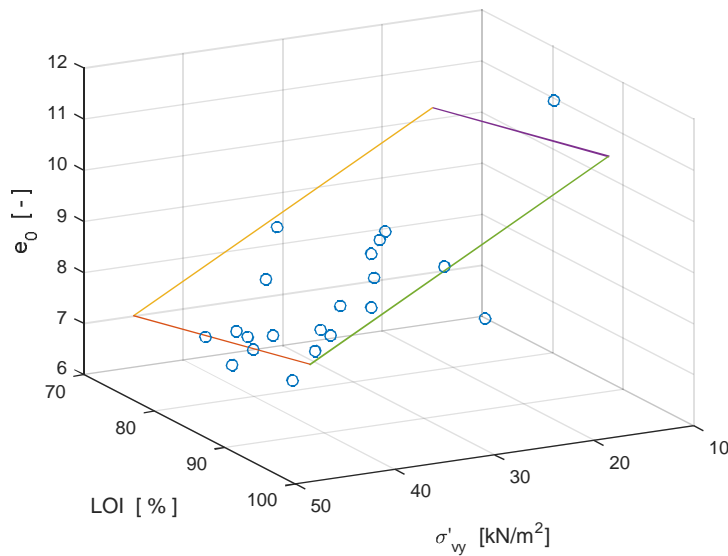


Figure 4.12 3D representation of initial void ratio, e_0 versus loss on ignition, LOI and yield stress, σ'_{vy}

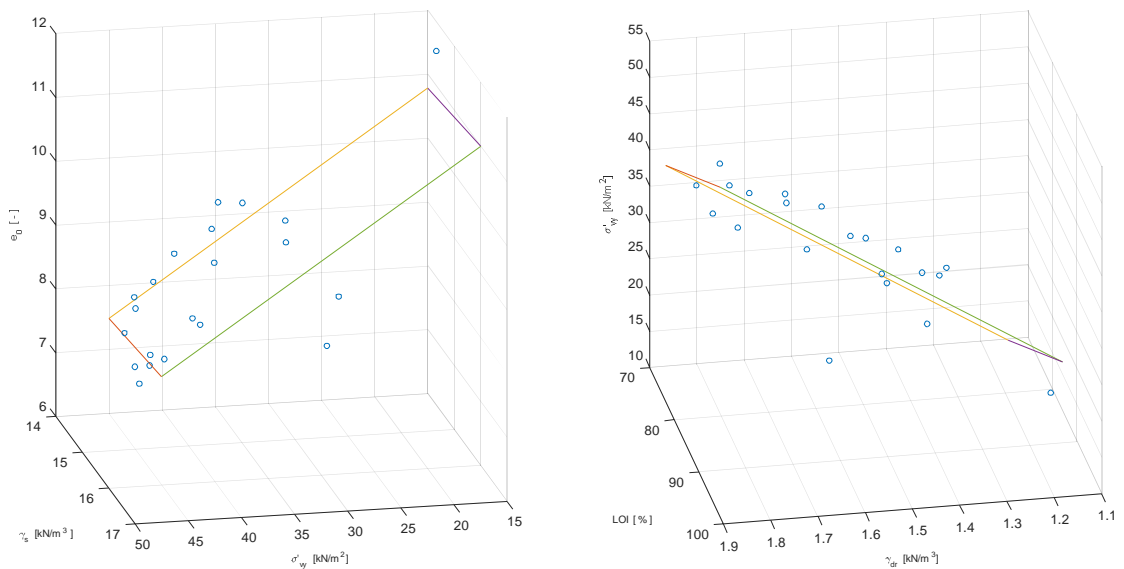


Figure 4.13 3D representation of initial void ratio, e_0 versus particle density, γ_s and yield stress σ'_{vy} (left) and yield stress, σ'_{vy} versus loss on ignition, LOI and dry density, γ_{dr}

Alternative parameter combinations are shown by Figure 4.13. The best fit for the left graph is given by:

$$e_0 = 10.982 - 0.11038 \times \sigma'_{vy} + 0.10477 \times \gamma_s, \quad R^2 = 0.59 \quad (4.5)$$

and for the right graph:

$$\sigma'_{vy} = -75.1208 + 38.5704 \times \gamma_{dry} + 0.58328 \times LOI, \quad R^2 = 0.59 \quad (4.6)$$

The right hand graph in Figure 4.13 shows one outlier; sample SB4A-A2-2B. Removing this sample gives:

$$\sigma'_{vy} = -96.0129 + 42.2621 \times \gamma_{dry} + 0.76425 \times LOI, \quad R^2 = 0.81 \quad (4.7)$$

In further analysis equation (4.7) will be used to estimate the yield stress for tests on samples for which the yield stress was not measured on a nearby specimen.

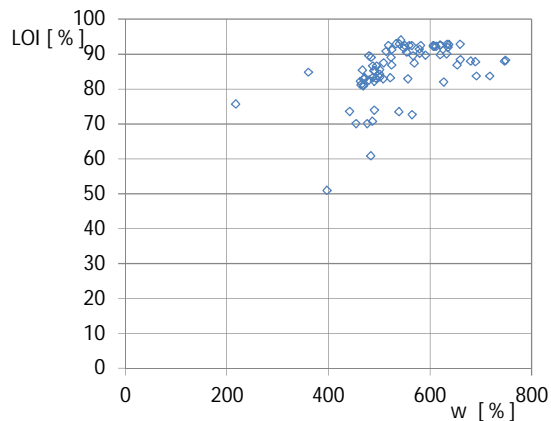


Figure 4.14 Loss on ignition, LOI , versus water content, w

Figure 4.14 shows the relation between the loss on ignition and water content. There seems a weak bi-linear relation. For $w < 500$ % is found that an increase in water content indicates an increase in LOI . For $w > 500$ % LOI is nearly constant for further increase in water content.

4.3.3 Stress – strain curves

Figure 4.15, Figure 4.17 and Figure 4.19 show the stress – strain curves found by the constant rate of strain, CRS, tests for each sample location. The CRS tests contain six phases, a loading phase, an unloading phase, a re-loading phase, a relaxation phase, a reloading phase and an unloading phase. During the relaxation phase the height is kept constant. The factual report, Zwanenburg & Konstantinou (2016) provides more details on the CRS tests. Due to creep the vertical effective stress decreases. The data from relaxation phase provides information the creep parameter, C_{α} . Figure 4.16, Figure 4.18 and Figure 4.20 show the void ratio versus vertical effective stress. It should be noted that in these graphs the vertical effective stress is presented on a normal, non- logarithmic, axis. For the Siddeburen and Schildmeer location the transition between re-loading and virgin compression behaviour is not visible when vertical effective stresses are plotted on a normal scale. This raises questions on the determination of the yield stress and to what extent the yield stresses derived in the classical way are an artefact of using a logarithmic scale to plot the vertical effective stress. This effect is often found for non-pre-loaded peats. Experience shows that, when numerically simulating CRS data of non-pre-loaded peat samples, a yield stress is

needed to reproduce the laboratory data correctly. Therefore, the values for yield stress obtained in the classical way, based on the logarithm of the vertical stresses, are used in the analysis.

Figure 4.15 and Figure 4.16 show that the stiffness of the Nieuwolda sample NW1A2-A5-1C deviates from the stiffness found in the other Nieuwolda samples. The classification parameters for sample NW1A2-A5-1C, like water content, organic content, dry density or particle density do not show clear differences with the values found for the other Nieuwolda samples. There is no clear explanation for the observed difference in stiffness. Schildmeer sample SM2C-A3-2A starts with a lower void ratio than found for the other Schildmeer samples. The difference in initial void ratio can be explained by the difference in yield stress, with $\sigma'_{vy} = 25 \text{ kN/m}^2$ for sample SM2C – A3 – 2A and approximately 15 kN/m^2 for the other Schildmeer samples.

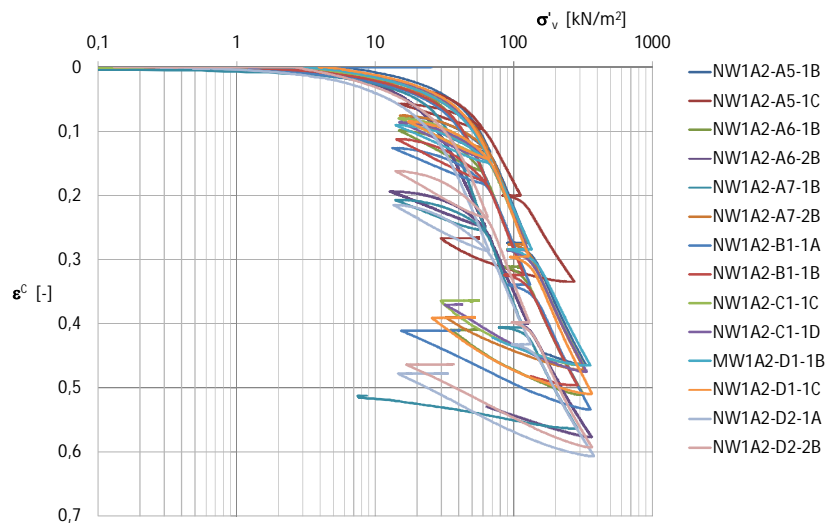


Figure 4.15 Stress – strain curve specimens Nieuwolda

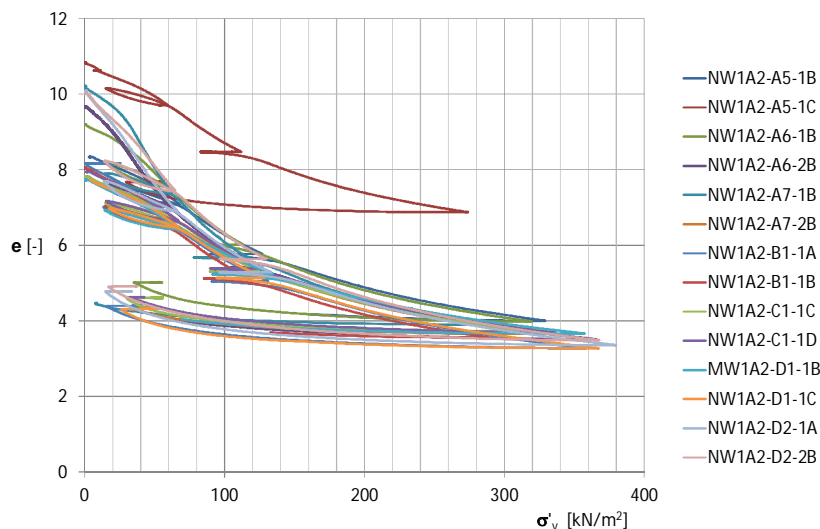


Figure 4.16 Stress – void ratio curve specimens Nieuwolda

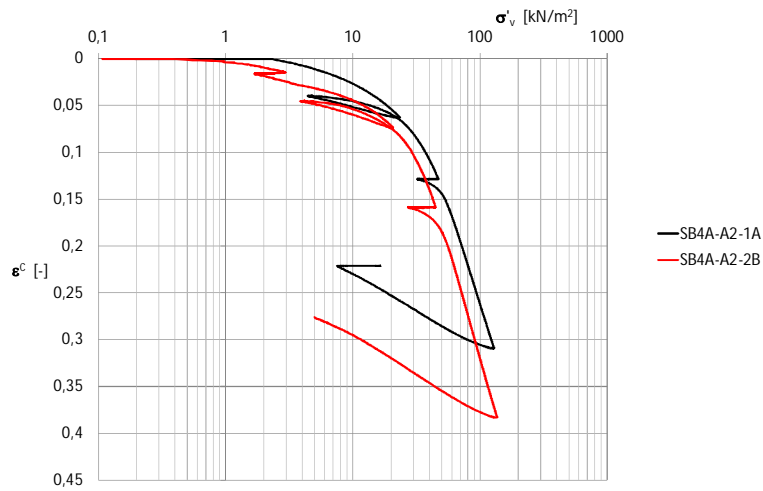


Figure 4.17 Stress – strain curve specimens Siddeburen

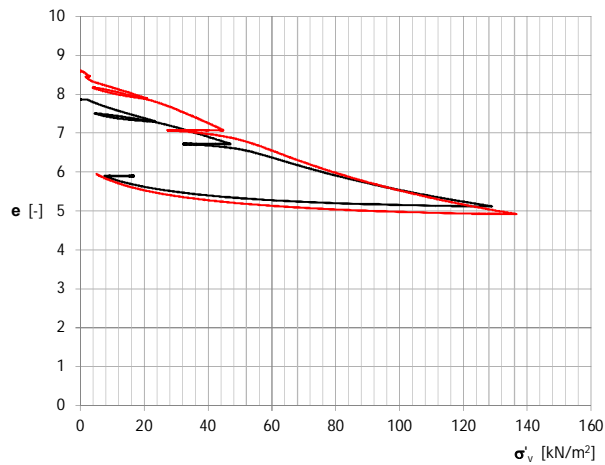


Figure 4.18 Stress – void ratio curve specimens Siddeburen

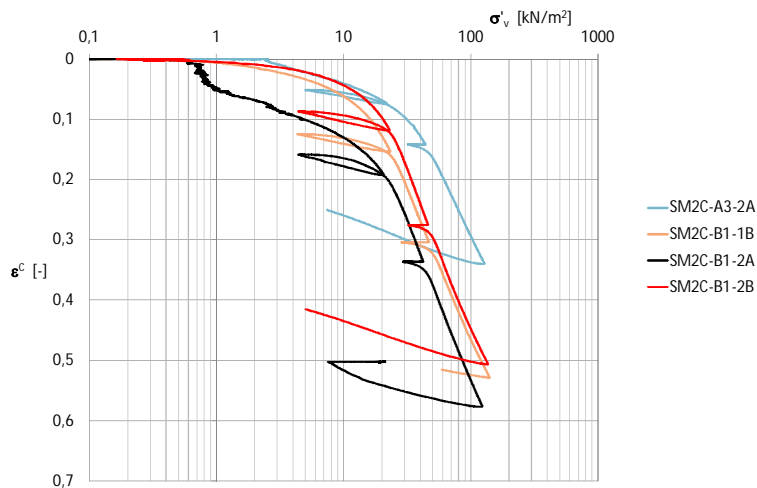


Figure 4.19 Stress – strain curve specimens Schildmeer

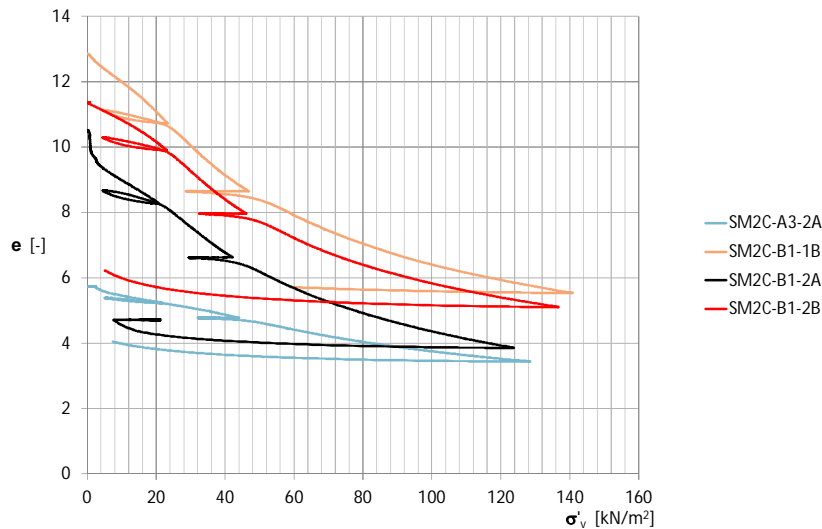


Figure 4.20 Stress – void ratio curve specimens Schildmeer

Location	γ_{sat} [kN/m ³]	ρ_{dry} [g/cm ³]	w [%]	RR [-]	CR [-]	C_{α} [-]	CR/RR [-]	C_{α}/CR [-]
Nieuwolda	9,66	1,54	534	0,09	0,51	0,04	5,73	0,08
Siddeburen	9,81	1,73	478	0,04	0,44	0,05	12,19	0,12
Schildmeer	9,74	1,43	629	0,04	0,50	0,05	11,61	0,10

Table 4.1 Summary CRS test results, averaged values for each location, γ_{sat} = saturated volume weight, ρ_{dry} , dry density, w = water content, RR = recompression index, CR = compression index, C_{α} = creep index

Table 4.1 Provides a summary of the CRS test results. The results agree well to oedometer and CRS parameters for peats found in literature, a.o. Mesri & Ajlouni (2007).

4.3.4 Undrained shear strength characteristics

In total 20 static Direct Simple Shear tests have been conducted. The results are presented in Zwanenburg & Konstantinou (2016). A summary of the test results is given Table 4.2. The table provides the OCR based on the yield stresses found in nearest CRS test. Table 4.2 gives the highest mobilised shear strength as the peak shear strength, $S_{u,peak}$.

Specimen	depth [gl m]	ρ [gr/cm ³]	w [%]	LOI [%]	σ'_{vc} [kN/m ²]	OCR [-]	$S_{u,peak}$ [kN/m ²]
NW1A2-A4-1B	-3.26	1.10	507.9	82.9	26.27	1.70	21.41
NW1A2-A5-1E	-4.16	1.05	479.4	89.5	27.39	1.63	20.44
NW1A2-a6-1C	-4.51	1.07	569.2	87.4	27.85	1.39	21.30
NW1A2-A7-1C	-5.46	1.06	653.9	86.9	28.89	1.08	19.14
NW1A2-A7-2A	-5.56	1.10	524.5	86.9	29.01	1.64	21.15
NW1A2-B1-2C	-4.01	1.07	469.9	82.8	27.20	1.46	20.43
NW1A2-B1-3B	-5.83	1.03	524.7	91.3	25.89	1.39	22.08
NW1A2-B2-2B	-5.26	0.99	633.4	92.8	29.83	1.09	21.10
NW1A2-C1-1B	-3.81	1.11	487.5	83.3	26.94	1.56	22.07
NW1A2-C1-2A	-4.16	1.07	554.1	90.5	27.41	1.43	22.47

Specimen	depth [gl m]	ρ [gr/cm ³]	w [%]	LOI [%]	σ'_{vc} [kN/m ²]	OCR [-]	$s_{u,peak}$ [kN/m ²]
NW1A2-C2-1A	-4.86	1.04	606.1	92.4	28.31	1.22	21.49
NW1A2-C2-2A	-5.16	1.07	581.6	92.4	28.55	1.13	23.50
NW1A2-d1-1D	-3.93	1.12	518.5	92.4	26.59	1.56	19.12
NW1A2-d2-1B	-4.81	1.13	659.3	92.8	28.20	1.04	17.24
NW1A2-d2-2C	-5.21	1.09	612.4	92.2	28.71	1.23	19.87
SB4A-A2-2C	-1.61	0.95	533.4	92.9	5.49	4.04	9.69
SM2C-A2-1A	-1.43	1.04	476.5	70.1	7.79	3.14	11.84
SM2C-A3-1B	-2.06	1.10	454.7	70.1	7.17	3.14	9.90
SM2C-B1-1C	-1.98	1.04	538.6	73.5	9.31	1.61	10.17
SM2C-C1-1B	-1.96	1.01	680.5	88	9.10	1.61	10.10

Table 4.2 Summary of Direct Simple Shear, DSS, test results, with gl = ground level, ρ = density of the sample, w = water content, LOI = loss on ignition, σ'_{vc} = vertical stress at which the sample is consolidated, OCR = Over Consolidation Ratio, s_u = undrained shear strength

According to Ladd (1991) the undrained shear strength is a function of the actual vertical stress, σ'_{vi} and the stress history, OCR:

$$s_u = S OCR^m \sigma'_{vi}, \quad S = \left(\frac{s_u}{\sigma'_{vi}} \right)_{nc} \quad (4.8)$$

In which S represents the normally consolidated shear stress ratio, m the strength gain parameter and σ'_{vi} the actual vertical effective stress. It should be noted that for DSS test conditions vertical stress at which the specimens are consolidated, σ'_{vc} is used for σ'_{vi} in equation (4.8).

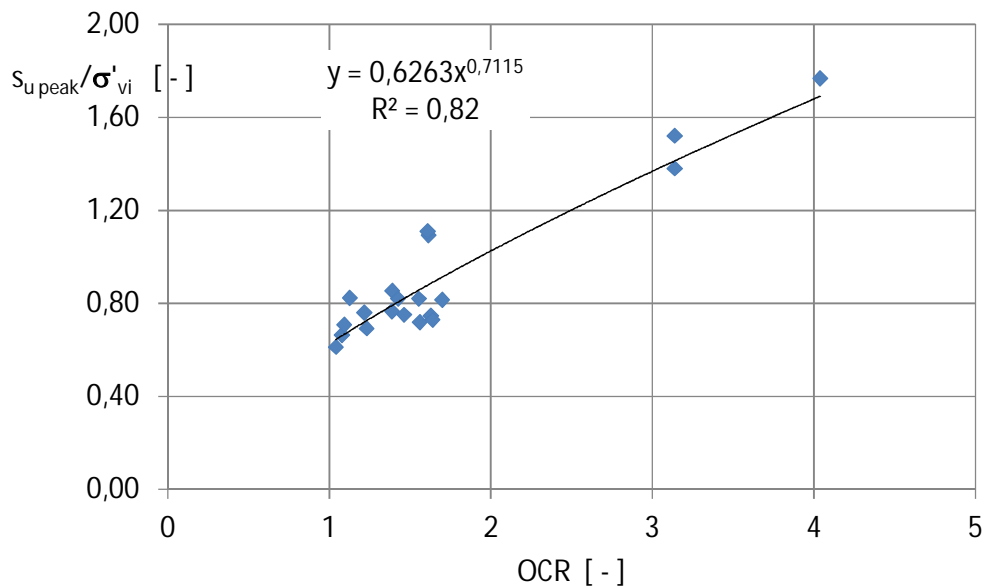


Figure 4.21 Fit of equation (4.8) to the data provided by Table 4.2

Figure 4.21 shows the result of fitting equation (4.8) to the data provided by Table 4.2 using a least squares approach. The weighted least square sum $R^2 = 0.82$ for the best fit, resulting in normally consolidated shear stress ratio $S = 0.62$ and $m = 0.71$. The found value for S seems somewhat high compared to Mesri & Ajlouni (2007) or Figure 2.4.

4.3.5 Statistical analysis; background theory

In order to come to general conclusions, it should be clear to what extent the different tested specimens represent the same material. The significance of the differences found between different subsets is given by statistical tests like the F and T -test. This section provides the formulas used in deriving the statistical parameters, like mean value and standard deviation and provides the formulas used for the F and T -test.

The statistical characterisation uses the following parameters:

mean value:

$$\mu_x = \frac{\sum_{j=1}^n x_j}{n} \quad (4.9)$$

in which:

μ_x = estimation of mean value of parameter x

x_j = j^{th} realisation of parameter x

n = number of measurements

Standard deviation:

$$\sigma_x = \sqrt{\frac{\sum_{j=1}^n (x_j - \mu_x)^2}{n-1}} \quad (4.10)$$

σ_x = estimation of the standard variation of parameter x

coefficient of variation:

$$VC = \frac{\sigma_x}{\mu_x} \quad (4.11)$$

T-test

The T -test tests the hypothesis, H_0 , that the mean value of two populations X and Y are equal given random selections, x and y , from each population. The hypothesis is defined as

$$H_0 : \mu_x = \mu_y \quad (4.12)$$

A testing parameter T is defined as:

$$T = \frac{\bar{x} - \bar{y}}{S \sqrt{\frac{1}{n_x} + \frac{1}{n_y}}}, \quad (4.13)$$

$$S^2 = \frac{(n_x - 1)S_x^2 + (n_y - 1)S_y^2}{n_x + n_y - 2}$$

in which:

H_0 = hypothesis

μ_x, μ_y = mean value for population X and Y
 T = testing quantity
 \bar{x}, \bar{y} = mean value of selection x respectively y
 n_x, n_y = number of data points of selection x respectively y
 S^2 = Weighted average of the selection variances
 S_x^2, S_y^2 =variance in selection x, respectively y.

The testing quantity T has Student-t distribution. To validate H_0 a 90% confidence level is chosen. This means that the bandwidth for which the hypothesis will be accepted has a lower boundary, $t^{0.05}_m$ and an upper boundary, $t^{0.95}_m$, with $m = n_x + n_y - 2$. If the value for T is outside these boundaries, $T < t^{0.05}_m$ or $T > t^{0.95}_m$, the hypothesis will be rejected. Then, the mean values for the selections deviate so strongly that the hypotheses stating that the mean value for the populations from which the selections are taken are equal is rejected, with a confidence level of 90%. This means that there is a 10% change that the rejection is not justified.

The T -test assumes that the variance of the two populations from which the selections are taken are equal. It should be noted that the variance of the both selections need not to be the same. This can be tested by the F -test, see below.

If the F -test shows that the variance of the selections differ, the T test should be replaced by a more sophisticated Welch test in which T is defined as:

$$T = \frac{\bar{x} - \bar{y}}{S_{x-y}}, \quad S_{x-y} = \sqrt{\frac{S_x^2}{n_x} + \frac{S_y^2}{n_y}} \quad (4.14)$$

and m is given by :

$$m = \frac{\left(\frac{S_x^2}{n_x} + \frac{S_y^2}{n_y} \right)^2}{\left(\frac{S_x^2}{n_x} \right)^2 / (n_x - 1) + \left(\frac{S_y^2}{n_y} \right)^2 / (n_y - 1)} \quad (4.15)$$

F-test

The F -test tests the hypothesis that the variance of two populations X and Y are equal given random selections, x and y, from each population. The hypothesis is defined as:

$$H_0 : \sigma_x^2 = \sigma_y^2 \quad (4.16)$$

In which σ_x and σ_y represent the standard deviation of population X and Y. The testing quantity is defined as:

$$F = \frac{S_x^2}{S_y^2} \quad (4.17)$$

In which S_x and S_y represent the standard deviation of the selections of the population X and Y.

The testing quantity F has an F - distribution. To validate H_0 a 90% confidence level is chosen. This means that the bandwidth for which the hypothesis will be accepted has a lower

boundary, $f^{0.05}_{(nx-1),(ny-1)}$ and an upper boundary, $f^{0.95}_{(nx-1),(ny-1)}$, with $m = n_x + n_y - 2$. If the value for F is outside these boundaries, $F < f^{0.05}_{(nx-1),(ny-1)}$ or $F > f^{0.95}_{(nx-1),(ny-1)}$, the hypothesis will be rejected. Then, the variances of the selections deviate so strongly that the hypothesis stating that the variances for the populations from which the selections are taken are equal is rejected, with a confidence level of 90%. This means that there is a 10% change that the rejection is not justified.

4.3.6 Statistical analysis, differences in tested material for the different sample locations

Figure 4.22 to Figure 4.24 gives the bar charts for the different classification parameters at the different sample locations. For each site the bar chart presents the mean value and the 5% upper and lower boundary value for the mean value. The exact numbers are presented in appendix A.

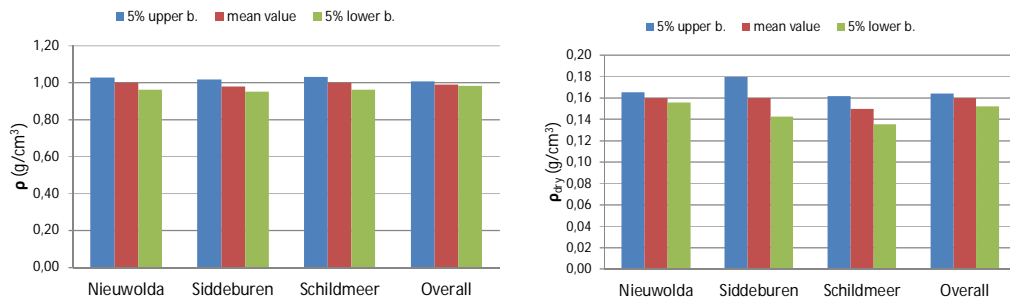


Figure 4.22 Bar chart for bulk density, ρ , (left) and dry density, ρ_{dry} , (right) for the different locations

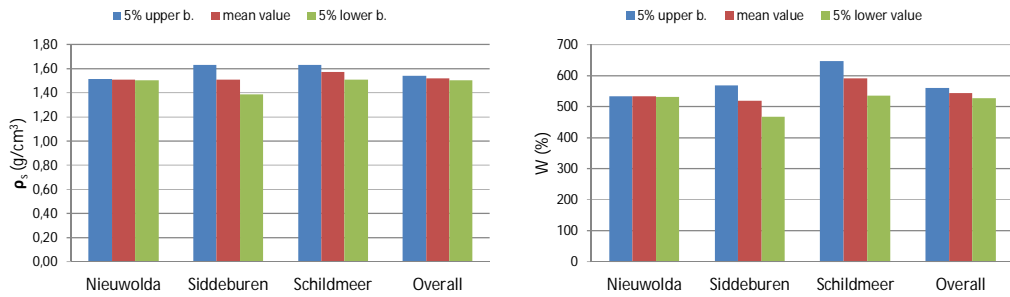


Figure 4.23 Bar chart for particle density, ρ_s , (left) and water content, w , (right) for the different locations

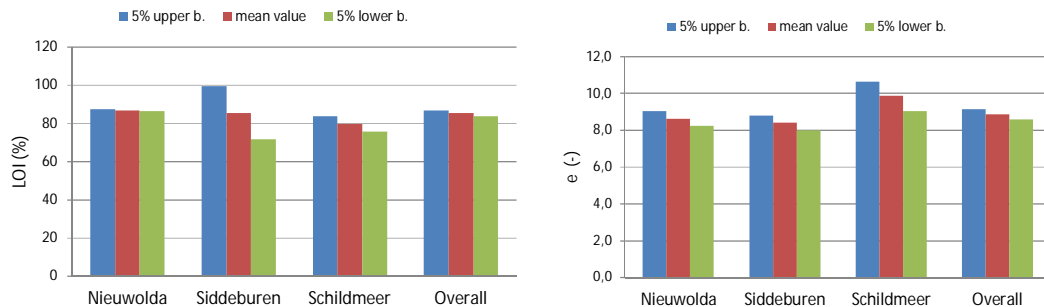


Figure 4.24 Bar chart for loss on ignition, LOI, (left) and initial void ratio, e_0 , (right) for the different locations

The bar charts above show the differences in classification parameters in the tested material from the three different sample locations. To test if the differences are statistically significant the F and T test are applied to the data. To avoid confusion with underlying dependencies only the material that has been classified as non to moderate humified is used in the tests. It should be noted that the number of specimens classified as humified material is small and that all specimens from the Siddeburen location are classified as humified material. Table 4.3 shows the results of the F and T test for the non and moderate humified material at Nieuwolda and Schildmeer.

		ρ [g/cm ³]	ρ_{dry} [g/cm ³]	ρ_s [g/cm ³]	w [%]	LOI [%]	e_0 [-]
Nieuwolda	mean, μ	0,99	0,16	1,51	542,00	87,40	8,78
	standard deviation, σ	0,06	0,02	0,06	62,70	4,77	1,10
	coefficient of variation, VC	0,06	0,12	0,04	0,12	0,05	0,13
	number of samples, n	51	51	51	51	51	51
Schildmeer	mean, μ	1,00	0,14	1,54	613,28	80,80	9,99
	standard deviation, σ	0,08	0,03	0,10	125,44	9,19	1,93
	coefficient of variation, VC	0,08	0,21	0,07	0,20	0,11	0,19
	number of samples, n	12	12	12	12	12	12
F-test	F	0,52	0,38	0,29	0,25	0,27	0,33
	$P(F < f; H_0)$	0,0582	0,0096	0,0014	0,0003	0,0007	0,0034
	$f^{0,05}_{(nx-1),(ny-1)}$	0,50	0,50	0,50	0,50	0,50	0,50
	$f^{0,95}_{(nx-1),(ny-1)}$	2,51	2,51	2,51	2,51	2,51	2,51
	conclusion	accepted	rejected	rejected	rejected	rejected	rejected
T-test	T	-0,36	3,91	-2,92	-5,96	7,51	-6,54
	$P(T < t; H_0)$	0,361	0,999	0,006	0,000	1,000	0,000
	$t^{0,05}_m$	-1,67	-1,77	-1,78	-1,78	-1,78	-1,78
	$t^{0,95}_m$	1,67	1,77	1,78	1,78	1,78	1,78
	conclusion	accepted	rejected	rejected	rejected	rejected	rejected

Table 4.3 F and T test for the non – moderate humified material at the Nieuwolda and Schildmeer locations, ρ = density, ρ_{dry} = dry density, ρ_s = solid density, w = water content, LOI = loss on ignition, e_0 = initial void ratio

The F -test shows that, except from the density, ρ , the variation found in the different classification parameter differs significantly between the Nieuwolda and Schildmeer location. As a consequence the more sophisticated welch test is used to compare the mean values. Again, except from the density, ρ , the differences in mean value for the different classification parameters are proven to be statistically significant.

4.3.7 Statistical analysis, differences between humified and non – moderate humified peat

At the start of the study a difference in material behaviour was expected between the humified and non to moderate humified peat. The classification between humified and non to moderate humified is made by visual inspection. This section checks if the classification

based on the visual inspection can be supported by differences in the classification parameters.

Appendix A shows the statistics of the classification tests for the humified and the non to moderate humified peat. A summary of the results are given by Figure 4.25 to Figure 4.27. To test whether these differences are statistically significant, the F and T test are applied to the data.

It is to be expected that strong humification will change the structure of the peat. The decay of (large) fibres will reduce the pore volume and amount of bounded water kept in the cell structure. A strongly humified peat will therefore have a lower water content, a lower void ratio and a larger (dry) density. Humification will reduce the organic content and therefore reduce the LOI. As a consequence an increase in particle density will be found for increasing humification. The differences in parameter values, as presented by the bar charts below, agree with these expectations. To tests if the observed differences are significant, the F and T -test are conducted. Table 4.4 shows the results of the F -test. The hypothesis regarding the variance in the different populations is accepted for each classification parameter. In the next step the mean value can be tested by the conventional T -test.

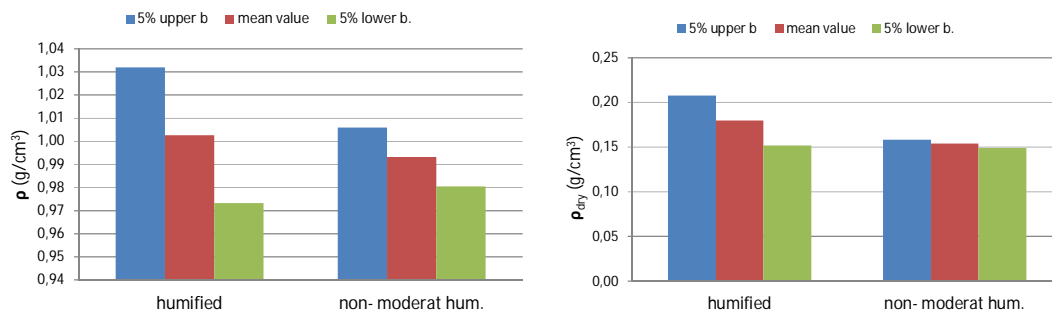


Figure 4.25 Bar chart for bulk density, ρ , (left) and dry density, ρ_{dry} , (right) for humified and non to moderate humified peat

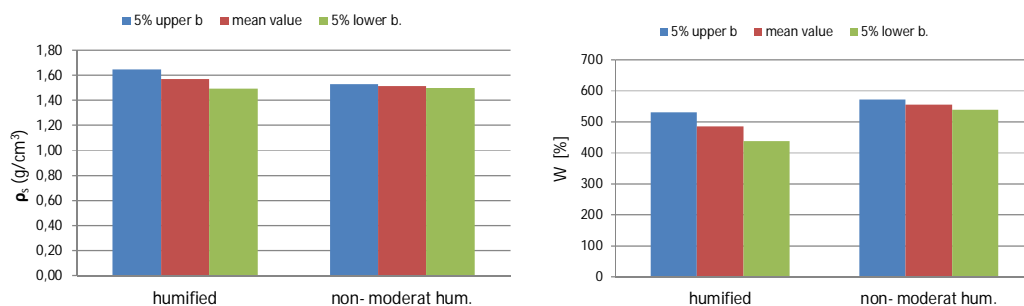


Figure 4.26 Bar chart for particle density, ρ_s , (left) and water content, w , (right) for humified and non to moderate humified peat

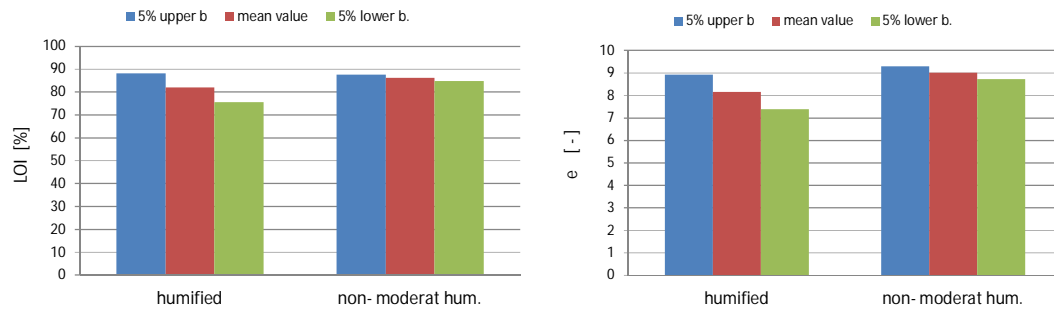


Figure 4.27 Bar chart for loss on ignition, LOI, (left) and void ratio, e, (right) for humified and non to moderate humified peat

	ρ [g/cm ³]	ρ_{dry} [g/cm ³]	ρ_s [g/cm ³]	w [%]	LOI [%]	e_0 [-]
F	0.97	6.64	5.25	1.32	3.94	1.31
P(F<f;H ₀)	0.51	1.00	1.00	0.77	0.99	0.77
$f^{0.05}_{(nx-1),(ny-1)}$	0.42	0.42	0.42	0.42	0.42	0.42
$f^{0.95}_{(nx-1),(ny-1)}$	1.91	1.91	1.91	1.91	1.91	1.91
conclusion	accepted	accepted	accepted	accepted	accepted	accepted

Table 4.4 Results of F test, ρ = density, ρ_{dry} = dry density, ρ_s = solid density, w = water content, LOI = loss on ignition, e_0 = initial void ratio

	ρ [g/cm ³]	ρ_{dry} [g/cm ³]	ρ_s [g/cm ³]	w [%]	LOI [%]	e_0 [-]
T	0,51	2,77	2,06	-2,75	-1,83	-1,99
P(T<t;H ₀)	0,695	0,997	0,979	0,004	0,036	0,025
$t^{0.05}_m$	-1,67	-1,67	-1,67	-1,67	-1,67	-1,67
$t^{0.95}_m$	1,67	1,67	1,67	1,67	1,67	1,67
conclusion	accepted	rejected	rejected	rejected	rejected	rejected

Table 4.5 Results of T-test, ρ = density, ρ_{dry} = dry density, ρ_s = solid density, w = water content, LOI = loss on ignition, e_0 = initial void ratio

Table 4.5 provides the results of the T test. The T-Test shows that, except from the density, ρ , for all classification parameters the differences are proven to be statistically significant; the hypothesis of identical mean value is rejected. This means that the visually made classification in humified and non to moderate humified is supported by the differences found in the classification parameters.

4.3.8 Statistical analysis, differences in material tested by different laboratories

Figure 4.28 to Figure 4.30 provide the characterisation parameters for the samples tested at the different laboratories. The bar charts also indicate the 5% upper and lower boundary of the estimated mean value. The exact values for the different parameters are given in Appendix A.

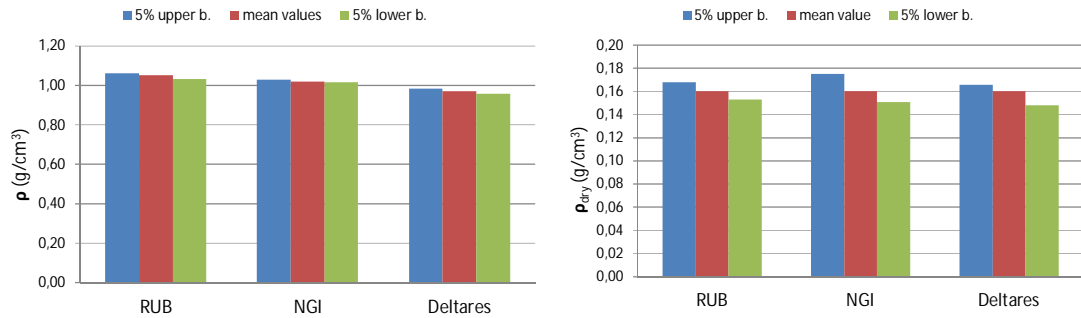


Figure 4.28 Bar charts for bulk density, ρ , (left) and dry density, ρ_{dry} , (right) for the different laboratories

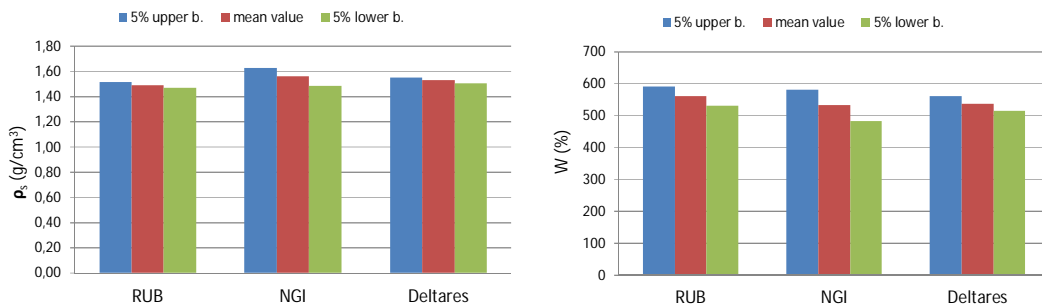


Figure 4.29 Bar chart for particle density, ρ_s , (left) and water content, w , (right) for the different locations

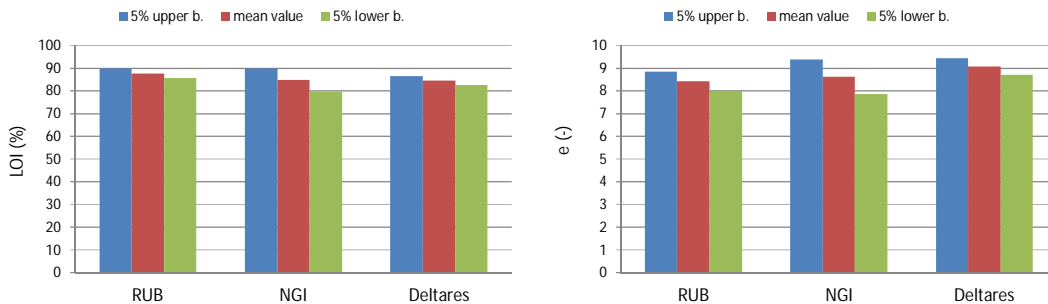


Figure 4.30 Bar chart for loss on ignition, LOI, (left) and void ratio, e , (right) for the different locations

The samples tested at the different laboratories are divided over the different sample locations and humidified and non-humidified samples. Since it is assumed that the differences in material dominate the observed differences in characterisation parameters and only a few samples were tested at NGI, the statistical sub sets are limited. Therefore, no F and T -test are conducted for the observed differences between the laboratories.

4.4 Small strain stiffness G_0

For each specimen, used for a resonant column testing, bender element measurements have been conducted. Details of the conducted measurements are given in appendix E and F of the factual report. The small strain modulus, G_0 is calculated from the bender element measurements by:

$$G_0 = \rho \times v_s^2 \tag{4.18}$$

in which ρ is the sample density and v_s the shear wave velocity. In the following the values for G_0 and v_s are compared to the characterisation parameters.

The different relations are plotted by Figure 4.31 to Figure 4.35. In general the G_0 values measured by NGI seem a bit lower than the values measured by RUB. As indicated in the RUB report, see appendix E of the factual report, the determination of the arrival time of the shear wave for peats in bender element testing is not straightforward. RUB and NGI use slightly different methods to detect the arrival time. RUB uses the start – to – start method, while NGI uses the peak – to – peak method. As reported by Yamashita et al (2005), regarding their tests on sand, the peak – to – peak method yields slightly lower values than the start – to start method. Also the difference in applied frequency, NGI used 500 – 600 Hz while RUB used 900 – 1100 Hz, might contribute to the observed differences in G_0 . This is further discussed in appendix C.

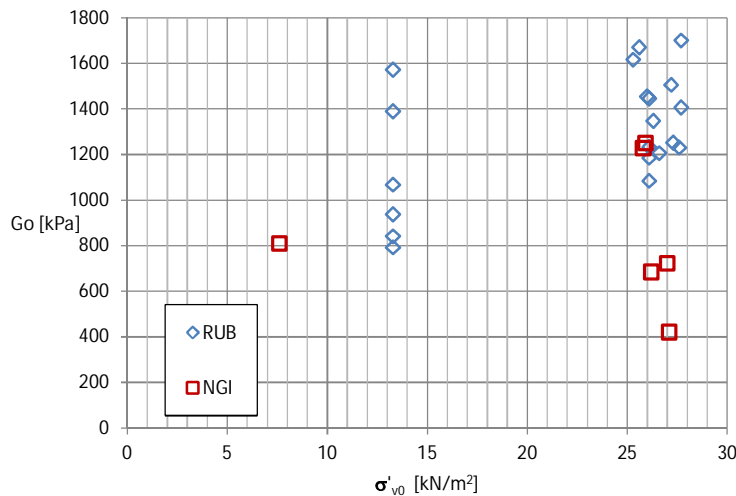


Figure 4.31 Small strain shear modulus, G_0 versus vertical effective stress, σ'_{v0}

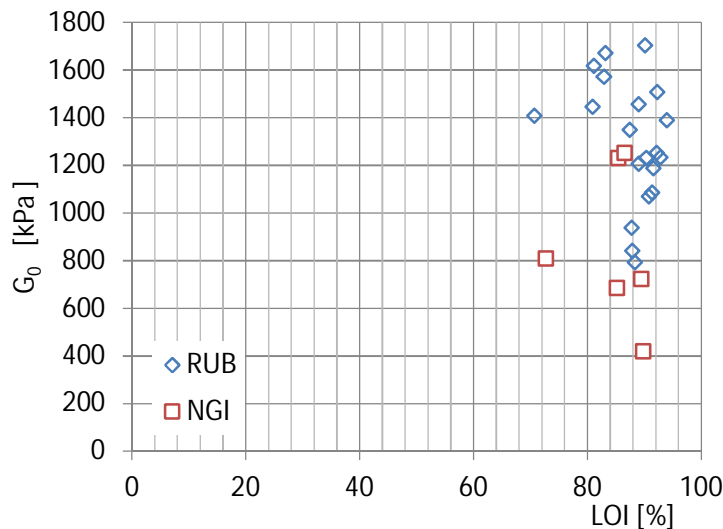


Figure 4.32 Small strain shear modulus, G_0 versus loss on ignition, LOI

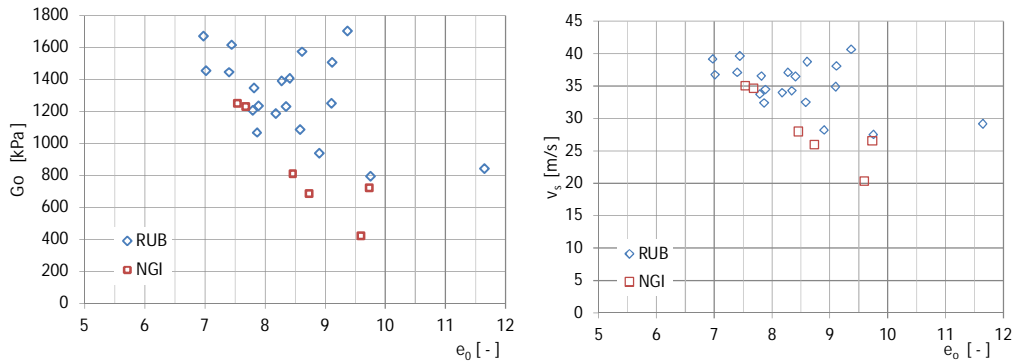


Figure 4.33 Left; Small strain shear modulus G_0 versus void ratio e_0 , right: shear wave velocity v_s versus e_0

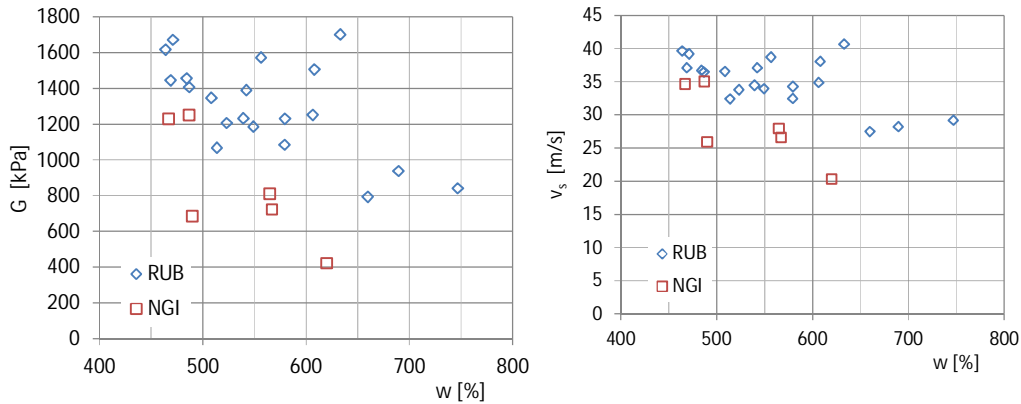


Figure 4.34 Left; Small strain shear modulus G_0 versus water content, w , right: shear wave velocity v_s versus water content, w

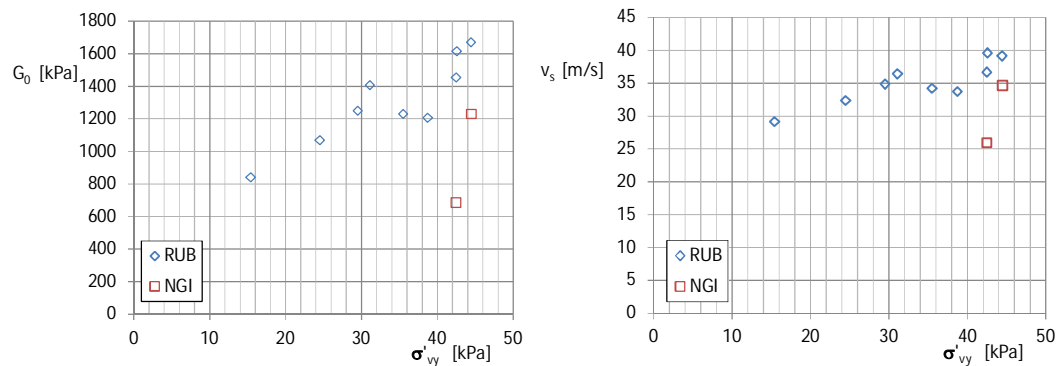


Figure 4.35 Left; Small strain shear modulus, G_0 versus yield stress, σ'_{vy} ; right, shear wave velocity v_s versus yield stress, σ'_{vy}

Figure 4.31 shows the G_0 values as a function of the actual vertical effective stress at testing. It should be noted that the level of vertical effective stress at testing is chosen equal to the estimated field value. The presented data does not show a clear correlation between G_0 and

σ'_{v0} . Figure 4.32 shows the G_0 values as a function of the Loss On Ignition, LOI, of the tested samples. The data does not show a clear correlation between G_0 and LOI.

Figure 4.33 shows G_0 respectively v_s as a function of e_0 . The graphs show a clear lower boundary, below which no points are found. Above this line the data is scattered.

Figure 4.34 shows that the relation between G_0 respectively v_s and w seems less clear than the relation between G_0 and e_0 .

Figure 4.35 shows the relation between G_0 and the yield stress σ'_{vy} . Since not all specimens, on which bender element measurements were conducted, had an adjacent specimen on which a CRS test was conducted, only a limited number of data points are available. The available data however seem to show a good correlation for the tests conducted at RUB. The number of data points for the measurements run at NGI is too small to find a clear correlation.

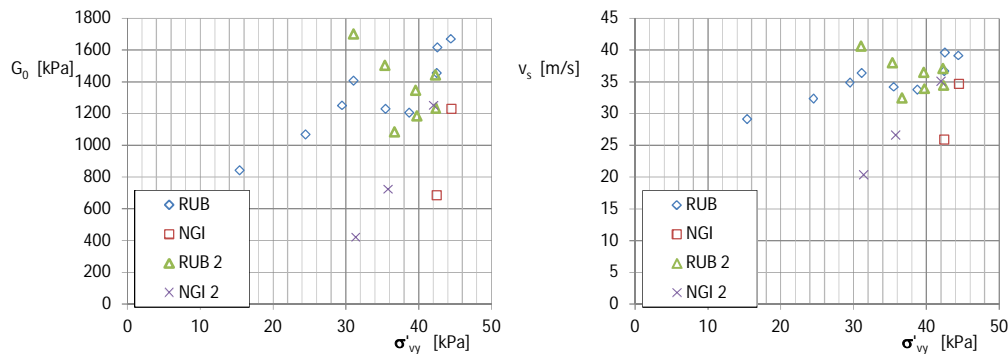


Figure 4.36 Left, small strain shear modulus, G_0 versus yield stress, σ'_{vy} ; right, shear wave velocity v_s versus yield stress, σ'_{vy} , for RUB 2 and NGI 2 the σ'_{vy} is estimated from equation (4.7)

For the Nieuwolda data a correlation between yield stress and initial void ratio is given by equation(4.7). When using this equation extra data points, from tests which have no direct yield stress measurement, can be added, see Figure 4.36. The extra data points do not improve the correlation between G_0 and e_0 or v_s and e_0 .

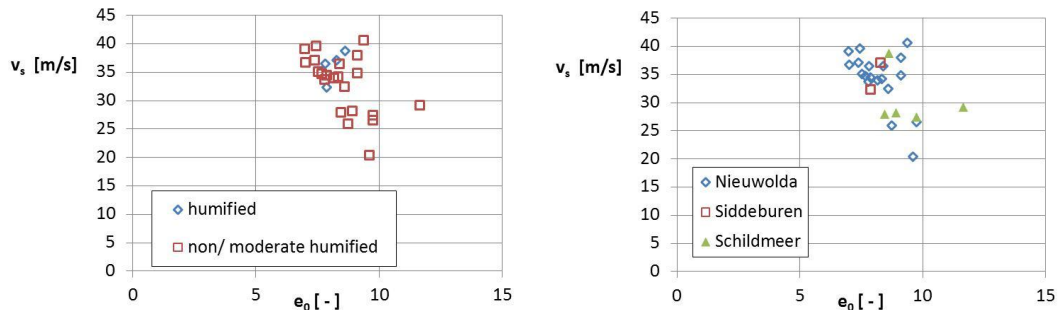


Figure 4.37 Shear wave velocity as a function of initial void ratio

Figure 4.37 shows again the relation between v_s and e_0 . In Figure 4.37 the data points are divided in humified and non to moderate humified samples in the left graph and in the different sample locations for the right graph. The differences in degree of humification and sample location seem not to explain the scatter found.

Kishida et al. (2006) provides a relation between the vertical effective stress level, σ'_v , the over consolidation ratio, OCR , the organic content, OC and small strain shear modulus G_0 by:

$$\frac{G_0}{p_a} = A \left(\frac{\sigma'_v}{p_a} \right)^n OCR^m$$

$$n = 1 - 0.37 \frac{2}{1 + \exp\left(\frac{OC}{23}\right)}$$

$$m = 0.8 - 0.4 \frac{2}{1 + \exp\left(\frac{OC}{23}\right)}$$

$$A = \exp \left(5.2 + 0.48 \frac{2}{1 + \exp\left(\frac{OC}{23}\right)} + 0.74 \left\{ \frac{3 \frac{2}{1 + \exp\left(\frac{OC}{23}\right)} - 1.5}{\ln \left(1 + 3 \exp \left(1 + 3 \frac{2}{1 + \exp\left(\frac{OC}{23}\right)} \right) \right)} - 1 \right\} \right) \quad (4.19)$$

In which p_a represents the atmospheric pressure, 100 kPa. All tests were done at field stress level. For the Nieuwolda samples the applied vertical effective stress ranges from 25.3 kN/m² to 27.7 kN/m², with an average of 26.5 kN/m².

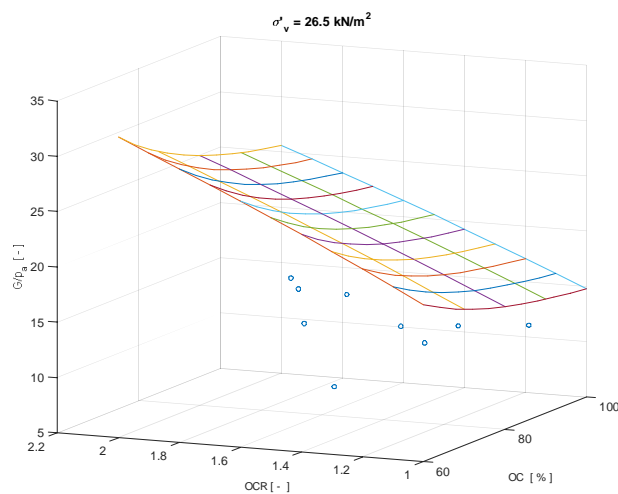


Figure 4.38 G_0/p_a as a function of OCR and OC for $\sigma'_v = 26.5 \text{ kN/m}^2$. The lines represent the Kashida formulation, the dots represent the measurements data

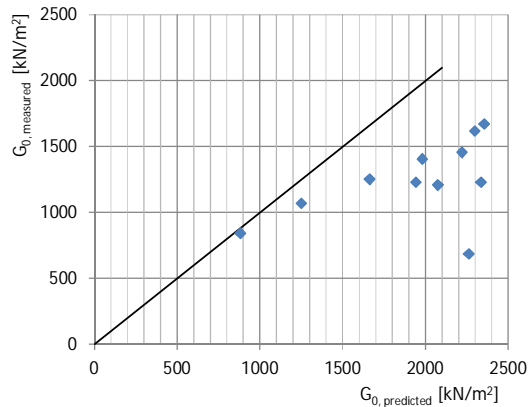


Figure 4.39 Measured and predicted G_0 using equation(4.19)

Figure 4.38 compares equation (4.19) to measurement data. The plane indicated by the coloured lines represent the equation results for $\sigma'_v = 26.5 \text{ kN/m}^2$. The dots represent the measurement data for the Nieuwolda case. It should be noted that the measurement data is depicted for their actual σ'_v which deviates slightly from $\sigma'_v = 26.5 \text{ kN/m}^2$. For each sample the loss on ignition, LOI is determined. The LOI is used to calculate the organic content, OC , by equation (2.3).

Figure 4.39 gives the relation between the measured G_0 and predicted G_0 using equation (4.19). The graph shows that equation (4.19) overestimates the G_0 values found for the Groningen peat. This also holds for the data from Siddeburen and Schildmeer, which are not shown in Figure 4.38 and Figure 4.39.

Hardin & Black (1966) proposes a relation between G_0 , e and s' , with $s' = (\sigma'_v + \sigma'_h)/2$. This equation is further elaborated in the appendix C by adding OC . This yields:

$$G_0 = \lambda (e)^M (OC)^D (s')^N \quad (4.20)$$

It should be noted that appendix C uses the denotation p' instead of s' . The fit of equation (4.20) yields, see Appendix C:

$$\begin{aligned} \lambda &= 132 \\ M &= -0.80 \\ D &= -0.85 \\ N &= 0.253 \end{aligned}$$

It should be noted that equation(4.19) includes the yield stress. Since the yield stress was not available for each sample, equation(4.19) was validated with the tests for which the yield stress is available. This selection is used to construct Figure 4.40. Appendix C validates equation(4.20) for all the available test data. Figure 4.40 shows that using equation(4.20), derived for all the data, slightly under predicts the G_0 for the selection of tests for which the yield stress was clear.

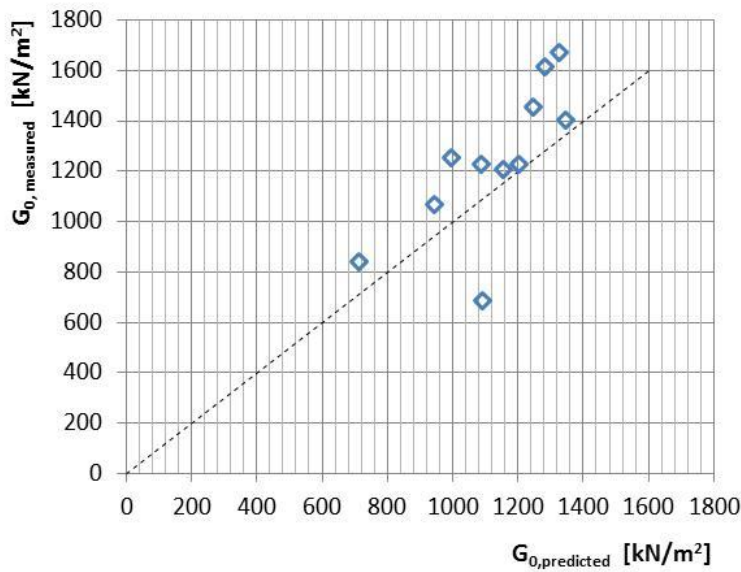


Figure 4.40 Measured and predicted G_0 for equation (4.20)

A fit based on linear least squares approach, between G_0 , OCR, OC and σ'_v yields:

$$G_0 = 22.25261 \sigma'_v + 275.0763 \text{OCR} - 11.8751 \text{OC} + 1310.686 \quad (4.21)$$

Which has a weighted least squares sum, $R^2 = 0.30$. The fit can be improved by omitting test NW1A2-C1-1D which yields $G_0 = 685$ kPa:

$$G_0 = 28.74761 \sigma'_v + 426.7729 \text{OCR} - 12.3744 \text{OC} + 1040.121 \quad (4.22)$$

Which has weighted least squares sum, $R^2 = 0.75$. Figure 4.41 shows the results for $\sigma'_v = 26.5$ kN/m². The measurement data are depicted by the dots. The red dot indicates the data point that is omitted in the derivation of equation (4.22). Figure 4.42 shows the measured versus predicted G_0 values for equation (4.22).

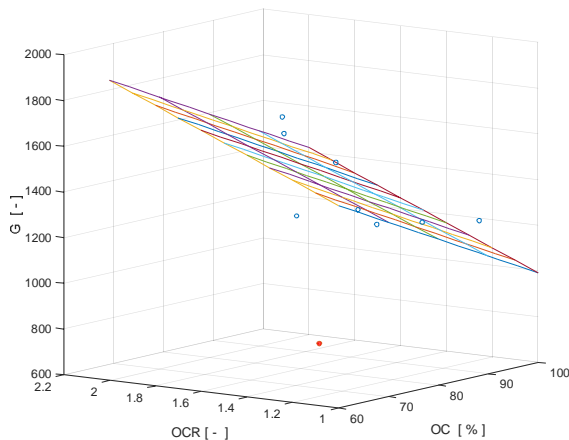


Figure 4.41 G as a function of OCR and OC for $\sigma'_v = 26.5$ kN/m². The lines represent the fit (4.22), the dots represent the measurements data, the red dot is omitted from the analysis

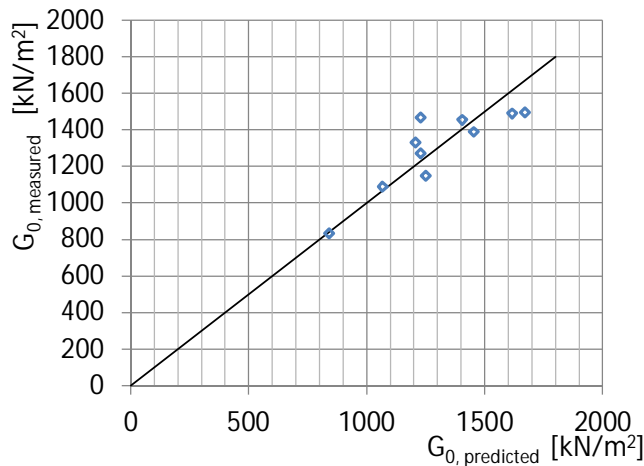


Figure 4.42 Measured and predicted G_0 using equation (4.22)

4.5 Summary and Conclusions

Chapter 4 discusses the classification parameters of the tested material. This section summarises the data and provides the following conclusions:

- The values found for the classification parameters comply with the general trends found for Dutch peats.
- The Loss on Ignition is a measure for the organic content and ranges from 70 to 90%. The trends presented in literature, see chapter 3, are usually derived from material with a lower organic content than found for the Groningen peat deposit.
- The water content ranges from 400 – 800 %, which is not exceptionally high for Dutch Peats.
- The small strain shear strain modulus, G_0 and shear wave velocity, v_s are derived from bender element measurements. G_0 ranges from 400 to 1700 kPa, v_s ranges from 15 to 40 m/s. These values comply well with the, limited, available literature data.
- For the Siddeburen site relatively high yield stresses are found for samples retrieved near the ground water table.
- In this study the difference between humified and non to moderate humified samples is shown. Differences in water content, dry density and loss on ignition support the deviation between humified and non – moderate humified.
- The differences in classification parameters for the humified and non to moderate humified samples were not only shown by a different mean value but mostly in a different coefficient of variation. This shows that the humified samples experience a larger heterogeneity than the non to moderate humified samples.
- The humified peat layers are relatively small and therefore difficult to sample. As a consequence, the number of humified samples, tested in this study, is smaller than the number of non to moderate humified samples.
- For the low stress locations, Siddeburen and Schildmeer, the transition between re-loading and virgin behaviour, as found from CRS tests, is not clearly visible unless stresses are plotted on a logarithmic scale. This makes the definition of yield stress for these tests questionable. Samples from the Nieuwolda site clearly show the transition between re-loading and virgin behaviour.
- The F and T -tests show that the samples taken from the different sites represent statistically different material in terms of density, water content and loss on ignition. This

means that averaged, overall, parameters should be used with care. Instead, correlations that reflect the local conditions will provide more accurate parameters. This can be done by using correlations between the dynamic properties and classification parameters.

- Classification parameters in general are meant for a first approximation of material behaviour. For peats, a first understanding for material behaviour comes from a combination of different classification parameters. For example section 4.3.2 shows that a correlation of the yield stress from the dry density and loss on ignition gives a more accurate result than a correlation based on the dry density alone.
- This also holds for the prediction of small strain shear modulus G_0 and shear wave velocity v_s . Although there is a clear trend between G_0 and σ'_{vy} , the accuracy of the prediction improves when parameters, reflecting the organic nature of the material, are involved. As shown by equation (4.22), G_0 can be estimated from the actual stress level, stress history and organic content. This complies to the conclusion of the literature review, section 3.7.
- There is no direct relation between the degree of humification and the small strain shear modulus, G_0 . This is to be expected since G_0 is not only a function of peat properties but also a function of stress and stress history. The influence of the differences in loss on ignition due to a different degree in humification is masked by differences in stress and stress history that also influences G_0 .
- Since G_0 is related to v_s by equation (4.18), the same conclusions hold for v_s .
- Since there is no number given to the degree of humification the dynamic properties can better be correlated to water content, dry density, solid density or loss on ignition that do have parametric value.

5 Construction of MRD-curves

5.1 Introduction

As explained in chapter 1, the aim of this study is to obtain the relevant dynamic parameters for the Groningen peat deposit in order to calculate the soil response to earthquakes. The most relevant input for this type of calculations are the shear modulus reduction curve and damping curve. The dynamic properties of Groningen peat have been assessed experimentally via the performance of Resonant Column (RC), Bender Elements (BE), Direct Simple Shear (DSS) and cyclic Direct Simple Shear (cyDSS) tests and subsequent analysis of basic parameters is shown in Chapter 4. Each of these types of tests produces data for a limited range of shear strain. To construct the shear modulus reduction and damping curves the data of the different test types need to be combined in order to obtain the curves for the entire shear strain range. This chapter combines the results of the different test types to the MRD-curves and makes a comparison to literature data. The next chapter gives a further analysis and parameter assessment. Hereafter the shear modulus reduction and damping curves are referred to as MRD-curves.

5.2 Shear modulus degradation curve

Figure 5.1 to Figure 5.3 show the degradation curves for each of the three sample locations. In each graph an average line is drawn through the data points. These average lines are drawn visually and are not based on some mathematical optimisation procedure, which will be done in chapter 6. The degradation curves combine the results of different testing devices. Each testing device has its own range in shear strain. Since there is no overlap between the resonant column tests and the DSS tests some interpretation is needed. In the NGI Resonant column tests a larger range in shear strain is applied than in the RUB tests. Figure 5.1 shows the combined data points for the different shear strains for the Nieuwolda site, Figure 5.2 for Schildmeer and Figure 5.3 for Siddeburen. The specifics of each of the sets are described below.

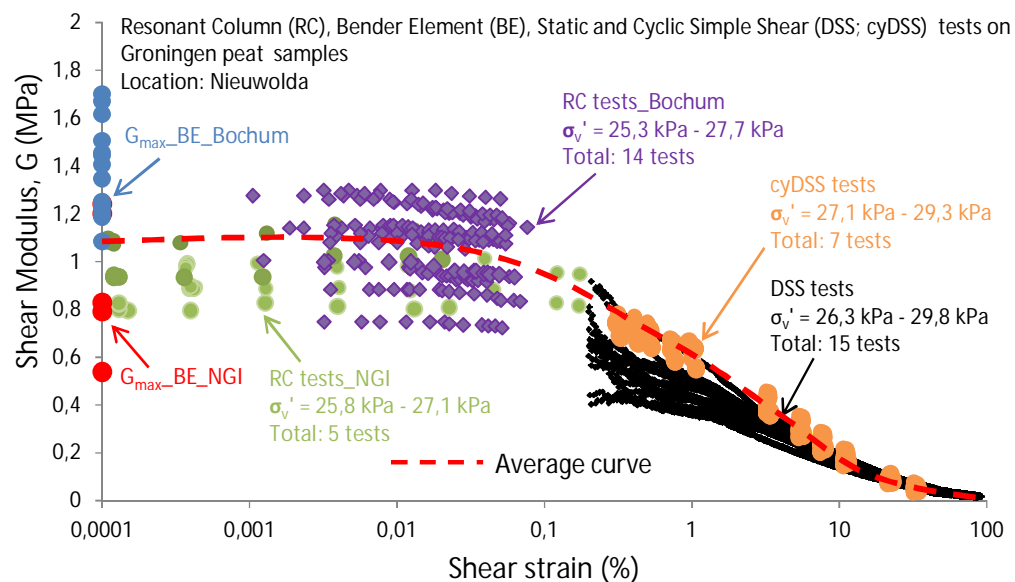


Figure 5.1 Shear modulus degradation curve for the Nieuwolda site

The G_{max} measurements on the left of the graph, smallest shear strain, show a large variation. For the Nieuwolda site, the resonant column measurements (up to 0.1% shear strain) show a nearly flat degradation curve. As a consequence the stiffness is nearly linear for shear strain up to 0.01 %. For larger strains the cyclic DSS tests have been shown on the right. These tests follow the traditional degradation shape towards negligible shear modulus at very large strains. The static DSS tests are shown for comparison reasons and appear below the average MRD curve for the cyclic tests.

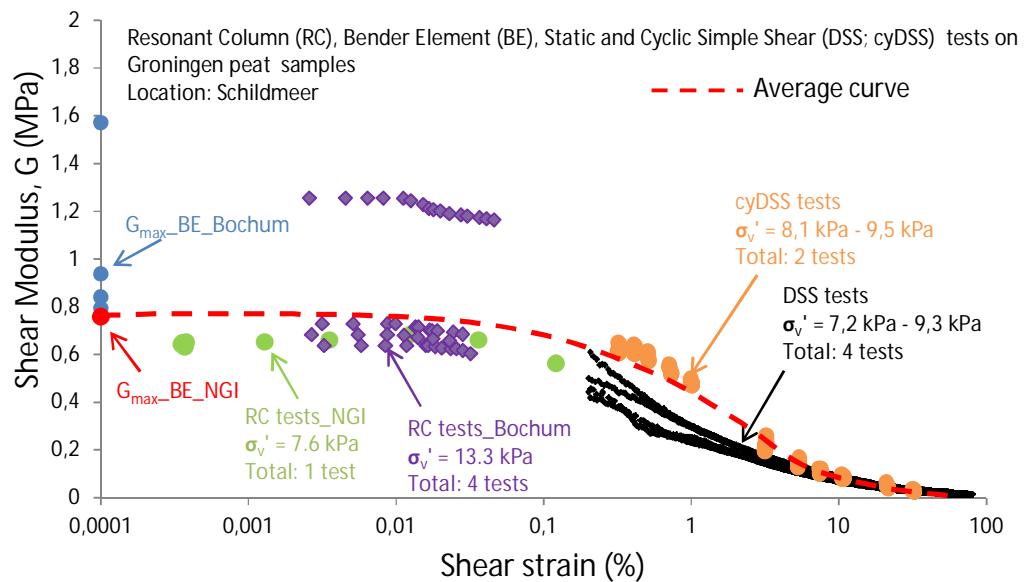


Figure 5.2 Shear modulus degradation curve for the Schildmeer site

A similar pattern is found for the specimens retrieved at the Schildmeer location, except for one test result. Figure 5.2 shows that results of one RUB resonant column test deviates strongly from the other results. These are the results of test SM2C-A3-1A. This is the only specimen from the Schildmeer location that is classified as humified. However the differences in loss on ignition, water content or density with the non-humified samples seem too small to explain the observed difference.

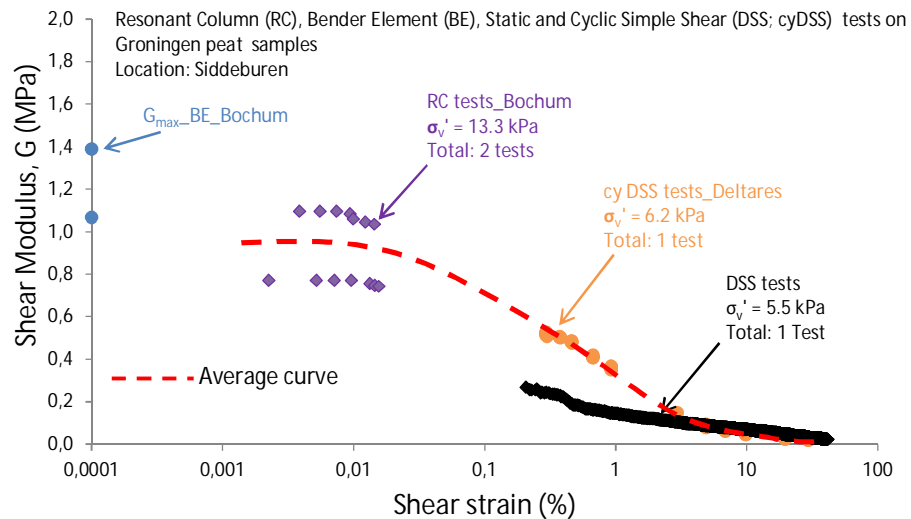


Figure 5.3 Shear modulus degradation curve for the Siddeburen location

The Siddeburen site has fewer test results, but in general follows the same trends. The static DSS test results are however found well below the dynamic line. The graphs show that for shear strain in excess of 0.2%, a difference among the shear modulus values can be observed for samples subjected to cyclic simple shear loading compared to the samples subjected to static simple shear loading. The latter ones exhibit for the same level of shear strain lower shear modulus values.

This behaviour is in agreement with existing findings in the literature on testing sands and clays. Only at extremely small strain, below 0.001%, the maximum stiffness does not appear to be affected by the type of loading, monotonic or cyclic. The coincidence of G_{max} between monotonic and cyclic loading tests has been observed for various types of sands, gravels, clays as sheared in torsional shear, in plane strain compression and in triaxial compression (Iwasaki et al., 1978; Bolton & Wilson, 1988; Shibuya et al., 1990; Shibuya et al., 1992;). Tatsuoka & Shibuya (1992) consider that at small strains (0.0001% - 0.001%) the soil behaviour is essentially elastic and therefore the same elastic initial tangent modulus (or small strain stiffness) is expected from monotonic and cyclic tests. As stated from Bolton and Wilson (1990) a practical implication of the coincidence of G_{max} amongst these types of loading is that G_{max} under dynamic loading conditions can be reliably evaluated by monotonic loading tests. However it was observed that for higher strain levels the stress-strain response of a soil element subjected to monotonic loading is softer than that to cyclic loading for both cohesive and cohesionless soils (Bolton & Wilson, 1988; Teachavorasinskun et al., 1991; Shibuya et al. 1992; Lo Presti et al. 1997). It should be noted that due to inaccuracy of the measurement of small displacements for the static DSS tests, data for shear strain < 0.2 % are considered unreliable and therefore not shown.

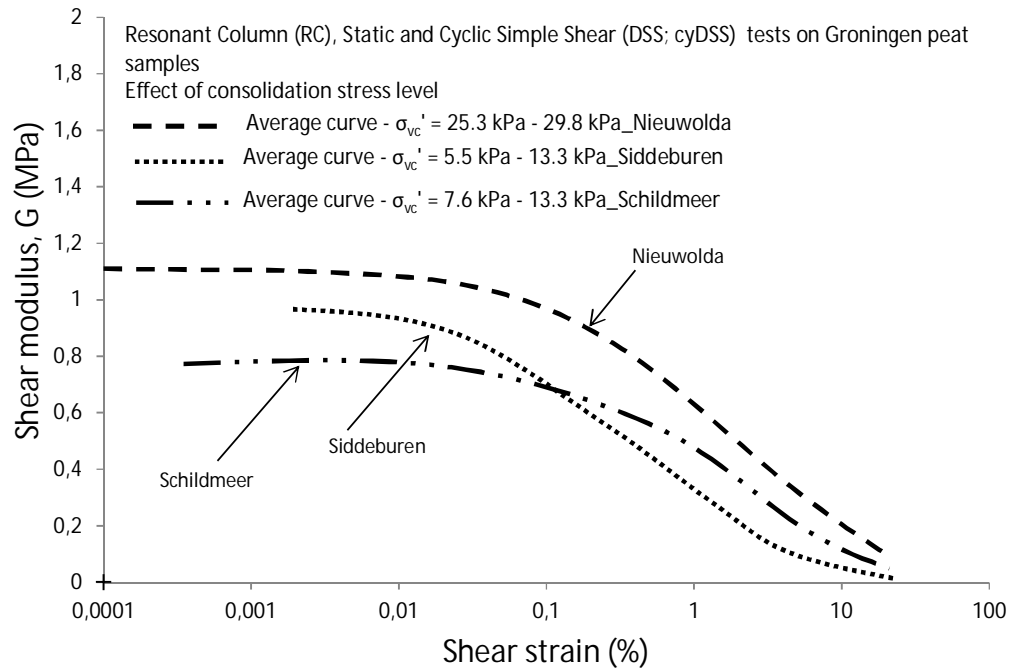


Figure 5.4 Comparison of general fit between the different sample locations

Figure 5.4 shows a comparison between the general fits found for the different sample locations. It should be noted that for the Siddeburen site only one resonant column and two cyclic DSS tests are conducted. The differences between the Nieuwolda and Schildmeer results can be explained by differences in stress level for which tests have been conducted.

5.3 Trends in shear modulus reduction curve

5.3.1 Normalised graphs

For normalization of the data the G_{max} value was taken as the largest measured secant shear modulus during RC testing, typically at shear strains of $\gamma < 0.003\%$. The specimens on which DSS and cyclic DSS tests have been conducted were taken directly adjacent to the specimens that have been used for resonant column testing. The DSS and cyclic DSS data were normalized by G_{max} values found for the adjacent resonant column specimen.

It can be observed that the Groningen peat samples exhibit shear modulus values that are almost linear up to approximately $\gamma = 0.01\%$. With increasing strain levels the shear modulus values decrease progressively. In Figure 5.5 to Figure 5.7 an average curved line that is considered to best-fit the experimental data is shown with red dashed line style. Appendix C discusses an analysis made by RUB on the RUB data. In this paragraph the general findings of Appendix C are repeated and applied to the entire dataset. The best fit for the Figure 5.5 to Figure 5.7 are based on equation(5.1),

$$\frac{G}{G_{max}} = \frac{1}{1 + \beta \left(\frac{\gamma}{\gamma_{ref}} \right)^\alpha} \quad (5.1)$$

In which α and β are fit parameters and γ_{ref} represents a reference shear strain. Two methods are applicable to determine the value of γ_{ref} . The first method is to estimate γ_{ref} using the equations proposed by Hardin & Drnevich (1972) in which $\gamma_{ref} = \tau_{max} / \gamma_{max}$.

The second method assumes that the value of γ_{ref} represents the strain level for which $G/G_{max} = 0.5$, as given by Stokoe et al (1999). This is valid if experimental data encompassing $G/G_{max} = 0.5$ is available. Using this approach yields that $\beta = 1$.

Figure 5.5 to Figure 5.7 shows the normalised shear modulus reduction curves and a fit by equation(5.1). For each location $\alpha = 0.8$, $\beta = 1.0$ and γ_{ref} defined as the strain level for which $G/G_{max} = 0.5$. The obtained values for γ_{ref} are summarized in Table 5.1.

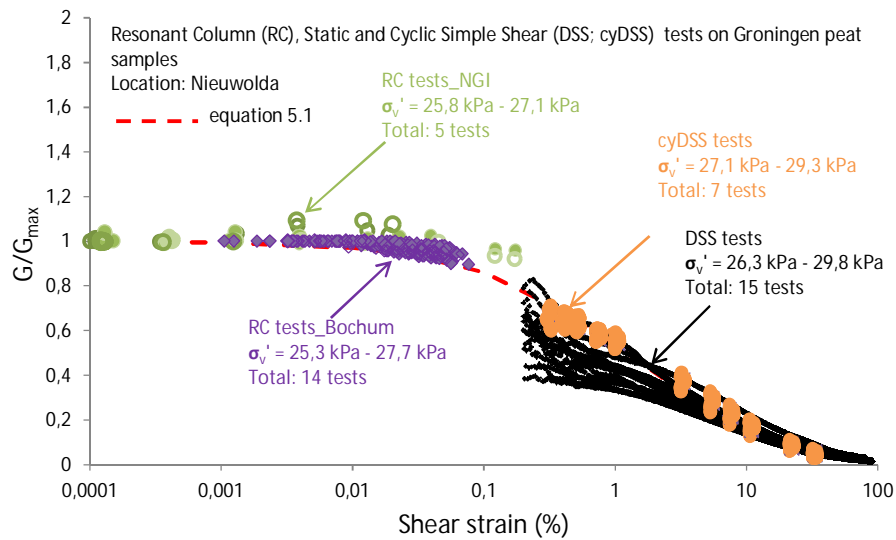


Figure 5.5 Normalised shear modulus reduction curve and best fit for Nieuwolda data, red dashed line gives equation (5.1) with the parameters given in Table 5.1

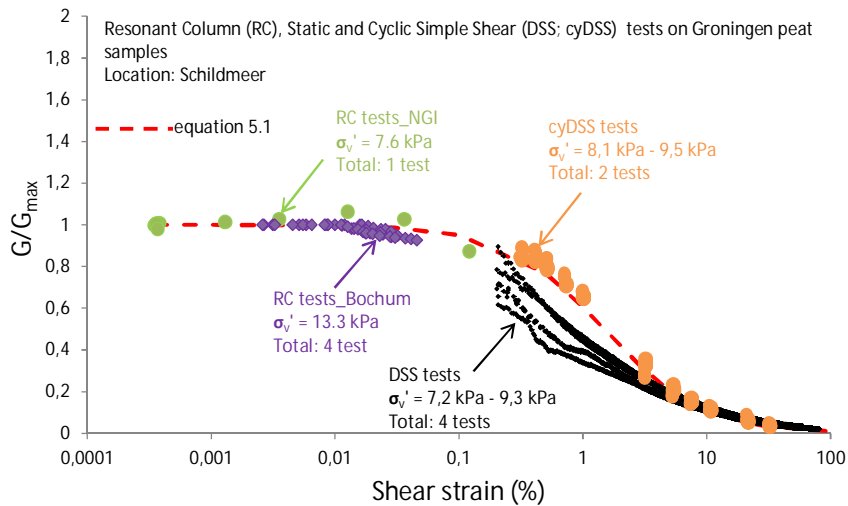


Figure 5.6 Normalised shear modulus reduction curve and best fit for the Schildmeer data, red dashed line gives equation (5.1) with the parameters given in Table 5.1

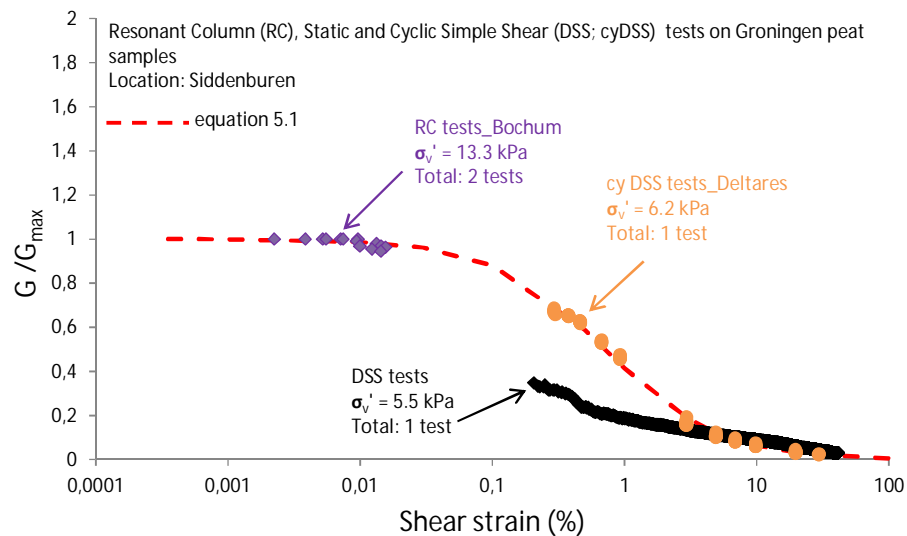


Figure 5.7 Normalised shear modulus reduction curve and best fit for Siddeburen data, red dashed line gives equation (5.1) with the parameters given in Table 5.1

Location	γ_{ref} [%]
Nieuwolda	1.00
Schildmeer	1.65
Siddeburen	0.80

Table 5.1 γ_{ref} for the three locations

Figure 5.5 to Figure 5.7 shows that with one set of values for α and β the curves for the three locations can be reproduced. Figure 5.8 to Figure 5.10 show the shear modulus degradation

curve normalised for the mean effective stress, $s' = (\sigma'_v + \sigma'_h)/2$. For the Nieuwolda case the results of the different test types agree well, while for the Schildmeer and Siddeburen location the cyclic DSS results seem not to comply to the resonant column results.

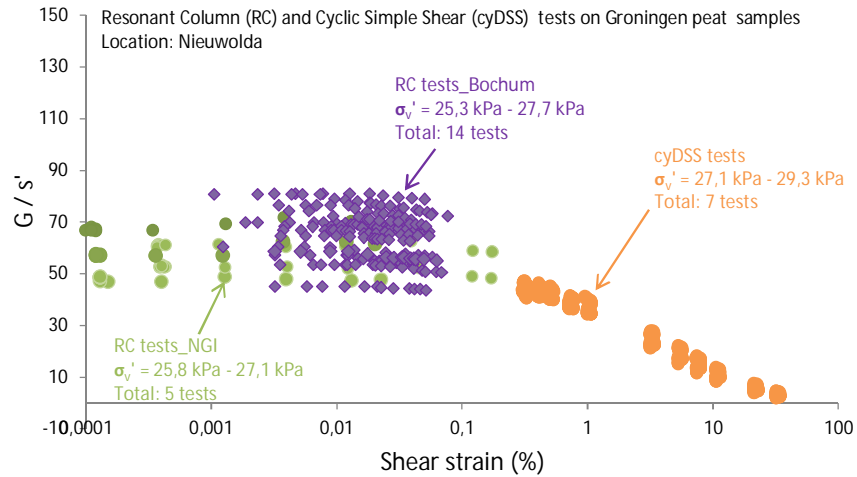


Figure 5.8 Shear modulus degradation curve, normalised for $s' = (\sigma'_v + \sigma'_h)/2$ for location Nieuwolda

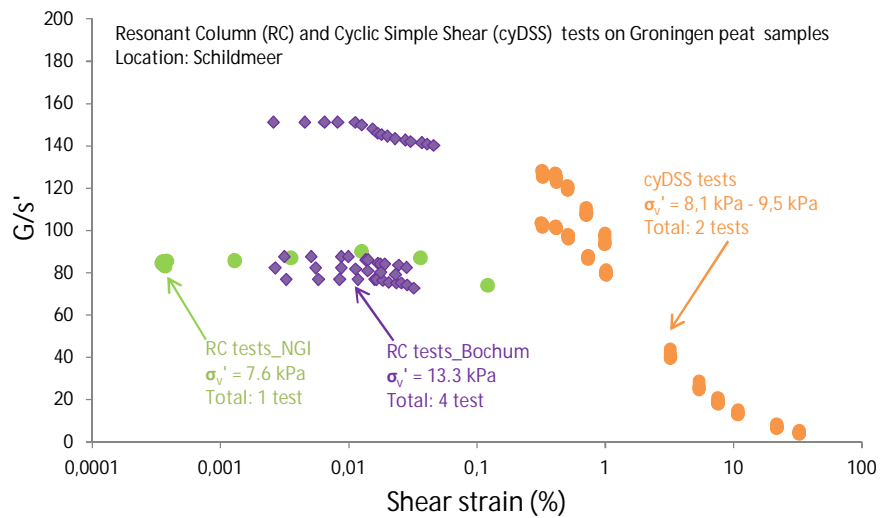


Figure 5.9 Shear modulus degradation curve, normalised for $s' = (\sigma'_v + \sigma'_h)/2$ for location Schildmeer

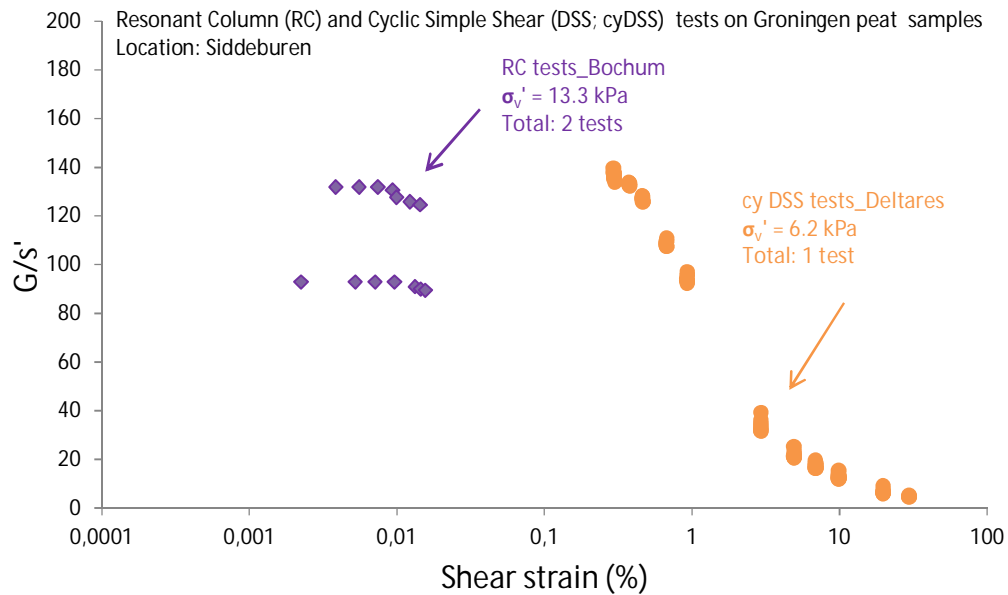


Figure 5.10 Shear modulus degradation curve, normalised for $s' = (\sigma_v' + \sigma_h')/2$ for location Siddeburen

Alternatively, it was suggested by Green & Rodriguez (2017) to plot G/s'^n , with $n = 0.4$ on the vertical axis of Figure 5.8 to Figure 5.10. Figure 5.11 to Figure 5.13 show the results. For the Schildmeer and Siddeburen tests, $n = 0.4$ results in a better agreement between the cyclic DSS test results and the resonant column test results than found for $n = 1$.

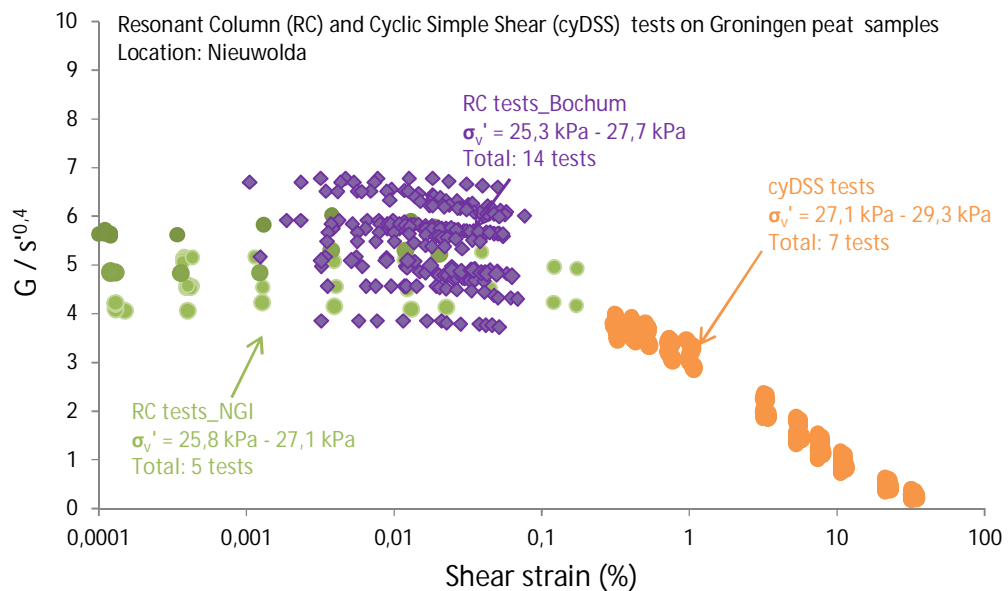


Figure 5.11 Shear modulus degradation curve, with $n = 0.4$, for location Nieuwolda

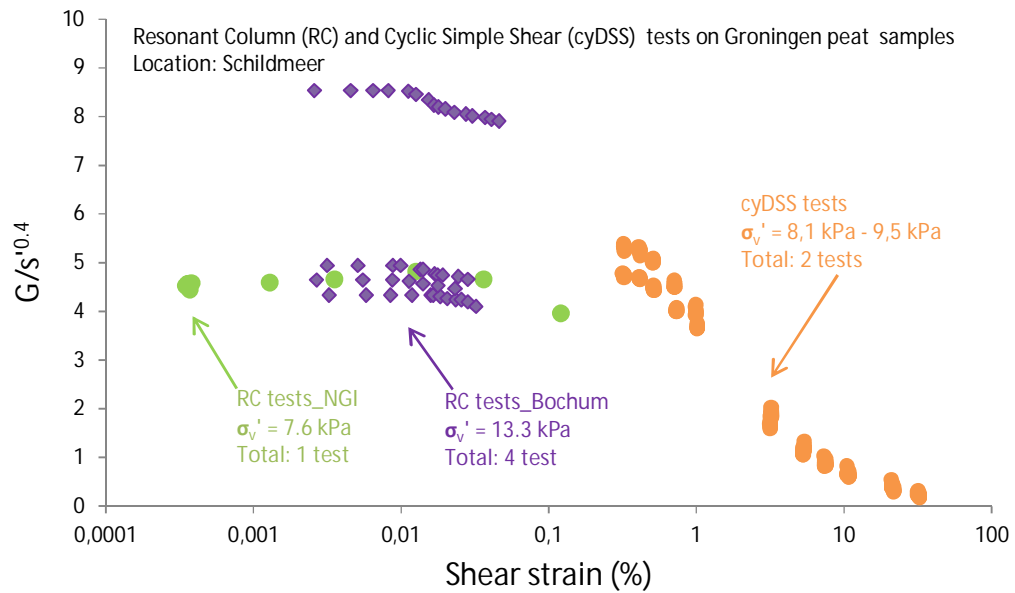


Figure 5.12 Shear modulus degradation curve, with $n = 0.4$, for location Schildmeer

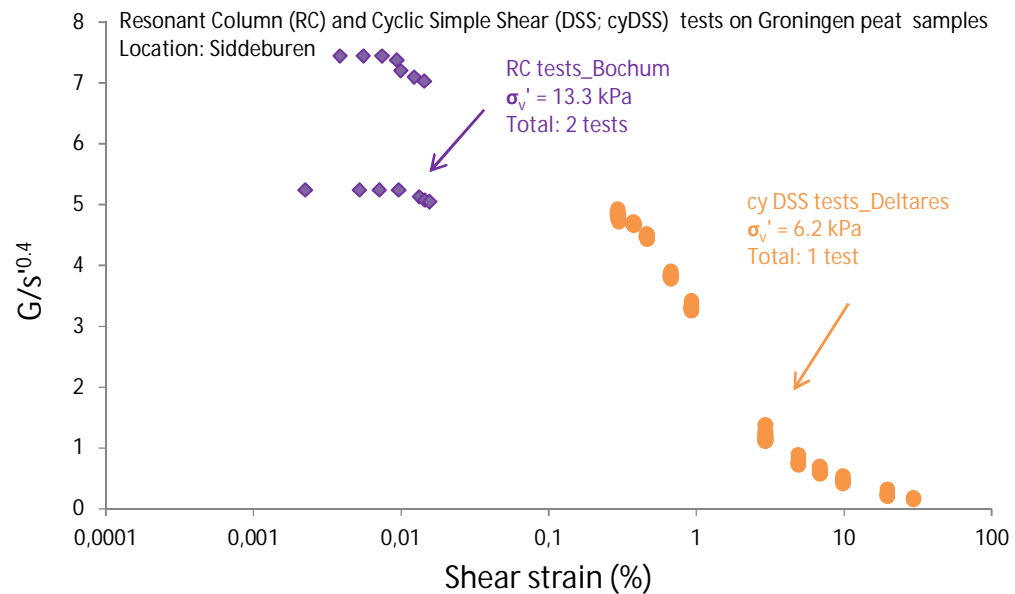


Figure 5.13 Shear modulus degradation curve, with $n = 0.4$, for location Siddeburen

For the Schildmeer location it seems if two different materials have been tested. The NGI test and three RUB tests show results that comply well with the Nieuwolda results, while one RUB test, SM2C-A3-1A, and both cyclic DSS tests, SM2C-A3-1C and SM2C-B1-2C, provide a deviating shear modulus degradation graph. The deviating graph lies well above the other results. To check if the different behaviour can be explained by differences in material

characteristics, Table 5.2 shows the classification parameters for the Schildmeer tests, while Table 5.3 shows the stress conditions at which the tests have been conducted.

ID	test type	depth [NAP m]	γ_t [kN/m ³]	γ_d [kN/m ³]	γ_s [kN/m ³]	w [%]	LOI [%]
SM2C-C1-2	RC-NGI	-3.75	10.15	1.53	14.47	565	72.7
SM2C-A2-1B	RC-RUB	-3.14	10.29	1.35	14.56	660	88.4
SM2C-B1-1A	RC-RUB	-3.39	9.90	1.15	14.49	747	87.9
SM2C-C1-1A	RC-RUB	-3.41	11.80	1.46	14.50	689	87.8
SM2C-A3-1A	RC-RUB	-3.57	10.50	1.57	15.06	557	79.9
SM2C-A3-1C	cyDSS	-3.68	8.90	1.51	16.49	491	73.9
SM2C-B1-2C	cyDSS	-3.78	9.30	1.57	17.93	484	60.8

Table 5.2 Comparison of the Schildmeer data, Tests SM2C-A3-1A, SM2C-A3-1C and SM2C-B1-2C, result in larger G/s' values

ID	test type	σ'_v [kN/m ²]	σ'_h [kN/m ²]	s' [kN/m ²]
SM2C-C1-2	RC-NGI	7.6	7.6	7.6
SM2C-A2-1B	RC-RUB	13.3	3.3	8.3
SM2C-B1-1A	RC-RUB	13.3	3.3	8.3
SM2C-C1-1A	RC-RUB	13.3	3.3	8.3
SM2C-A3-1A	RC-RUB	13.3	3.3	8.3
SM2C-A3-1C	cyDSS	8.1	2.0	5.1
SM2C-B1-2C	cyDSS	9.5	1.7	5.6

Table 5.3 Comparison of the Schildmeer data, Tests SM2C-A3-1A, SM2C-A3-1C and SM2C-B1-2C, result in larger G/s' values

The differences in applied stress level are small and therefore not considered to be the cause of the differences in test results. Table 5.2 shows the differences in classification parameters. The deviating tests SM2C-A3-1A, SM2C-A3-1C and SM2C-B1-2C have a lower water content, a higher particle density and lower LOI than the other tests. It should be noted that SM2C-A3-1A and SM2C-A3-1C are classified as humified peat while the other samples are classified as non to moderate humified peat. For specimen SM2C-B1-2C, which is classified as non to moderate humified, the water content, LOI and densities seem to agree with humified values. This specimen could have been wrongly classified as non-moderate humified.

For the Siddeburen case the cyclic DSS test results do not comply with the resonant column test. It should be noted that in resonant column testing the horizontal stress is applied by the cell pressure and therefore known for each test. In normalizing the cyclic DSS test data the K_0 value is used which is found from K_0 -CRS tests conducted on specimens that were sampled directly above or below the cyclic DSS samples. For the Siddeburen case the K_0 -CRS test shows a low K_0 -value, $K_0 = 0.14$. This low value might result in a high G/s'. The applied K_0 value might have been too low, although for the Nieuwolda case K_0 -values have been used in the range of 0.12 – 0.25.

5.3.2 Comparison with literature data

Figure 5.14, Figure 5.15 and Figure 5.16 show a comparison of the test results to literature data. The results of the tests on Groningen peat correspond to the literature data. It should be noted that organic content of the Groningen samples is larger than the organic contents reported for the literature data given in Figure 5.14. The consolidation stress applied in the Groningen test series seem low, compared to the literature data. The literature review in chapter 3 indicates that both organic content and consolidation stress influences the shear modulus degradation curve. Both effects might counterbalance each other, resulting in a good agreement between the Groningen data and the literature data.

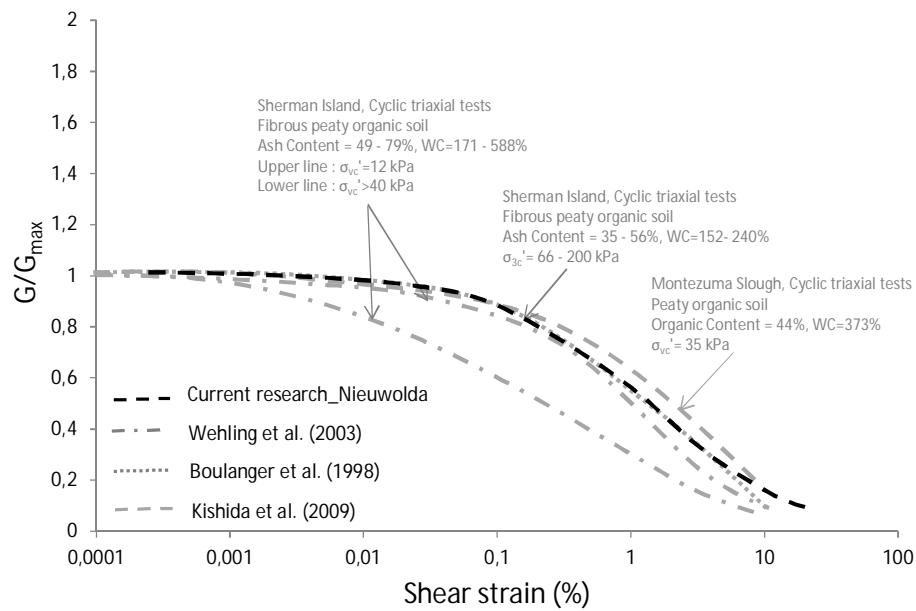


Figure 5.14 Comparison Nieuwolda test results to literature data

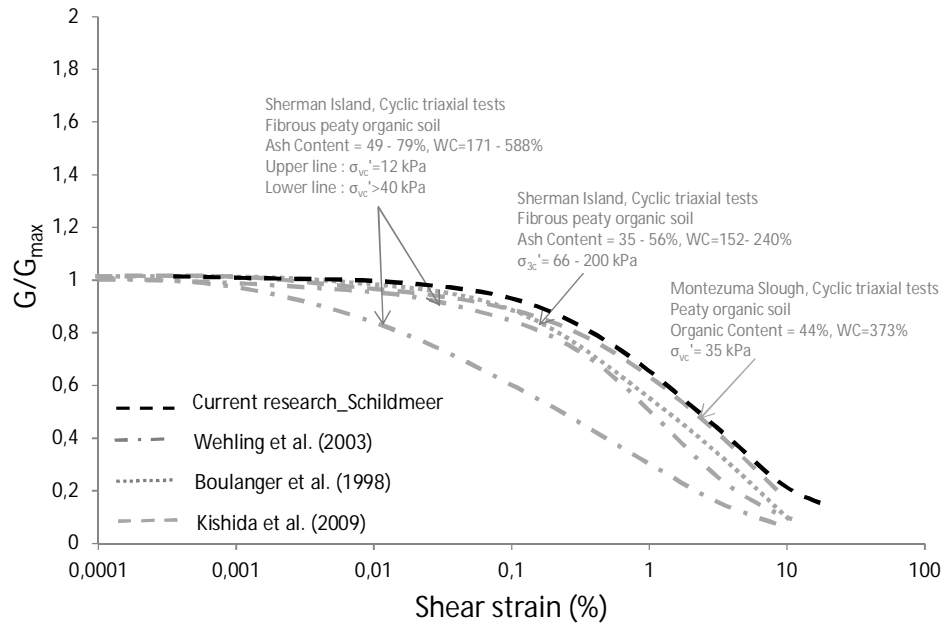


Figure 5.15 Comparison Schildmeer test results to literature data

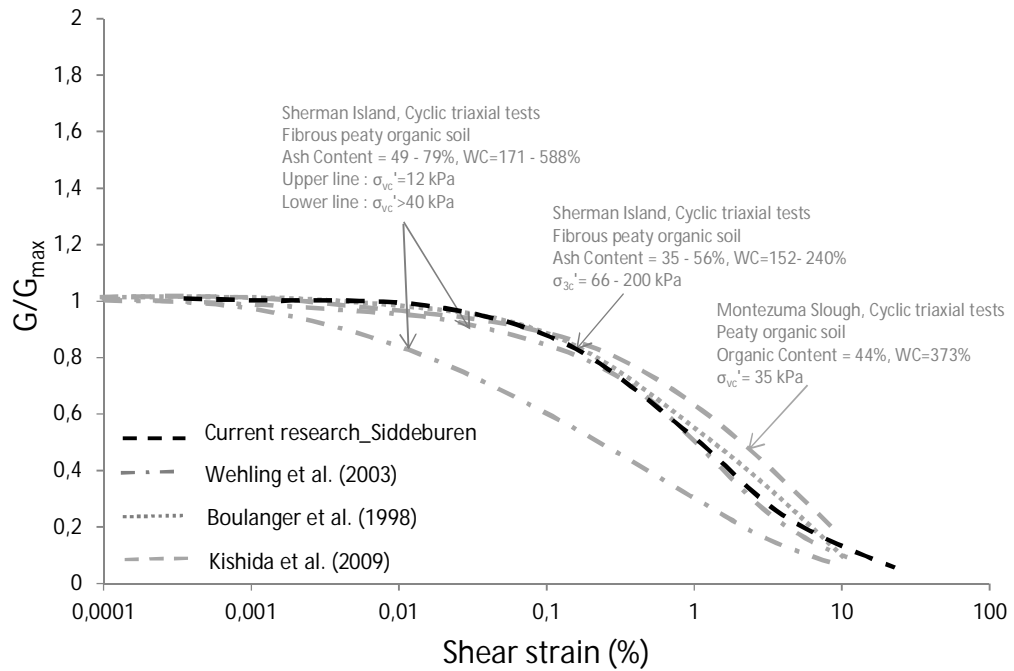


Figure 5.16 Comparison Siddeburen test results to literature data

5.4 Damping curve

Figure 5.17 to Figure 5.19 show the damping curves for the three different locations. In plotting the damping curve the data shows more scatter than found for the shear modulus degradation curve. For each location a curve through the data is drawn visually. This curve is indicated as average curve in the successive figures.

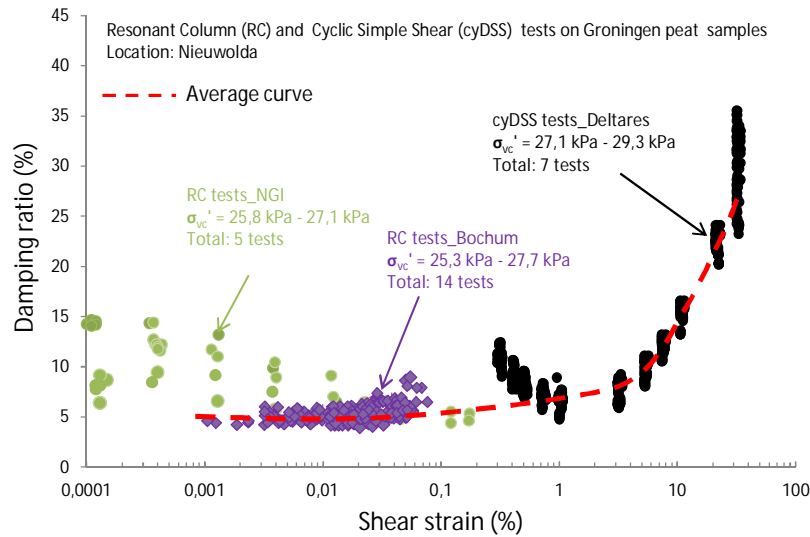


Figure 5.17 Damping curve for the Nieuwolda data

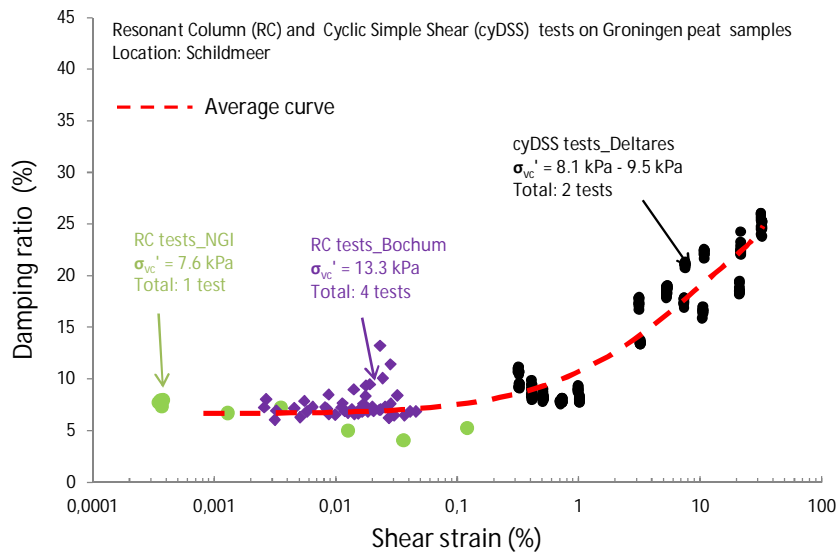


Figure 5.18 Damping curve for the Schildmeer data

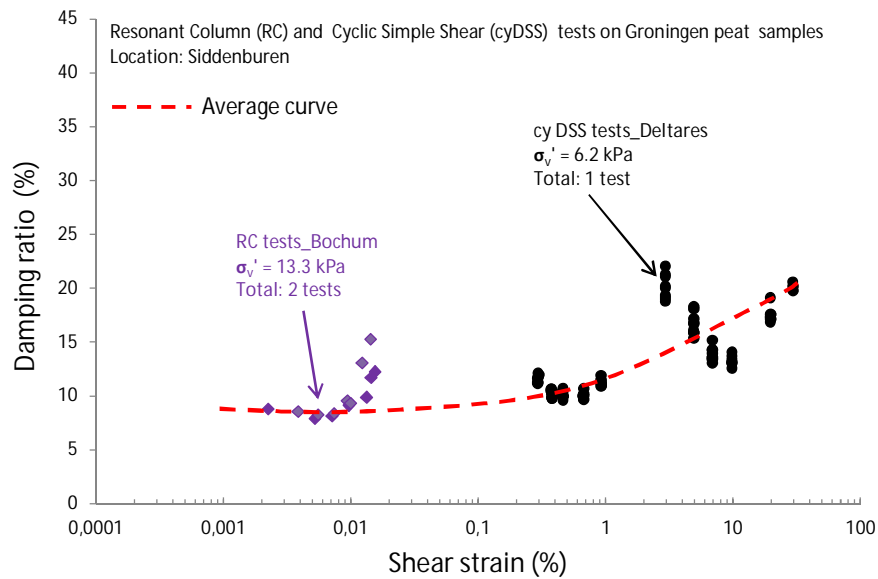


Figure 5.19 Damping curve for the Siddeburen data

The NGI data show an (initial) decrease in the damping parameter D for increasing shear strain, γ . As indicated by NGI in their report this behaviour is inconsistent with the general behaviour. This is most visible in the Nieuwolda data, Figure 5.17. For shear strain in the range of $0.01\% < \gamma < 0.1\%$ the NGI and RUB data converge nicely. For Schildmeer and Siddeburen location, some RUB data seem to show a dramatic increase for $\gamma > 0.01\%$. This increase is larger than expected from the average curve.

For the cyclic DSS tests the results for shear strains smaller than 1% seem to deviate from the average curve. This might be explained by measurement inaccuracies, like stiffness of the device, rings and membrane.

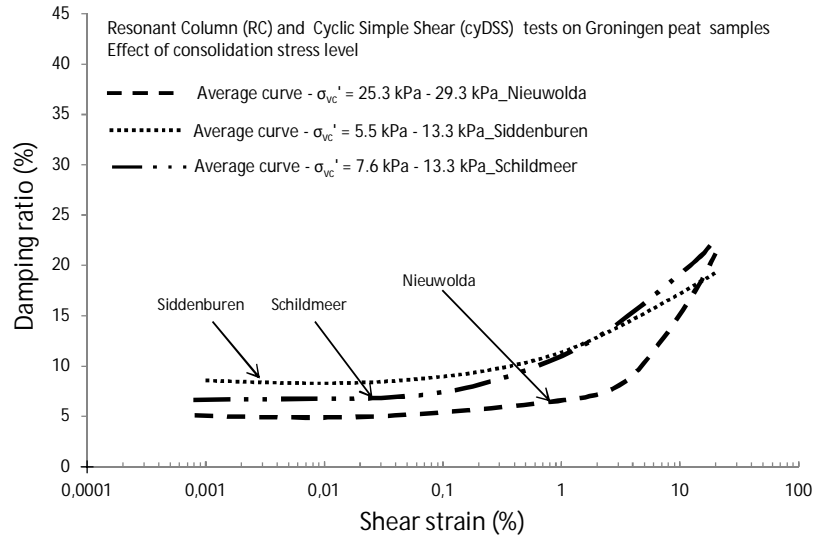


Figure 5.20 Summary of average damping curves for the three locations

Figure 5.20 shows the average curves for each of the three locations. It should be noted that Siddenburg curve is based on a small number of tests. The differences between the Schildmeer and the Nieuwolda curves can be explained by differences in stress level at which the tests are conducted. It should be noted that the specimens are consolidated at the field stress, which is below the yield stress. From literature it is known that the damping ratio decreases with increasing stress level. The Groningen data seem to follow this trend; the Schildmeer curve, low stresses, lies above the Nieuwolda curve found at higher stress level.

Appendix C suggests equation (5.2) to fit the data. Figure 5.21 to Figure 5.23 compares the test data to the best fit using equation (5.2) and the parameters given by Table 5.4 for each of the sample locations.

$$\frac{D}{D_{min}} = A \left(\frac{\gamma / \gamma_{ref}}{1 + \gamma / \gamma_{ref}} \right)^B + 1 \quad (5.2)$$

in which

- γ_{ref} = reference shear strain
- A, B = fitting parameters
- D_{min} = damping at small shear strain amplitude

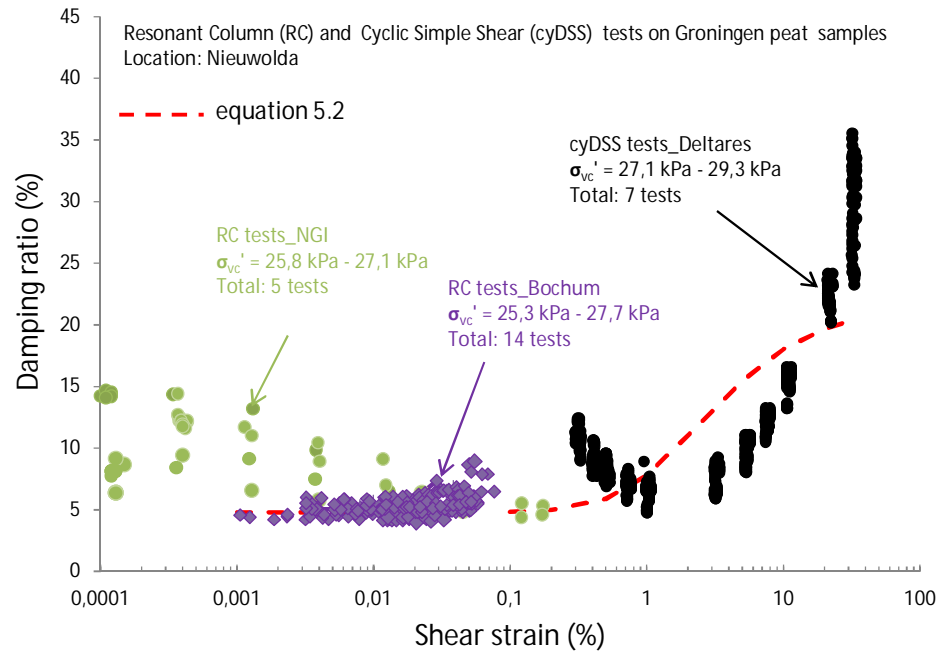


Figure 5.21 Fit Damping curve Nieuwolda data, red dashed line gives equation (5.2) and parameters from Table 5.4

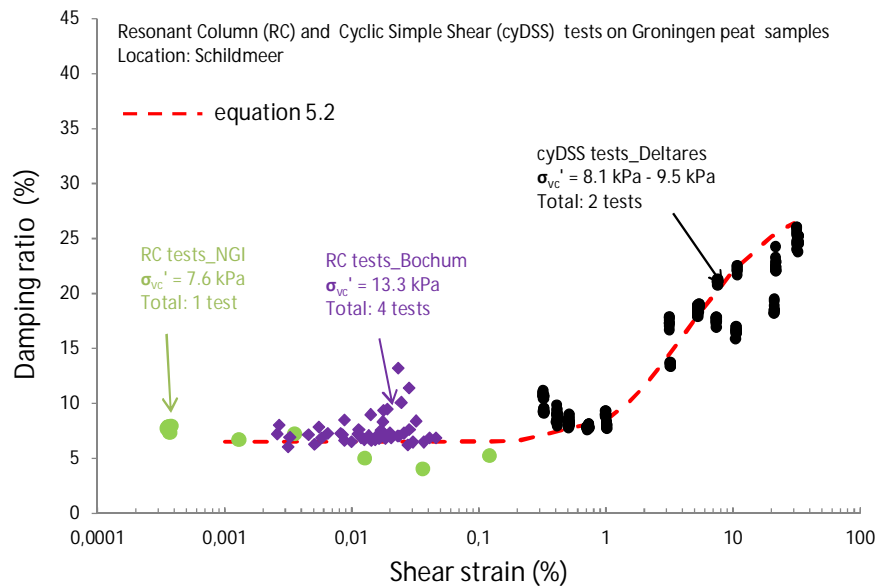


Figure 5.22 Fit Damping curve Schildmeer data, red dashed line gives equation (5.2) and parameters from Table 5.4

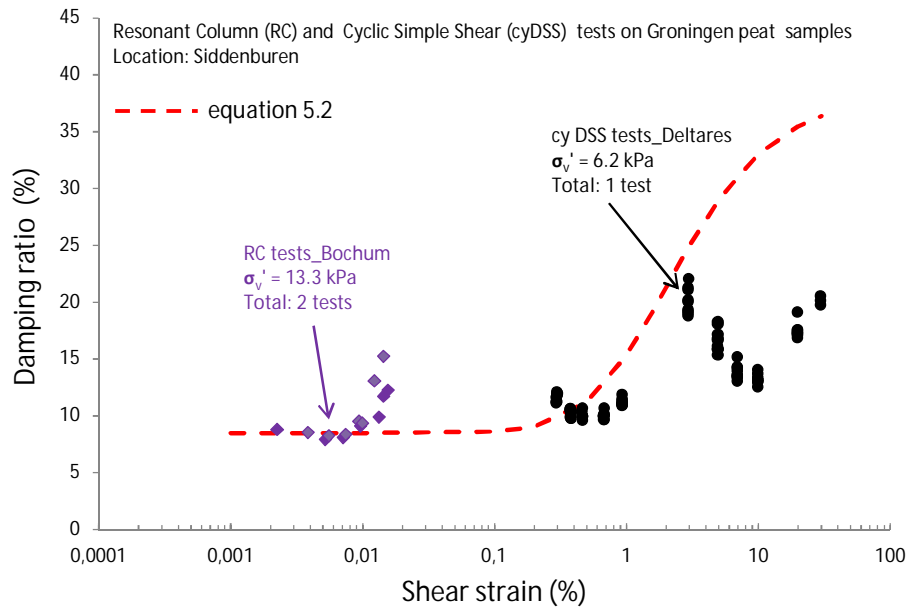


Figure 5.23 Fit damping curve Siddeburen location, red dashed line gives equation (5.2) and parameters from Table 5.4

parameter	Nieuwolda	Schildmeer	Siddeburen
A	3.5	3.5	3.5
B	2.5	2.5	2.5
D_{\min} [%]	4.8	6.5	8.5
γ_{ref} [%]	1.0	1.65	0.8

Table 5.4 Fitting parameters for equation (5.2) for each of the sample locations

5.5 Trends in damping curve

The dynamic properties of highly organic soils have been reported in a limited number of studies in the literature (Seed and Idriss, 1970; Boulanger et al., 1998; Kramer, 2000; Wehling et al., 2003; Tokimatsu and Sekiguchi, 2007; Kishida et al., 2009).

A comparison of the dynamic behaviour of the Groningen peat samples to those of other researchers that performed tests on organic soils (Boulanger et al., 1998; Wehling et al., 2003; Kishida et al., 2009) is presented in Figure 5.24 for the damping curve.

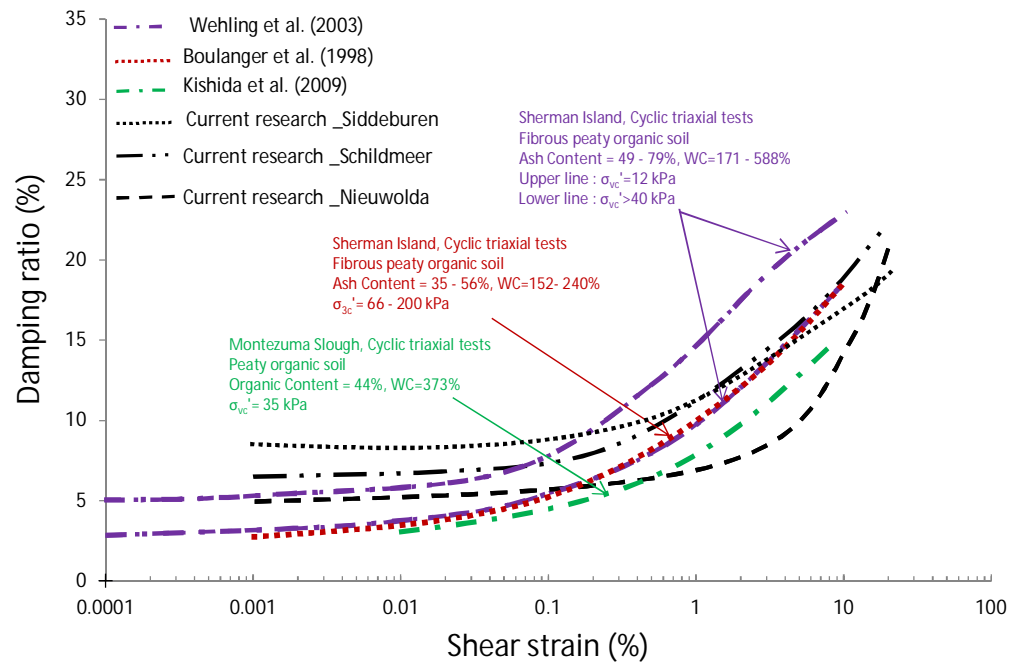


Figure 5.24 Comparison damping curve current research (black dashed lines) with literature data

To facilitate comparison among the testing data presented in these figures it is considered essential to clearly state the testing conditions (consolidation stress, testing mode) and the type of the tested soils (in terms of percentage of organic content) that correspond to each data series. The applied consolidation stress level and the percentage of organic content had been identified as two of the dominant factors that affect the dynamic behaviour of organic soils (Kishida et al., 2009; Kramer, 2000) while comparison of data from samples subjected to different testing modes (triaxial, resonant column, torsional shear) did not show any significant effect of shearing direction on the dynamic parameters, G , G/G_{max} or D (Kishida et al., 2009).

Wehling et al. (2003) performed a total of 25 cyclic triaxial tests on isotropically consolidated fibrous peaty organic soils. Samples were taken from the Sherman Island in California and had ash contents that ranged from 35% to 79% (52% average) and were tested at their in situ vertical stress. It should be noted that the ash content is the complement of the organic content. So, an ash content in the range of 35 % to 79 % refers to an organic content in the range of 65 – 21%. The mean damping ratio and the normalized shear modulus degradation data from these tests are shown with purple dashed lines in Figure 5.24 respectively for two sets of consolidation stress ($\sigma_{vc}' = 12$ kPa and $\sigma_{vc}' > 40$ kPa).

The dynamic properties of the Sherman Island's fibrous peaty organic soils had also been examined by Boulanger et al. (1998). The samples tested at this study had ash contents of 35% to 56%, organic content of 65% - 44%. In total a number of 12 cyclic triaxial tests were performed on samples isotropically consolidated to a range of stresses of 66 kPa to 200 kPa.

In the same figures the damping curve of an organic highly decomposed soil from the Montezuma Slough area in California (Kishida et al. 2009) is shown with green dashed line. The tested sample had an organic content of 44% and was subjected to triaxial testing after isotropic consolidation at in situ vertical stress.

It can be concluded from Figure 5.24 that:

- The influence of consolidation stress on the damping ratio values is more evident at low stress levels. As stated by Wehling et al. (2003) there might be some threshold consolidation stress above which the G and D relations for organic soils are relatively independent of consolidation stress. At this threshold value the fiber matrix is believed to have reached a condition where further increases in σ_{vc}' do not significantly change the relative micro mechanisms of nonlinearity and the damping relation is relatively unaffected. This appears to be the case for the damping ratio data from Boulanger et al. (1998) that are not influenced by a raise of consolidation stress ranged from 66 kPa to 200 kPa. The observed behaviour might be related to the peat samples from this series of tests having a yield stress that was close to, or greater than 200 kPa. The effect of consolidation stress on the damping data for the Groningen peat samples is evident at least for the range of stresses considered. The D values with $\sigma_{vc}'=5.5$ kPa – 13.3 kPa show the tendency of being higher than that of samples with $\sigma_{vc}'=25.3$ kPa – 29.3 kPa.
- In general it can be concluded that the damping ratio curves for the Groningen peat samples fell approximately within the area of values for organic soils. Nevertheless the Groningen peat damping data for both sets of consolidation stresses and for shear strains higher than 0.01% tend to be lower when compared to the other published data for similar stress levels. This behaviour might be attributed to the fact that the tested Groningen peat samples had the highest organic content, ranged from 60% to 95%, compare to the other test data. As concluded by Kishida et al. (2009) the samples with the higher OC tend to have - for similar consolidation stress - lower damping ratio values than the samples with lower OC. In any case, differences in damping behaviour could also be attributed to the differences in the organic components' characteristics of each series of tests (fibrous, decomposed or amorphous soil structure).

6 Parameter Assessment

6.1 Introduction

In this chapter an empirical relation for the MRD curves for use in the soil response calculations is derived. Rather than deriving a complete new relation use is made of the functional form of two available relations, (Darendeli, 2001) and (Kishida et al, 2009). These relations are given in detail in annex B. Chapter 6 seeks a relation for the entire range of tested shear strain. Tailor made correlations for specific strain ranges can be made, if required in later studies. So far, the three sites, Nieuwolda, Siddeburen and Schildmeer have been dealt with separately. However in practical application it is preferred to have general MRD curves that can be applied for the entire Groningen area instead of having different curves for which the exact area of application is not known. Therefore, the data of the three locations are combined in section 6.4 to derive general applicable relations for the entire Groningen area.

Darendeli (2001) derived general expressions for the MRD curves for sand and clay, no expressions for peat were derived. As part of the development of version 2 Ground Motion Equations for Groningen a separate set of equations was derived using a larger dataset of published test results on peat. This is described in section 7.6 of (Bommer et al, 2015). As functional form the expressions by Darendeli (2001) were used, resulting in a much simpler form as the set of expressions by Kishida (2009). The organic content is not a parameter in the derived expressions. Contrary to the expressions by Darendeli (2001) also the frequency and the number of cycles is not included as parameter as well. These parameters were not included as the number of available test data was considered to be too limited for determining the possible effect of these parameters on the MRD curves with sufficient reliability.

Kishida et al (2009) derived a set of equations using test data from the Sacramento-San Joaquin Delta (Sherman Island, Clifton Court, Montezuma Slough). In this set of equations the organic content is taken into account as a parameter determining the MRD curves.

An advantage of the expression by Kishida (2009) is that the organic content is included as a parameter. This makes it possible to also derive the MRD curves for clayey peat and organic clay. A disadvantage is the complex nature of their set of expressions.

In this chapter first a comparison of the results of the tests on Groningen peat with these two empirical relations, Bommer et al (2015) and Kishida (2009) is made in section 6.2. Next, section 6.3, the test data for the three locations (Nieuwolda, Schildmeer and Siddeburen) are matched to the functional form of Darendeli (2001). Section 6.4 gives a comparison to literature data and section 6.5 provides the proposed relations.

6.2 Comparison of test data with existing MRD curves

The three sets of test data first will be compared with the two existing correlation curves, from Bommer et al (2015) and Kishida (2009), for peat. For each location first the relevant material parameters for drafting the empirical lines are given. Figure 6.1 to Figure 6.6 show the graphs of the resulting MRD curves per location.

Nieuwolda

$$\sigma'_v = 27 \text{ kPa}$$

$$K_0 = 0.35$$

$$\text{OC} = 87\%$$

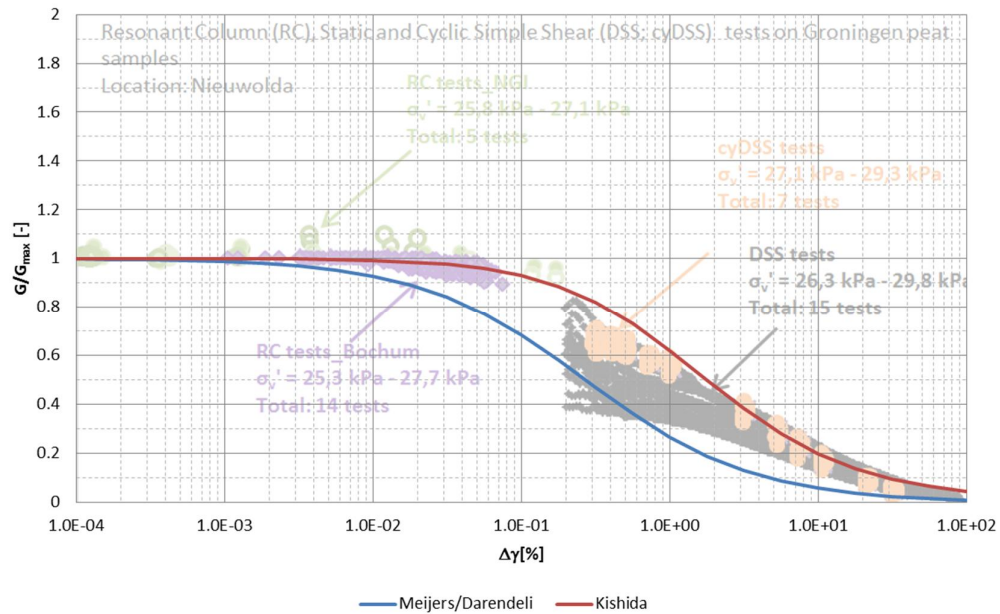


Figure 6.1 Comparison measured shear modulus reduction curve with existing empirical curves, Meijers/Darendeli refers to the curves according to section 7.6 of (Bommer et al 2015).

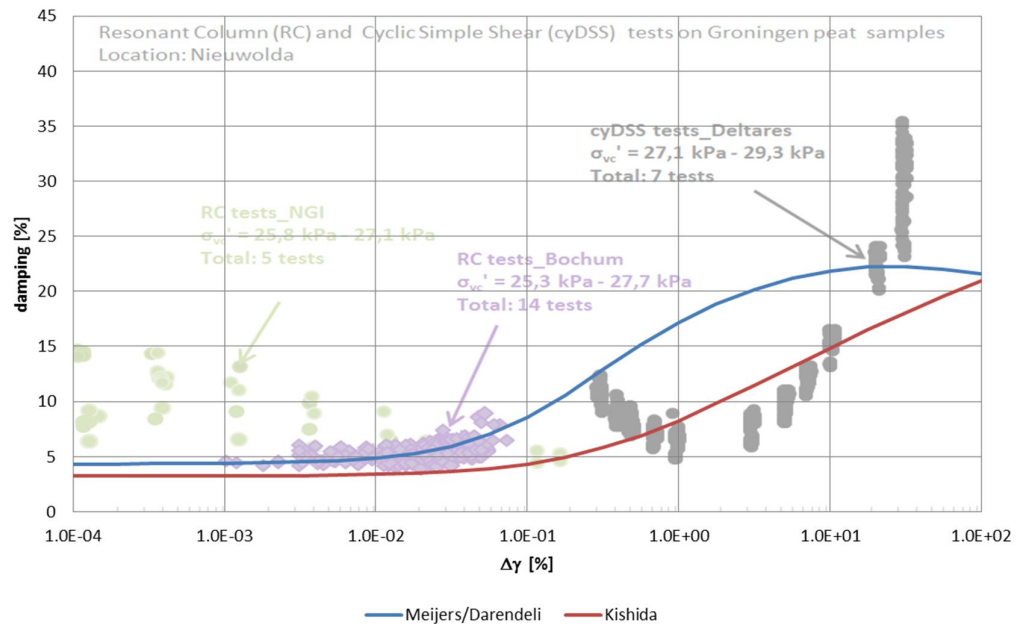


Figure 6.2 Comparison measured damping curve with existing empirical curves, Meijers/Darendeli refers to the curves according to section 7.6 of (Bommer et al 2015)

Siddeburen

$\sigma'_v = 9 \text{ kPa}$
 $K_0 = 0.35$
 $OC = 86\%$

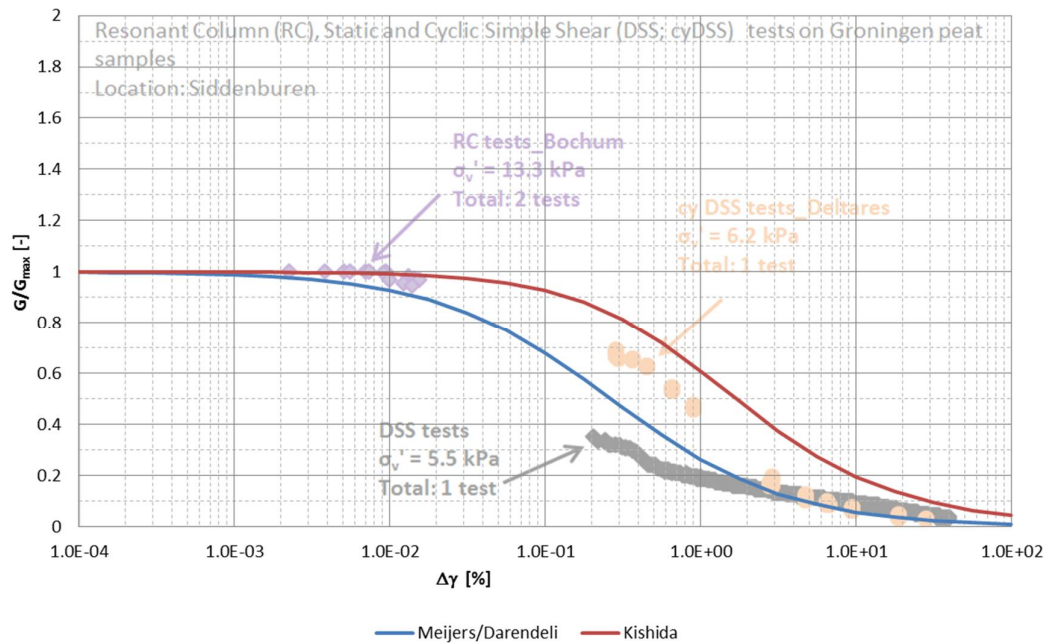


Figure 6.3 Comparison measured shear modulus reduction curve with existing empirical curves, Meijers/Darendeli refers to the curves according to section 7.6 of (Bommer et al 2015)

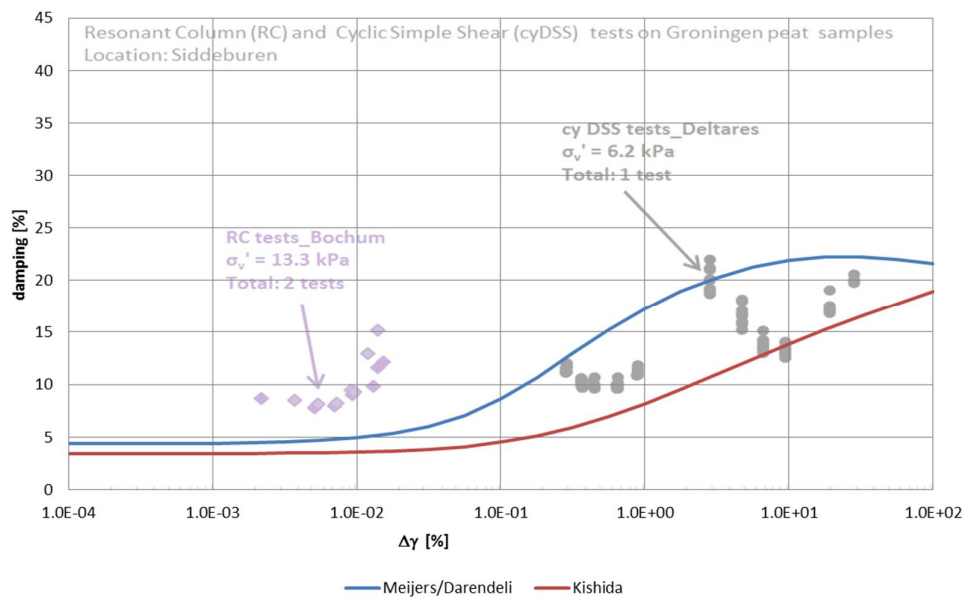


Figure 6.4 Comparison measured damping curve with existing empirical curves, Meijers/Darendeli refers to the curves according to section 7.6 of (Bommer et al 2015)

Schildmeer

$\sigma'_v = 6$ kPa

$K_0 = 0.35$

OC = 80 %

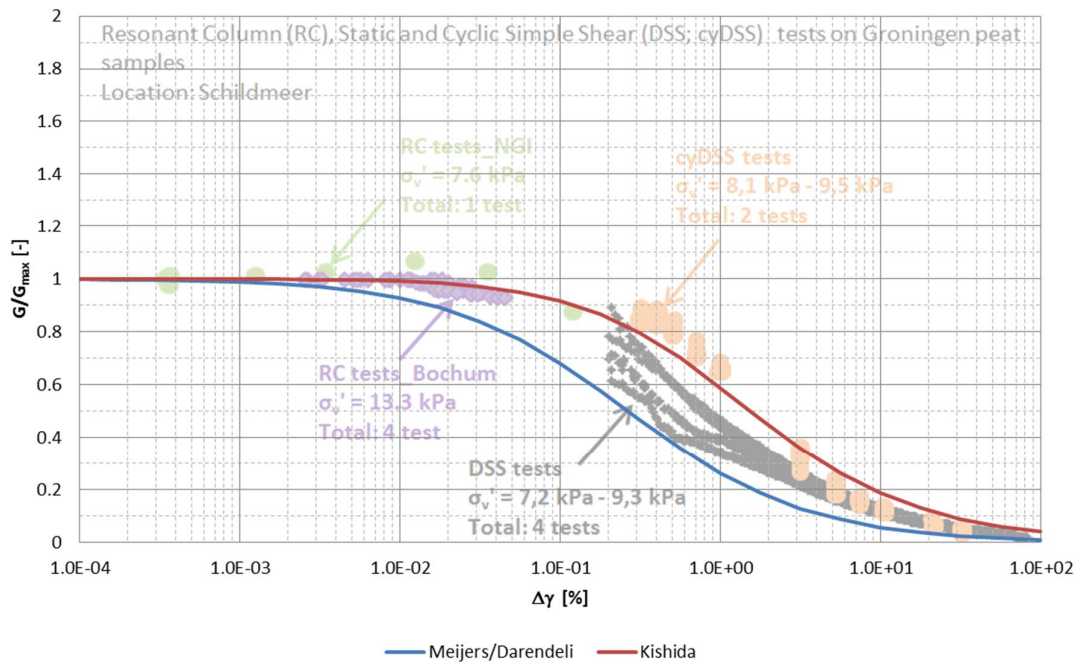


Figure 6.5 Comparison measured shear modulus reduction curve with existing empirical curves, Meijers/Darendeli refers to the curves according to section 7.6 of (Bommer et al 2015)

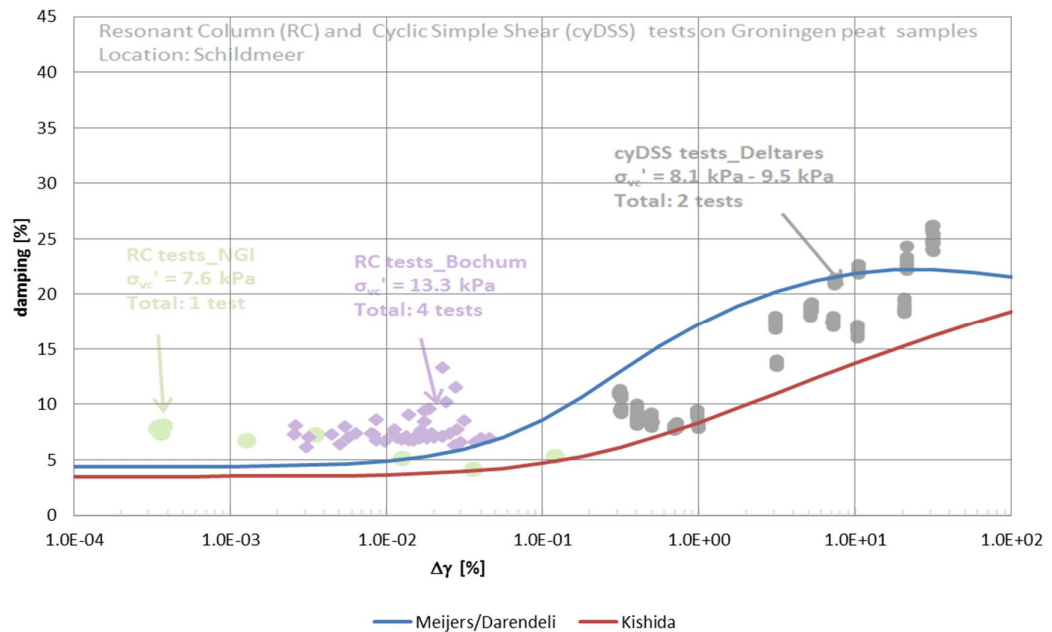


Figure 6.6 Comparison measured damping curve with existing empirical curves, Meijers/Darendeli refers to the curves according to section 7.6 of (Bommer et al 2015)

From these graphs the following can be concluded:

The predicted curves by Kishida give a better agreement with the test data than the predicted curves by Meijers/Darendeli. For Schildmeer there is a nearly perfect match, for the other two locations Kishida slightly overpredicts G/G_0 . The predicted curves by Meijers/Darendeli give a lower value of the G/G_0 than the test data. This can also be expressed by stating that the value of the reference shear strain, the shear strain at which $G/G_0 = 0.5$, is too low.

Bommer et al 2015 does not use the organic content as an input parameter. Most of the test data used to derive the expressions have an organic content of about 50%; much lower than the organic content of the tested material. This may explain the observed differences.

The predicted damping by Kishida (2009) is in reasonable agreement with the test data for Nieuwolda. For Siddeburen and Schildmeer the measured values are well above the predicted values.

The predicted damping by Meijers/Darendeli is well above the measured values for large strains and below the measurement data for low strains. This is consistent with the trends in the predicted values for G/G_0 .

6.3 Fitting measured data

6.3.1 Fitting shear modulus reduction curve

The test data of the modulus reduction are fitted using the functional form of Darendeli. In this expression the curve is determined by two parameters:

$$\frac{G}{G_{\max}} = \frac{1}{1 + \left(\frac{\gamma}{\gamma_{ref}} \right)^a} \quad (6.1)$$

in which:

- γ_r = shear strain amplitude for $G/G_0 = 0.5$, this determines the location of the curve
- a = power; determines the steepness of the curve

The loading frequency in the cyclic DSS tests is 0.1 Hz. As described in section 3.5 there is a frequency effect on the measured stiffness. In order to correct for the low frequency used in the cyclic DSS tests a correction factor of 1.2 on the stiffness is applied. The value of the correction factor is chosen in accordance with Figure 3.18. In this figure the difference between the low frequency stiffness for frequencies < 0.1 Hz and high frequency stiffness, for frequencies > 10 Hz, is in the order of 1.2.

For each location a least squares approach is used, using all available test data. Figure 6.7, Figure 6.9, Figure 6.11 show the resulting fitted curve per location. Figure 6.8, Figure 6.10, Figure 6.12 show the residuals. Please note that in these graphs the plotted results of the cyDSS tests include the correction factor of 1.2.

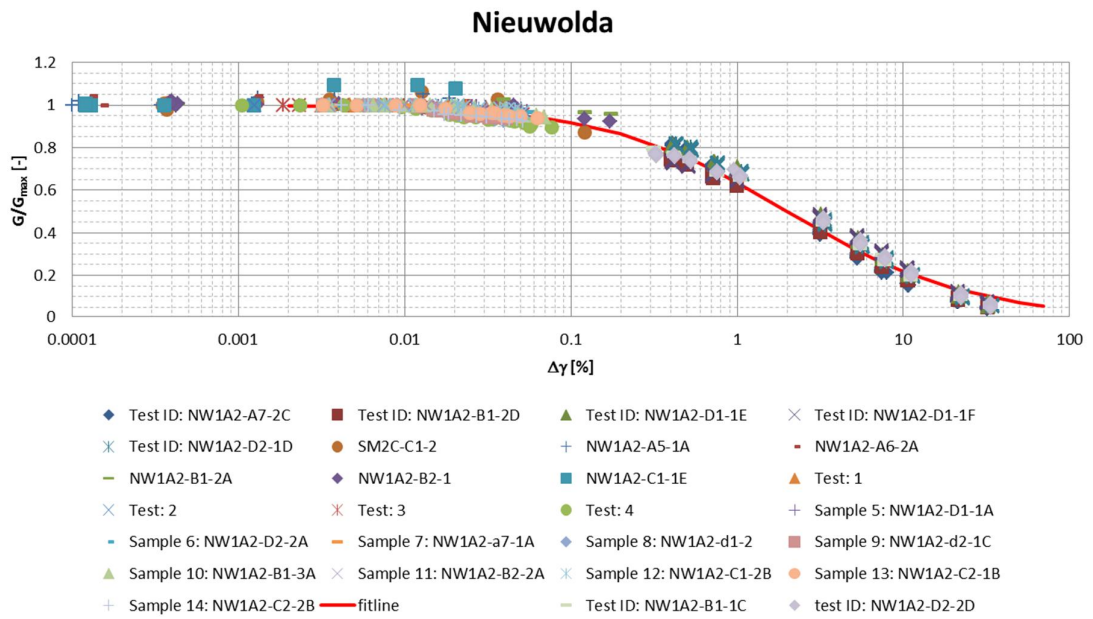


Figure 6.7 Fitting test data Nieuwolda, derived curve

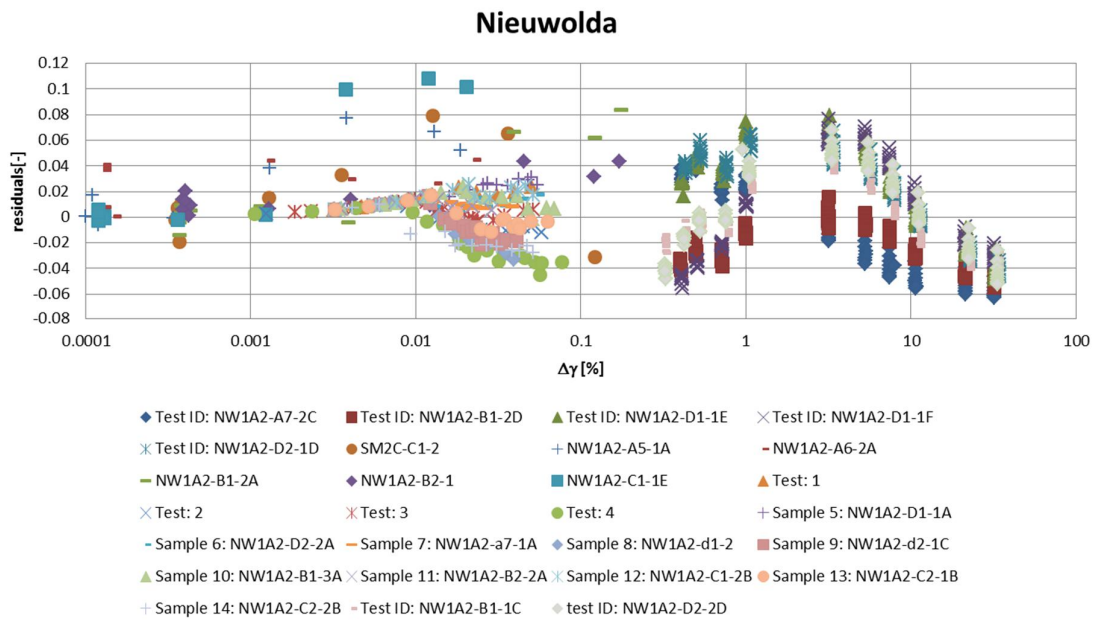


Figure 6.8 Fitting test data Nieuwolda, residuals

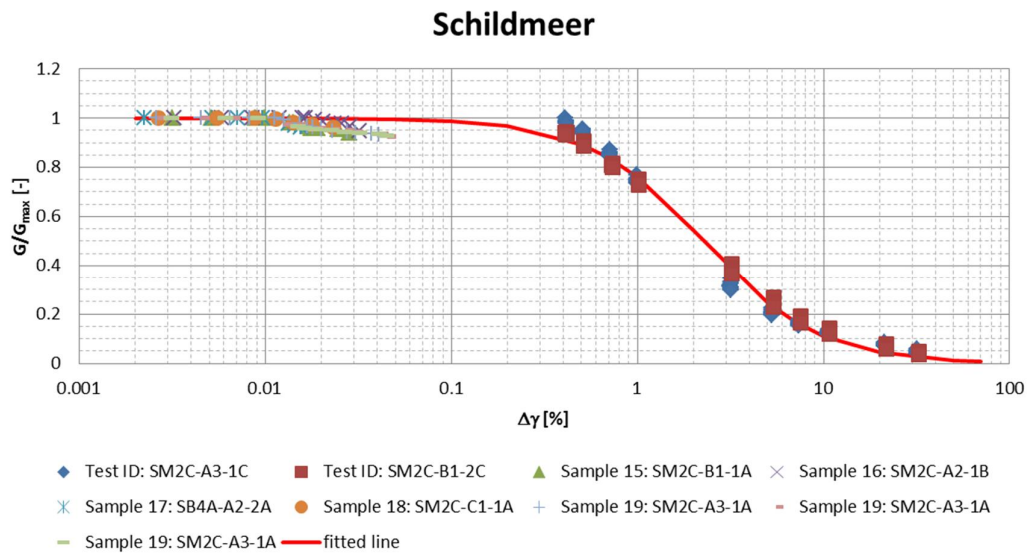


Figure 6.9 Fitting test data Schildmeer, derived curve

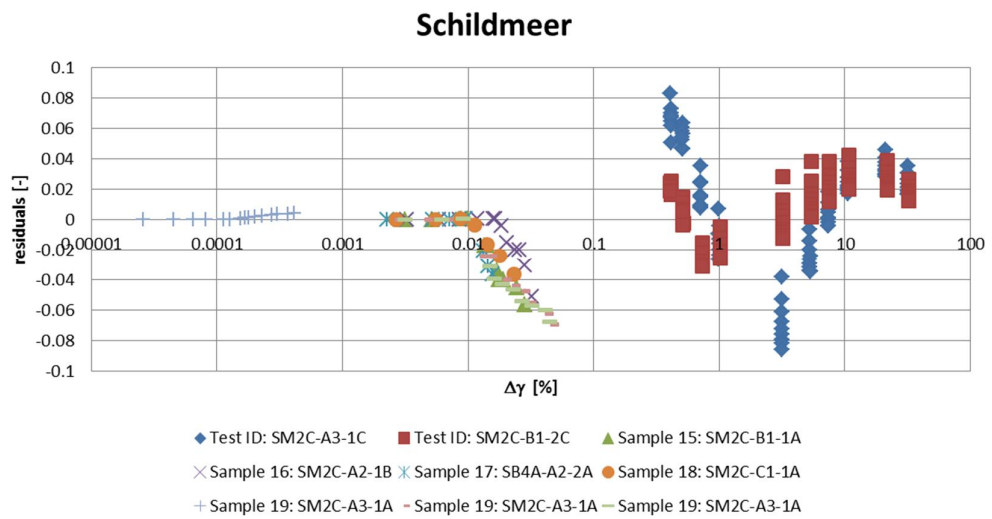


Figure 6.10 Fitting test data Schildmeer, residuals

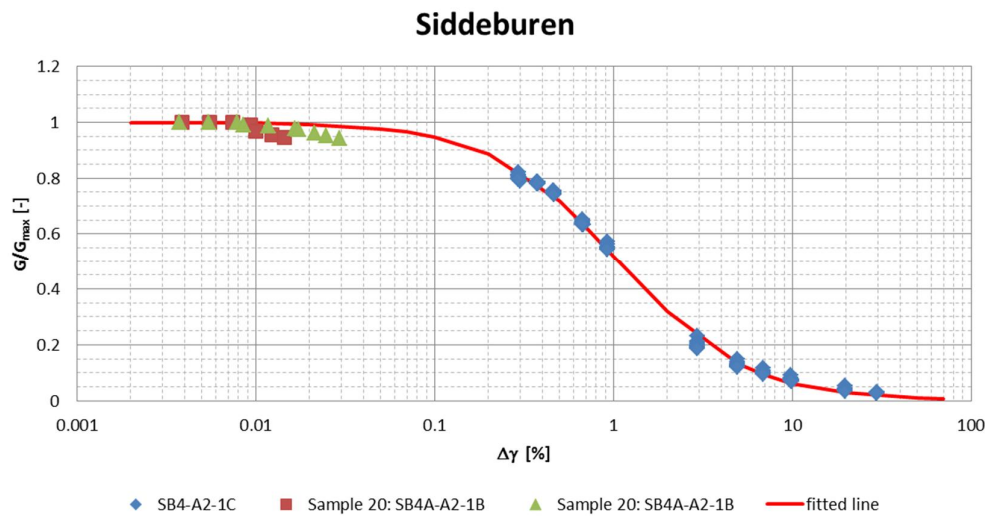


Figure 6.11 Fitting test data Siddeburen, derived curve

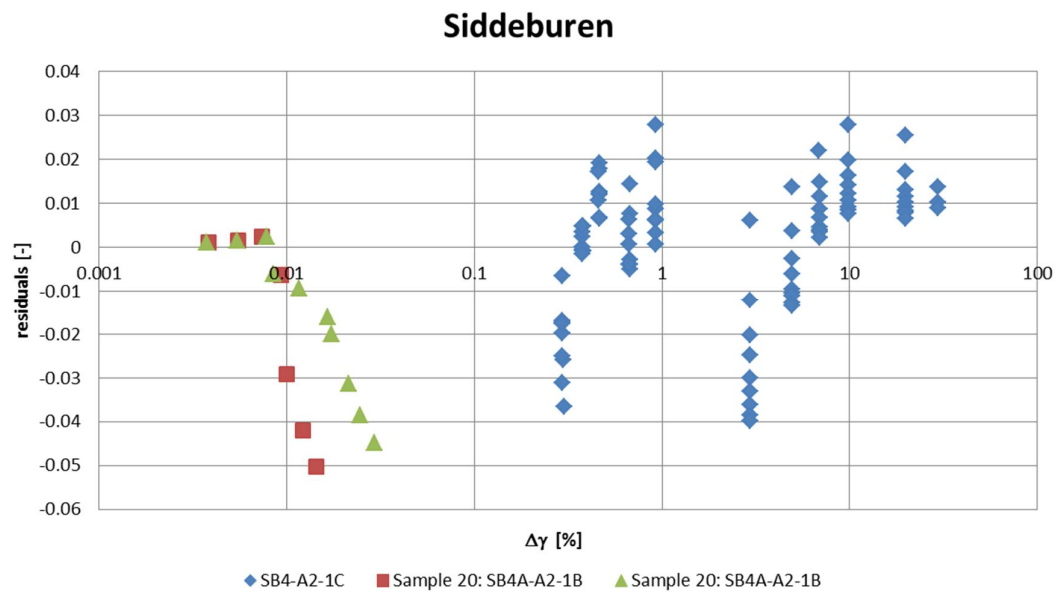


Figure 6.12 Fitting test data Siddeburen, residuals

The resulting fit parameters are given in Table 6.1. For completeness also the obtained values are given in case the results of the cyclic DSS tests are not corrected for the difference in loading frequency.

Location	Organic content [%]	Vertical effective stress [kPa]	No correction cyclic DSS test results		Correction factor 1.2 on cyclic DSS test results	
			γ_r [%]	a [-]	γ_r [%]	a [-]
Nieuwolda	87	27	1.22	0.73	2.12	0.83
Schildmeer	80	6	1.48	1.1	2.26	1.41
Siddeburen	86	9	0.71	1.02	1.07	1.22

Table 6.1 Fit parameters for the modulus reduction curve, γ_{ref} and a according equation (6.1)

6.3.2 Fitting material damping

The damping curve is fitted by:

$$D = F D_{Masing} + D_{min}$$

$$F = b \left(\frac{G}{G_{max}} \right)^p$$

$$D_{Masing} = c_1 \cdot D_{Masing,a=1} + c_2 \cdot D_{Masing,a=1}^2 + c_3 \cdot D_{Masing,a=1}^3 \quad (6.2)$$

$$D_{Masing,a=1} = \frac{100}{\pi} \left[4 \frac{\gamma - \gamma_{ref} \ln \left(\frac{\gamma + \gamma_{ref}}{\gamma_{ref}} \right)}{\gamma^2} - 2 \right]$$

in which:

- D_{min} = damping at small strain level
- b = fitting parameter
- p = power; $p = 0.1$
- γ_{ref} = reference strain, according to Table 6.1
- c_1, c_2, c_3 = fit parameters

Appendix B gives background information on the fitting procedure and explains the used parameters. For fitting the results the parameters D_{min} and b are used. The parameter p was fixed by Darendeli (2001) at $p = 0.1$. It has been found that varying this parameter has little influence on the obtained damping curve, therefore using this parameter in the fitting procedure was found to be little added value.

The parameter D_{min} is read directly from the test results. For obtaining the parameter b this parameter was varied until an acceptable agreement with the measured damping was obtained. The results are shown by Figure 6.13 to Figure 6.15 and Table 6.2.

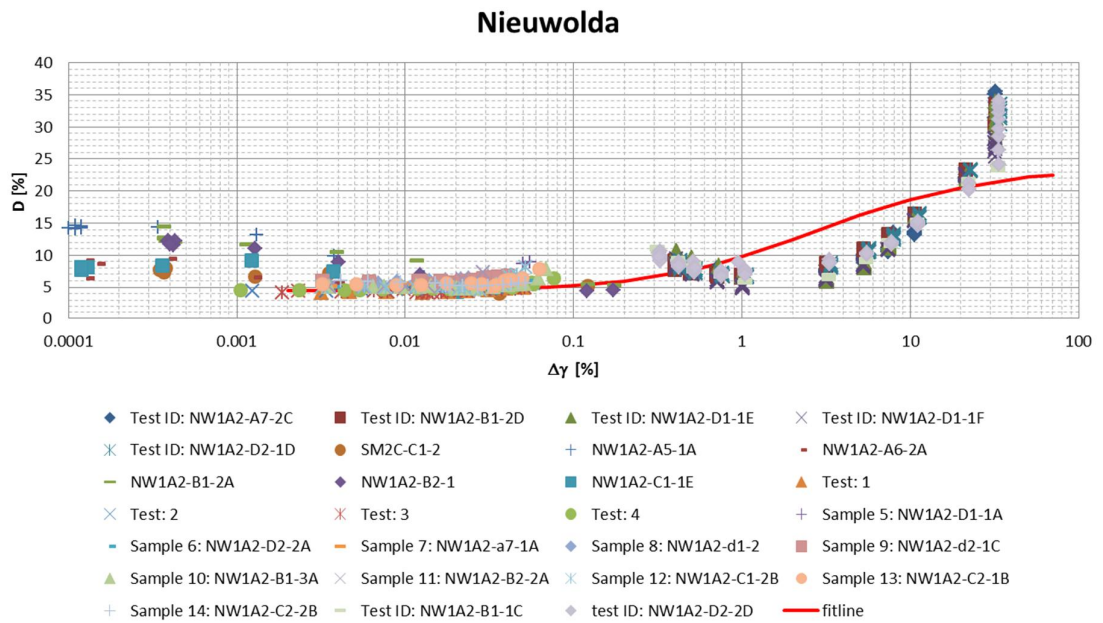


Figure 6.13 Fitting test data damping Nieuwolda

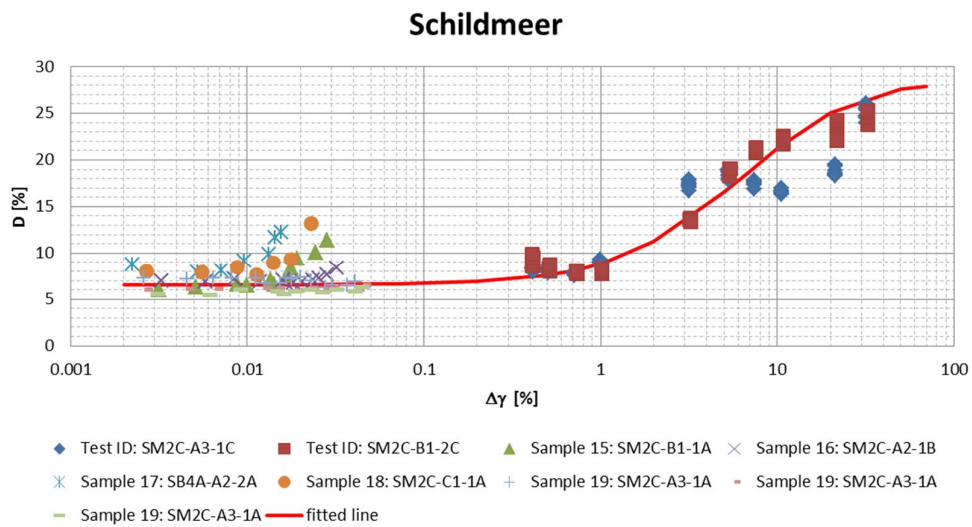


Figure 6.14 Fitting test data damping Schildmeer

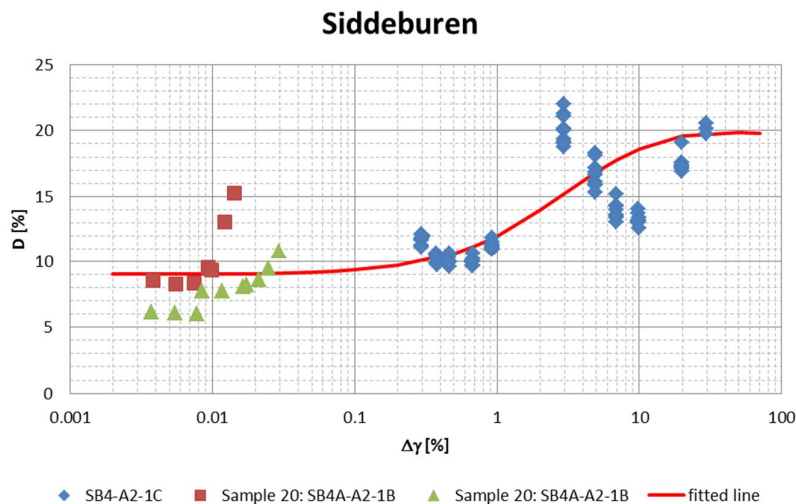


Figure 6.15 Fitting test data damping Siddeburen

The resulting fit parameters are given in Table 6.2.

Location	Organic content [%]	Vertical effective stress [kPa]	D_{min} [%]	b [-]
Nieuwolda	87	27	4.5	0.6
Schildmeer	80	6	6.5	0.3
Siddeburen	86	9	9.0	0.2

Table 6.2 Fit parameters for the damping curve, correction factor 1.2 on stiffness from cyDSS tests

For Schildmeer and Siddeburen the shape of the fitted damping curve follows well the test data. The value of b however is much lower than previously derived from published test data. For Nieuwolda the fitted line overestimates the damping for shear strain amplitudes between 1% and 10% and under predicts the damping for shear strain amplitudes above 10%. A better fit for shear strains below 5% is obtained by decreasing the value of b (using e.g. $b = 0.3$). This however will result in a large underestimation of the damping for larger shear strain amplitudes.

6.4 Derivation general curves for Groningen peat

6.4.1 Selected approach

In this section a general expression for the MRD curves for Groningen peat is derived. Starting point are the derived parameters describing the MRD curves for the three locations. Using these data a general set of parameters is derived. The resulting curves according to this set are compared with the test data.

As functional form the Darendeli equations are used. Reason for this is:

- Already implemented in the Deltares software for batch processing.
- More easily to adjust parameters for fitting with test data.

6.4.2 Derivation general modulus reduction curve

For practical purposes, and in order to be in line with published test data, a fixed value of $a = 0.8$ is selected for equation (6.1). Using this pre-set value for the parameter a , a new fit of the test data is made for obtaining the value of the reference strain γ_{ref} , using a least squares approach. Comparing these values with the values given in Table 6.3 it is found that these values are nearly the same as derived in section 6.3.1.

Location	Consolidation stress [kPa]	Organic content [%]	a [-]	γ_{ref} [%]
Nieuwolda	27	87	0.8	2.12
Schildmeer	6	80	0.8	2.25
Siddeburen	9	86	0.8	1.08

Table 6.3 Results fitting modulus reduction curve, using $a = 0.8$ as fixed value

The limited dataset does not allow the determination of the dependency of the MRD curves on the consolidation stress and/or the organic content. From a practical point of view therefore it is recommended to use $\gamma_{ref} = 2\%$ for the top peat layers in the Groningen area.

Figure 6.16, Figure 6.17 and Figure 6.18 show a comparison of the fit according to the selected values, Table 6.3 and the test data. It should be noted that the factor 1.2 for effect frequency on results cyclic DSS tests is incorporated. For Nieuwolda a good agreement is found, for Siddeburen the curve overestimate the shear modulus at large shear strain amplitudes ($\gamma > 1\%$) while for Schildmeer the shear modulus at intermediate strain ($0.1\% < \gamma < 1\%$) is slightly underestimated.

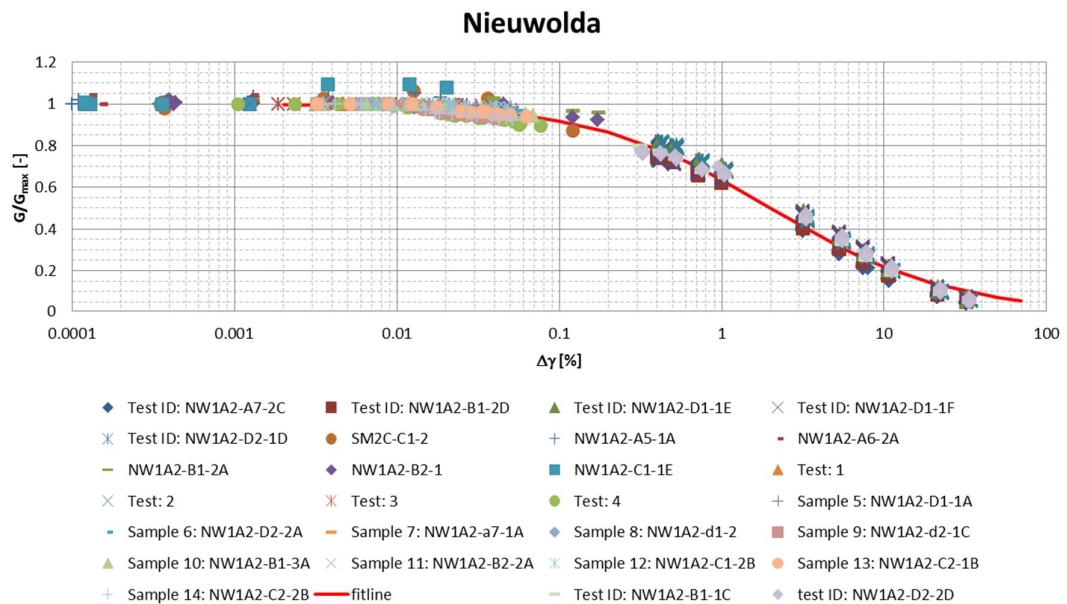


Figure 6.16 Comparison test data with the selected general curve for Groningen peat, location Nieuwolda

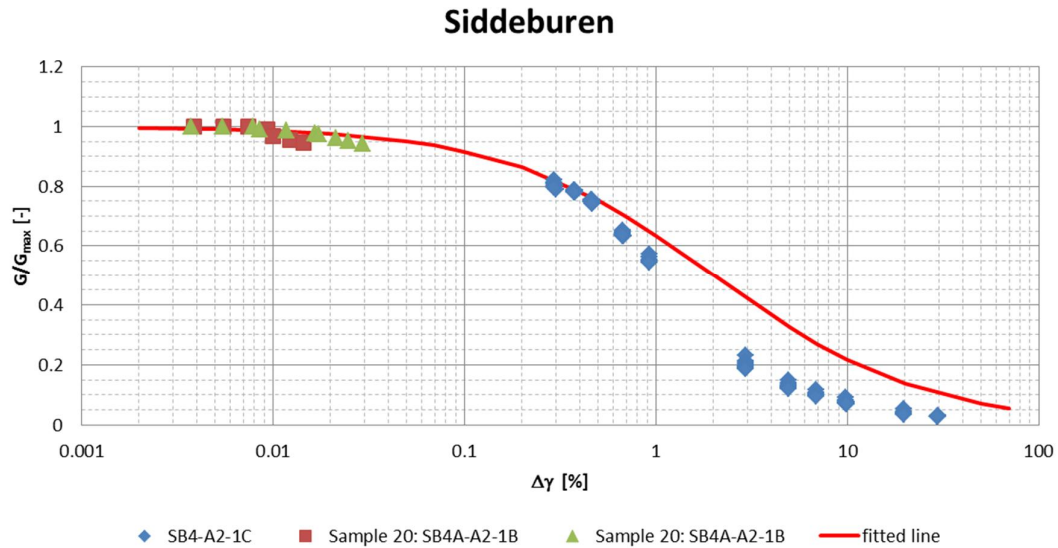


Figure 6.17 Comparison test data with the selected general curve for Groningen peat, location Siddeburen

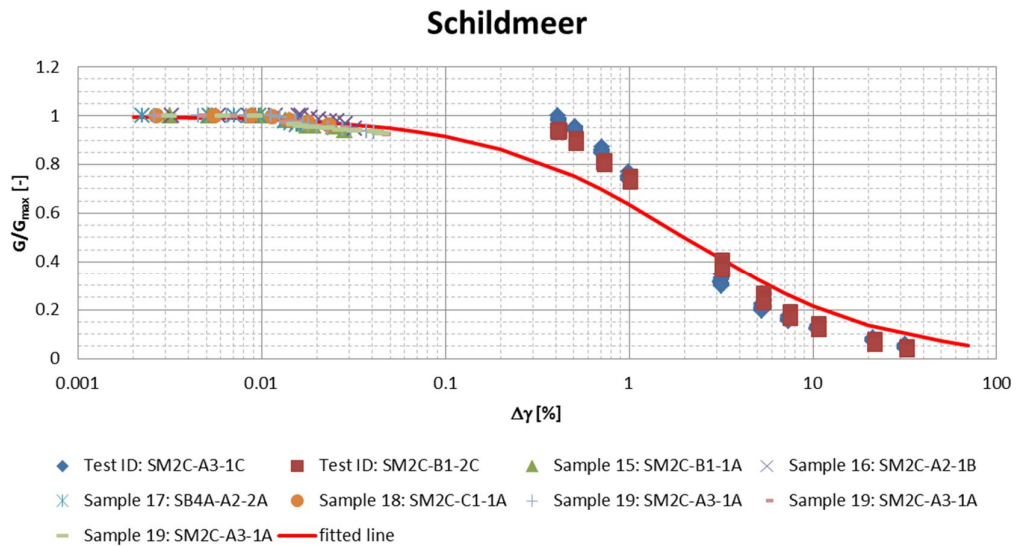


Figure 6.18 Comparison test data with the selected general curve for Groningen peat, location Schildmeer

6.4.3 Comparison with literature data

Chapter 3 gives an overview of published test data on peat. Most tested peats have an organic content, OC of about 50%, which is lower as the organic content of the Groningen peat. The published data provide only one case with a high OC. This is the case Mercer Slough with OC = 70 – 80% and consolidation stress was 1.5 kPa, 12.5 kPa and 19 kPa (Kramer 1996, 2000).

Figure 6.19 shows a comparison between the Groningen data and the Mercer Slough data.

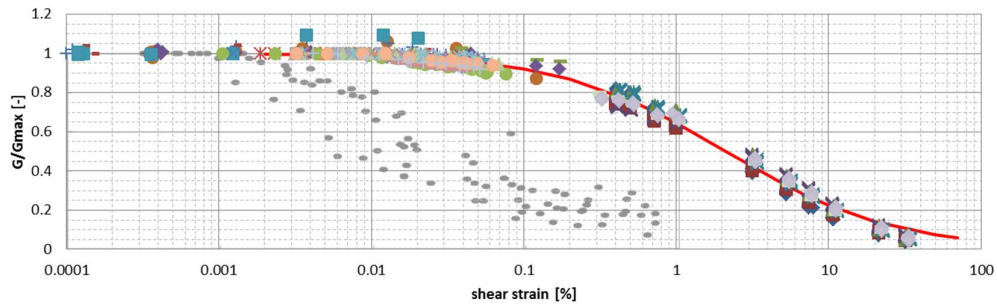


Figure 6.19 Comparison Groningen peat with Mercer Slough, grey dots are data for Mercer Slough, taken from (Kramer 2000)

A huge difference in the location of the modulus reduction curve is observed, despite the nearly equal organic content and consolidation stress. The test data resembles more the case Sherman Island, as tested by Boulanger et al. (1997 – 1998), OC = 35 – 65%, consolidation stress in the range of 132 to 200 kPa.

Compared with the other data the reference shear strain γ_{ref} for Mercer Slough is in fact remarkable low, see Figure 6.20.

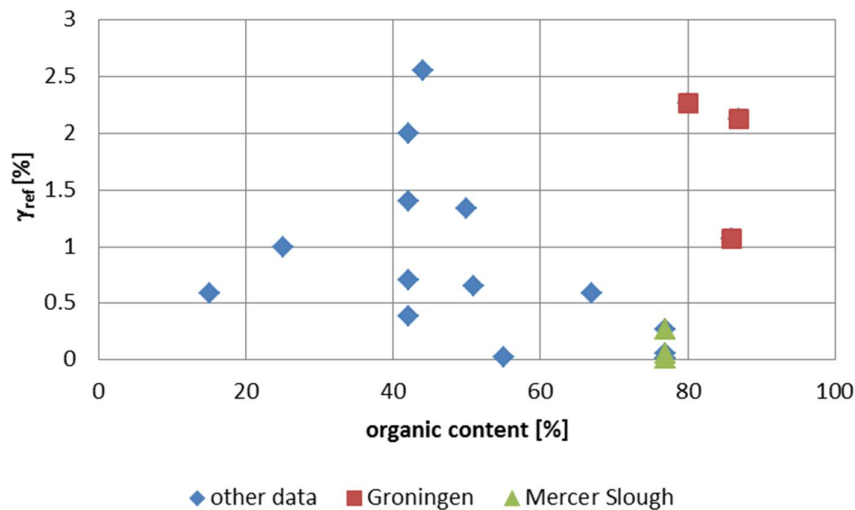


Figure 6.20 Comparison values reference strain

As the value of γ_{ref} is expected to be a function of at least both, the stress level and OC, the data in Figure 6.20 might be clarified when stress level is accounted for. Figure 6.21 shows the literature data subdivided in different stress ranges. The Groningen data is derived for stress levels ranging from 6 kPa to 27 kPa and do not show relation between γ_{ref} and stress level, see Table 6.3.

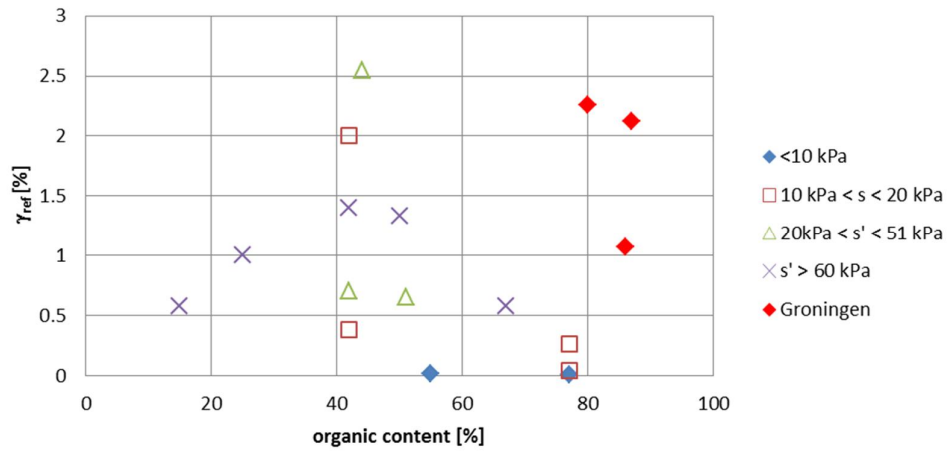


Figure 6.21 Reference strain, γ_{ref} versus Organic Content, with subdivision for different stress ranges

Figure 6.22 and Figure 6.23 show a further investigation of the stress dependency of the parameters a and γ_{ref} . The figures seem to show that the parameters for Groningen peat fall outside the general trend found in literature.

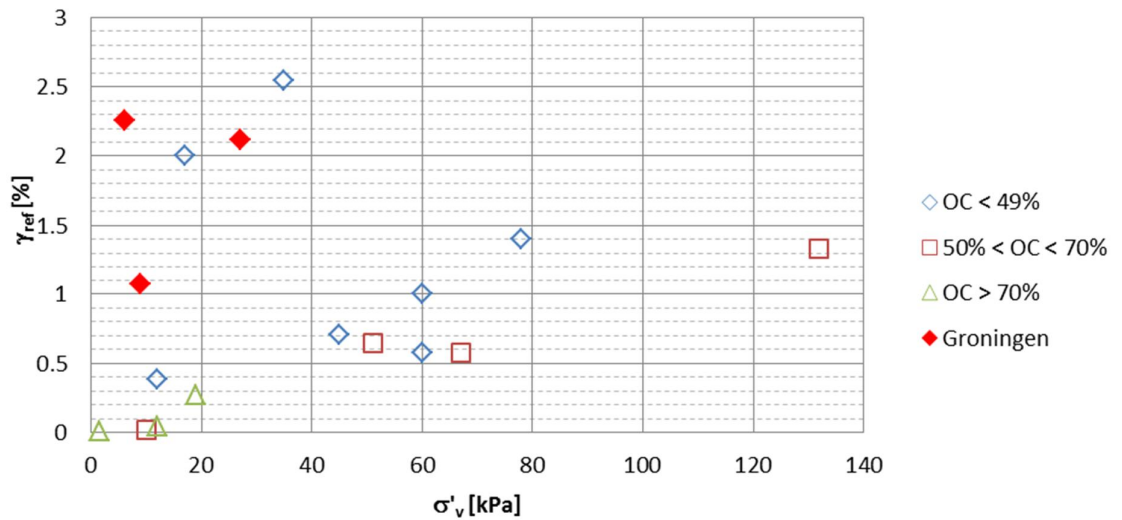


Figure 6.22 Reference strain, γ_{ref} versus vertical effective stress, with subdivision for different Organic Content ranges

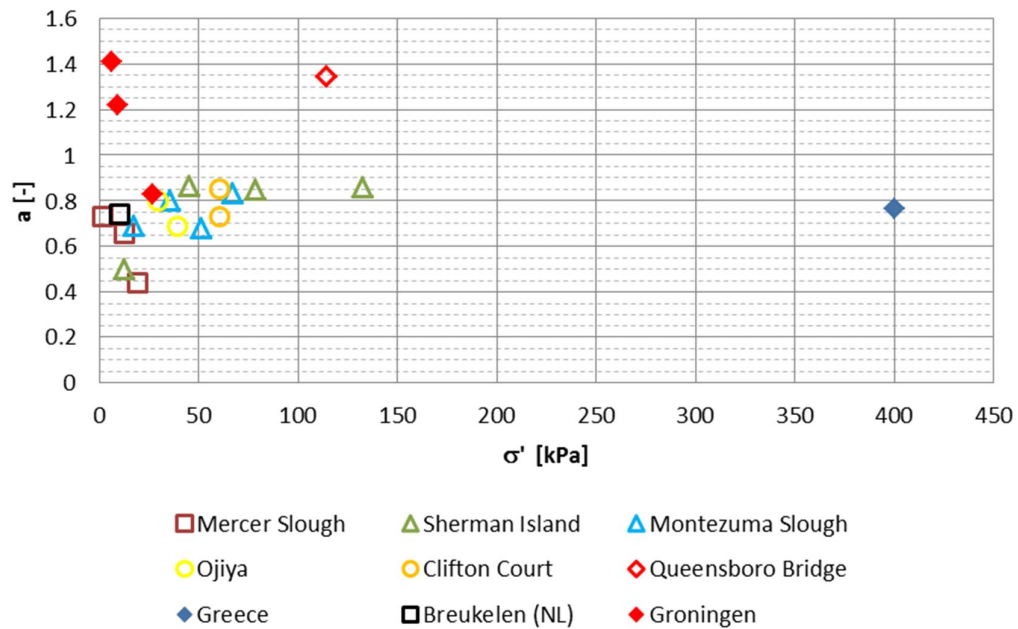


Figure 6.23 Value of a as function of consolidation stress

From the test data in the literature a more or less fixed value $a \approx 0.8$ was derived. From fitting of the Groningen test data values of 0.8, 1.2 and 1.4 are observed.

Compared to the modulus reduction curve of Queensboro bridge the newly derived curve compares well, see Figure 6.24. Unfortunately little information on the type of peat etc. of the Queensboro case has been published.

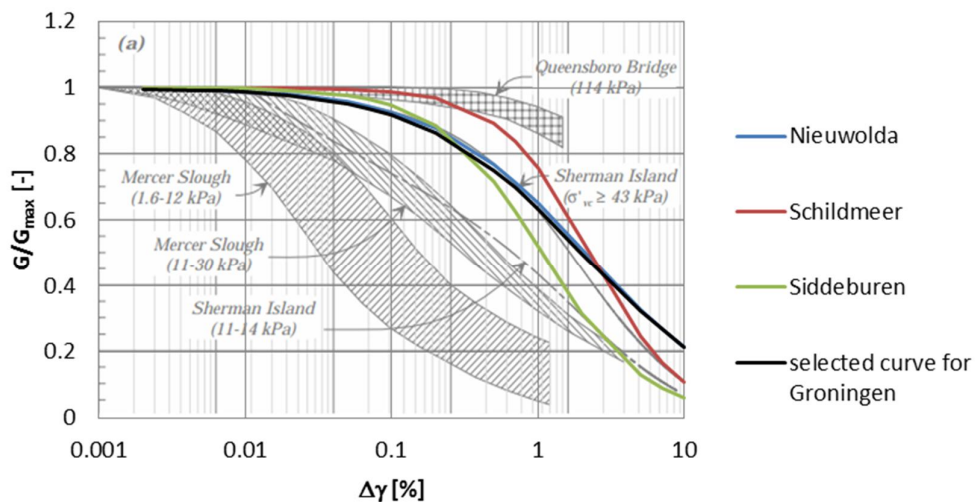


Figure 6.24 Comparison shear modulus reduction curve Groningen peat with published test data, shaded areas are published test data

6.4.4 Damping curves

Table 6.2 gives the derived parameters for the damping curve. From the published test data on peat $b = 0.712$ was derived. The value of b for Nieuwolda is fairly comparable to this value, but the other two locations show a lower b value and higher D_{min} . Figure 6.25 compares the derived values for D_{min} with the literature data.

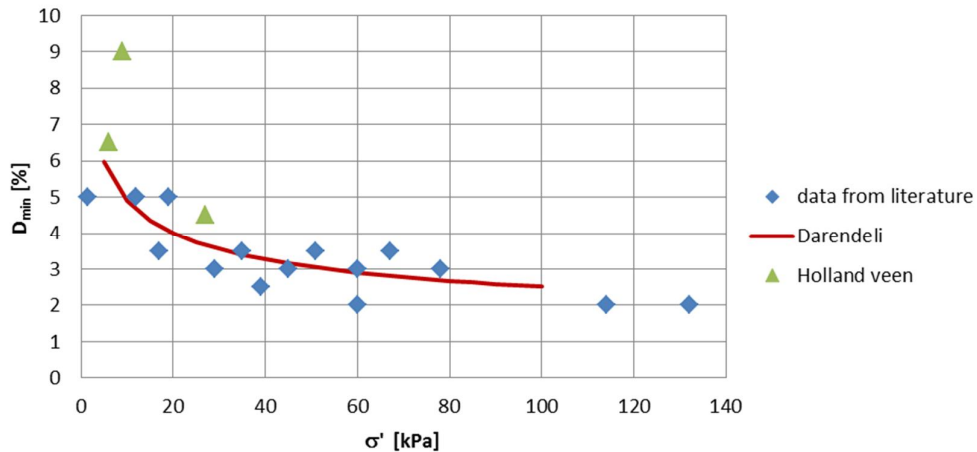


Figure 6.25 Comparison value of D_{min} for Groningen peat with published data

The value of D_{min} is fairly in line with the literature data, but slightly at the upper side. Fitting a line through all available datapoints gives nearly the same trendline. Using only the three datapoints for the Groningen peat yields a trendline above the general trendline. The equation of that line is:

$$D_{min} = 3.54 \left(\frac{\sigma'}{p_a} \right)^{-0.3} \tag{6.3}$$

In which p_a represents the atmospheric pressure.

Opting for a Groningen specific correlation will result in slightly higher values for D_{min} . As such a correlation would be based on just three data points it is proposed to retain the original correlation.

Figure 6.26 compares the obtained values for b with the results from published tests on peat.

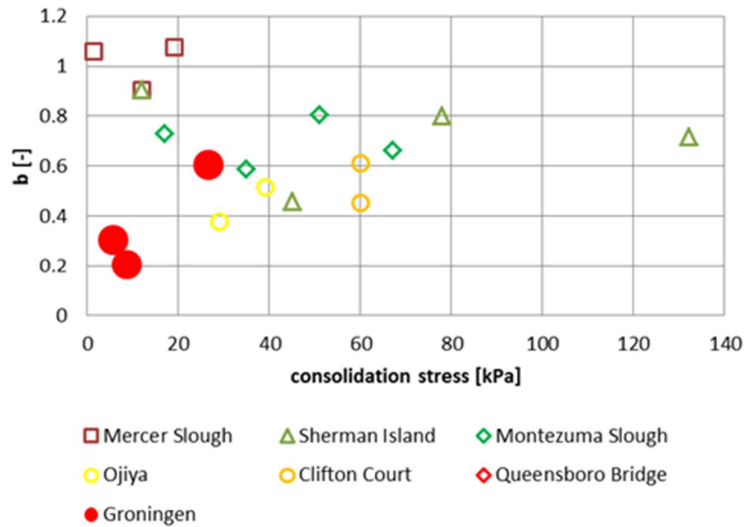


Figure 6.26 Comparison value of b for Groningen peat with data from published tests on peat

For low stress levels (5 – 10 kPa) the obtained value for b is below the data from literature, but for slightly higher values (25 kPa) it is well in line with other data. Therefore it is proposed to retain for the parameter b the original value.

Figure 6.27 to Figure 6.29 compare the damping curve, using these values, with the test data for Groningen peat. The agreement is considered reasonable.

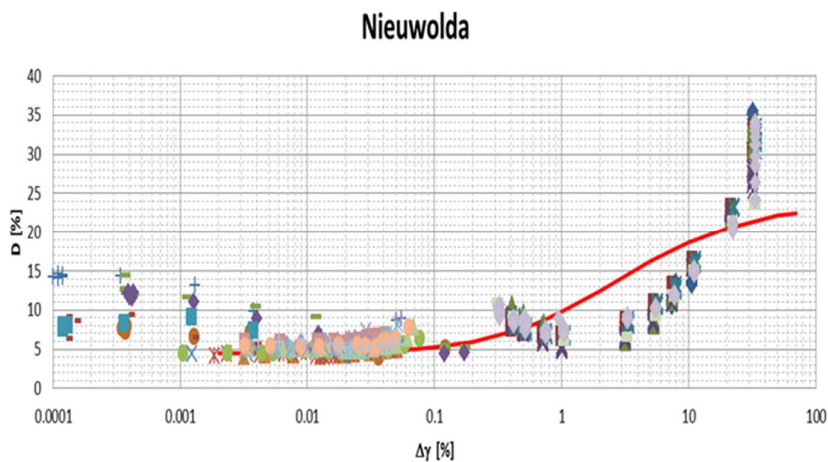


Figure 6.27 Comparison test data with the selected general curve for Groningen peat, location Nieuwolda

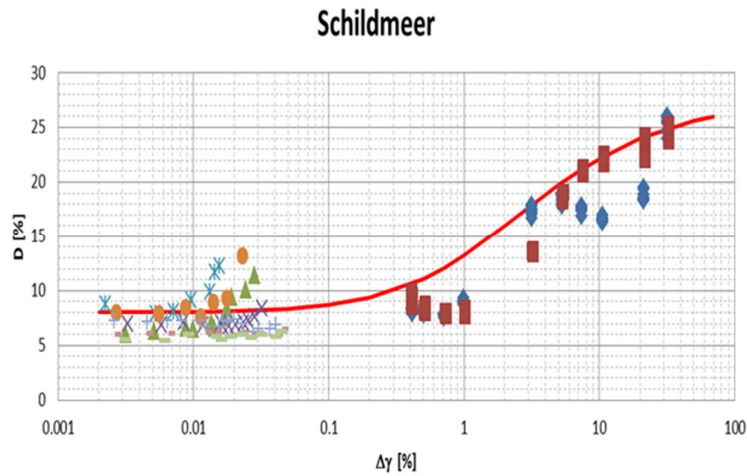


Figure 6.28 Comparison test data with the selected general curve for Groningen peat location Schildmeer

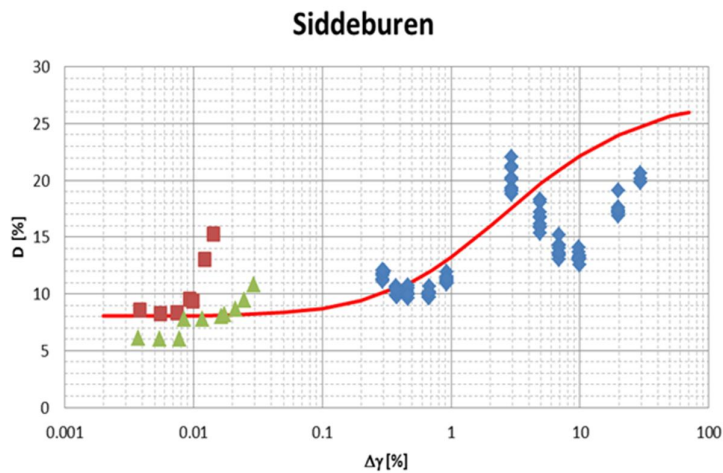


Figure 6.29 Comparison test data with the selected general curve for Groningen peat, location Siddeburen

6.4.5 Summary recommended MRD curves for Groningen peat

From the preceding analysis the following MRD curves are recommended for the Groningen peat:

- Use as functional form the Darendeli equations, with the following parameters.
- For the modulus reduction curve:
 - $\gamma_{ref} = 2\%$, independent of the consolidation stress.
 - $a = 0.8$.
- For the damping curve, retain the previous values:
 - $D_{min} = 2.512 \cdot (\sigma'/p_a)^{-0.2889}$.
 - $b = 0.712$.
- For the basal peat: Retain the current equation in (Bommer et al 2015).

7 Summary and conclusions

Resonant column and cyclic DSS tests are performed on shallow peat from three locations in Groningen. The purpose of these tests is to obtain the MRD curves for Groningen peat.

Properties of the peat in Groningen

The tested samples all have a high organic content of 80% to 90%. This is well above the organic content of the peat for which MRD curves have been published.

The small strain shear modulus of the peat is found to be low, between 0.75 MPa and 1.2 MPa. This corresponds to a shear wave velocity of about 30 m/s.

Description of curves in functional forms for site response calculations

The test results are compared with predicted MRD curves by Kishida et al (2009) and from a recent developed set of equations using a larger database, as described in Bommer et al (2015). This comparison shows that the equations given by Kishida (2009) predict less shear modulus reduction and a much lower damping than found in the test data. The MRD curves according to Bommer et al (2015) predict a higher shear modulus reduction and higher damping than found in the test data. The last effect is attributed to the high organic content of the Groningen samples compared to the organic content of the peat samples used in the published test results.

Selection MRD curves for Groningen peat

The test data are fitted using the functional form of Darendeli (2001). To account for the difference in frequency between the RC and the cyclic DSS test results the shear modulus from the cyclic DSS tests is multiplied with a factor of 1.2. The resulting parameters are given in Table 6.1 and Table 6.2.

Comparing the test data on Groningen peat with results from published tests on peat and with the previously derived equations yields the following recommendations for the MRD curves.

- Nieuwkoop formation, in this report referred to as Groningen peat:
 - Use as functional form the Darendeli equations, with the following parameters.
 - For the modulus reduction curve:
 - $\gamma_{ref} = 2\%$, independent of the consolidation stress.
 - $a = 0.8$.
 - For the damping curve, retain the previous values:
 - $D_{min} = 2.512 \cdot (\sigma'/p_a)^{-0.2889}$.
 - $b = 0.712$.
- Basal peat:
 - Retain the current equation in (Bommer et al 2015).

References

ASTM D4015-15 (2015) Standard Test Methods for Modulus and Damping of Soils by Fixed Base Resonant Column Devices, *American Society for Testing and Materials*, October 2015

Bate, B., H. Choo, H. & S.E. Burns (2013). Dynamic properties of fine-grained soils engineered with a controlled organic phase. *Soil Dynamics and Earthquake Engineering*, 53, 2013, pp 176–186

Bolton, M.D., & Wilson, J.M.R. (1988). An experimental and theoretical comparison between static and dynamic torsional soil tests.

Bolton, M.D., & Wilson, J.M.R. (1990). Discussion. *Geotechnique* 40, No. 4, 659-664.

Bommer, J.J., Dost, B., Edwards, B., Kruiver, P.P., Meijers, P., Ntinalexis, M., Polidoro, B., Rodriguez-Marek, A., Stafford, P.J. (2015). Development of Version 2 GMPEs for Response Spectral Accelerations and Significant Durations from Induced Earthquakes in the Groningen Field. Available at: <http://feitenencijfers.namplatform.nl/download/rapport/cbef666c-607b-4be2-a6e6-3d0dd0271b52?open=true>

Boulanger, R.W., R. Arulnathan, L.F. Harder, R.A. Torres & M.W. Driller (1997). Dynamic properties of Sherman Island peat. Department of Civil & Environmental Engineering, University of California, Davis, California. Report UCD/CGM-97/01

Boulanger, R.W., R. Arulnathan, L.F. Harder Jr., R.A. Torres & M.W. Driller (1998). Dynamic Properties of Sherman Island Peat. *Journal of Geotechnical and Geoenvironmental Engineering*, Vol. 124, No. 1, January 1998, pp 12-20

Cola S, Cortellazzo G (2005) The shear strength behavior of two peaty soils *Geotechnical and Geological Engineering* 23:679-695

Darendeli, M.B. (2001). Development of a New Family of Normalized Modulus Reduction and Material Damping Curves. Ph.D thesis The University of Texas at Austin, August, 2001

Dobry, R., L. Liu & K.H. Stokoe II (1996). Queensboro Bridge in New York City: geotechnical seismic hazard assessment. Eleventh world conference on Earthquake Engineering, 1996

Goudarzy M. (2015) Micro and macro mechanical assessment of small and intermediate properties of granular materials, *PhD thesis* Ruhr Universität Bochum

Green R., Rodriguez-Marek A. (2017) Comments on Deltares report entitled “Dynamic behaviour of Groningen peat” *Memorandum* 9 September 2017

Haan, E.J. den & G.A.M. Kruse (2007). Characterisation and engineering properties of Dutch peats. Characterisation and Engineering Properties of Natural Soils. Proceedings of 2nd Int. Workshop, Singapore, Taylor & Francis, London, 2007, 3: 2101–2133.

- Haan, E.J. den (1999) Stress independent parameters for primary and secondary compression *Proceedings XIIIth International Conference on Soil Mechanics and Foundation Engineering*, New Delhi, Vol I, p 65 - 70
- Hardin B.O., Black W.L. (1966) Sand stiffness under various triaxial stresses *journal of soil mechanics and foundations* Vol 92 p 27-42
- Hardin B.O., Drnevich V.P. (1972) Shear modulus and damping in soils: design equations and curves *Soil Mechanics and Foundation Division* **98** p 667-692
- Hendry M.T., Sharma J.S., Derek Martin C., Lee Barbour S. (2012) Effect of fibre content and structure on anisotropic elastic stiffness and shear strength of peat *Can. Geotechnical Journal* no 49 p 403-415
- Hobbs N.B. (1986) Mire morphology and the properties and behaviour of some British and foreign peats *Quarterly Journal of Engineering Geology* vol 19 pp 7-80
- Iwasaki, T., Tatsuoka, F., & Takagi, Y. (1978). Shear moduli of sands under cyclic torsional shear loading *Soils and Foundations* 18, No. 1, 39-50.
- Kallioglou, P., Th. Tika, G. Koninis, St. Papadopoulos & K. Pitilakis (2009). Shear Modulus and Damping Ratio of Organic Soils. *Geotechnical and Geological Engineering*. Volume 27, Issue 2, April 2009, pp 217-235,
- Kishida, T., R.W. Boulanger, T.M. Wehling & M.W. Driller (2006). Variation of Small Strain Stiffness for Peat and Organic Soil. Proceedings of the 8th U.S. National Conference on Earthquake Engineering. April 18-22, 2006, San Francisco, California, USA, Paper No. 1057
- Kishida, T., T.M. Wehling, R.W. Boulanger, M.W. Driller & K.H. Stokoe II (2009). Dynamic Properties of Highly Organic Soils from Montezuma Slough and Clifton Court *Journal of Geotechnical and Geoenvironmental Engineering*, Vol. 135, No. 4, April 2009, pp 525 - 532
- Kishida, T., R.W. Boulanger, N.A. Abrahamson, T.W. Wehling & M.W. Driller (2009a). Regression Models for Dynamic Properties of Highly Organic Soils *Journal of Geotechnical and Geoenvironmental Engineering*, Vol. 135, No. 4, April 1, 2009 pp 533-543
- Kishida, T., R.W. Boulanger, N.A. Abrahamson, M.W. Driller & T.M. Wehling (2009b). Site Effects for the Sacramento-San Joaquin Delta *Earthquake Spectra*, Volume 25, No. 2, May 2009, pages 301–322
- Kramer, S.L. (1996). Dynamic response of peat. Washington State Department of Transportation, report WA-RD 412.2, November 1996
- Kramer S.L. (2000). Dynamic Response Of Mercer Slough Peat. *Journal of Geotechnical and Geoenvironmental Engineering*, Vol. 126, No. 6, June 2000, pp 504 - 510
- Ladd C.C. (1991) Stability Evaluation during Staged Construction *Journal of Geotechnical Engineering*, Vol 117 No 4, 1991 p 540-615, 22nd Karl Terzaghi lecture

- Landva A.O. (2007) Characterization of Escuminac peat and construction on peatland *in: Characterisation and Engineering Properties of Natural Soils, Tan, Phoon, Hight & Leroueil (eds) Taylor& Francis Group London ISBN 978-0-415-42691-6*
- Lo Presti, D.C.F, Jamiolkowski, M., Pallara, O., Cavallaro, A., & Pedroni, S. (1997). Shear modulus and damping of soils. *Geotechnique* 47, No. 3, 603-617.
- Meijers P., Rodriguez-Marek A. (2017) A Model for the Modulus Reduction and Damping Curves for Peats using World-Wide Data, to be published
- Menq, F.Y. (2003). Dynamic properties of sandy and gravelly soils. Ph.D thesis University of Texas at Austin.
- Mesri, G., Hayat, T. M. (1993). The coefficient of earth pressure at rest. *Can. Geotech. J.*, 30(4), 647-666
- Mesri G., Ajlouni M. (2007) Engineering properties of fibrous peats *Journal of geotechnical and geoenvironmental engineering* no 133 p 850-866
- Molendijk W.O., Dykstra C.J. (2003) Restzetting na oplevering: Het belang van een verbeterde voorspellingskracht. Casus Betuweroute Sliedrecht – Gorinchem *Geotechniek* 2003 nr 4, p 36
- Moreno, C.A. & E.E. Rodriguez (2004). Dynamic Behavior of Bogota's Subsoil Peat and its Effect in Seismic Wave Propagation, *13th World Conference on Earthquake Engineering*, Vancouver, B.C., Canada, August 1-6, 2004, Paper No. 2632
- Sato, N., T. Ogino, T. Takahashi, H. Hayashi, H. Oikawa (2013). Empirical equations of elastic shear modulus and reference strain for soils containing organic matters *Japanese Geotechnical Journal*, Vol. 8, No. 1, 2013, pp 133-142 (in Japanese)
- Seed, H.B., & I.M. Idriss (1970a). Analysis of ground motions at Union Bay, Seattle, during earthquakes and distant nuclear blasts. *Bulletin Seismological Society of America*, Vol. 60, No. 1, February 1970
- Seed, H.B., & i.M. Idriss. (1970b). Soil moduli and damping factors for dynamic response analyses. College of engineering, University of California – Berkely. Report EERC 70-10, December 1970
- Shafiee, A., S.J. Brandenberg & J.P. Stewart (2013). Laboratory investigation of the pre- and post-cyclic volume change properties of Sherman Island peat, *Geocongress 2013 – Stability and Performance of Slopes and Embankments III*, San Diego
- Shibuya, S., Tatsuoka, F., Teachavorasinskun, S., Jing Kong, X., Abe, F., Kim, Y.S, & Park, C. S. (1992). Elastic deformation properties of geomaterials *Soils and Foundations* Vol. 32, No. 3, 26-46.
- Skempton A.W., Petley D.J. (1970) Ignition loss and other properties of peats and clays from Avonmouth, King's Lynn and Cranberry Moss, *Géotechnique* 20 no 4 pp 343-356

Stewart, J.P., S.J. Brandenburg & A. Shafiee (2013). Laboratory Evaluation of Seismic Failure Mechanisms of Levees on Peat, Structural and Geotechnical Engineering Laboratory Department of Civil & Environmental Engineering University of California, Los Angeles, Report UCLA-SGEL 2013/04, September 2013

Stokoe II. K., Darendeli M.B., Andrus R.D., Brown L.T. (1999) Dynamic soil properties: laboratory, field and correlation studies *Earthquake Geotechnical Engineering* pp 811-845

Stokoe II K, Santamarina C. (2000) Seismic wave based testing in geotechnical engineering *Technical Report*

Tatsuoka F., Iwasaki T., Fukushima S. Sudo H. (1979) Stress conditions and stress histories affecting shear modulus and damping of sand under cyclic loading *Soils and Foundations* **19** p 30-43

Tatsuoka, F., Shibuya, S. (1992). Deformation characteristics of soil and rocks from field and laboratory tests. Keynote Lecture, *Proceedings IX Asian Conference on SMFE, Bangkok*, No. 2, 101-190.

Teachavorasinskun, S., Shibuya, S., & Tatsuoka, F. (1991). Stiffness and damping of sands in torsion shear. *Proceedings of the 2nd International Conference on Recent Advances in Geotechnical Earthquake Engineering and Soil Dynamics*. St. Louis, Missouri. Paper No. 1.40

Tokimatsu, K. & T. Sekiguchi (2006a). Effects of Nonlinear Dynamic Soil Properties on Strong Motions at Ojiya K-Net and JMA Stations during 2004 Mid Niigata Prefecture Earthquake Proceedings of the 8th U.S. National Conference on Earthquake Engineering, San Francisco, California, USA, April 18-22, 2006

Tokimatsu, K & T. Sekiguchi (2006b). Effects of nonlinear properties of surface soils on strong ground motions recorded in Ojiya during 2004 mid Niigata Prefecture earthquake *Soils and Foundations*, Vol. 46, No. 6, December 2006, pp 765-775

Tokimatsu, K. & T. Sekiguchi (2007). Effects of Dynamic Properties of Peat on Strong Ground Motions during 2004 Mid Niigata Prefecture Earthquake. 4th International Conference on Earthquake Geotechnical Engineering June 25-28, Paper No. 1531, 2007

Von Post L. (1922) Sveriges Geologiska Undersøknings torvinventering och några av dess hittills vunna resultat *Svenska Mosskulturforeningens Tidsskrift* vol **36**

Vucetic, M. & R. Dobry (1991). Effect of Soil Plasticity on Cyclic Response *Journal of Geotechnical Engineering*. 1991.117:89-107.

Vucetic, M. (1994). Cyclic Threshold Shear Strains in Soils. *Journal of Geotechnical Engineering*, Vol 120, No. 12, December 1994, pp 2208-2228.

Wehling, T.M., R.W. Boulanger, L.F. Harder & M.W. Driller (2001). Dynamic Properties Of Sherman Island Peat: Phase II Study. Department of Civil & Environmental Engineering, College of Engineering, University of California at Davis Report No. UCD/CGM-01/05, March 2001

- Wehling, T.M., R.M. Boulanger, R. Arulnathan, L.F. Harder & M. Driller (2003). Nonlinear Dynamic Properties of a Fibrous Organic Soil. *Journal of Geotechnical and Geoenvironmental Engineering*, Vol. 129, No. 10, October 2003, pp 929 - 939
- Wood D.M. (1990) Soil Behaviour and Critical State Soil Mechanics *Cambridge University Press* ISBN 0-521-33782-8
- Yamaguchi H., Ohira Y., Kogure K., Mori S. (1985) Undrained shear characteristics of normally consolidated peat under triaxial compression and extension. *Soils and Foundations* **25** No. 3, 1-18
- Yamashita S., Fujiwara T., Kawaguchi T., Mikami T., Nakata Y., Shibuya S. (2005) International parallel test on the measurement of G_{max} using bender element *TC29 Technical report* Japanese Domestic Committee for TC 29
- Yniesta, S., (2016). Constitutive Modeling of Peat in Dynamic Simulations. Ph.D thesis University of California, 2016. <http://escholarship.org/uc/item/7j25282w>
- Zainorabidin, A. & D.C. Wijeyesekera (2009). Shear Modulus and Damping Properties of Peat Soils. Proceedings of the Advanced in Computing Technology, The School of Computing, Information Technology and Engineering, 4th Annual Conference, 2009, pp 61 -67.
- Zhang J., Andrus R.D., Juang C.H. (2005) Normalized shear modulus and material damping ratio relationships *Journal of Geotechnical and Geoenvironmental Engineering* **131** p 453-464
- Zwanenburg, C. (2005). The influence of anisotropy on the consolidation behaviour of peat, Ph.D thesis Delft University of Technology, October 2005
- Zwanenburg C., Haan E.J. den, Kruse G.A.M. Koelewijn A.R. (2012) Failure of a trial embankment on peat in Booneschans, The Netherlands *Géotechnique* **62** no 6, 479-490
- Zwanenburg, C. Jardine, R.J. (2015), Laboratory, in situ and full-scale load tests to assess flood embankment stability on peat, *Géotechnique*, 65(4), 309-326, doi: 10.1680/get.14.P.257
- Zwanenburg C., Konstantinou M. (2016) Assessment of dynamic properties for peat, Factual report *Deltares report nr 1209862-011-GEO-003*
- Zwanenburg C., Van M.A. (2015) Comparison between conventional and large scale triaxial compression test on peat *XVth Pan American Conference on Soil Mechanics and Geotechnical Engineering* Buenos Aires

A Characterisation parameters for the tested material

Table A.1 shows a summary of the characterisation parameters for all tested specimens. Table A.2 to Table A.4 gives the summary of the characterisation parameters for the individual sampling sites.

Total	ρ [g/cm ³]	ρ_{dry} [g/cm ³]	ρ_s [g/cm ³]	w [%]	LOI [%]	e [-]
mean, μ	0.99	0.16	1.52	543.51	85.41	8.86
standard deviation, σ	0.06	0.03	0.09	87.94	7.82	1.43
coefficient of variation, VC	0.06	0.20	0.06	0.16	0.09	0.16
number of samples, n	76	76	76	76	76	76

Table A.1 Statistical characterisation of the total data set

Nieuwolda	ρ [g/cm ³]	ρ_{dry} [g/cm ³]	ρ_s [g/cm ³]	w [%]	LOI [%]	e [-]
mean, μ	1.00	0.16	1.51	533.36	86.93	8.64
standard deviation, σ	0.14	0.02	0.03	5.05	1.70	1.77
coefficient of variation, VC	0.14	0.14	0.02	0.01	0.02	0.21
number of samples, n	55	55	55	55	55	55

Table A.2 Statistical characterisation of all tested material from the Nieuwolda site

Siddeburen	ρ [g/cm ³]	ρ_{dry} [g/cm ³]	ρ_s [g/cm ³]	w [%]	LOI [%]	e [-]
mean, μ	0.98	0.16	1.51	518.39	85.58	8.41
standard deviation, σ	0.04	0.02	0.15	62.12	17.02	0.49
coefficient of variation, VC	0.04	0.14	0.10	0.12	0.20	0.06
number of samples, n	6	6	6	6	6	6

Table A.3 Statistical characterisation of all tested material from the Siddeburen site

Schildmeer	ρ [g/cm ³]	ρ_{dry} [g/cm ³]	ρ_s [g/cm ³]	w [%]	LOI [%]	e [-]
mean, μ	1.00	0.15	1.57	590.76	79.77	9.86
standard deviation, σ	0.07	0.03	0.14	122.15	8.79	1.75
coefficient of variation, VC	0.07	0.20	0.09	0.21	0.11	0.18
number of samples, n	15	15	15	15	15	15

Table A.4 Statistical characterisation of all tested material from the Schildmeer site

Table A.5 to Table A.7 gives a summary of the characterisation parameters for the samples tested at the different laboratories.

RUB	ρ [g/cm ³]	ρ_{dry} [g/cm ³]	ρ_s [g/cm ³]	w [%]	LOI [%]	e [-]
mean, μ	1.05	0.16	1.49	560.56	87.71	8.42
standard deviation, σ	0.04	0.02	0.06	78.02	5.54	1.07
coefficient of variation, VC	0.04	0.12	0.04	0.14	0.06	0.13
number of samples, n	20	20	20	20	20	20

Table A.5 Statistical characterisation of all material tested at RUB

NGI	ρ [g/cm ³]	ρ_{dry} [g/cm ³]	ρ_s [g/cm ³]	w [%]	LOI [%]	e [-]
mean, μ	1.02	0.16	1.56	532.67	84.87	8.62
standard deviation, σ	0.01	0.01	0.09	60.12	6.28	0.93
coefficient of variation, VC	0.01	0.09	0.06	0.11	0.07	0.11
number of samples, n	6	6	6	6	6	6

Table A.6 Statistical characterisation of all material tested at NGI

Deltares	ρ [g/cm ³]	ρ_{dry} [g/cm ³]	ρ_s [g/cm ³]	w [%]	LOI [%]	e [-]
mean, μ	0.97	0.16	1.53	537.98	84.55	9.07
standard deviation, σ	0.06	0.04	0.10	94.57	8.65	1.57
coefficient of variation, VC	0.06	0.24	0.07	0.18	0.10	0.17
number of samples, n	50	50	50	50	50	50

Table A.7 Statistical characterisation of all material tested at Deltares

Humified	ρ [g/cm ³]	ρ_{dry} [g/cm ³]	ρ_s [g/cm ³]	w [%]	LOI [%]	e [-]
mean, μ	1.00	0.18	1.57	485.02	81.85	8.16
standard deviation, σ	0.06	0.06	0.16	94.58	12.58	1.57
coefficient of variation, VC	0.06	0.31	0.10	0.20	0.15	0.19
number of samples, n	13	13	13	13	13	13

Table A.8 Statistical characterisation of the material classified as humified

Non to moderate humified	ρ [g/cm ³]	ρ_{dry} [g/cm ³]	ρ_s [g/cm ³]	w [%]	LOI [%]	e [-]
mean, μ	0.99	0.15	1.51	555.57	86.14	9.01
standard deviation, σ	0.06	0.02	0.07	82.21	6.34	1.37
coefficient of variation, VC	0.06	0.14	0.05	0.15	0.07	0.15
number of samples, n	63	63	63	63	63	63

Table A.9 Statistical characterisation of the material classified as non to moderate humified

B Expressions for the MRD curves

B.1 Expressions Kishida

In (Kishida 2009) the following expressions for the MRD curves are given. These expressions are based on tests from the Sacramento-San Joaquin Delta (Sherman Island, Montezuma Slough, Clifton Court) only:

$$\ln G_{lab} = b_0 + b_1 \cdot X_1 + b_2 \cdot X_2 + b_3 \cdot X_3 + b_4 \cdot X_4 + b_5 \cdot (X_1 - \bar{X}_1)(X_2 - \bar{X}_2) + b_6 \cdot (X_1 - \bar{X}_1)(X_3 - \bar{X}_3) + b_7 \cdot (X_2 - \bar{X}_2)(X_3 - \bar{X}_3) + b_8 \cdot (X_1 - \bar{X}_1)(X_2 - \bar{X}_2)(X_3 - \bar{X}_3)$$

$$X_1 = \ln(\gamma_c + \gamma_3)$$

$$X_2 = \ln \sigma'_v$$

$$X_3 = 2/[1 + \exp(OC/23)]$$

$$X_4 = \ln LCR$$

$$\gamma_r = \exp[b_9 + b_{10}(X_3 - \bar{X}_3)]$$

$$\bar{X}_1 = -2.5$$

$$\bar{X}_2 = 4.0$$

$$\bar{X}_3 = 0.5$$

$$b_0 = 5.11$$

$$b_1 = -0.729$$

$$b_2 = 1 - 0.37\bar{X}_3 \left[1 + \frac{\ln(\gamma_r) - \bar{X}_1}{\ln(\gamma_l/\gamma_r + \gamma_c/\gamma_r)} \right]$$

$$b_3 = -0.693$$

$$b_4 = 0.8 - 0.4\bar{X}_3$$

$$b_5 = \frac{0.37\bar{X}_3}{\ln(\gamma_l/\gamma_r + \gamma_c/\gamma_r)}$$

$$b_6 = 0.0$$

$$b_7 = -0.37\bar{X}_3 \left[1 + \frac{\ln(\gamma_r) - \bar{X}_1}{\ln(\gamma_l/\gamma_r + \gamma_c/\gamma_r)} \right]$$

$$b_8 = \frac{0.37}{\ln(\gamma_l/\gamma_r + \gamma_c/\gamma_r)}$$

$$b_9 = -1.41$$

$$b_{10} = -0.95$$

$$\gamma_l = 1$$

OC: organic content (%)

For damping the following expression is given by Kishida:

$$\ln D_{lab} = c_0 + c_1 \cdot X_1 + c_2 \cdot X_2 + c_3 \cdot X_3 + c_4 \cdot (X_1 - \bar{X}_1)(X_2 - \bar{X}_2) + c_5 \cdot (X_2 - \bar{X}_2)(X_3 - \bar{X}_3)$$

$$X_1 = \ln \left[\ln \left(\frac{\hat{G}_{max}}{\hat{G}} \right) + 0.103 \right]$$

No separate definitions/expressions for X_2 and X_3 are given. Therefore it may be assumed that they are equal to the expressions for these parameters for the shear modulus.

$$\begin{aligned}\overline{X}_1 &= -1 \\ \overline{X}_2 &= 4.0 \\ \overline{X}_3 &= 0.5\end{aligned}$$

$$\begin{aligned}c_0 &= 2.86 \\ c_1 &= 0.571 \\ c_2 &= -0.103 \\ c_3 &= -0.141 \\ c_4 &= 0.0419 \\ c_5 &= -0.24\end{aligned}$$

An advantage of this set of parameters is that the organic content is included as a parameter. This allows to derive also the MRD curves for clayey peat and organic clay.

B.2 Expressions Darendeli for sand and clay

Darendeli (2001) has derived general expressions for the shear modulus reduction and damping curves for sand and clay. The format of these curves will be used as basis for the generalised curves for peat. In this document similar expressions for peat are derived, using test results on peat collected from literature. Therefore, first a description of these expressions will be given.

$$\frac{G}{G_{max}} = \frac{1}{1 + (\gamma/\gamma_r)^a}$$

with:

- γ shear strain amplitude
- γ_r reference shear strain amplitude (shear strain amplitude at which the value of $G/G_{max} = 0.5$)
- a parameter describing the curvature of the shear modulus reduction curve

The parameter γ_r determines the location of the shear modulus reduction curve and the parameter “a” determines the curvature.

For the damping a set of equations is used.

$$D = F * D_{Masing} + D_{min}$$

with:

- F multiplication factor
- D_{Masing} damping according to the Masing rule
- D_{min} damping at small shear strain amplitude

$$D_{Masing} = c_1 \cdot D_{Masing,a=1} + c_2 \cdot D_{Masing,a=1}^2 + c_3 \cdot D_{Masing,a=1}^3$$

The parameters c_1 , c_2 and c_3 are fit parameters. According to Darendeli these coefficients can be derived from the parameter a as follows:

$$\begin{aligned}c_1 &= -1.1143 \cdot a^2 + 1.8618 \cdot a + 0.2523 \\ c_2 &= 0.0805 \cdot a^2 - 0.071 \cdot a - 0.0095 \\ c_3 &= -0.0005 \cdot a^2 + 0.0002 \cdot a + 0.0003\end{aligned}$$

$$D_{Masing,a=1} = \frac{100}{\pi} \left[4 \frac{\gamma - \gamma_r \ln \left(\frac{\gamma + \gamma_r}{\gamma_r} \right)}{\frac{\gamma^2}{\gamma + \gamma_r}} - 2 \right]$$

For the multiplication factor F Darendeli developed the following expression:

$$F = b \cdot \left(\frac{G}{G_{max}} \right)^p$$

with:

- b, p parameters that control the characteristics of the function

To simplify the model a fixed value of $p=0.1$ is used by Darendeli.

The above results in a 4-parameter model (G_{max} , γ_r , a and b)

In section 9.1 of Darendeli (2001) a set of constants is given to fit the 4 parameters. The parameters are given as a function of the mean effective stress, plasticity index PI, over consolidation ratio OCR, number of cycles N and frequency f. the resulting expressions are given below;

$$\gamma_r = (0.0352 + 0.001 \cdot PI \cdot OCR^{0.32463}) \cdot (\sigma'/p_a)^{0.34834}$$

$$a = 0.919$$

$$D_{min} = (0.8005 + 0.0129 \cdot PI \cdot OCR^{-0.1069}) \cdot (\sigma'/p_a)^{-0.2889} \cdot (1 + 0.2919 \cdot \ln(f))$$

$$b = 0.6329 - 0.0057 \cdot \ln(N)$$

B.3 Adjusted Darendeli expression for peat

The expressions by Darendeli are derived for sand and clay, but not for peat.

As part of the development of the GMPE V2 an investigation of available test data in the literature was made (Bommer et al 2015). Based on the available test data, and using the functional form of Darendeli, expressions were derived. The resulting expressions are:

Shear modulus reduction

The shear modulus reduction curve is described by:

$$\frac{G}{G_{max}} = \frac{1}{1 + \left(\frac{\gamma}{\gamma_r} \right)^a}$$

The parameters a and γ_r are:

- $a = 0.776$
- $\gamma_r = 0.995 \cdot (\sigma'/p_a)^{0.694}$ [%]

Damping

The damping is described by:

$$D = F * D_{masing} + D_{min}$$

$$F = b \cdot \left(\frac{G}{G_{max}} \right)^{0.1}$$

For D_{masing} the same expressions as by Darendeli are used. The parameters D_{min} and b become:

- $D_{\text{min}} = 2.512 \cdot (\sigma' / p_a)^{-0.2889}$
- $b = 0.712$

Isotropic stress

The effective vertical stress is calculated from the soil profile and the water table. As minimum value $\sigma'_v = 15$ is to be used.

The effective isotropic stress is calculated from the effective vertical stress as:

$$\sigma'_i = \sigma'_v \cdot 0.57$$

In these expressions the organic content is not a parameter. Contrary to the expressions by Darendeli also the frequency and the number of cycles is not a parameter. These parameters were not included as the available test data were considered to be too limited for determining the possible effect on the MRD curves in a sufficient reliable form.

C External review on draft report

20. Dezember 2016

Dr. Cor Zwanenburg
DELTARES
Postbus 177

2600 MH Delft
The Netherlands

Project

Dynamic properties of Groningen peat
(ref. 1209862-006-GEO-0003)
here: expert review on two DELTARES reports

Dear Sirs.

Find my expert report in the attachment.

Best regards,



Prof. Dr.-Ing. habil. T. Schanz

Univ. Prof. Dr.-Ing. habil. Tom Schanz

GEO RUHR

Ingenieurgesellschaft für Geotechnik

Am alten Wasserwerk 12
D-45886 Gelsenkirchen

Telefon:

+49 (0) 0151 67442786

tom.schanz@georuhr.de

Finanzamt Gelsenkirchen
Steuernummer 319/5383/5890

Bankverbindung
Sparkasse Mittelthüringen
IBAN: DE57 8205 1000 1310 1130 21
BIC: HELADEF1WEM

Response to the review questions belonging to report of: Dynamic behaviour of Groningen peat, analysis and parameter assessment

This memo provides a response on the review questions belonging to report 1209862-011 Dynamic behaviour of Groningen peat, analysis and parameter assessment and report 1209862-011 Dynamic behaviour of Groningen peat, factual report. The reviewer responses are as follows:

Review question:

- *The aim of the study is to derive the dynamic parameters for Groningen peat, and in particular the parameters needed for the soil response calculations. Is, in the reviewers opinion, the study focused on the correct parameters or are, in the reviewers opinion, important parameters missing? If so, please explain.*

Response:

Different parameters (e.g. depth or distance of vibration source, soil properties and duration of vibration) make significant effects on response of structure or ground motion during a vibration. Among these parameters, soil properties can make significant effects on soil-structure interaction during wave propagation (Darendeli 2001). Shear modulus, G , and material damping, D , are soil properties which have a significant effect on ground motion during vibration (Seed et al. 1986). These properties are used to determine the velocities and decay of stress waves propagating through the geotechnical materials. Depending on the type of soil (e.g. granular, plastic or organic soils) various parameters can make effect on dynamic properties of soils. G and D in organic soils can be affected by various parameters. Previous studies (e.g. Kramer 2000, Wehling et al. 2003 and Kishida et al. 2009) reported that dynamic properties of organic soils can be mainly affected by organic content, stress state, void ratio, over consolidation ratio. Furthermore, Kramer (2000) and the preformed analysis on peat samples (Figure 2) revealed that the results can be also affected by frequency of loading, although, this effect in organic soils is not significant (see attached report). The effect of these main parameters were studied on the dynamic behaviour of Groningen peat samples. The empirical relationships were also developed and modified to predict G_{max} , $G(\gamma)$ and $D(\gamma)$ on Groningen peat samples. To predict the G_{max} the well-known empirical relationship developed by Hardin (Hardin and Black 1966) was correlated to organic content, stress state and void ratio. $G(\gamma)$ is estimated through the hyperbolic relationship developed by Hardin (Hardin and Black 1966) or Equation 1 as a modified form of Hardin's relationship (e.g. Hashash and Park 2001 and Arefi et al. 2012) or another hyperbolic model developed by Hardin (Hardin and Drnevich 1972), which has been presented in my former report (see detailed analysis in the appendix).

$$\frac{G}{G_{max}} = \frac{1}{1 + \beta \left(\frac{\gamma}{\gamma_r}\right)^\alpha} \quad (1)$$

These models are a function of reference shear strain γ_r . The effect of organic content and stress state on reference shear strain were also studied. Furthermore, damping ratio were also written as a function of reference shear strain. Therefore, one can estimate maximum shear modulus, G_{max} and reference shear strain, γ_r , using the correlated models to organic content and mean effective stress. Afterwards, the curves of $G(\gamma)$ and $D(\gamma)$ can be predicted.

Review question:

- *Are the testing procedures followed correct, consistent and state of the art? And is the quality of the test result sufficient for the purpose of the study?*

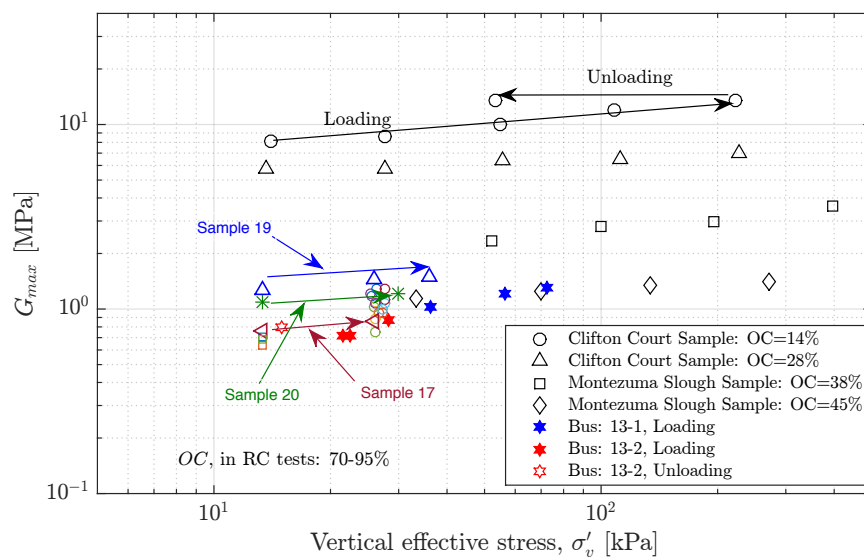
Response:

The goal of study was to determine the small and intermediate dynamic properties of Groningen peat samples. The experiment were conducted using three devices: i) bender elements to determine stiffness at small strain region ii) resonant column device, to determine stiffness and damping ratio at small and intermediate region and, ii) direct shear device for intermediate to large strain levels.

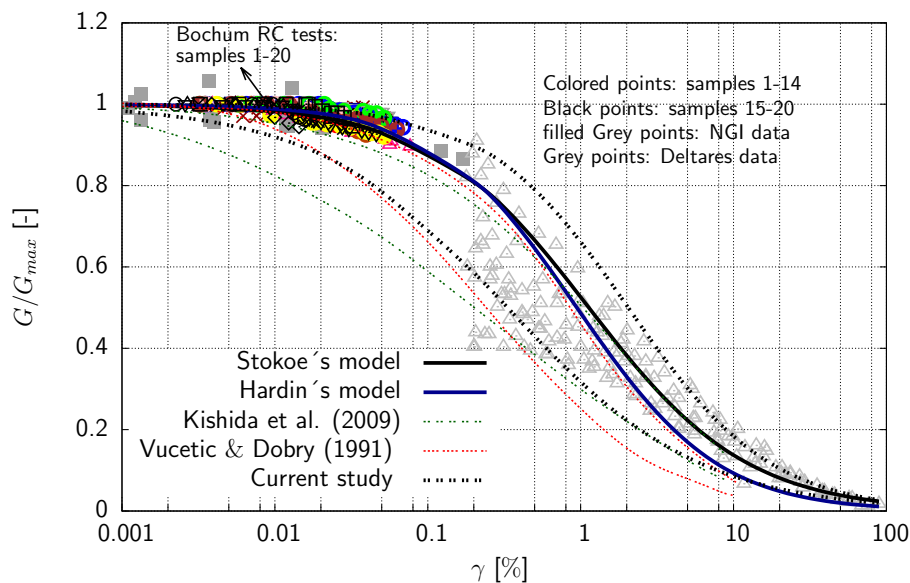
Piezoelectric elements are mounted in different laboratory devices to measure the maximum shear stiffness at low amplitude of deformations in last few decades (e.g. Jovicic and Coop 1988, Kuwano et al. 2000, Kuwano and Jardine 2004, Sadek et al. 2007, Wang and Mok 2008). Bender element test is not a standard procedure to determine modulus degradation and damping ratio curves.

Beside of piezoelectric elements, resonant column device is one of the standard methods (ASTM D-4015) to measure the small strain properties at very small to medium level of deformations. The resonant column device is an accurate device but, the accuracy of results depends on the calibration of device.

Therefore, before performing tests on Groningen peat samples using the resonant column device, calibration of devices for stiffness and damping ratio were done using the numerical and experimental methods (see attached report). Furthermore, the test results from this experiment were also compared with the published data for inorganic and organic soils (e.g. Figure 1). This Figure shows a good agreement between the measured results from this experiment in comparison with the proposed lines for inorganic and organic soils. This confirms that experiment has been done with sufficient accuracy.



(a)



(b)

Figure 1: The results from this experimental program in comparison with the published data: (a) G_{max} from this experiment, colored points, in comparison with G_{max} from literature, black points; (b) G/G_{max} versus γ from this experiment in comparison with the defined ranges by Vucetic and Dobry (1991) for plastic soils and Kishida et al. (2009) for organic soils

Review question:

- *Laboratory tests were conducted by different laboratories and results are combined in the analysis. Is, in the reviewers opinion, the data, derived by the different laboratories, sufficiently consistent? Meaning there are no significant systematic differences between the laboratories due to different testing techniques, equipment etc.*

Response:

Different dynamic devices don't yield similar results in most of the times. These differences could be due to the number of applied cycle of loading (e.g. Tatsuoka et al. 1978) and the frequency of loading (e.g. Stokoe and Santamarina 2000). Resonant column and Bender element tests were conducted to determine the dynamic properties of the Groningen peat samples. The effect of frequency on the results have been explained in the attached report.

However, the performed analysis showed that the stiffness of Groningen peat is affected by frequency and the existing scatter between the measured stiffness using various devices was due to the frequency of loading (details can be found in attached report). However, the influence of frequency on stiffness of peat is not significant in comparison to plastic soils .

Stokoe and Santamarina (2000) showed that small strain properties of cohesive soils can be significantly affected by the frequency of vibration during laboratory tests (Figure 2). The normalized stiffness using experiment at RUB on Groningen peat samples show the significant effect of frequency on shear modulus (attached report). Grey zone in Figure 2 shows the predicted range for the effect of frequency on stiffness of Groningen peat samples. The red line in this Figure is the estimated average line for the effect of frequency in adopted samples. NGI did bender element tests on Groningen peat with frequency between 500 to 600 Hz but, unfortunately, the frequency of their RC tests is not available.

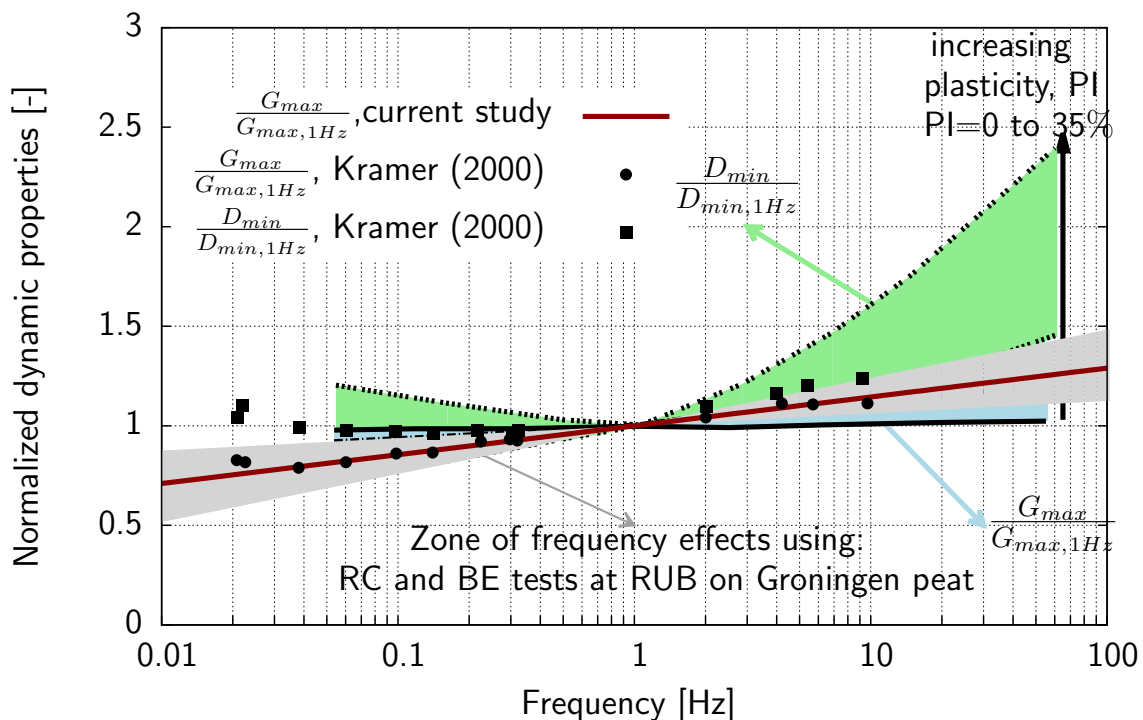


Figure 2: General effect of excitation frequency on small strain shear modulus, G_{max} , and small strain damping ratio, D_{min} , Deltares experiment has been done with frequency of 0.1 Hz (modified after Stokoe and Santamarina 2000)

Furthermore, the experimental data by Kramer (2000) on Mercer Slough Peat was also normalized with the estimated reference shear modulus for their data. Figure 2 shows the normalized average line of maximum shear modulus from the experiment at RUB on peat samples in comparison with the proposed zones for cohesive soils and data by Kramer (2000) for peat samples. The data shows that the increasing of stiffness in peat samples are in agreement with literature.

Therefore, test results on peat samples from different dynamic devices do not yield similar values when the frequency of loading is different.

Review question:

- *Is the analysis of the data correct, consistent and sufficient for the purpose of the study?*

Response:

Two analysis are available to determine the value of G_{max} in this study: i) the developed model based on the analysis of Deltares; ii) developed model from my report (attached report). Deltares model is based on the regression of experimental data from Groningen peat samples. The regression has been done to find the equation with the maximum R^2 . However, this model could be also validated by existing published data on peats (e.g. data from Kishida et al. 2009). On the other hand, the model from my report has been based on the well-known model developed by Hardin (Hardin and Black 1966). This Equation has been already used for organic and inorganic soils (e.g. Kishida et al. 2009 and Ishihara 1996). However, in this model 3 functions have been adopted in my report to capture the effect of e , OC and p' : a) void ratio function that is in the form of $f(e) = e^d$ which was originally developed by Jamiolkowski et al. (1995) for clays ; b) organic content function, OC , which was assumed to be in the form of void ratio function and, c) pressure function, which is in form of developed function by Hardin for soils. The fitting parameters of these functions were determined by optimization analysis of data in 3D space (see section 1.1.1 in attached report). However, one can improve the scatter of data by developing another organic content function.

Review question:

- *The study shows low values for G_0 and vs. These values are considerably lower than usually found for clays and sands. Can in the reviewers opinion the obtained values for peat in this study be used for further analysis?*

Response:

The experiment has been done on samples containing high amount of organic content. As can be seen in Figure 1a, organic content has a negative effect on maximum shear modulus. However, for samples containing low amount of organic content the proposed models must be re-calibrated. Because, this

models have been proposed for Groningen peat sample containing high amount of *OC*.

Review question:

- *The analysis focuses on producing correlations for the Groningen area. By these correlations parameters can be assessed for locations other than the sample locations. Is the number of tests, quality of the tests and applied correlations sufficient for this purpose in relation to the aim of the project?*

Response:

As mentioned above, the experiment has been conducted on samples containing high amount of organic content and samples subjected to vertical stress 13-30 kPa. For samples containing the same amount of organic content the equations could be applicable, but for samples containing low amount of organic content the proposed models must be re-calibrated. It must be noted that in the case of low organic content, the models are similar in their mathematical representations but fitting parameters will be different.

Review question:

- *The study showed difficulty in measuring the damping curve. Is the analysis of the damping curve and its parameters sufficient for the purpose of this study? Are there any suggestions to improve the damping curve measurements or the interpretation of the available test data?*

Response:

The originality of the proposed model was for sand samples (see attached report), however, this model was compared with the comprehensive data points and models from published data in Figure 3.

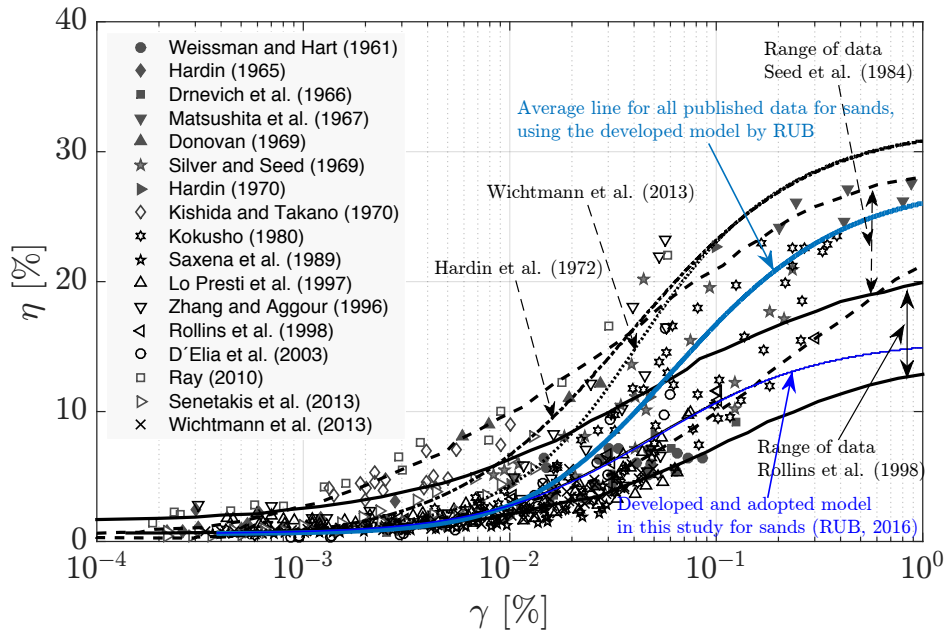


Figure 3: The developed model for damping ratio in comparison with published data for sands

The fitting parameters of developed model was determined for Groningen peat samples. The predicted curve using this model has been compared with the defined range for inorganic and organic soils in Figure 4.

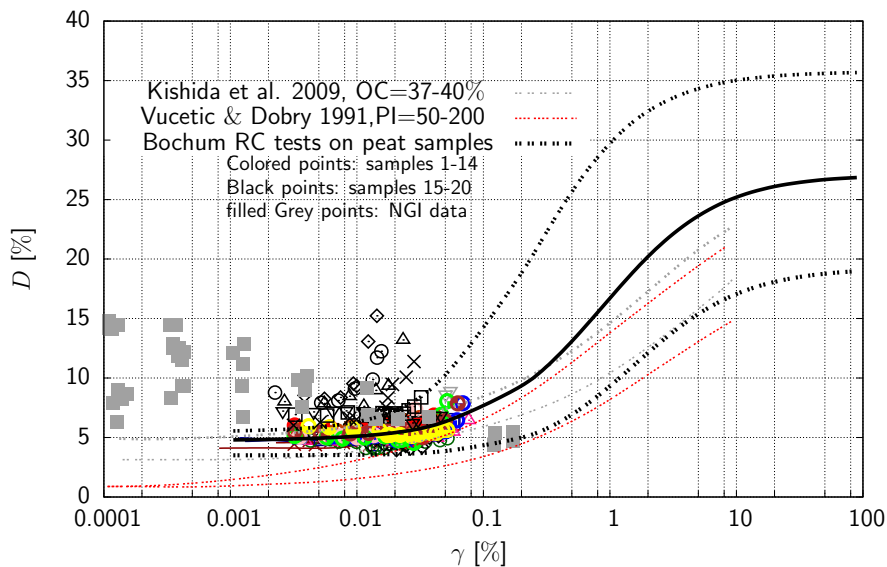


Figure 4: The results from this experimental program in comparison with the published data. D versus γ from this experiment in comparison with the defined ranges by Vucetic and Dobry (1991) for plastic soils and Kishida et al. (2009) for organic soils. Solid line is the defined average line for damping ratio based on the RC results

To improve the measured damping ratio, damping of NGI and Deltares devices must be clarified. Furthermore, the effect of frequency on the measured damping ratio must be also taken into account.

Review question:

- *The study focuses on the superficial peat layer, the Nieuwkoop formation. In the area there is also a thin basal peat layer present. Is it, in the reviewers opinion, possible to use the data, found for the superficial layers, for parameter assessment of the basal peat layer? Does the reviewer have any further suggestions about dealing with the basal peat layer?*

Response:

The experimental results showed that G_{max} increases with an increase in mean effective stress, p' . The trend of data was the same as the proposed curve by Hardin and Black (1966) ($G_{max} = Kf(p') = K(p'/p_a)^n$) for geo-materials. Additionally, the trend of G_{max} versus effective stress is in agreement with the published works. Furthermore, the developed model to predict G_{max} is in the form of Hardin's relationship, therefore, we expect that the effect of p' will be covered for wide range of stress states. This has been shown in Figure 1.7 (attached report). The experimental data from current study and published data by Kishida et al. (2009) show that the effect of mean effective stress on G/G_{max} and D versus γ curves in samples containing high amount of organic contents is not significant, although, the value of γ_r in attached report has been also correlated to the mean effective stress (Figure 1.11 in attached report). This means G_{max} , G/G_{max} and D can be roughly estimated in basal layers, when we are dealing with the same amount of organic content.

Review question:

- *Are there any further comments the reviewer wants to make about this study?*

Response:

The performed analysis was maximum possible analysis for this experimental program. For an accurate analysis, the experiment must be done on a wide range of stress state and samples containing wide range of organic content. However, the data from this experimental study was limited to a narrow range of organic content and stress state. This makes difficulty in more general analysis of data.

References

- Arefi, M. J., Cubrinovski, M. and Bradley, B. A. (2012), A model for nonlinear total stress analysis with consistent stiffness and damping variation, *in* '15WCEE'.
- Darendeli, M. B. (2001), Development of a new family of normalized modulus reduction and material damping curves, PhD thesis, University of Texas at Austin.
- Hardin, B. O. and Black, W. L. (1966), 'Sand stiffness under various triaxial stresses', *Soils Mechanics and Foundations Division* ., 27–42.
- Hardin, B. O. and Drnevich, V. P. (1972), 'Shear modulus and damping in soils: Design equations and curves', *Soil Mechanics and Foundation Division* **98**, 667–692.
- Hashash, Y. M. A. and Park, D. (2001), 'Non-linear one-dimensional seismic ground motion propagation in the mississippi embayment', *Engineering Geology* **62**, 185–206.
- Ishihara, K. (1996), *Soil behavior in earthquake geotechnics*, Oxford Engineering Science.
- Jamiolkowski, M., Lancellotta, R. and Lo Presti, D. (1995), 'Remarks on the stiffness at small strains of six italian clays', *Pre-failure Deformation of Geomaterials* **1**, 817–836.
- Jovicic, V. and Coop, M. R. (1988), 'The measurement of stiffness anisotropy in clays with bender element tests in the triaxial apparatus', *Geotechnical Testing Journal* **21**, 3–10.
- Kishida, T., M., W. T., Boulanger, R. W., Driller, M. W. and Stokoe, II, K. (2009), 'Dynamic properties of highly organic soils from montezuma slough and clifton court', *Journal of Geotechnical and Geoenvironmental Engineering* **135**, 525–531.
- Kramer, S. L. (2000), 'Dynamic response of mercer slough peat', *Journal of Geotechnical and Geoenvironmental Engineering* **126**, 504–510.
- Kuwano, R., Connolly, T. M. and Jardine, R. J. (2000), 'Anisotropic stiffness measurements in a stress-path triaxial cell', *Geotechnical Testing Journal* **23**, 141–157.
- Kuwano, R. and Jardine, R. J. (2004), 'On the applicability of cross-anisotropic elasticity to granular materials at very small strains', *Géotechnique* **52**, 727–749.
- Sadek, T., Lings, M., Diloru, L. and Wood, D. M. (2007), 'Wave transmission in hostun sand: multiaxial experiments', *Rivista Italiana Di Geotecnica* **2**, 69–84.
- Seed, B., Wong, R., Idriss, I. and Tokimatsu, K. (1986), 'Moduli and damping factors for dynamic analyses of cohesionless soils', *Journal of Geotechnical and Geoenvironmental Engineering* **112**, 1016–1032.

- Stokoe, II, K. and Santamarina, C. (2000), Seismic wave based testing in geotechnical engineering, Technical report.
- Tatsuoka, F., Iwasaki, T. and Takagi, Y. (1978), 'Hysteretic damping of sands under cyclic loading and its relation to shear modulus', *Soils and Foundations* **18**, 26–39.
- Vucetic, M. and Dobry, R. (1991), 'Effect of soil plasticity on cyclic response', *J. Geotech. Eng.* **117**, 89–107.
- Wang, Y. and Mok, C. (2008), 'Mechanisms of small strain shear modulus anisotropy in soils', *Journal of Geotechnical and Geoenvironmental Engineering* **134**, 1516–1530.
- Wehling, T. M., Boulanger, R. W., Arulnathan, R., Harder, L. F. and Driller, M. W. (2003), 'Non-linear dynamic properties of a fibrous organic soil', *J. Geotech. Geoenviron. Eng.* **129**, 929–939.

Appendix A

Contents

Appendix	1
1 Empirical relationships	9
1.1 Derivation of empirical relationships	9
1.1.1 Maximum shear modulus, G_{max}	9
1.1.1.1 Prediction of G_{max} using shear wave velocity	10
1.1.1.2 Prediction of G_{max} using Hardin's relationship	14
1.1.2 Prediction of S_{su}	19
1.1.3 Intermediate shear modulus and damping ratio, $G(\gamma)$ & $D(\gamma)$	19
1.2 Comparison of derived empirical relationships with published data	28
2 Discussion	31
2.1 Influence of frequency on dynamic properties	31

List of Figures

1.1	Shear wave velocity versus organic content, OC, and mean effective stress, $p' = \frac{(\sigma'_v + \sigma'_h)}{2}$. Solid points are results from BE test and open points are from RC test	11
1.2	Normalized v_s versus organic content, OC	11
1.3	Measured v_s using Bochum RC device versus predicted v_s using Equation 1.7	12
1.4	(a) Normalized v_s versus organic content, OC. Data from RC and BE tests are open and solid points respectively; (b) v_s versus frequency, (Santamarina 2001)	13
1.5	Measured G_{max} using Bochum RC device versus predicted G_{max} using Equations 1.7 and 1.1	13
1.6	G_{max} versus void ratio, e and organic content, OC , for stress level of: a) $p'=8$ kPa, $p' \approx 8$ kPa is related to the samples subjected to the $\sigma'_h=3.3$ kPa from RUB data; b) $p'=16$ kPa, $p' \approx 16$ kPa is related to the samples subjected to the $p'=15.6$ to 16.4 kPa from RUB and NGI data using RC device; c) $p'=17$ kPa, $p' \approx 17$ kPa is related to the samples subjected to the $p'=16.6$ to 17.4 kPa from RUB and NGI data using RC device	16
1.7	(a) Normalized G_{max} versus mean effective stress, p' , for all of the data from RUB and NGI using resonant column device: a) M and D are from Figures 1.6a; b) M and D are from Figure 1.6b; c) M and D are from Figure 1.6c	17
1.8	Normalized G_{max} versus void ratio, e and organic content, OC , for all of the data from RUB and NGI using resonant column device	18
1.9	Measured G_{max} using RUB and NGI resonant column device versus predicted G_{max} using Equation 1.10 and determined fitting parameters	18
1.10	Normalized S_{su} versus density, ρ for all samples	19
1.11	Normalized γ_r versus organic content, OC	21
1.12	Normalized γ_r versus S_{su}	21

List of Figures

1.13	Experimental data from Deltares, Bochum and NGI, provided by Deltares	23
1.14	G/G_{max} versus shear strain, Deltares data were:(a) normalized with the minimum measured value for G_{max} for samples 1 to 14 using Bochum RC device; (b) normalized with the maximum measured value of G_{max} for samples 1 to 14 using Bochum RC device	24
1.15	G/G_{max} , normalized with the average values of G_{max} for samples 1 to 14, versus shear strain. Solid lines are Equations 1.13 and 1.14 with determined fitting parameters from analysis of Bochum RC test on samples 1 to 14 and Deltares data	25
1.16	G/G_{max} versus shear strain, solid lines are Equations 1.13 and 1.14 with determined fitting parameters from analysis of Bochum RC test on samples 1 to 14 and Deltares data	25
1.17	D versus shear strain, solid line is Equation 1.16 with fitting parameters defined for samples 1 to 14 from Bochum RC test	27
1.18	Normalized D versus shear strain for dutch peat samples, measured by Bochum RC device, and Equation 1.16 with fitting parameters obtained from Figure 1.17	27
1.19	The measured G_{max} by Kishida et al. (2009) versus the predicted G_{max} using Equations 1.7 and 1.1	28
1.20	Small and intermediate properties of peat samples in comparison with the published data: a) shear modulus versus shear strain; b) damping ratio versus shear strain the solid and dashed black lines are curves from Equations 1.13 and 1.16 using the determined fitting parameters from this experiment for samples 1 to 14, $D_{min}=4.75\%$, dashed lines are the proposed bonds for organic and inorganic soils, solid lines are the estimated curves using the proposed models	29
2.1	The effect of frequency on small strain shear modulus, G_{max} , of sample No. 10 (NW1A2-B1-3A)	32
2.2	General effect of frequency on small strain shear modulus, G_{max} , of Geroningen peat samples, RC and BE frequency from RUB data and BE frequency from NGI data	32
2.3	General effect of frequency on small strain shear modulus, G_{max} , (modified after Kramer 2000)	33

2.4 General effect of excitation frequency on small strain shear modulus, G_{max} , and small strain damping ratio, D_{min} , Deltares experiment has been done with frequency of 0.1 Hz (modified after Stokoe & Santamarina 2000) . . . 34

1 Empirical relationships

1.1 Derivation of empirical relationships

1.1.1 Maximum shear modulus, G_{max}

Resonant column device was initially adopted by [Iida \(1937\)](#), Japanese researcher, to evaluate the influence of water content on wave velocity. Equation 1.1 is employed to estimate the value of shear stiffness from wave velocity in this report.

$$G_{max} = \rho v_s^2 \quad (1.1)$$

where, ρ is density, v_s is shear wave velocity and G_{max} is maximum shear modulus. This Equation was widely used to measure the stiffness in geo-materials using wave velocity (e.g. Piezoelectric element tests, resonant column device and etc.) in last decades.

However, for ease of discussion, Equation 1.1 will be employed to estimate G_{max} in this section. Therefore, as first step, empirical relationships will be written to determine the value of shear wave velocity, v_s . Afterwards, G_{max} will be estimated using Equation 1.1. Among various relationships between v_s and factors which have an effect on v_s , two simplest forms (Equations 1.2 and 1.3) have been used to illustrate the stress and void ratio dependency of v_s (e.g. [Moon & Ku 2016](#)):

$$v_s = \Gamma_1 \sigma_r \left(\frac{p'}{\sigma_r} \right)^{m_1} \quad (1.2)$$

$$v_s = \Gamma_2 (e)^{m_2} \quad (1.3)$$

where, p' is mean effective stress, e is void ratio, the coefficients Γ_1 (m/s) and Γ_2 (m/s) are material constants, and the exponents m_1 and m_2 represent the sensitivity of stress and void ratio respectively. σ_r is a reference pressure, which is assumed to be 1 kPa, therefore, we do not write it in the next Equations for v_s in this report.

[Schanz et al. \(2016\)](#) reported that v_s must be written as a function of constant parameter

1 Empirical relationships

Γ , mean effective stress and void ratio (Equation 1.4) as a unique function:

$$v_s = \Gamma f(e) f(p') \quad (1.4)$$

where, Γ is fitting parameter, $f(e)$ and $f(p')$ are void ratio and pressure functions.

1.1.1.1 Prediction of G_{max} using shear wave velocity

However, for simplicity of analysis, Equations 1.2 and 1.3 are used independently (e.g. Moon & Ku 2016) in literature. In this report, the goal is to find the effect of organic content on v_s . Therefore, Equation 1.2 was employed and correlated to the organic content.

Shear wave velocities from RC and BE test were drawn versus organic content and mean effective stress in 3D space (Figure 1.1). This Figure reveals that v_s decreases with an increase in the organic content and increases with an increase in the mean effective stress. A preliminary analysis of data shows that a unique surface could be derived for data in this Figure, where the effect of OC and p' may be estimated through Equations 1.5 and 1.6 as follows:

$$f(OC) = (OC)^\eta \quad (1.5)$$

$$f(p) = (p')^\zeta \quad (1.6)$$

where, ζ and η are fitting parameters. From Figure 1.1, the value of ζ was equal to 0.20. v_s was normalized with respect to the $f(p')$ which is determined using Equation 1.6.

1.1 Derivation of empirical relationships

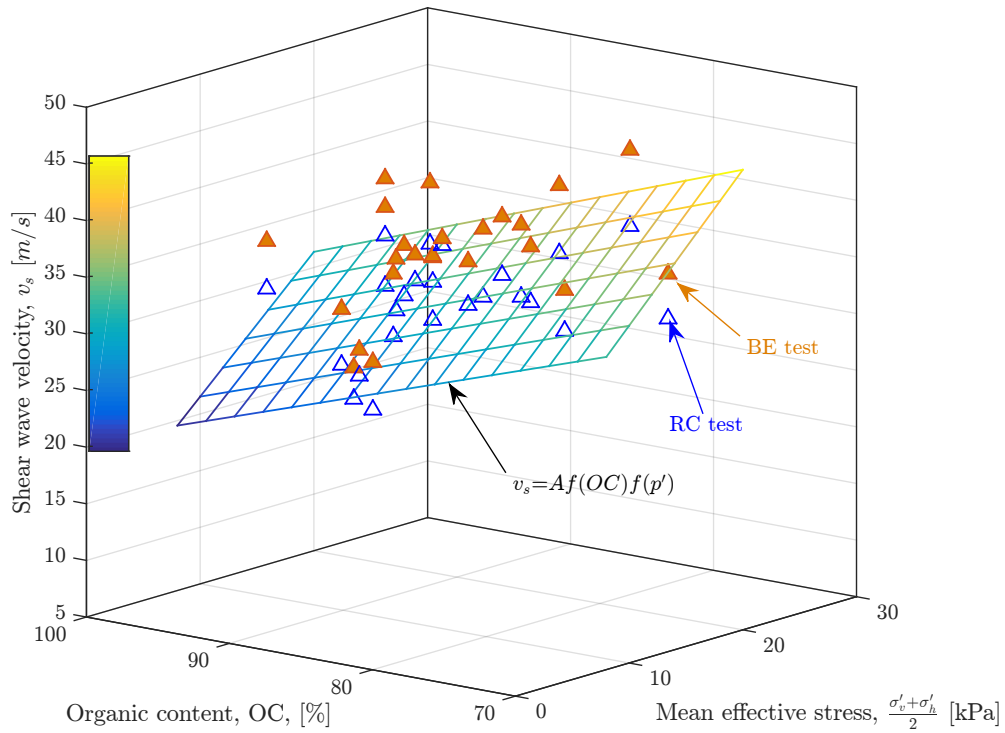


Figure 1.1: Shear wave velocity versus organic content, OC, and mean effective stress, $p' = \frac{(\sigma'_v + \sigma'_h)}{2}$. Solid points are results from BE test and open points are from RC test

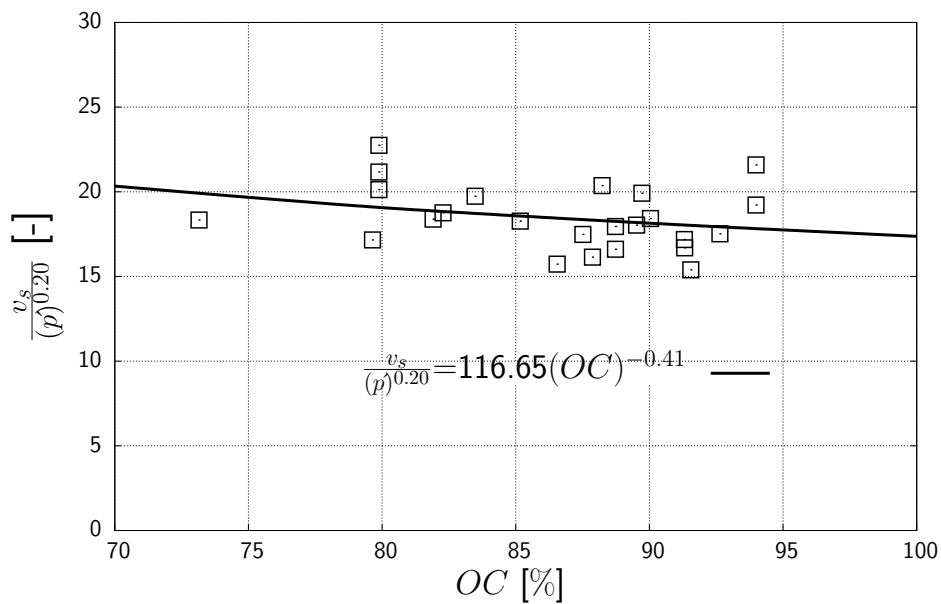


Figure 1.2: Normalized v_s versus organic content, OC

1 Empirical relationships

Normalized v_s was drawn versus OC in Figure 1.2. This Figure shows also the reduction of wave velocity with organic content. Therefore, Equation 1.5 could be an appropriate relationship to capture the effect of OC in adopted peat samples. Therefore, Equation 1.7 can be written as:

$$v_s = \mu f(OC) f(p') = \mu (OC)^\eta (p')^\zeta \quad (1.7)$$

where, μ is equal to 116.65, η and ζ are equal to -0.41 and 0.20 for test data on Groningen peat samples using resonant column device. Figure 1.3 shows predicted results using Equation 1.7 and measured v_s using Bochum RC device.

Maximum shear modulus, G_{max} , is estimated using Equation 1.1, where ρ is density of sample from Table 1.1 and v_s is shear wave velocity from Equation 1.7.

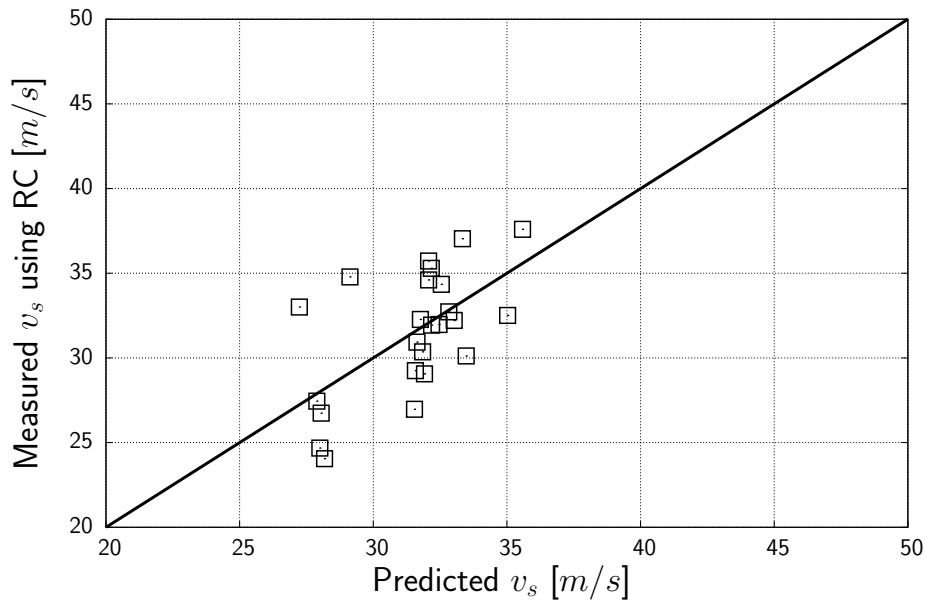


Figure 1.3: Measured v_s using Bochum RC device versus predicted v_s using Equation 1.7

It is worthwhile to mention that all of the analysis have been done on the results obtained from RC test, because RC results will be used to propose a model for $D(\gamma)$ and $G(\gamma)$ in the next sections.

Measured wave velocity using BE test have been compared to the model suggested for RC data in Figure 1.4a. This Figure shows that the wave velocity, measured using BE test, are approximately 3-5 m/s larger than the values from RC test for all the samples. This difference could be due to the frequency of waves in both tests. RC tests were conducted under frequency of 4-5 Hz but the frequency of waves in BE test were variable

1.1 Derivation of empirical relationships

between 800-1300 Hz and we were dealing with the wet samples. Regarding to [Biot \(1955\)](#) theory, the effect of frequency on water content must be taken into account. The effect of frequency on wave velocity can be explained through Figure 1.4b ([Biot 1955](#) and [Santamarina 2001](#)). As can be seen in this Figure, the wave velocity, in moist porous media, increases with an increase in frequency.

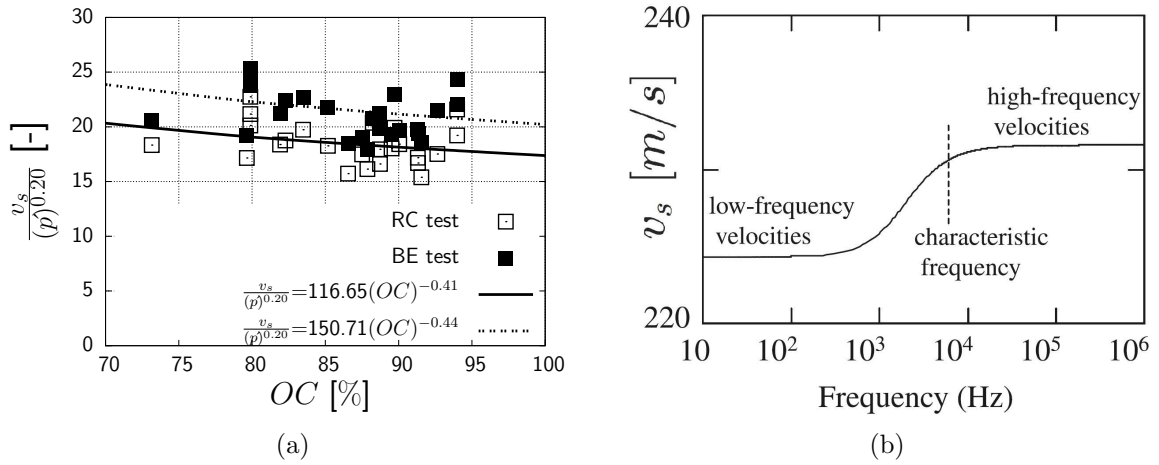


Figure 1.4: (a) Normalized v_s versus organic content, OC. Data from RC and BE tests are open and solid points respectively; (b) v_s versus frequency, ([Santamarina 2001](#))

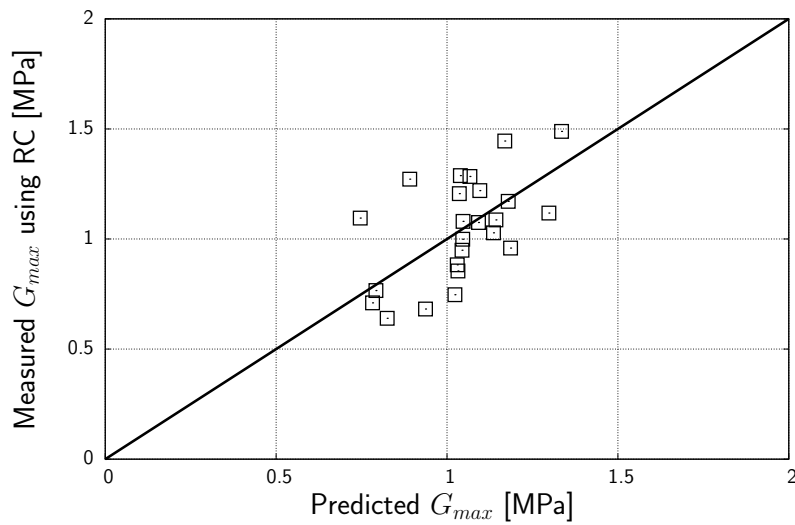


Figure 1.5: Measured G_{max} using Bochum RC device versus predicted G_{max} using Equations 1.7 and 1.1

1 Empirical relationships

Figure 1.5 shows the measured G_{max} using Bochum RC device versus predicted G_{max} with Equations 1.7 and 1.1.

1.1.1.2 Prediction of G_{max} using Hardin's relationship

Previous studies have illustrated the influence of effective confining stress (σ'_h), void ratio (e), soil structure and fabric, and other factors on maximum shear modulus, G_{max} . Hardin & Black (1966), arguably, the first to propose one of the most widely used empirical relation to predict G_{max} (Equation 1.8) which was assumed to be a function of void ratio, e and mean effective stress, p' (Goudarzy et al. 2016).

$$G_{max} = \lambda f(e) f(p') = \lambda f(e) \sigma_r \left(\frac{p'}{\sigma_r} \right)^N \quad (1.8)$$

where, λ is a material constant which depends on the type of soil, σ_r is a reference pressure to balance the unit of Equation. We assume that σ_r is equal to 1 kPa and we do not write it in the next Equations for G_{max} in this report. n is an exponent and $f(e)$ is void ratio function.

In this section, Hardin's relationship, Equation 1.8, is calibrated to predict G_{max} in adopted peat samples. General form of Hardin's relationship consists of three main parts: i) constant fitting parameter of λ , ii) pressure function, $f(p')$, which is a power function of mean effective stress, $f(p') = \left(\frac{p'}{\sigma_r} \right)^N$ (See Equation 1.8) iii) void ratio function, $f(e)$. Various void ratio functions have been developed to capture the effect of e on G_{max} , however, in this report, we employed Jamiolkowski's void ratio function, $f(e) = e^M$ (Jamiolkowski et al. 1995). Therefore, general form of Hardin's relationship can be written as:

$$G_{max} = \lambda(e)^M (p')^N \quad (1.9)$$

However, to predict G_{max} in organic soils, the effect of organic content must be also taken into account. In this report, we assume a power function, $f(OC) = (OC)^D$, to capture the effect of organic content. Therefore, Hardin's relationship can be written as:

$$G_{max} = \lambda(e)^M (OC)^D (p')^N \quad (1.10)$$

where, λ , M , N and D are fitting parameters of this relation that must be determined. Therefore, there are four unknown fitting parameters in Equation 1.10 that must be determined for the adopted peat samples. The following steps could be done to find these fitting parameters:

1.1 Derivation of empirical relationships

1- most of the samples have been subjected to the mean effective stress between 8 to 17 kPa. We determine the integer value of each mean effective stress using floor and ceiling functions. Therefore, most of the samples have been subjected to the three mean effective stress levels: 8, 16 and 17 kPa (i.e. samples with the mean effective stress between 8 to 8.4 kPa, 15.8 to 16.4 kPa and 16.5 to 17.4 kPa have the stress level of 8, 16 and 17 kPa respectively). It must be noted that some of the samples had mean effective stress out of the defined range, therefore, they are not included in this step and they will be considered in the next steps. Figures 1.6a, 1.6b and 1.6c show the G_{max} versus, e and OC in 3D space for stress levels 8, 16 and 17 kPa respectively. Therefore, as preliminary estimation, a surface of $G_{max} = Kf(e)f(OC) = K(e)^M(OC)^D$ could be fitted to the presented data in these Figures. Optimization analysis was done using MATLAB on the data in Figures 1.6a, 1.6b and 1.6c to get the optimum values for M and D . These values have been presented in Figure 1.6 for each stress level. Now, we have three values for M and D for each stress level. These values are used in the next step to determine the value of N in pressure function ($f(p') = (p')^N$).

1 Empirical relationships

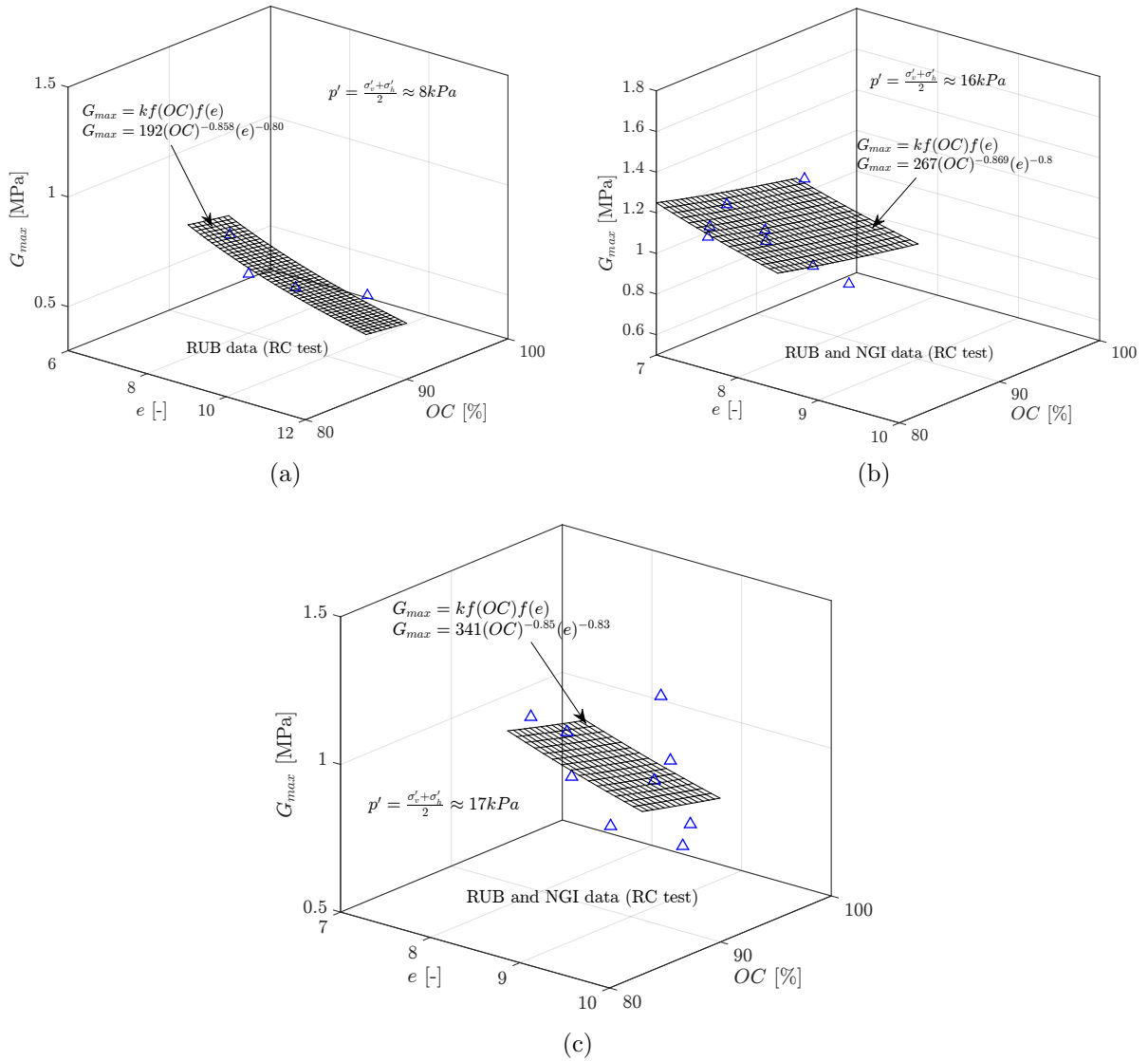


Figure 1.6: G_{max} versus void ratio, e and organic content, OC , for stress level of: a) $p' = 8$ kPa, $p' \approx 8$ kPa is related to the samples subjected to the $\sigma'_h = 3.3$ kPa from RUB data; b) $p' = 16$ kPa, $p' \approx 16$ kPa is related to the samples subjected to the $p' = 15.6$ to 16.4 kPa from RUB and NGI data using RC device; c) $p' = 17$ kPa, $p' \approx 17$ kPa is related to the samples subjected to the $p' = 16.6$ to 17.4 kPa from RUB and NGI data using RC device

2- G_{max} was normalized with respect to $(e)^M$ and $(OC)^D$. M and D are from Figures 1.6a, 1.6b and 1.6c respectively. This means we have three values for M and D . Normalized G_{max} was drawn versus mean effective stress, p' in Figure 1.7. In this step, p' is the real value of mean effective stress, that RC tests at RUB and NGI have been done for this stress level and the results for all of the samples have been presented in this Figure. The

1.1 Derivation of empirical relationships

values of λ and n in Equation 1.10 are determined by a simple power regression of data ($Y = X^n$) in Figure 1.7. The results in Figures 1.7a, 1.7b and 1.7c show that the value of N is around 0.253. Therefore, this value will be used as a power of pressure function for the adopted peat samples.

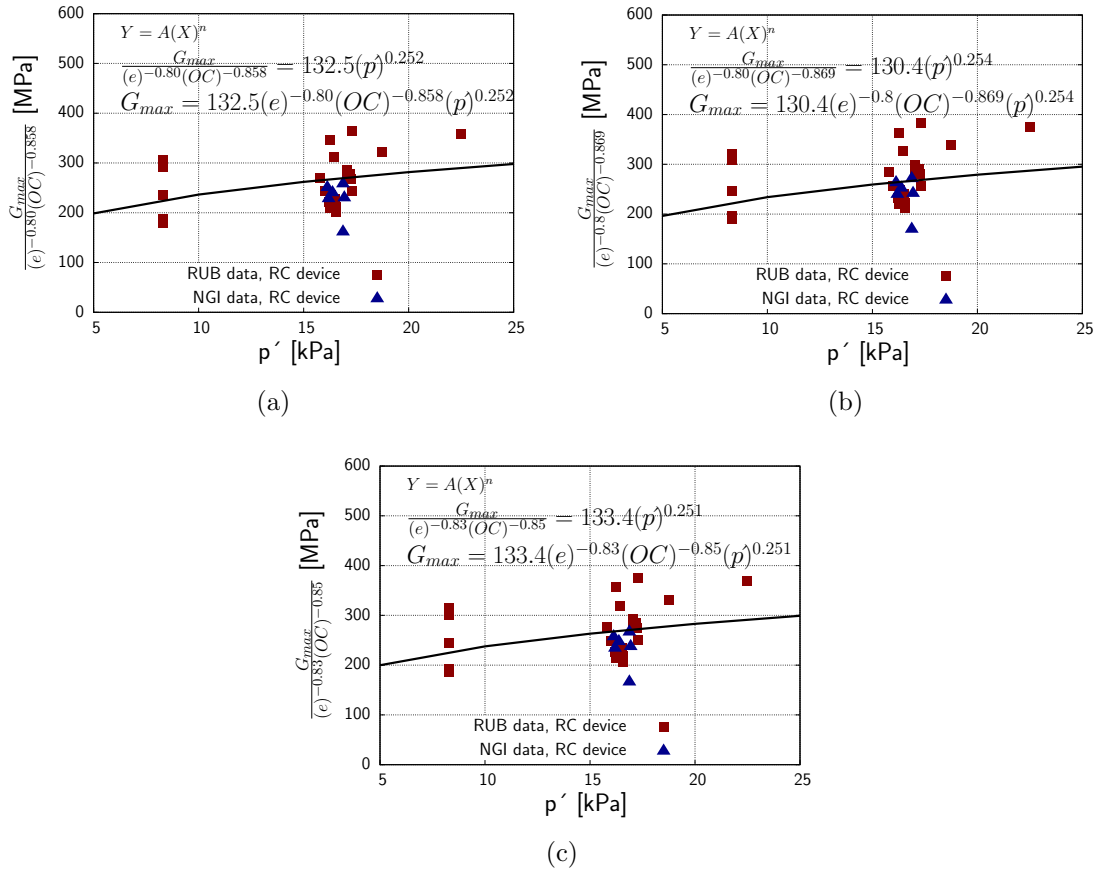


Figure 1.7: (a) Normalized G_{max} versus mean effective stress, p' , for all of the data from RUB and NGI using resonant column device: a) M and D are from Figures 1.6a; b) M and D are from Figure 1.6b; c) M and D are from Figure 1.6c

3- G_{max} was normalized with respect to the $f(p') = p'^N$, where, N is 0.253. Normalized G_{max} was drawn versus OC and e for all of the data from RUB and NGI using RC device in Figure 1.8. Again, optimization analysis was done to determine the optimum values of M , D and λ for all of the data. The analysis revealed that the optimum values of M , D and λ are -0.80, -0.85 and 132 respectively.

1 Empirical relationships

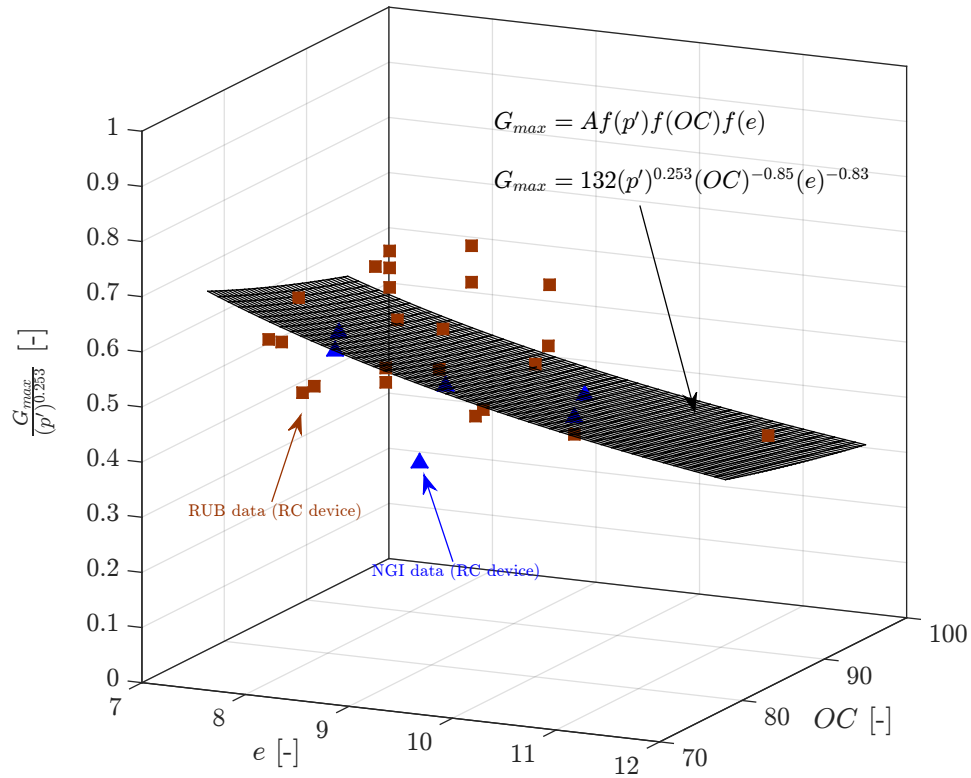


Figure 1.8: Normalized G_{max} versus void ratio, e and organic content, OC , for all of the data from RUB and NGI using resonant column device

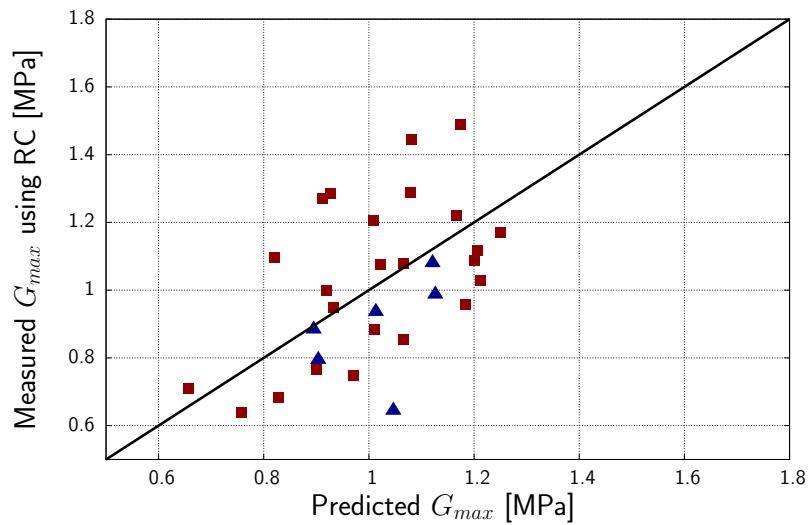


Figure 1.9: Measured G_{max} using RUB and NGI resonant column device versus predicted G_{max} using Equation 1.10 and determined fitting parameters

Figure 1.9 shows the measured G_{max} using resonant column device at RUB and NGI versus the predicted G_{max} using Equation 1.10.

1.1.2 Prediction of S_{su}

The analysis was also conducted to find the influence of organic content and density on the undrained shear strength, S_{su} , of peat samples. S_{su} was normalized with organic content function, $(OC)^\kappa$. Normalized S_{su} was drawn versus density of sample, ρ (Figure 1.10).

Figure 1.10 shows significant scatter for samples 15, 16 and 18 in comparison with the other samples, but, a unique curve could be fitted to the other data in S_{su} -OC- ρ space.

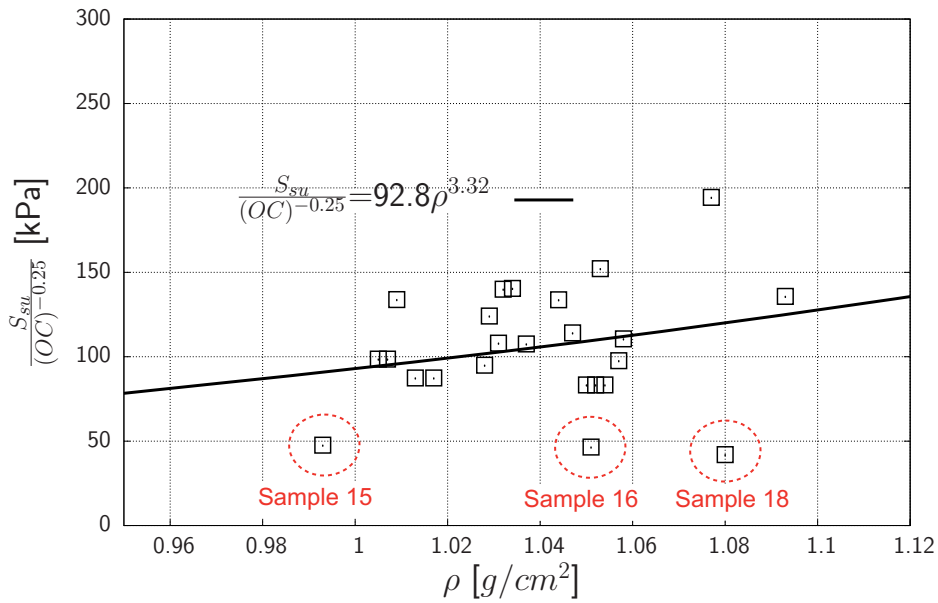


Figure 1.10: Normalized S_{su} versus density, ρ for all samples

1.1.3 Intermediate shear modulus and damping ratio, $G(\gamma)$ & $D(\gamma)$

Empirical relationships have been also developed to predict modulus degradation, $G(\gamma)$, and damping ratio, $D(\gamma)$, of soils. Hardin & Drnevich (1972a) proposed well known empirical relation 1.11 to predict the G/G_{max} curve.

1 Empirical relationships

$$\frac{G}{G_{max}} = \frac{1}{1 + \frac{\gamma}{\gamma_r}} \quad (1.11)$$

where, G_{max} is maximum shear modulus, γ is a shear strain and γ_r is the reference shear strain. Hardin's relationship is based on two main parts: maximum shear modulus and reference shear strain that must be determined.

Empirical relationships to predict γ_r (Seed & Idriss 1970) are not applicable to predict γ_r in samples subjected to anisotropic loading (Tatsuoka et al. 1979 and Goudarzy 2015). However, Goudarzy (2015) reported that the value of γ_r for samples subjected to anisotropic loading could be estimated through Equation 1.12:

$$\gamma_r = \gamma_{r100} (\sigma_v/p_a)^{m_v} (\sigma_h/p_a)^{m_h} \quad (1.12)$$

where, γ_{r100} is the reference shear strain for sample subjected to 100 kPa isotropic cell pressure, p_a is atmospheric pressure (100 kPa). Equation 1.12 can not be also used to predict γ_r in this study, because, our experiment on Dutch peat samples was limited to the maximum cell pressure of 7 kPa, therefore, the value of γ_{r100} was not available.

Two method can be used to estimate the value of γ_r in this study:

1) the value of γ_r was determined by back analysis of test data in $G/G_{max}-\gamma$ space (Goudarzy 2015). Stokoe et al. (1999) and Hashash & Park (2001) proposed a modified form of Equation 1.11 as Equation 1.13 that is called Stokoe's model in this report:

$$\frac{G}{G_{max}} = \frac{1}{1 + \beta \left(\frac{\gamma}{\gamma_r}\right)^\alpha} \quad (1.13)$$

where, γ is the shear strain, γ_r is the reference shear strain, and α , β are curve fitting parameters. Therefore, the fitting parameters of Equation 1.13 (α and β) were also determined by back analysis of test data to get the maximum R^2 . The obtained values of γ_r from our experiment for all of the Dutch peat samples, using Bochum RC device, are summarized in Table 1.1. The average value of γ_r , for samples 1 to 14, from this Table 1.1 is 1.08%, which is close to the estimated value from Figure 1.15.

Hardin & Drnevich (1972b) defined a hyperbolic strain, γ_h and proposed Equation 1.14 to predict the modulus degradation. This model is called Hardin's model in this report.

$$\frac{G}{G_{max}} = \frac{1}{1 + \gamma_h} = \frac{1}{1 + \frac{\gamma}{\gamma_r} [1 + a \exp(-b \frac{\gamma}{\gamma_r})]} \quad (1.14)$$

Where a and b are fitting curve parameters and γ_r is reference strain.

Figure 1.11 shows the effect of organic content on reference shear strain, γ_r . This Figure shows that a unique curve could be fitted to the data in $\gamma_r - OC$ space.

1.1 Derivation of empirical relationships

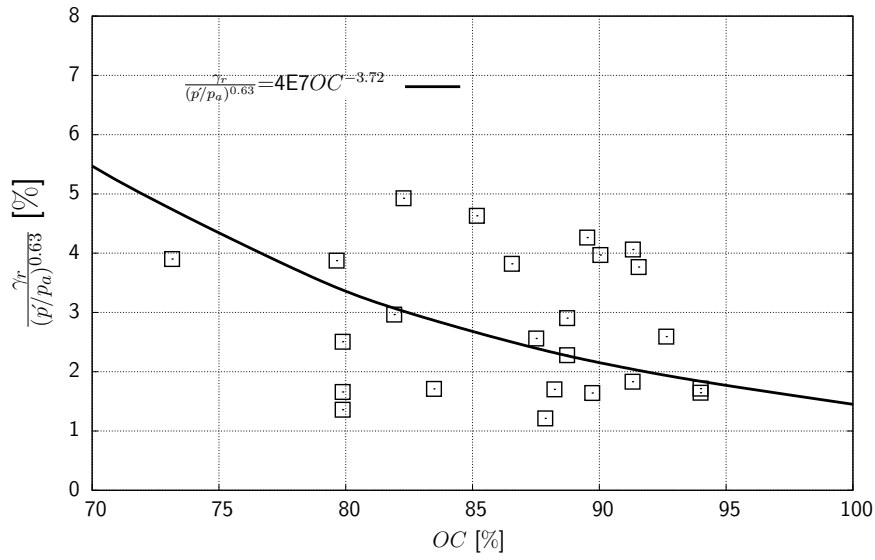


Figure 1.11: Normalized γ_r versus organic content, OC

Figure 1.12 shows the relation between γ_r and S_{su} . This Figure shows that γ_r could also be a function of p' and OC . However, the scatter of data in Figures 1.11 and 1.12 may be reduced by considering the effect of other parameters on γ_r (e.g. water content, density).

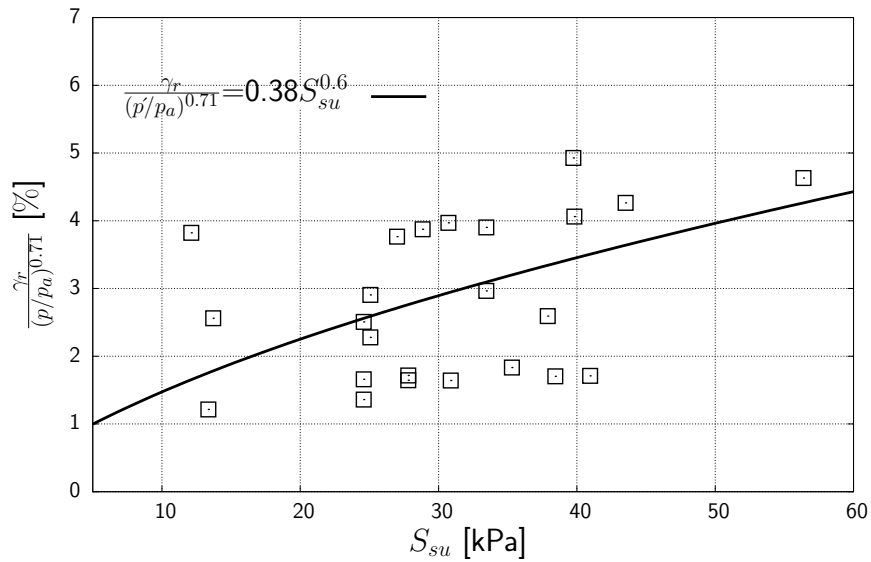


Figure 1.12: Normalized γ_r versus S_{su}

1 Empirical relationships

Table 1.1: The value of γ_r for all samples

Sample No.	Sample name	σ_h' [kPa]	σ_v' [kPa]	$(\sigma_h' + \sigma_v')/2$ [kPa]	G_{max} [Mpa]	ρ [g/cm^3]	OC [%]	S_{su} [kPa]	α [-]	β [-]	γ_r [-]	γ_r [%]
1	NW1A2-A5-1D	6.40	25.60	16.00	1.171	1.093	82.280	39.740	1.0000	1.0000	0.0154	1.5446
2	NW1A2-A6-1A	6.40	26.60	16.50	0.959	1.057	79.640	28.850	0.9999	1.0036	0.0124	1.238
3	NW1A2-B1-2B	6.60	26.10	16.35	1.087	1.047	81.910	33.450	0.9984	0.9995	0.0094	0.942
4	NW1A2-C1-1A	6.30	25.30	15.80	1.220	1.034	83.480	40.960	0.9801	0.9916	0.0053	0.531
5	NW1A2-D1-1A	6.50	26.00	16.25	1.028	1.077	85.170	45.910	1.0227	1.1005	0.0146	1.466
6	NW1A2-D2-2A	6.90	27.60	17.25	1.075	1.053	89.520	43.520	1.0087	1.0023	0.0140	1.402
7	NW1A2-a7-1A	7.00	27.70	17.35	1.118	1.058	73.150	33.450	1.0200	1.0049	0.0128	1.287
8	NW1A2-d1-2	6.60	26.30	16.45	1.288	1.009	88.230	38.440	1.0257	1.0083	0.0054	0.543
9	NW1A2-d2-1C	6.80	27.30	17.05	0.949	1.029	91.310	35.300	1.0103	1.0033	0.0059	0.598
10	NW1A2-B1-3A	6.60	26.10	16.35	0.883	1.032	91.320	39.820	1.0408	1.0115	0.0129	1.291
11	NW1A2-B2-2A	6.60	26.10	16.35	1.080	1.037	90.040	30.710	1.0311	1.0071	0.0126	1.262
12	NW1A2-C1-2B	6.60	26.10	16.35	0.747	1.028	91.550	27.000	1.0276	1.1067	0.0119	1.197
13	NW1A2-C2-1B	6.80	27.20	17.00	0.999	1.044	92.640	37.890	1.0012	0.9987	0.0084	0.845
14	NW1A2-C2-2B	6.90	27.70	17.30	1.284	1.031	89.720	30.880	0.9846	0.9942	0.0054	0.540
15	SM2C-B1-1A	3.30	13.30	8.30	0.710	0.993	87.510	13.710	1.0290	1.0084	0.0052	0.529
16	SM2C-A2-1B	3.30	13.30	8.30	0.640	1.051	87.870	13.360	1.1	1.6	0.0025	0.251
17	SB4A-A2-2A	3.30	13.30	8.30	0.766	1.017	88.730	25.070	1.0412	1.0100	0.0060	0.601
		6.50	26.00	16.25	0.855	1.013	88.730	25.070	1.0517	1.0122	0.0072	0.721
18	SM2C-C1-1A	3.30	13.30	8.30	0.682	1.180	86.550	12.120	1.0410	1.0199	0.0079	0.790
19	SM2C-A3-1A	3.30	13.30	8.30	1.272	1.050	79.880	24.590	1.0313	1.0093	0.0052	0.519
		6.50	26.00	16.25	1.445	1.052	79.880	24.590	0.9987	1.0196	0.0053	0.525
		9.00	36.00	22.50	1.489	1.054	79.880	24.590	0.9952	0.9983	0.0053	0.5291
20	SB4A-A2-1B	3.30	13.30	8.30	1.095	1.005	93.990	27.810	1.0455	1.0122	0.0035	0.355
		7.50	30.00	18.75	1.206	1.007	93.990	27.810	1.0306	1.0088	0.0057	0.570

1.1 Derivation of empirical relationships

2) in this method, γ_r is assumed as a point that G/G_{max} is equal to 0.5 (Stokoe et al. 1999).

The second method was also used to determine the value of γ_r for dutch peat samples. It must be noted that all of the analysis have been done on the results from Bochum RC, at small and intermediate strain region and the data from Deltares for large strain level. It is worthwhile to mention that Figure 1.13 was used to get the data from Deltares for our analysis in this report. As can be seen the data for large strain (data by deltares, black points) are so close to each other, therefore, some points were chosen, as an example, for our analysis. Samples 1 to 14 have boundary conditions close to the data in Figure 1.13 (Table 1.1), therefore, the results for these samples, were used for our analysis on small and intermediate strain region. The obtained model from these analysis will be compared with the experimental data for samples 15 to 20 from the Bochum resonant column and the results from NGI (obtained from Figure 1.13).

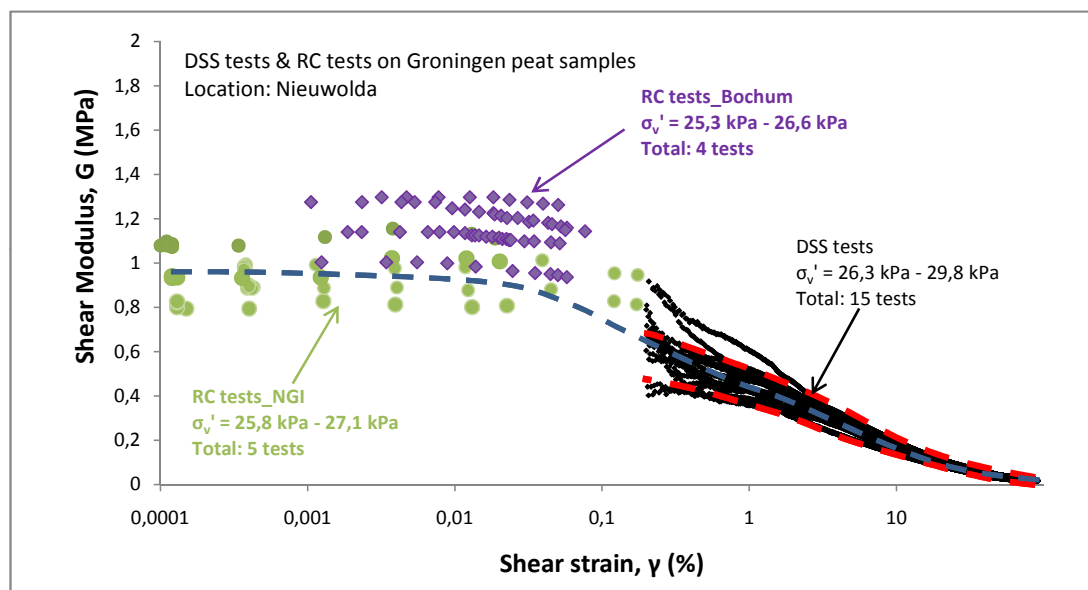


Figure 1.13: Experimental data from Deltares, Bochum and NGI, provided by Deltares

Three values were assumed for G_{max} :

- i) minimum G_{max} from Bochum RC test on samples 1 to 14
- ii) maximum G_{max} from Bochum RC test on samples 1 to 14
- iii) average G_{max} from Bochum RC test for samples 1 to 14

1 Empirical relationships

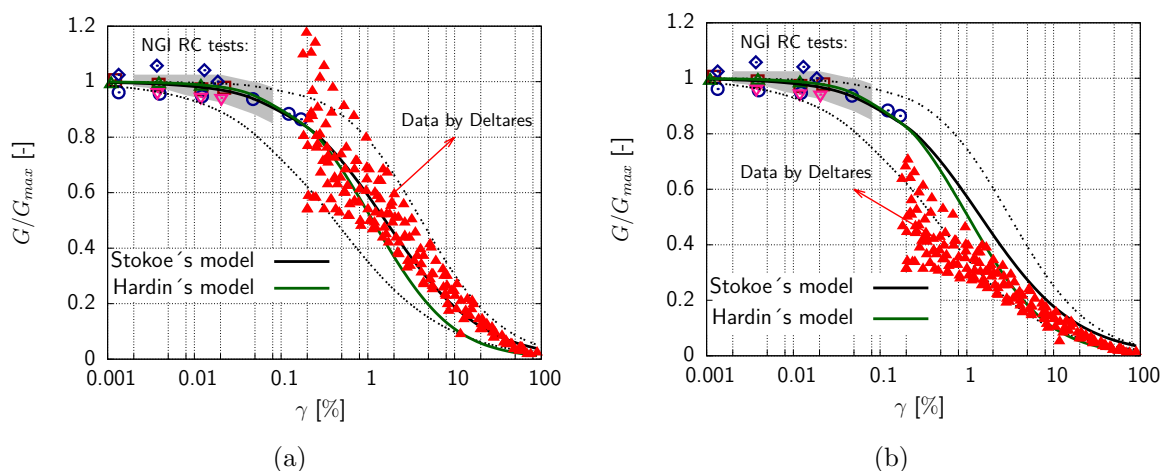


Figure 1.14: G/G_{max} versus shear strain, Deltares data were:(a) normalized with the minimum measured value for G_{max} for samples 1 to 14 using Bochum RC device; (b) normalized with the maximum measured value of G_{max} for samples 1 to 14 using Bochum RC device

Firstly, G_{max} was assumed to be equal to minimum and maximum G_{max} which were measured using Bochum RC device for samples 1 to 14. Figures 1.14a and 1.14b show the G/G_{max} versus shear strain when G was normalized with minimum and maximum measured value for G_{max} respectively. Dashed lines show the upper and lower bands for data and solid line is the fitted curve using Equation 1.13 to the data. Black points in this Figures are the results for samples 15 to 20 measured by Bochum resonant column device.

In next try, G_{max} was assumed to be the average of G_{max} values which were measured for samples 1 to 14 by Bochum RC device. The average value was equal to 1 MPa and this value was used as G_{max} in this analysis. Figure 1.15 shows G/G_{max} versus γ for experimental data from Bochum and Deltares. This Figure is used to determine the value of γ_r . γ_r is a shear strain that G/G_{max} is equal to 0.5. Therefore, from, Figure 1.15, γ_r is approximately equal to 1%. The experimental data from Bochum RC test for samples 15 to 20 were also added to this Figure (black points). The solid line is Equation 1.13 where the value of α and β are equal to 0.9 and 0.8 respectively.

Defined model using Bochum and Deltares data were also compared with the results from NGI in Figure 1.16. It must be noted that the data by Deltares were normalized with G_{max} from Bochum data and data by NGI were normalized with G_{max} from NGI. The grey zone in these Figures shows results from Bochum for samples 1-20, dashed lines are

1.1 Derivation of empirical relationships

suggested upper and lower bands solid line is a suggested curve to predict G/G_{max} of Dutch peat samples (details are in Figure 1.15).

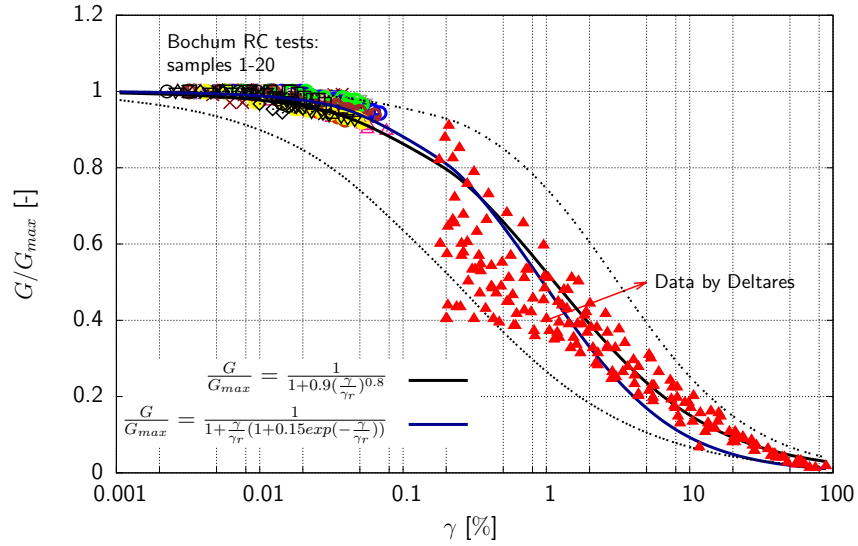


Figure 1.15: G/G_{max} , normalized with the average values of G_{max} for samples 1 to 14, versus shear strain. Solid lines are Equations 1.13 and 1.14 with determined fitting parameters from analysis of Bochum RC test on samples 1 to 14 and Deltares data

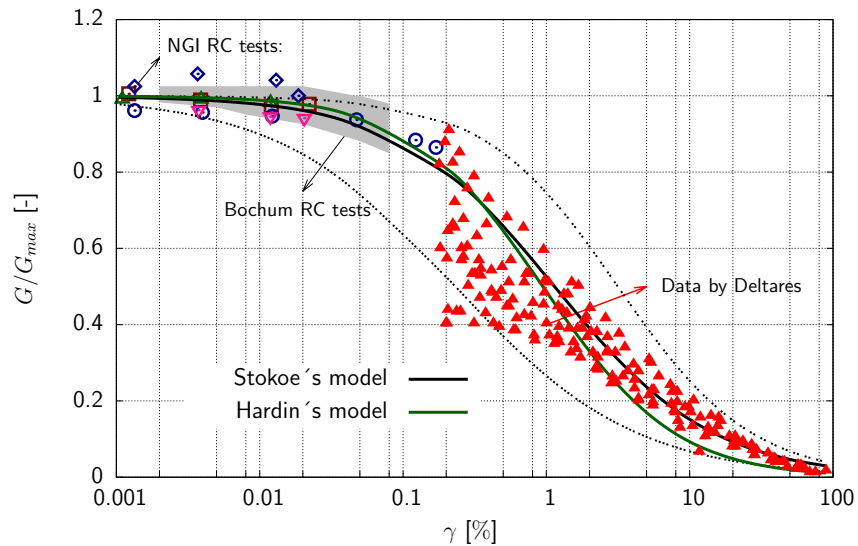


Figure 1.16: G/G_{max} versus shear strain, solid lines are Equations 1.13 and 1.14 with determined fitting parameters from analysis of Bochum RC test on samples 1 to 14 and Deltares data

1 Empirical relationships

Hardin & Drnevich (1972a) proposed the Equation 1.15 to predict damping ratio respect to shear strain.

$$\frac{D}{D_{max}} = \frac{\frac{\gamma}{\gamma_r}}{1 + \frac{\gamma}{\gamma_r}} \quad (1.15)$$

where, D_{max} is maximum damping ratio which was suggested to be a value between 25% to 33% for sands. However, D_{max} is an unknown value for peats, therefore, this Equation is not applicable to estimate the value of D for peats.

From the analysis of our experimental data on sand samples, we concluded that Equation 1.16 which can be used to estimate damping ratio. This Equation is based on the minimum damping ratio, D_{min} and γ_r which are available from RC test results.

$$\frac{D}{D_{min}} = A \left(\frac{\frac{\gamma}{\gamma_r}}{1 + \frac{\gamma}{\gamma_r}} \right)^B + 1 \quad (1.16)$$

where, D_{min} is the minimum damping ratio and A and B are fitting parameters. Therefore, Equation 1.16 was used to estimate damping ratio of Dutch peat soils. The fitting parameters of Equation 1.16 were determined using the experimental data from Bochum RC for samples 1 to 14.

Analyze of Bochum experimental data revealed that for Dutch peat samples, the values of A and B must be equal to 4.7 and 0.9 respectively. The fitted line using Equation 1.16 and obtained fitting parameters has been shown by black solid line in Figure 1.17. It must be noted that D_{min} for samples 1 to 14 was assumed to be 4.75%. Dashed lines in Figure 1.17 are the suggested upper and lower bands for Dutch peat samples. Damping ratio were normalized with respect to the minimum damping ratio, D_{min} for all of the peat samples (samples 1 to 20). Normalized damping ratio was drawn versus shear strain in Figure 1.18. The solid line in this Figure is Equation 1.16 with proposed fitting parameters for samples 1 to 14.

1.1 Derivation of empirical relationships

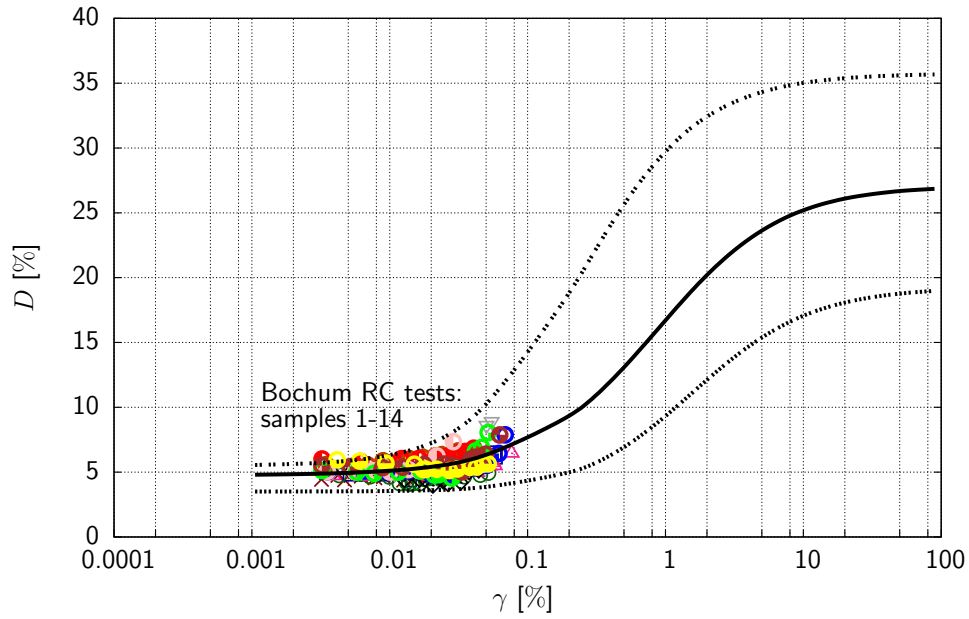


Figure 1.17: D versus shear strain, solid line is Equation 1.16 with fitting parameters defined for samples 1 to 14 from Bochum RC test

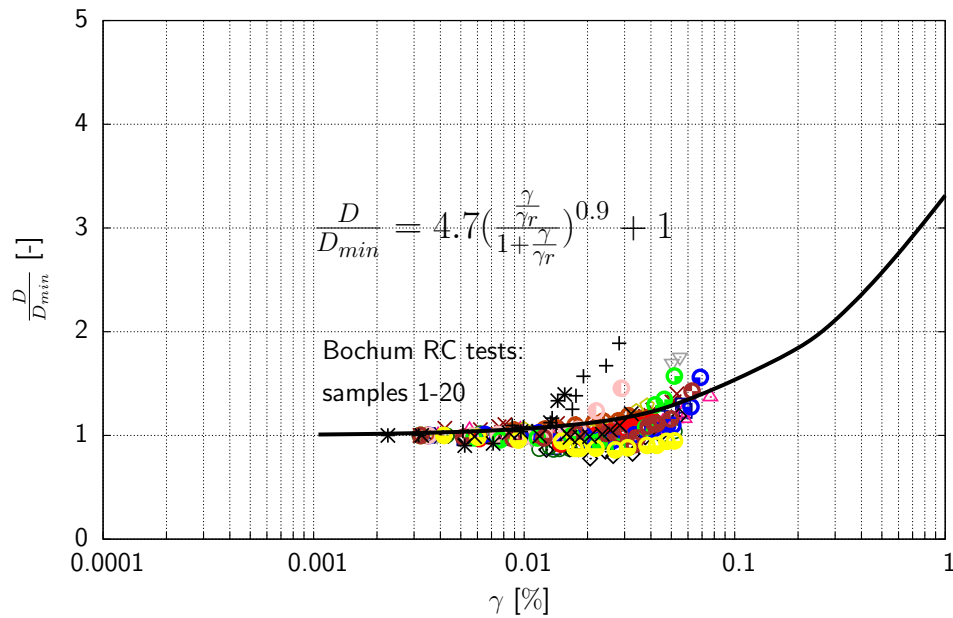


Figure 1.18: Normalized D versus shear strain for dutch peat samples, measured by Bochum RC device, and Equation 1.16 with fitting parameters obtained from Figure 1.17

1.2 Comparison of derived empirical relationships with published data

Kishida et al. (2009) conducted RC and torsional shear tests to assess dynamic properties of highly organic soils ($OC \approx 15\%-61\%$). Samples were compiled from the Montezuma Slough and Clifton Court in their experiment. The value of G_{max} has been compared with the predicted G_{max} using Equations 1.7 and 1.1 in Figure 1.19.

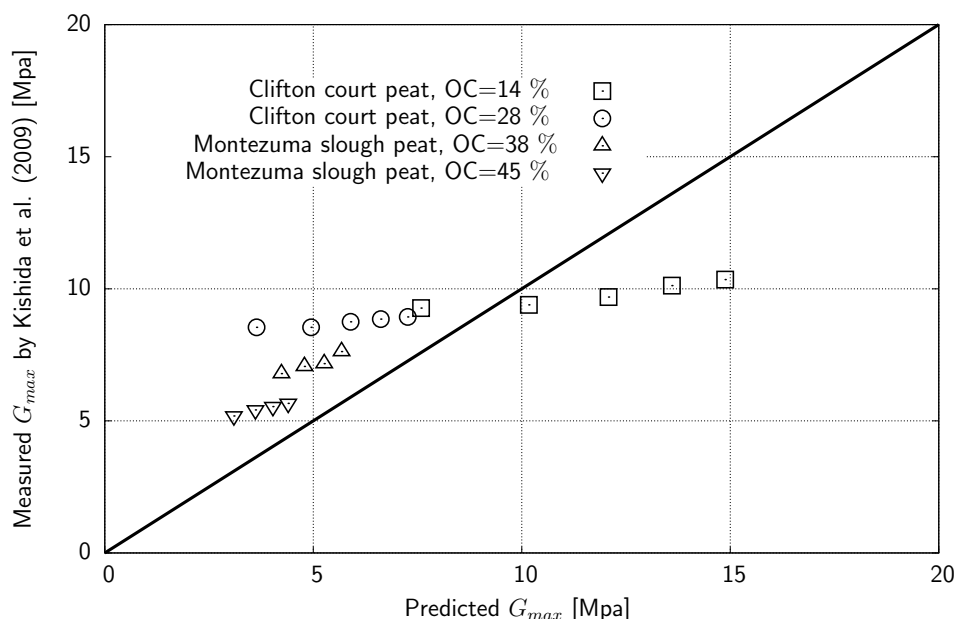


Figure 1.19: The measured G_{max} by Kishida et al. (2009) versus the predicted G_{max} using Equations 1.7 and 1.1

However, the fitting parameters of Equations 1.7 and 1.1 were determined from the experiment on the peat samples with high amount of organic content (more than 70% OC) but, the experimental results by Kishida et al. (2009) are for samples with low amount of organic content ($15\% < OC < 45\%$). Therefore, this could be a reason for the scatter between predicted results using Equations 1.7 and 1.1 and fitting parameters from our experiment in comparison with the measured results by Kishida et al. (2009).

Experimental data obtained from the current study on peat samples and the proposed curves regarding the experimental data were compared with the proposed bands by Vucetic & Dobry (1991) for inorganic soils and Kishida et al. (2009) for organic soils in Figure 1.20.

1.2 Comparison of derived empirical relationships with published data

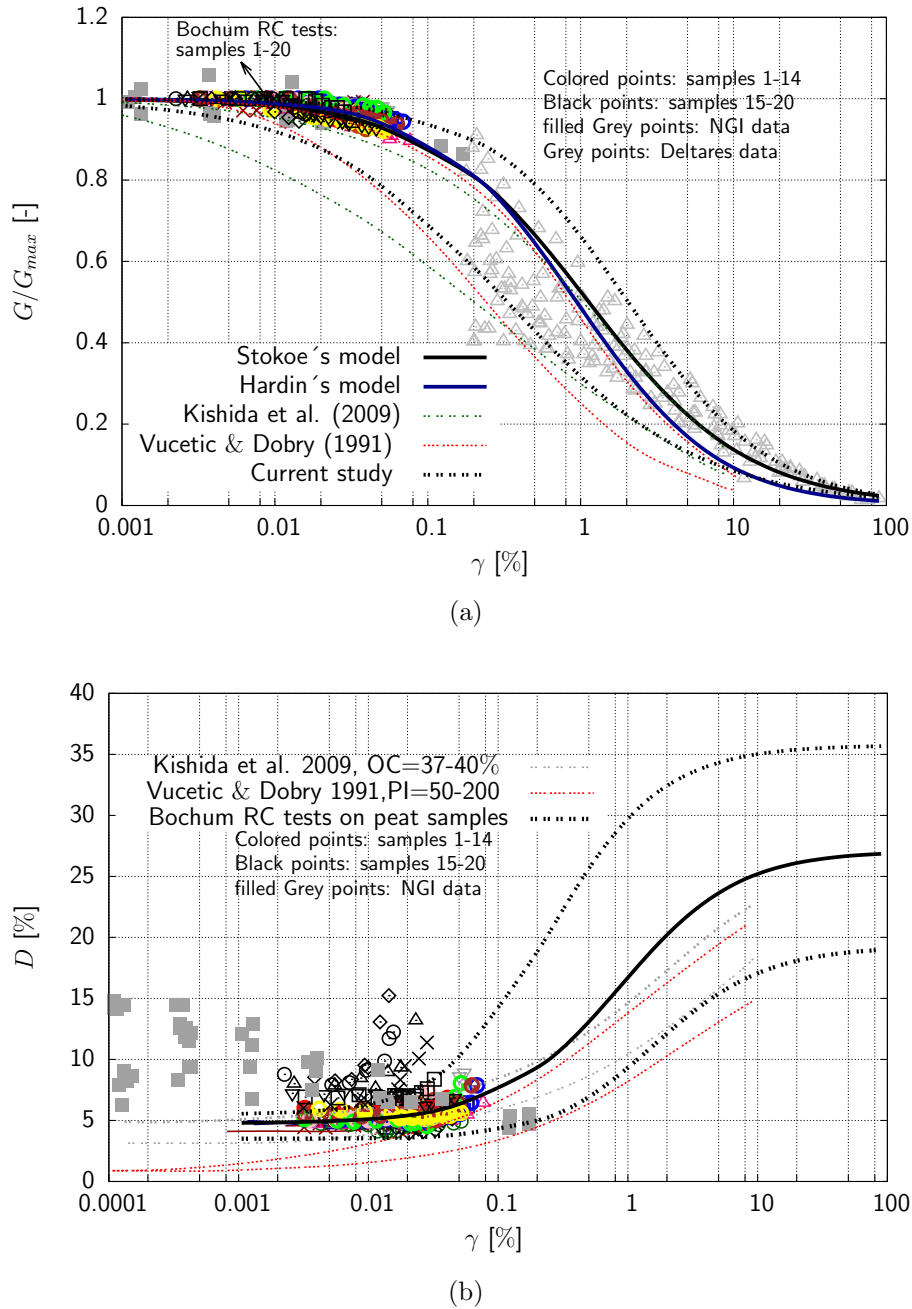


Figure 1.20: Small and intermediate properties of peat samples in comparison with the published data: a) shear modulus versus shear strain; b) damping ratio versus shear strain the solid and dashed black lines are curves from Equations 1.13 and 1.16 using the determined fitting parameters from this experiment for samples 1 to 14, $D_{min}=4.75\%$, dashed lines are the proposed bonds for organic and inorganic soils, solid lines are the estimated curves using the proposed models

2 Discussion

2.1 Influence of frequency on dynamic properties

Resonant column and Bender element tests were conducted to determine the dynamic properties of the Groningen peat samples. The effect of frequency on the results have been explained in this chapter. It must be noted that analysis have been done on the resonant column and bender element tests from RUB and bender element tests from NGI. The value of frequency of tests in Deltares was 0.1 Hz.

Dynamic soil properties in resonant column tests are evaluated at the resonant frequency of the specimen (ASTMD4105-92). The resonant frequency of Groningen peat samples using RUB resonant column device was a value between 3.5 to 5 Hz. On the other hand, bender element tests were conducted to determine the maximum shear stiffness of the adopted peat samples. The frequency of waves in BE tests was between 900-1100 Hz. For an example, the measured G_{max} using resonant column and Bender element tests were drawn versus frequency in logarithmic scale for sample No.10 (NW1A2-B1-3A) in Figure 2.1. The trend line in Figure 2.1 is the best fitted line to the data ($R^2=1$). This line shows that the value of G_{max} using BE is more than the measured G_{max} using RC in. This could be due to the effect of frequency. This is in agreement with the published data by [Stokoe & Santamarina \(2000\)](#) and [Kramer \(2000\)](#) where, they reported that the dynamic properties of cohesive soils and peats are strongly affected by frequency of loading. For ease of discussion, maximum shear modulus at frequency of 1 Hz was assumed as a reference value, hereafter $G_{max,1Hz}$. $G_{max,1Hz}$ was estimated by replacing f by 1 in the Equation of trend line in G_{max} - f plot. For an example, by replacing f by 1 in Figure 2.1, $G_{max,1Hz}$ will be equal to 0.876 for sample No.10.

The same analysis was done for all of the samples, the summary of them is represented in Figure 2.2. The trend of lines in this Figure show that the value of G_{max} using RC device was less than the results using BE for all of the samples. The value of $G_{max,1Hz}$ was also estimated for them using the Equation of their trend lines (Figure 2.2).

2 Discussion

We can assume one line, as an average line, for all of the data in Figure 2.2.

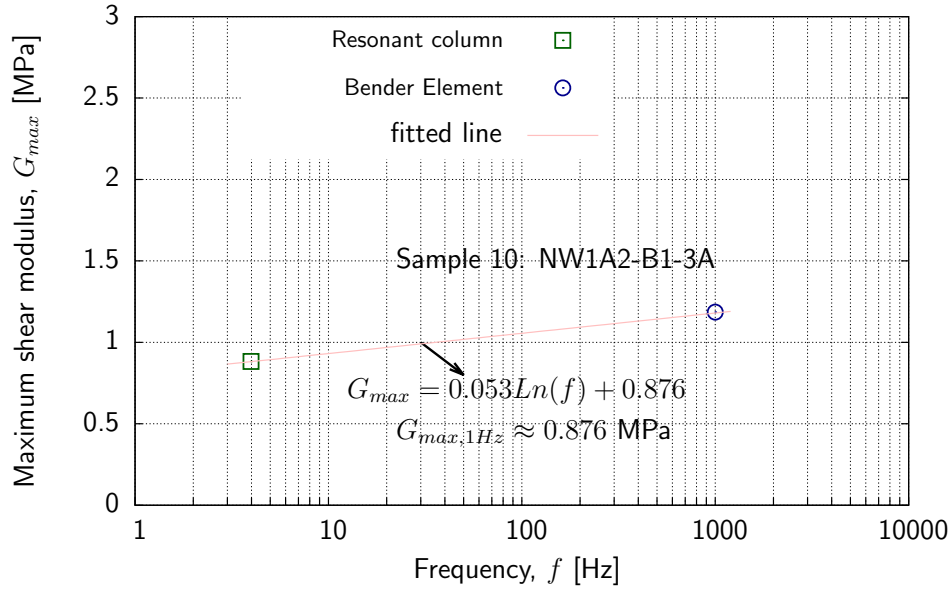


Figure 2.1: The effect of frequency on small strain shear modulus, G_{max} , of sample No. 10 (NW1A2-B1-3A)

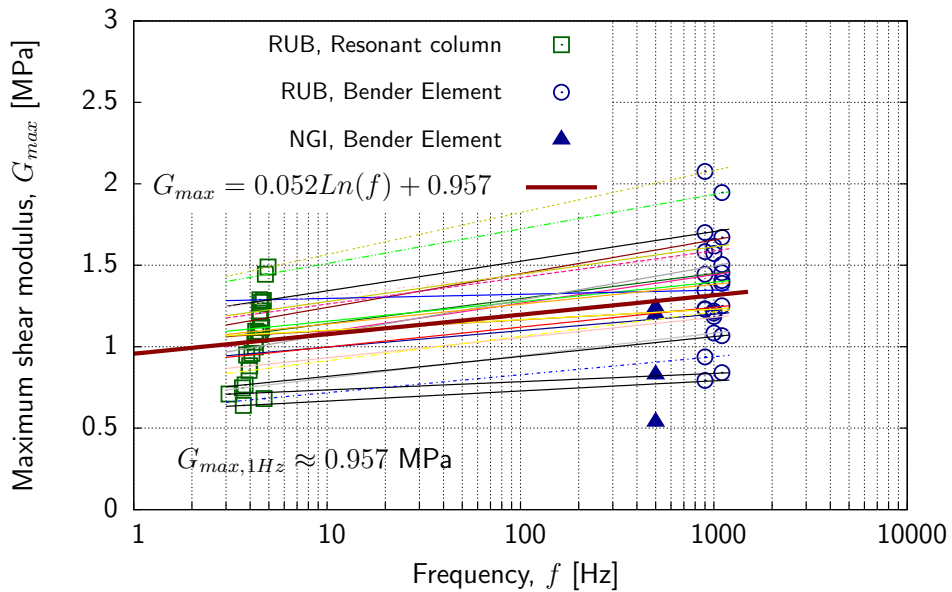


Figure 2.2: General effect of frequency on small strain shear modulus, G_{max} , of Geroningen peat samples, RC and BE frequency from RUB data and BE frequency from NGI data

2.1 Influence of frequency on dynamic properties

The average line, solid red line in this Figure, could be chosen as a reference trend line for Groningen peat samples. It is worthwhile to mention that the scatter of data in Figure 2.2 is due to the differences in the boundary conditions and material properties of samples. Kramer (2000) reported that dynamic properties of Mercer Slough Peat was also affected by frequency of loading (Figure 2.3). The same analysis was also conducted on the published data by Kramer (2000) (Figure 2.3). Again, shear stiffness at frequency of 1 Hz was estimated for Kramer's data, and assumed as a reference value for their data.

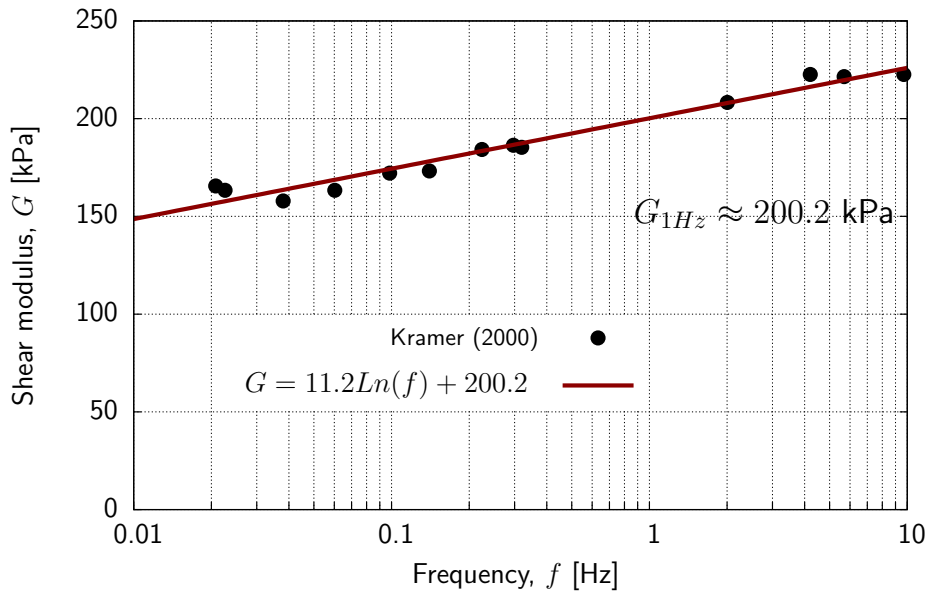


Figure 2.3: General effect of frequency on small strain shear modulus, G_{max} , (modified after Kramer 2000)

Stokoe & Santamarina (2000) showed that small strain properties of cohesive soils can be significantly affected by the frequency of vibration during laboratory tests (Figure 2.4). The normalized stiffness using experiment at RUB on Groningen peat samples (Figure 2.2) show the significant effect of frequency on shear modulus. Grey zone in Figure 2.4 shows the predicted range for the effect of frequency on stiffness of Groningen peat samples. The red line in this Figure is the estimated average line for the effect of frequency in adopted samples. Furthermore, the experimental data by Kramer (2000) on Mercer Slough Peat was also normalized with the estimated reference shear modulus for their data (Figure 2.3). Figure 2.4 shows the normalized average line of maximum shear modulus (Figure 2.2) from the experiment at RUB on peat samples in comparison with the proposed zones for cohesive soils and data by Kramer (2000) for peat samples. The data shows that the

2 Discussion

increasing of stiffness in peat samples are in agreement with literature.

Therefore, test results on peat samples from different dynamic devices do not yield similar values when the frequency of loading is different.

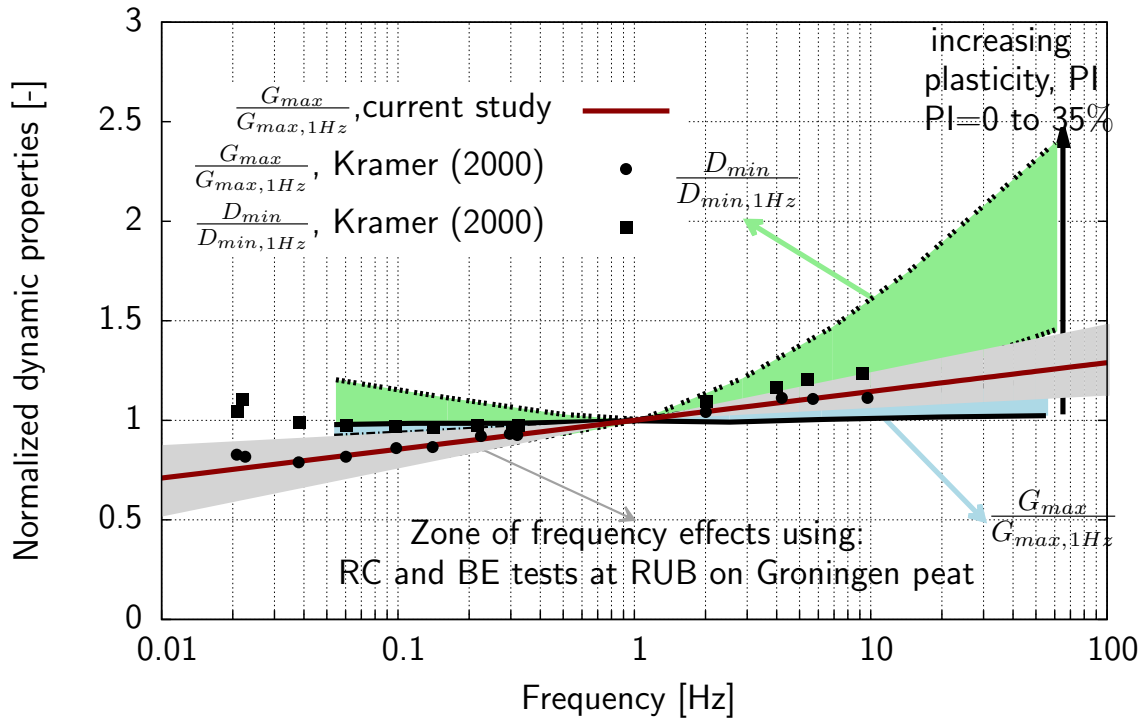


Figure 2.4: General effect of excitation frequency on small strain shear modulus, G_{max} , and small strain damping ratio, D_{min} , Deltares experiment has been done with frequency of 0.1 Hz (modified after [Stokoe & Santamarina 2000](#))

Bibliography

- Biot, M. A. (1955), 'Theory of propagation of elastic waves in a fluid saturated porous solid. ii. higher frequency range', *The journal of the Acoustical Society of America* **28**, 179–191.
- Goudarzy, M. (2015), Micro and macro Mechanical assessment of small and intermediate properties of granular materials, PhD thesis, Ruhr Universität Bochum.
- Goudarzy, M., Rahman, M., König, D. & Schanz, T. (2016), 'The influence of non-plastic fines content on maximum shear modulus of sands', *Soils and Foundations* **56** No.6 (in-press).
- Hardin, B. O. & Black, W. L. (1966), 'Sand stiffness under various triaxial stresses', *Soils Mechanics and Foundations Division* ., 27–42.
- Hardin, B. O. & Drnevich, V. P. (1972a), 'Shear modulus and damping in soils: Design equations and curves', *Soil Mechanics and Foundation Division* **98**, 667–692.
- Hardin, B. O. & Drnevich, V. P. (1972b), 'Shear modulus and damping in soils measurement and parameter effects', *Soils Mechanics and Foundations Division* **98**, 603–624.
- Hashash, Y. M. A. & Park, D. (2001), 'Non-linear one-dimensional seismic ground motion propagation in the mississippi embayment', *Engineering Geology* **62**, 185–206.
- Iida, K. (1937), 'The velocity of elastic wave in sands', *Earthquake research institute* ., 132–145.
- Jamiolkowski, M., Lancellotta, R. & Lo Presti, D. (1995), 'Remarks on the stiffness at small strains of six italian clays', *Pre-failure Deformation of Geomaterials* **1**, 817–836.
- Kishida, T., M., W. T., Boulanger, R. W., Driller, M. W. & Stokoe, II, K. (2009), 'Dynamic properties of highly organic soils from montezuma slough and clifton court', *Journal of Geotechnical and Geoenvironmental Engineering* **135**, 525–531.

Bibliography

- Kramer, S. L. (2000), 'Dynamic response of mercer slough peat', *Journal of Geotechnical and Geoenvironmental Engineering* **126**, 504–510.
- Moon, S. W. & Ku, T. (2016), 'Development of global correlation models between in-situ stress normalized shear wave velocity and soil unit weight', *Canadian Geotechnical Journal* **10.1139/cgj-2016-0015**.
- Santamarina, J. C. (2001), *Soils and Waves*, John wiley & sons.
- Schanz, T., Goudarzy, M., Rahemi, N. & Baille, W. (2016), 'Discussion of comparing cpt and vs liquefaction triggering methods by p. k. robertson', *Journal of Geotechnical and Geoenvironmental Engineering* **10.1061/(ASCE)GT.1943-5606.0001527** , **07016017**.
- Seed, H. & Idriss, I. (1970), Soil moduli and damping factors for dynamic response analyses, Technical report, Earthquake Engineering Research Center, University of California, Berkeley.
- Stokoe, II, K., Darendeli, M. B., Andrus, R. D. & Brown, L. T. (1999), 'Dynamic soil properties: Laboratory, field and correlation studies', *Earthquake Geotechnical Engineering* pp. 811–845.
- Stokoe, II, K. & Santamarina, C. (2000), Seismic wave based testing in geotechnical engineering, Technical report.
- Tatsuoka, F., Iwasaki, T., Fukushima, S. & Sudo, H. (1979), 'Stress conditions and stress histories affecting shear modulus and damping of sand under cyclic loading', *Soils and Foundations* **19**, 30–43.
- Vucetic, M. & Dobry, R. (1991), 'Effect of soil plasticity on cyclic response', *J. Geotech. Eng.* **117**, 89–107.

D External review on final report

21. März 2017

Dr. Cor Zwanenburg
DELTARES
Postbus 177

2600 MH Delft
The Netherlands

Project

Dynamic properties of Groningen peat
(ref. 1209862-006-GEO-0003)
here: expert review on two DELTARES reports

Dear Sirs.

Hereby I send you my review with respect to the following two reports by Deltares:
Report „1209862-011 Dynamic behaviour of Groningen peat, analysis and parameter assessment, December 2016 and
Report „1209862-011 Dynamic behaviour of Groningen peat, factual report, March 2017“.

1. The aim of the study is to derive the dynamic parameters for Groningen peat, and in particular the parameters needed for the soil response calculations. With the analysis of maximum shear stiffness, degradation curve of shear stiffness with strain and damping curve the study focused on the correct parameters.
2. The testing procedures followed are correct, consistent and state of the art. They cover different strain levels and different experimental protocols. The results gained by NGI, RUB & Deltares are of excellent quality showing very good overlapping for similar test conditions. Minor deviations can both qualitatively and quantitatively be explained by details of experimental procedures (slightly different frequencies for RC tests at NGI & RUB). The test results allow the theoretical interpretation and derivation of constitutive relations by Deltares with a very high quality. In the reviewer's opinion, the data, derived by the different laboratories, is sufficiently consistent, meaning there are no significant systematic differences between the laboratories.

Univ. Prof. Dr.-Ing. habil. Tom Schanz

**GEO
RUHR**

Ingenieurgesellschaft für Geotechnik

Am alten Wasserwerk 12
D-45886 Gelsenkirchen

Telefon:
+49 (0) 0151 67442786

tom.schanz@georuhr.de

Finanzamt Gelsenkirchen
Steuernummer 319/5383/5890

Bankverbindung
Sparkasse Mittelthüringen
IBAN: DE57 8205 1000 1310 1130 21
BIC: HELADEF1WEM

3. The analysis of the data is correct, consistent and sufficient for the purpose of the study. It follows theoretical concepts of established international standards.
4. The study shows relatively low values (compared to literature) for maximum shear stiffness and shear wave velocity. Those values are considerably lower than usually found for clays and sands. In the reviewers opinion the obtained values for peat in this study can be perfectly used for further analysis as specific material properties for organic soils in this study differ from those of the literature (OC, OCR, stress state etc.).
5. The analysis focuses on producing correlations for the Groningen area. By these correlations parameters can be assessed for locations other than the sample locations but showing material and state parameters similar to the samples studied (OC, stress state, stress history etc.). From my point of view, also considering natural heterogeneities of peat, the number of tests, quality of the tests and applied correlations are highly sufficient for this purpose in relation to the aim of the whole project.
6. Even the study showed difficulties in measuring the damping curve of peat at low stress level for higher strain amplitudes the analysis of the damping curve by Deltares and its parameters derived are sufficient for the purpose of this study. Our suggestions to improve the damping curve measurements and the interpretation of the available test data were fully considered by Deltares.
7. The study here focuses on the superficial peat layer, the Nieuwkoop formation. In the area there is also a thin basal peat layer present. In the reviewers opinion, it is only possible to use the data, found for the superficial layers, for parameter assessment of the basal peat layer if similar constitutive characteristics and stress level are guaranteed (see my remarks above). For dealing with the basal peat layer it can be additionally checked if similarities are there for these parameters with those from studies from the literature. Also sensitivities of the dynamic analysis with respect to the presence of a thin basal layer at all can be studied.

To summarize my statements above the following can be concluded:

The experimental program and the theoretical analysis documented in the reports by Deltares are of excellent quality. The study under qualitative and quantitative considerations is fully sufficient to be used in the safety assessment calculation for the Groningen earthquakes. This statement especially holds under consideration of the fact that beyond this research there is limited information on the dynamic (small strain) parameters of peat. The results obtained by Deltares

showed that the trends of curves are similar to the published data for different sites. Furthermore, peats are not homogenous materials and it makes it difficult to compare the results from each sample with the other sample. Therefore, the presented data from the performed experiment can only be used for seismic or dynamic analysis (i.e. estimate ground motion parameters) of soil layers that the experiment has been done for them. For other layers one has to do additional experiment on them because stress state will be out of the range covered by the current study.

If we want to find and predict the dynamic behaviour of Groningen peat precisely using a unique and general equation, an extended experimental program must be executed covering a wide range of OC, OCR and stress states.

Best regards,

A handwritten signature in black ink, appearing to read 'T. Schanz', with a stylized, cursive script.

Univ. Prof. Dr.-Ing. habil. T. Schanz